
IXO

**PAYLOAD DEFINITION
DOCUMENT**

<i>prepared by/préparé par</i>	SRE-PA
<i>reference/référence</i>	SRE-PA/2009.019/
<i>issue/édition</i>	6
<i>revision/révision</i>	1
<i>date of issue/date d'édition</i>	24/04/2009
<i>status/état</i>	Final
<i>Document type/type de document</i>	Technical Note
<i>Distribution/distribution</i>	SRE-PA, IXO CDF team, NASA IXO Project team, IXO-IWG, Assessment study contractors

A P P R O V A L

Title <i>titre</i>	issue <i>issue</i>	revision <i>revision</i>
-----------------------	-----------------------	-----------------------------

author <i>auteur</i>	date <i>date</i>
-------------------------	---------------------

approved by <i>approuvé by</i>	date <i>date</i>
-----------------------------------	---------------------

C H A N G E L O G

reason for change / <i>raison du changement</i>	issue/ <i>issue</i>	revision/ <i>revision</i>	date/ <i>date</i>
First release & preparation for CDF activity	1	0	21/05/2004
Including updates resulting from CDF studies	2	0	March/2005
Overall update	2	1	April/2005
Revision based on payload working group and instrument experts inputs & responsive to SciRD	3	0	Sep/2005
Updated with input from payload accommodation study and	4	0	January 2007
Updated with input from CV2015-2025 planning and XEUS proposal	4	1	March 2008
Updated according to inputs from Instrument teams, prior to CDF study	5	0	May 2008
Updated with results from October 2008 CDF & IXO definition	6	0	April 2009
Public Document	6	1	April 2009

CHANGE RECORD APRIL / 2009

Issue: 6 Revision: 0

<i>reason for change/raison du changement</i>	<i>page(s)/page(s)</i>	<i>paragraph(s)/paragraph(s)</i>

TABLE OF CONTENTS

PART 1	PREFACE	13
1	List of acronyms	14
2	Reference list	16
2.1	Applicable Documents	16
2.2	Reference Documents	16
3	The IXO mission	17
4	Spacecraft Reference coordinate system.....	19
5	Introduction.....	20
6	Payload overview.....	21
7	Mission profile & science operations - summary	23
PART 2	DESCRIPTION OF THE BASELINE INSTRUMENTS	25
1	Introduction.....	26
2	Wide Field Imager (WFI).....	28
2.1	Instrument Description	28
2.1.1	Introduction	28
2.1.2	Instrument performance specifications.....	30
2.1.3	Instrument configuration	31
2.1.4	Instrument optical design - filters.....	44
2.1.5	Instrument units' mechanical design and dimensions	44
2.1.6	Mechanisms.....	45
2.1.7	Instrument units' thermal design.....	45
2.1.8	Electrical design	46
2.1.9	On-board Software	54
2.1.10	Ground support equipment.....	56
2.1.11	Instrument mode description.....	56
2.2	Mechanical Interfaces and Requirements	60
2.2.1	Location requirements	60
2.2.2	Alignment requirements	61
2.2.3	Pointing requirements and performance goals	61
2.2.4	Interface control drawing	61
2.2.5	Instrument mass.....	62
2.3	Thermal Interfaces and Requirements.....	63
2.3.1	Temperature limit in space environment.....	63
2.3.2	Temperature limits in laboratory environment.....	63
2.3.3	Temperature sensors.....	63
2.3.4	Heaters.....	63
2.3.5	Thermal schematics.....	64
2.3.6	Thermal control requirements	64
2.4	Electrical Interfaces and Requirements.....	65
2.4.1	Electrical resources requirement summary	65
2.4.2	Instrument power distribution block diagram	65
2.4.3	Power budget.....	65

2.4.4	Instrument modes' duration.....	68
2.4.5	Telecommands.....	68
2.4.6	Telemetry.....	68
2.4.7	Electrical interfaces.....	69
2.5	Electromagnetic Compatibility and Electrostatic Discharge Interface	70
2.5.1	Susceptibility requirements	70
2.6	Optical Requirements.....	71
2.6.1	Straylight requirements	71
2.6.2	Baffling requirements.....	71
2.6.3	Charged Particle Rejection Requirements.....	72
2.7	Transportation, Handling, Cleanliness and Purging Requirements.....	72
2.7.1	Transportation requirements.....	72
2.7.2	Handling requirements	72
2.7.3	Cleanliness requirements.....	72
2.7.4	Purging requirements	72
2.8	Ground and flight operations requirement	73
2.8.1	Ground and pre-flight operation.....	73
2.8.2	Flight operations.....	73
2.9	Deliverable Models and GSE.....	74
2.9.1	Structural Thermal Model	74
2.9.2	Engineering Qualification Model.....	74
2.9.3	Flight model	75
2.9.4	Flight spare model.....	75
3	X-ray Microcalorimeter Spectrometer (XMS).....	76
3.1	Introduction.....	76
3.2	Instrument description	77
3.2.1	Introduction	77
3.2.2	Instrument performance specifications.....	79
3.2.3	Instrument configuration	83
3.2.4	Instrument optical design	100
3.2.5	Instrument units mechanical design	103
3.2.6	Mechanisms.....	103
3.2.7	Instrument units thermal design	103
3.2.8	Electrical design	106
3.2.9	Onboard software	106
3.2.10	Ground support equipment.....	107
3.2.11	Instrument mode description.....	107
3.3	Mechanical Interfaces and Requirements	110
3.3.1	Location requirements.....	110
3.3.2	Alignment requirements	110
3.3.3	Pointing requirements and performance goals	111
3.3.4	Interface control drawing	111
3.3.5	Instrument mass.....	118
3.4	Thermal Interfaces and Requirements.....	122
3.4.1	Temperature limit in space environment.....	122
3.4.2	Temperature limits in laboratory environment.....	123
3.4.3	Temperature sensors.....	123
3.4.4	Heaters.....	123
3.4.5	Thermal schematics.....	123

3.4.6	Thermal control requirements	129
3.5	Electrical interfaces and requirements	130
3.5.1	Electrical resources requirement summary	130
3.5.2	Instrument power distribution block diagram	130
3.5.3	Power budget	131
3.5.4	Instrument modes' duration	133
3.5.5	Telecommands	133
3.5.6	Telemetry	134
3.5.7	Electrical interfaces	136
3.6	Electromagnetic Compatibility and Electrostatic Discharge Interface	137
3.6.1	Susceptibility requirements (EMC cleanliness and grounding)	137
3.6.2	Susceptibility for microphonics	140
3.6.3	Susceptibility to radiation	140
3.7	Optical Requirements	141
3.7.1	Stray-light requirements	141
3.7.2	Baffling requirements	141
3.8	Transportation, Handling, Cleanliness and Purging Requirements	142
3.8.1	Transportation requirements	142
3.8.2	Handling requirements	142
3.8.3	Cleanliness requirements	142
3.8.4	Purging requirements	142
3.9	Ground and flight operations requirements	143
3.9.1	Ground and pre-flight operation	143
3.9.2	Flight operations	144
3.10	Deliverable models and GSE	146
3.10.1	Structural Thermal Model	146
3.10.2	Engineering Qualification Model	146
3.10.3	Flight model	146
3.10.4	Flight spare model	146
3.10.5	Ground Support Equipment	147
4	Hard X-ray Imager (HXI)	148
4.1	Instrument Description	148
4.1.1	Introduction	148
4.1.2	Instrument performance specifications	149
4.1.3	Instrument configuration	150
4.1.4	Instrument Optical Design	154
4.1.5	Instrument units' mechanical design and dimensions	154
4.1.6	Mechanisms	155
4.1.7	Instrument units' thermal design	155
4.1.8	Electrical design	156
4.1.9	Onboard software	156
4.1.10	Ground support equipment	156
4.1.11	Instrument mode description	157
4.2	Mechanical interface and requirements	157
4.2.1	Location and alignment requirements	157
4.2.2	Pointing requirements and goal	157
4.2.3	Interface control drawing	157
4.2.4	Instrument mass	158
4.3	Thermal interface and requirements	158

4.3.1	Temperature limit in space environment	158
4.3.2	Temperature limit in laboratory environment	158
4.3.3	Temperature sensors	158
4.3.4	Heaters	159
4.3.5	Thermal schematics	159
4.3.6	Thermal control requirements	159
4.4	Electrical Interfaces and requirements.....	159
4.4.1	Electrical resources requirement summary	159
4.4.2	Instrument power distribution block diagram	160
4.4.3	Power budget	160
4.4.4	Instrument modes' duration.....	160
4.4.5	Telecommands.....	160
4.4.6	Telemetry.....	160
4.4.7	Electrical interfaces	161
4.5	Electromagnetic compatibility and Electrostatic discharge interface	161
4.5.1	Susceptibility requirements	161
4.6	Optical requirements.....	161
4.6.1	Stray-light requirements	161
4.6.2	Baffling requirements	161
4.7	Transportation, Handling, Cleanliness and Purging requirements.....	162
4.7.1	Transportation requirements.....	162
4.7.2	Handling requirements	162
4.7.3	Cleanliness requirements.....	162
4.7.4	Purging requirements	162
4.8	Ground and Flight Operation requirements.....	162
4.8.1	Ground and pre-flight requirements	162
4.8.2	Flight operations.....	162
4.9	Deliverable Models and GSE.....	162
4.9.1	Structural Thermal model.....	162
4.9.2	Engineering Qualification model	162
4.9.3	Flight model	162
4.9.4	Flight spare model.....	163
5	High Time Resolution Spectrometer (HTRS)	164
5.1	Instrument Description	164
5.1.1	Introduction	164
5.1.2	Instrument performance specifications.....	164
5.1.3	Instrument configuration	165
5.1.4	Instrument optical design – filters	169
5.1.5	Instrument units' mechanical design and dimensions	169
5.1.6	Mechanisms.....	171
5.1.7	Instrument units' thermal design	173
5.1.8	Electrical design	173
5.1.9	On-board software.....	174
5.1.10	Ground support equipment.....	174
5.1.11	Instrument mode description.....	175
5.2	Mechanical Interfaces and Requirements	176
5.2.1	Location requirements	176
5.2.2	Alignment requirements	176
5.2.3	Pointing requirements and performance goals	176

5.2.4	Interface control drawing	177
5.2.5	Instrument mass	178
5.3	Thermal interfaces and requirements.....	179
5.3.1	Temperature limit in space environment	179
5.3.2	Temperature limits in laboratory environment.....	179
5.3.3	Temperature sensors.....	179
5.3.4	Heaters.....	179
5.3.5	Thermal schematics.....	179
5.3.6	Thermal control requirements	180
5.4	Electrical interfaces and requirements.....	181
5.4.1	Electrical resources requirement summary	181
5.4.2	Instrument power distribution block diagram	181
5.4.3	Power budget.....	181
5.4.4	Instrument modes' duration.....	182
5.4.5	Telecommands.....	182
5.4.6	Telemetry.....	183
5.4.7	Electrical interfaces	184
5.5	Electromagnetic compatibility and electrostatic discharge interface	185
5.5.1	Susceptibility requirements	185
5.6	Optical requirements.....	187
5.6.1	Stray-light requirements	187
5.6.2	Baffling requirements.....	187
5.6.3	Charge particle deflection	188
5.7	Transportation, handling, cleanliness and purging requirements	188
5.7.1	Transportation requirements.....	188
5.7.2	Handling requirements	188
5.7.3	Cleanliness requirements.....	188
5.7.4	Purging requirements	188
5.8	Ground and flight operation requirements	189
5.8.1	Ground and pre-flight operation	189
5.8.2	Flight operations.....	189
5.9	Deliverable models and GSE	190
5.9.1	Structural Thermal Model	190
5.9.2	Engineering Qualification Model	190
5.9.3	Flight model	191
5.9.4	Flight spare model.....	192
5.10	Open issues for the HTRS	192
6	X-ray Polarimeter (XPOL)	193
6.1	Instrument Description	193
6.1.1	Introduction	193
6.1.2	Instrument performance specifications.....	193
6.1.3	Instrument configuration	194
6.1.4	Instrument optical design – filters	196
6.1.5	Instrument units' mechanical design and dimensions	196
6.1.6	Mechanisms.....	198
6.1.7	Instrument units' thermal design (TBD)	198
6.1.8	Electrical design	198
6.1.9	On-board software.....	207
6.1.10	Ground support equipment.....	207

6.1.11	Instrument mode description.....	208
6.2	Mechanical Interfaces and Requirements	211
6.2.1	Location requirements	211
6.2.2	Alignment requirements	211
6.2.3	Pointing requirements and performance goals	211
6.2.4	Interface control drawing	212
6.2.5	Instrument mass.....	212
6.3	Thermal Interfaces and Requirements	213
6.3.1	Temperature limit in space environment.....	213
6.3.2	Temperature limits in laboratory environment.....	213
6.3.3	Temperature sensors.....	213
6.3.4	Heaters.....	213
6.3.5	Thermal schematics.....	213
6.3.6	Thermal control requirements	214
6.4	Electrical Interfaces and Requirements.....	215
6.4.1	Electrical resources requirement summary	215
6.4.2	Instrument power distribution block diagram	215
6.4.3	Power budget.....	215
6.4.4	Instrument modes duration.....	215
6.4.5	Telecommands.....	216
6.4.6	Telemetry.....	216
6.4.7	Electrical interfaces	218
6.5	Electromagnetic Compatibility and Electrostatic Discharge Interface	219
6.5.1	Susceptibility requirements	219
6.6	Optical Requirements.....	220
6.6.1	Stray-light requirements	220
6.6.2	Baffling requirements.....	220
6.6.3	Charged particles deflector.....	220
6.7	Transportation, Handling, Cleanliness and Purging Requirements.....	221
6.7.1	Transportation requirements.....	221
6.7.2	Handling requirements	221
6.7.3	Cleanliness requirements.....	221
6.7.4	Purging requirements	221
6.8	Ground and Flight Operation Requirements.....	221
6.8.1	Ground and pre-flight operation.....	221
6.8.2	Flight operations.....	222
6.9	Deliverable Models and GSE.....	222
6.9.1	Structural Thermal Model	222
6.9.2	Engineering Qualification Model.....	222
6.9.3	Flight Model.....	223
6.9.4	Flight Spare Model.....	223
7	Critical-angle transmission grating spectrometer (CAT-GS).....	224
7.1	Instrument Description	224
7.1.1	Introduction	224
7.1.2	Instrument performance specifications.....	226
7.1.3	Instrument configuration	226
7.1.4	Instrument optical design – filters	226
7.1.5	Instrument units’ mechanical design and dimensions	227
7.1.6	Mechanisms.....	230

7.1.7	Instrument units thermal design	230
7.1.8	Electrical design	232
7.1.9	On-board software	235
7.1.10	Ground support equipment.....	236
7.1.11	Instrument mode description.....	236
7.2	Mechanical Interfaces and Requirements	237
7.2.1	Location requirements	237
7.2.2	Alignment requirements	238
7.2.3	Pointing requirements and performance goals	238
7.2.4	Interface control drawing	239
7.2.5	Instrument mass.....	239
7.3	Thermal Interfaces and Requirements	240
7.3.1	Temperature limit in space environment.....	240
7.3.2	Temperature limits in laboratory environment.....	240
7.3.3	Temperature sensors.....	240
7.3.4	Heaters.....	240
7.3.5	Thermal schematics.....	240
7.3.6	Thermal control requirements	240
7.4	Electrical Interfaces and Requirements.....	241
7.4.1	Electrical resources requirement summary	241
7.4.2	Instrument power distribution block diagram	241
7.4.3	Power budget.....	241
7.4.4	Instrument modes' duration.....	242
7.4.5	Telecommands.....	242
7.4.6	Telemetry.....	242
7.4.7	Electrical interfaces	243
7.5	Electromagnetic Compatibility and Electrostatic Discharge Interface	243
7.5.1	Susceptibility requirements	243
7.6	Optical Requirements.....	243
7.6.1	Stray-light requirements	243
7.6.2	Charged particle requirements.....	244
7.7	Transportation, Handling, Cleanliness and Purging Requirements.....	244
7.7.1	Transportation requirements.....	244
7.7.2	Handling requirements	244
7.7.3	Cleanliness requirements.....	244
7.7.4	Purging requirements	244
7.8	Ground and Flight Operation Requirements.....	245
7.8.1	Ground and pre-flight operation.....	245
7.8.2	Flight operations.....	245
7.8.3	Contamination Requirements	245
7.9	Deliverable Models and Ground Support Equipment	245
7.9.1	Structural Thermal Model	245
7.9.2	Engineering Qualification Model.....	245
7.9.3	Flight model	245
7.9.4	Flight spare model.....	245
7.10	Other requirements	246
8	Off-Plane X-ray Grating Spectrometer (OP-XGS).....	247
8.1	Instrument Description	247
8.1.1	Introduction	247

8.1.2	Instrument performance specifications.....	248
8.1.3	Instrument configuration	248
8.1.4	Instrument optical design – filters	251
8.1.5	Instrument units’ mechanical design and dimensions	251
8.1.6	Mechanisms.....	254
8.1.7	Instrument units’ thermal design.....	254
8.1.8	Electrical design	255
8.1.9	On-board software.....	256
8.1.10	Ground support equipment.....	256
8.1.11	Instrument mode description.....	257
8.2	Mechanical Interfaces and Requirements	258
8.2.1	Location requirements	258
8.2.2	Alignment requirements	258
8.2.3	Pointing requirements and performance goals	258
8.2.4	Interface control drawing	258
8.2.5	Instrument mass.....	259
8.3	Thermal Interfaces and Requirements.....	260
8.3.1	Temperature limit in space environment.....	260
8.3.2	Temperature limits in laboratory environment.....	260
8.3.3	Temperature sensors.....	260
8.3.4	Heaters.....	261
8.3.5	Thermal schematics.....	261
8.3.6	Thermal control requirements	262
8.4	Electrical Interfaces and Requirements.....	263
8.4.1	Electrical resources requirement summary	263
8.4.2	Instrument power distribution block diagram	263
8.4.3	Power budget.....	263
8.4.4	Instrument modes’ duration.....	264
8.4.5	Telecommands.....	264
8.4.6	Telemetry.....	264
8.4.7	Electrical interfaces	264
8.5	Electromagnetic Compatibility and Electrostatic Discharge Interface	264
8.5.1	Susceptibility requirements	264
8.6	Optical Requirements.....	265
8.6.1	Stray-light requirements	265
8.6.2	Baffling requirements.....	265
8.7	Transportation, Handling, Cleanliness and Purging Requirements.....	265
8.7.1	Transportation requirements.....	265
8.7.2	Handling requirements	265
8.7.3	Cleanliness requirements.....	265
8.7.4	Purging requirements	265
8.8	Ground and Flight Operation Requirements.....	266
8.8.1	Ground and pre-flight operation	266
8.8.2	Flight operations.....	266
8.9	Deliverable Models and GSE.....	266
8.9.1	Structural thermal model	266
8.9.2	Engineering qualification model	266
8.9.3	Flight model	266
8.9.4	Flight spare model	266

PART 3	PAYLOAD ACCOMMODATION AND INTERFACES	267
1	Introduction.....	268
2	Accommodation.....	269
2.1	Instrument accommodation issues	269
2.2	Instrument alignment requirements	270
3	Interfaces.....	271
3.1	Data handling system	271
3.2	Power	272
3.3	Thermal	272
3.4	Cryogenics	273
3.5	Baffling and particle deflection	274
3.5.1	X-ray stray light baffles.....	274
3.5.2	Optical stray light baffling	275
3.5.3	Particle deflectors	275
3.6	Pointing requirements	275
4	Space Craft provided items.....	276
4.1	Alignment equipment	277
4.2	Stray light and background related equipment	277
4.2.1	X-ray Baffling	277
4.2.2	Optical stray light baffling	280
4.2.3	Charged particle deflectors.....	280
4.3	Cryogenic chain for XMS	281
4.4	Additional Items.....	281
4.4.1	CAT-XGS baffle, mount and wavelength calibration sources	281

Part 1 Preface

The Payload Definition Document (PDD) has been compiled by ESA with major inputs from the various instrument teams, forming part of the IXO Instrument Working Group (IWG). This document is agreed by the IWG chairmen as well as the IWG Instrument contact persons and contributors and describes a reference payload that satisfies the measurement requirements given in the Mission Requirements Document [AD-1]. This reference payload is used to establish the overall system design and the corresponding cost envelope.

1 LIST OF ACRONYMS

AC	Alternating Current
ACIS	AXAF CCD Imaging Spectrometer
ADC	Analog to Digital Converter
ADR	Adiabatic Demagnetisation Refrigerator
AGN	Active Galactic Nuclei
AIV	Assembly, Integration and Verification
AMA	Average Measurement Accuracy
AOCS	Orbit and Attitude Control System
APD	Avalanche PhotoDiodes
APE	Absolute Pointing Error
APS	Active Pixel Sensor
ASIC	Application Specific Integrated Circuit
BGO	Bi ₄ Ge ₃ O ₁₂
BOL	Beginning Of Life
CA	Camera Assembly
CAT[GS]	Critical Angle Transmission [Grating Spectrometer]
CAN	Controller Area Network
CC	Continuous Clocking mode
CCD	Charge Coupled Device
CEU	Central Electronic Unit
CPPS	Centralized Payload Power Supply
CRB	Contamination Review Board
CSA	Charge Sensitive Amplifier
CTE	Coefficient of Thermal Expansion
DAC	Digital to Analog Converter
DC	Direct Current
DEA	Detector Electronics Assembly
DEPFET	Depletion Mode Field Effect Transistor
DPA	Digital Processing Assembly
DPU	Digital Processing Unit
DSP	Digital Signal Processor
ECS	External Calibration Source
EMC	Electromagnetic Cleanliness/compatibility
EMCB	Electromagnetic Cleanliness Board
EMI	Electromagnetic Interference
EOL	End of Life
FEE	Front End Electronics
FET	Field Effect Transistor
FIP	Fixed Instrument Platform
FMA	Flight Mirror Assembly
FPGA	Field Programmable Array
FWHM	Full Width Half Maximum
GAS	Grating Assembly Structure

GEM	Gas Electron Multiplier
HETGS	High Energy Transmission Grating Spectrometer
HGA	High Gain Antenna
HTRS	High Time Resolution Spectrometer
H/W	Hardware
HXI	Hard X-ray Imager
ICU	Instrument Control Unit
I/O	Input/Output
J-T	Joule-Thomson (cooler)
LEOP	Low Earth Orbit Phase
LOS	Line Of Sight
MLI	Multi Layer Insulation
NVR	Non-Volatile Residual
OBF	Optical Blocking Filter
O[T]G	Off-plane [Transmission] Grating
PA	Product Assurance
PDD	Payload Definition Document
PDMU	Payload Data Management Unit
PSE	Payload Support Equipment
PSU	Power Supply Unit
RAM	Random Access Memory
RPE	Relative Pointing Error
RTU/C	Remote Terminal Unit / Control
S/C	Spacecraft
SciRD	Science Requirements Document
SDD	Single Drift Diode
SNR	Super Nova Remnant
SpW	Space Wire
SRE-PA	Advanced Studies and Technology Preparation Division
SSMM	Solid State Mass Memory
STE	Supra-Thermal Electron detector
SWT	Science Working Team
SXRP	Stellar X-Ray Polarimeter
TBC	To Be Confirmed
TBD	To Be Determined
TC/TM	Tele-command / Telemetry
TDA	Technology Development Activity
TDP	Technology Development Plan
TE	Timed Exposure
TES	Transition Edge Sensor
WFI	Wide Field Imager
XGS	X-ray Grating Spectrometer
XMS	X-ray Micro-calorimeter Spectrometer
XPOL	X-ray Polarimeter
XRБ	X-ray Binary

2 REFERENCE LIST

2.1 Applicable Documents

- [AD-1] IXO Mission Requirements Document,
- [AD-2] IXO Mirror Module Specification and Interface Requirement Document,
- [AD-3] IXO Mission analyses document,
- [AD-4] IXO Environment analyses document,
- [AD-5] ARIANE V users manual,
- [AD-6] Margin philosophy for science assessment studies

2.2 Reference Documents

- [RD-1] XEUS Mirror Spacecraft Definition Document, SCI-A/2006.013/AL, issue 1 revision 0, 26 April 2006,
- [RD-2] XEUS Detector Spacecraft Definition Document, SCI-A/2004/173-DL, issue 3 revision0, 20 January 2006,
- [RD-3] Constellation-X IMDC study report,
- [RD-4] XEUS Physics of the hot evolving universe, proposal to CV2015-2025, June 2007,
- [RD-5] IXO CDF report,
- [RD-6] IXO reference observation scenario,
- [RD-7] Requirements for the cooling chain for the XMS on IXO, SRE-PA/2009.022/

3 THE IXO MISSION

The Cosmic Vision 2015-2025 Call for Mission Proposals was issued by ESA in March 2007. Following this Call for Missions, five Medium-class missions and three Large-class missions have been recommended by the Space Science Advisory Committee (SSAC) for further assessments by ESA. The XEUS X-ray observatory proposal [RD-4] was initially selected as a candidate L-class mission for the Cosmic Vision programme. However, a Phase 0 study conducted at ESA demonstrated that the mission proposal was not feasible within the budget envelope of an ESA L-class mission.

A coordination group involving ESA, NASA and JAXA was established in spring 2008 with the intent of exploring a possible scenario towards a joint mission merging the European XEUS and U.S. Constellation-X efforts. The coordination group proposed to engage in a joint study of an International X-ray Observatory (IXO) concept, which will be the input to the U.S. decadal process and to the ESA selection for the Cosmic Vision Plan. The proposal for a joint ESA/JAXA/NASA study of an International X-ray Observatory was accepted at an ESA-NASA bilateral meeting on 2008, July 14, with JAXA concurrence.

The International X-Ray Observatory (IXO) is a facility-class mission that will address the leading astrophysical questions in the "hot universe" through its breakthrough capabilities in X-ray spectroscopy, imaging, timing, and polarimetry.

IXO will measure the spin of black holes, a fundamental property driven by galaxy formation and evolution for super-massive black holes, and by the nature of core collapse for stellar mass black holes. IXO will reveal the physics of accretion near the last stable orbit, measuring General Relativistic effects in the strong field limit.

For neutron stars, IXO will determine the mass-radius relationship, thereby constraining the equation of state and QCD models of matter at these densities. For neutron stars with ultra-high magnetic fields (magnetars), IXO's polarimeter will measure the predicted QED effects.

In galaxy clusters, IXO will measure the velocity structure, mass, and metallicity distribution of the dominant baryon component, the hot intra-cluster gas. Not only will this provide a deep understanding of evolution of large-scale structure, but samples of clusters at various redshifts provide important and independent constraints on the cosmological model and dark energy.

Extending away from clusters and groups is the Cosmic Web, where half of the baryons in the local universe are expected to reside, yet have not been detected. IXO will detect these missing baryons and it can test predictions for the formation and topology of the Cosmic Web.

Furthermore, IXO will yield insight into feedback mechanisms in the universe on many scales: through studies of supernova remnants, outflows in starburst galaxies, and AGNs across cosmic time.

Several of these and other science issues require a panchromatic approach. IXO covers the 0.1-40 keV energy range, complementing the capabilities of the next generation observatories, such as ALMA, LSST, JWST, and 30-m ground-based telescopes.

The performance requirements and the implementation constraints of the IXO mission are given in the IXO mission requirement document [AD-1].

Input elements to the IXO configuration include:

- A single large X-ray mirror assembly compatible with both pore optics and slumped glass technology,
- An extensible optical bench to reach $F=20$ to 25m and ways to maximise A_{eff} above 6 keV,

- a set of six Payload Instruments including a wide field imager (WFI), a high resolution non-dispersive spectrometer (XMS), an X-ray grating spectrometer (XGS) an X-ray Polarimeter (XPOL) a High-Energy X-ray Imager (HXI) and a High Time resolution Spectrometer (HTRS),
- The IXO concept must be compatible with both Ariane V and Atlas V 551 launchers.

A description of the mission scenario has been refined during a Concurrent Design Facility (CDF) study. The IXO CDF report [RD-5] describes the IXO spacecraft configuration that consists of a Mirror Assembly (MA), a Service Module (SVM), an Extendable Bench and an Instrument Module (IM).

The IXO mirror assembly integrates a large number of mirror modules built using a high density pore optics technology. A back-up technology to build these mirror modules is the thermally slumped glass plate technology.

The IXO instrument module accommodates the payload instruments which will be provided by institutes after an instrument Announcement of Opportunity (AO). The mirror assembly and the instrument module are connected by a mechanical structure that consists of a fixed structure carrying the service module and of a deployable bench.

The mission profile considers a single launch into an L2 halo orbit with an Ariane V or an Atlas V 551 launcher around 2020. In this L2 orbit it is possible to always have the same side of the spacecraft nominally pointing towards the Sun. However, to increase the instantaneous coverage of IXO, the S/C has been designed for a pitch angle of up to 20 degrees (see Figure 3-1). Thus at any point in time the IXO telescope can access a 40 degrees wedge at all ecliptic latitudes. In addition, the S/C is designed to enable a roll angle of up to +/-10 degrees, such that the observation conditions for XGS can be optimised with respect to avoiding off-axis sources.

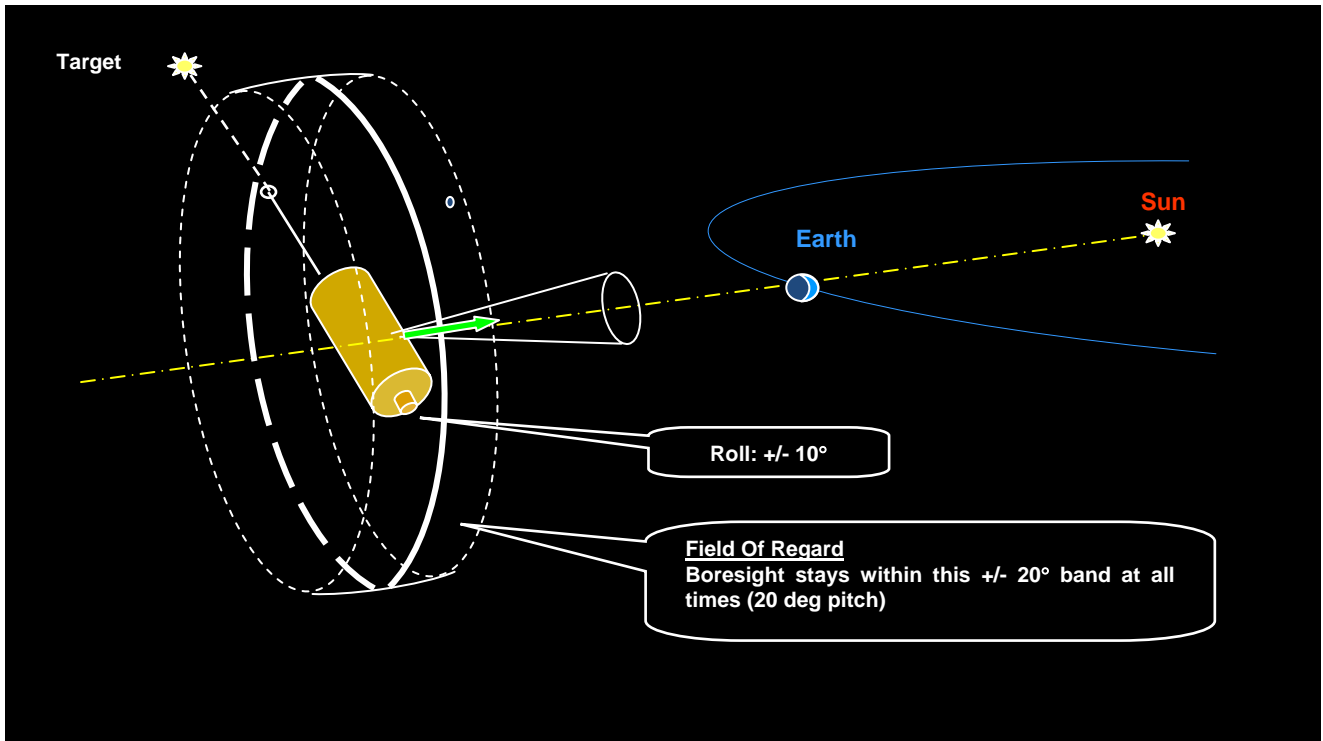


Figure 3-1: Sun Aspect Angle during observations.

4 SPACECRAFT REFERENCE COORDINATE SYSTEM

The Spacecraft Co-ordinate System is an axis reference frame physically attached to the spacecraft.

All reference frames shall be right-handed orthogonal triads.

The Geometrical Fixed Reference Frame shall be defined as in Table 4-1

Table 4-1: Geometrical Fixed Reference Frame

Item	Definition
Origin	In the geometric center of the mirror face in the direction of the telescope focal point
+X	Normal to the Z axis, pointing towards the sunshield
+Y	Axis that is completing the right-handed orthogonal triad ($Y = Z \times X$)
+Z	Along the boresight of the telescope pointing towards the mirror incoming photons

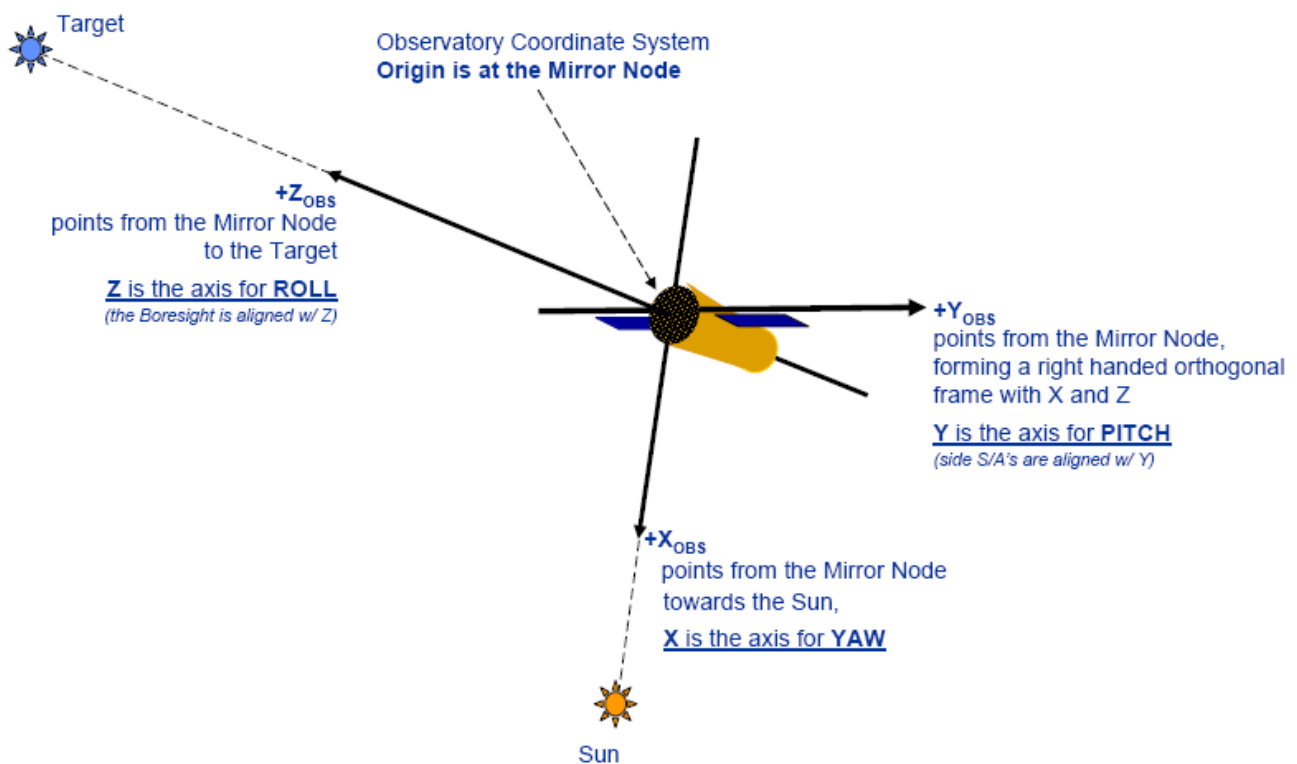


Figure 4-1: Spacecraft coordinate system

5 INTRODUCTION

This Payload Definition Document (PDD) is a compilation of the IXO reference payload requirements and of their related reference design. The PDD plays a key role in defining the resources required by the IXO instruments and in providing the information necessary to conduct the mission assessment study and the preliminary spacecraft design.

The model payload described in this document originates from the scientific objectives of the mission as spelled out in the associated Mission Requirements Document [AD-1]. Information on the reference payload has been provided by selected experts of the IXO Instrument Working Group. The initial descriptions were provided in the Instrument Working Group report and then used as a basis for the preliminary versions of the PDD in the framework of the formation-flying Xeus mission concept. After a first compilation, an internal study of the XEUS mission was carried out in the Concurrent Design Facility, but this concerned mainly the Mirror Spacecraft (MSC) elements, and where the Detector Spacecraft (DSC) was taken with a baseline of 3 core instruments and estimated resources, not subject to verification. As a consequence of the study of MSC sub-systems and the initial PDD, a DSC definition Document was produced [RD-2]. A study of a DSC version in the context of the Constellation-X project was carried out in the NASA GSFC Integrated Mission Design Center activity, and reported in [RD-3]. However this included mainly payload elements related to the NASA mission, and not representative of the XEUS payload. Subsequently, the XEUS Science Advisory Team prepared an updated science case in the context of submissions to the Cosmic Vision 2015- 2025 programme, and compared the science case with that of the NASA Con-X project with a view to internationalising and harmonizing the project. As a result, the XEUS Science Requirements Document was provided and the PDD revised to support a payload that fully met the required objectives. In the course of that activity, it was realized that a severe and possibly unsustainable mass growth in the DSC could occur. The early assessment showed that the previously identified payload resources were largely under-estimated, especially with respect to the growth of field of view requirements and spectral resolution requirements that drive the design and the resources of cryogenic instruments. These thermal issues were also found to have a major impact on system resources and spacecraft design, and had not been adequately researched. Therefore PDD version 3.1, based on refined inputs from the instrument experts, distinguished between 'core' instruments (WFI and NFI) and 'ancillary' instruments.

After selection for assessment study in the Cosmic Vision plan, and in preparation of the May-June 2008 CDF, the PDD underwent a thorough iteration by the instrument experts as well as by SRE-PA (Advanced Studies and Technology Preparation Division). During that review, the outcome of two parallel Payload Accommodation Studies as well as the XEUS proposal [RD-4] for CV2015-2025 were taken into consideration.

Since then the overall mission concept has been revised to reflect the needs of a possible international collaboration with NASA and JAXA. The current version of the PDD follows the results of an updated Mission requirements document [AD-1], assumes a 20-25m focal length telescope mounted on an extendible bench and incorporates a baseline payload consisting of 6 instruments and includes inputs from the November 2008 and March 2009 CDF studies.

6 PAYLOAD OVERVIEW

The Baseline Mission could be accomplished by an instrument complement comprising the following:

- Wide Field Imager [WFI]
- X-ray microcalorimeter spectrometer [XMS]
- X-ray Grating Spectrometer [XGS]
- High Time Resolution Spectrometer [HTRS]
- Hard X-ray Imager [HXI]
- X-ray Polarimeter [XPOL]

It should be noted that, although the WFI and HXI are listed separately, these two instruments are intimately linked as their sensors will be in close proximity of each other and co-aligned. Each instrument shall first be fabricated, tested and calibrated separately; however an integration of both instruments is foreseen to take place by one of the instrument teams, followed by integrated tests and calibrations. It will then be delivered as a single instrument to the project, reducing system level AIV requirements to that of a single instrument.

The WFI/HXI, XMS, HTRS and XPOL are mounted on a moveable platform and each can be positioned onto the optical axis to perform observations. The XGS camera is mounted off-axis and will be observing in parallel to any of the other instruments. A possible configuration is shown in Figure 6-1 and Figure 6-2.

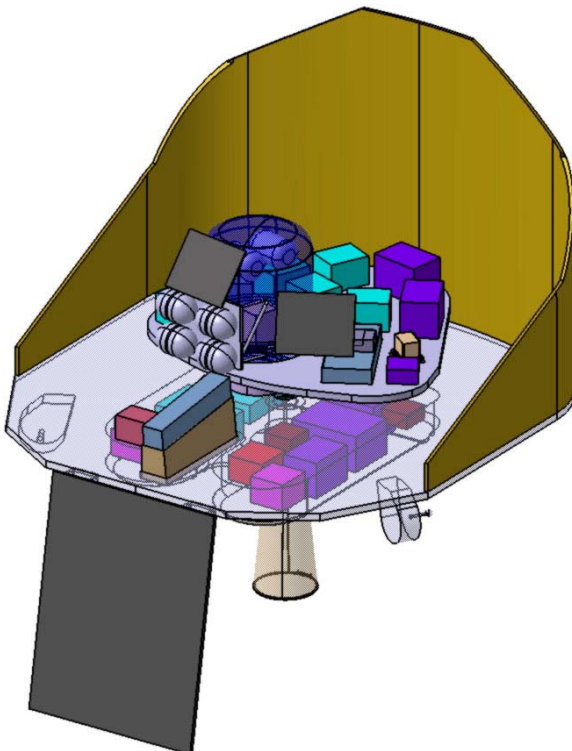


Figure 6-1: instrument platform 3-D view

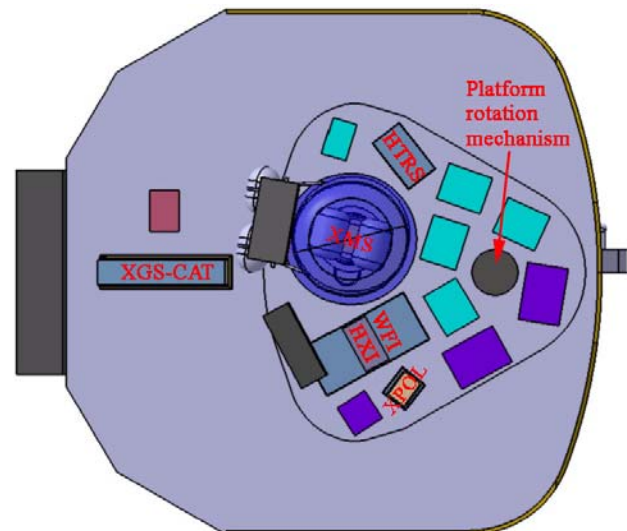


Figure 6-2: instrument platform showing distribution of the various instruments on the fixed and moveable platforms.

Concerning the XGS, there are currently two technologies being developed respectively based on critical angle transmission gratings (CAT) and Off-plane transmission gratings (OT). Both instrument concepts are detailed in this PDD, however the spacecraft system level studies have so far only considered the requirements of the CAT grating.

The XMS requires its detectors to be cooled in the mK range. In order to achieve this temperature, a number of coolers are required. Many different technical solutions exist to this problem and technology is available and is being further developed in Japan, Europe and the United States. Currently there is no firm decision on which alternative is best and various options are therefore described in the relevant section of this PDD. For the system level studies, we have considered the requirements of the 'European' redundant concept.

7 MISSION PROFILE & SCIENCE OPERATIONS - SUMMARY

The IXO mission comprises a folded spacecraft that carries an instrument module and a mirror assembly. The spacecraft is launched on either an Ariane 5 or Atlas 5 with a direct injection towards a large-amplitude orbit around L2. The Ariane launch is considered more constraining, both in payload capability as well as in terms of launch window constraints.

The orbit is designed to be eclipse-free in the transfer and for at least the mission lifetime of 5 years and does not require any deterministic manoeuvres. Correction manoeuvres are needed, however, to compensate the dispersion of the injection state vector due to the limited launcher accuracy, and thus to precisely target the spacecraft for the libration orbit around the Lagrange point. The details of the mission time line are determined by operational requirements rather than mission analysis considerations.

A framework of the time line can however be given here as the correction manoeuvres do require some scheduling. After the injection by the launcher there are two days needed for obtaining tracking data, which can also be used for initial commissioning. Two days after the injection a correction manoeuvre of less than 34 m s^{-1} (on a 99% confidence level) is performed. In addition 28 m s^{-1} have been allocated to allow a fixed launch orbit (one flight program on Ariane), simplifying the interface with the launch service provider. This combined day-2 manoeuvre can therefore be expected to be smaller than 62 m s^{-1} .

More tracking is needed after this first correction, which can again be performed in parallel with operational activities (commissioning). A second correction manoeuvre is scheduled for day 10 after the injection and has a size of less than 3 m s^{-1} .

The deployment of the telescope can take place after the day-10 manoeuvre, after which the spacecraft commissioning can be finalized.

Science Operations

The XGS being at a fixed location in the focal plane, this instrument can be used in parallel to any of the other instruments. The HXI is mounted directly behind the WFI and therefore shares the same optical axis. From an operational point of view, both instruments shall be operated together and can therefore be considered as a 'single' unit. The four instrument groups, XMS, WFI/HXI, HTRS and X-POL, will be mounted on a movable platform such that each can be located at the telescope's focus. Only one of these instrument configurations will be operational at a time for data taking. However internal calibration of another instrument for a limited period of time may take place while another unit is performing actual measurements. Furthermore, the pre-cooling chains of XMS will be permanently operated to maintain their operational temperature. Nominal operations will be performed from a stored pre-programmed sequence, the instrument configuration will be selected, operational modes enabled and data taking commences. Data will be stored to mass memory for downlink typically one TM session of 2-3 hours per day. The Payloads must automatically enter safe mode if necessary such as for high rate charged particle background conditions.

Subject to science team definition, observations will mostly have durations between 50ks to several days. TM communications windows are therefore not synchronous with observations. A number of critical science observations have been identified in which very bright sources will be observed for a short duration. This will be of order 10ks, and partly depends on availability of mass memory storage capability. These events are not expected to happen more than 5 times per year

Between observations the spacecraft will slew to the next pointing. During this period it is TBC if instruments will be on, off or in configuration for the next observation.

Earth Communications

Operations would be via a single ESA ground station and hence communications with the spacecraft would only be possible for circa 3 hours per day. Housekeeping telemetry will be prioritised for transmission over science data for safety reasons.

Part 2 Description of the Baseline Instruments

1 INTRODUCTION

In this part, the baseline design of each instrument is described and the corresponding resources, in terms of mass, envelope size, power and data rate are quantified. Such estimates play an important role in the context of the definition of the IXO mission as they strongly influence the spacecraft requirements and corresponding resources. Under- or over-estimating the required resources would in fact lead to inaccurate choices at system level, thus significantly increasing the development risks and/or the cost at completion.

Open issues, critical areas and the need for specific technology developments are also indicated for each instrument.

A summary of all baseline instruments is given in Table 1-1.

Table 1-1: Summary of Payload

Characteristic	WFI&HXI Combined		XMS	HTRS	XPOL	XGS ¹
	WFI	HXI				
Detector type	Si APS (DEPFET)	CdTe + Si strip detectors	Microcalorimeter/ TES	Silicon Drift Diodes (SDD)	Gas Pixel Detector	CCD
Mass (kg) excluding baffle and S/C provided radiators and including margin	83	33	389² 352³	30	11	6.7 + 43.8⁴
	116					
Peak Power (W) including DC/DC converters and including margin ⁵	283	61	1221² 1080³	165	61	115
	344					
Operating temp.	210 K	233 K	50 mK	253 K	283 K	183K
Cooling	Radiator	Radiator	Closed cycle coolers / ADR	Radiator	Peltier	Radiator
Detector Size (mm)	102.4 × 102.4	70 × 70	31.2 × 31.2	16.1 (Hexagonal)	15 × 15	786 × 24
Energy Range (keV)	0.1 – 15	10 – 40	0.3 – 10	0.3 – 10	2 – 10	0.3-1
Energy resolution (FWHM)	50 eV @ 282 eV 125 eV @ 6 keV	1 keV @ 40 keV	2.5 eV @ 6 keV	200 eV @ 6 keV	1200 eV @ 6 keV	E/ΔE > 3000
Pixel size (μm)	100	220	300 (& 600)	4000	50	24
Number of pixels in one dimension	1024	320 strips	40 (+ 32)	7	300	32768
Field of View (arcmin square)	17.6	12	2 (& 5.4)	2.8 (Hexagonal)	2.6	N/A
Unvignetted FOV (arcmin)	17.6 (diam)	12	5.4 (diam)	2.8 (diam)	2.6	N/A
Baffle length / Diameter (cm)	TBD/TBD	TBD/TBD	TBD/TBD	TBD/TBD	TBD/TBD	TBD/TBD

¹ Assuming the CAT grating option

² JAXA redundant cooler option

³ ESA CDF baseline cooler option

⁴ 6.7kg for both grating boxes, 43.8kg for the camera, does not include focussing mechanism

⁵ Also includes peak power required for filter operation

2 WIDE FIELD IMAGER (WFI)

2.1 Instrument Description

2.1.1 Introduction

The IXO wide field imager is an imaging X-ray spectrometer with a large field of view. The purpose of the WFI is to provide images in the energy band 0.1-15keV, simultaneously with spectrally and time resolved photon counting. The device consists of an array of DEPFET (Depleted p-channel FET) active pixels integrated onto a common silicon bulk. Based on the principle of sideways depletion, these devices combine the advantages of sideways depleted silicon detectors with new benefits arising from the innovative DEPFET concept.

The DEPFET is a combined detector-amplifier structure. Every pixel consists of a p-channel MOSFET, which is integrated onto a fully depleted silicon bulk. By means of the sideways depletion principle, the bulk is fully depleted. With the help of an additional deep-n implantation, a potential minimum for electrons, the so-called internal gate, is generated and laterally constrained to the region below the transistor channel. Incident X-rays interact with the bulk material, and the resulting charge is separated; while holes drift to the most nearby p-contact, the electrons are collected in the internal gate of the adjacent pixels. There, their presence influences the conductivity of the MOSFET channel; sensing the increase of channel conductivity of the MOSFET is therefore a measure of the quantity of collected charge.

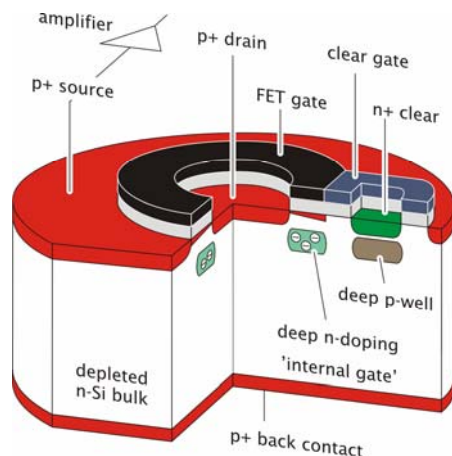


Figure 2-1: Cutaway display of a circular MOS-type DEPFET pixel as implemented as prototype for IXO. The bulk thickness is 450 μm .

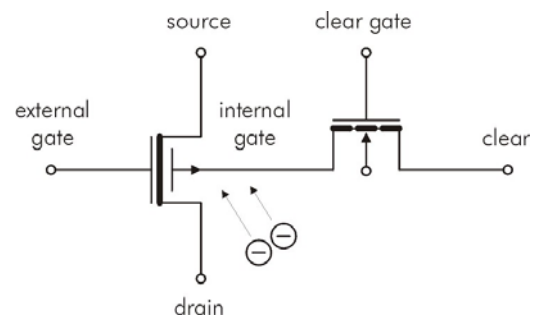


Figure 2-2: Schematic representation of a DEPMOSFET pixel as a combination of a dual-gate p-channel MOSFET and the parasitic n-channel ClearFET structure.

As the internal gate persists regardless of the presence of a transistor current, the pixel can be turned off during a certain exposure time, and only turned on for readout. The amount of integrated charge can then be sensed by turning on the transistor current, measuring the conductivity, removing the charge completely by a nearby parasitic n-channel MOSFET, the so-called ClearFET, and measuring the conductivity again. Considering a linear response of the channel conductivity to charge in the internal gate, calculating the difference is a measurement of the integrated charge.

The prototype devices designed for IXO have circular transistor geometry. A cutaway of a DEPMOSFET pixel and its schematic circuit representation are shown in Figure 2-1 and Figure 2-2. Figure 2-3 and Figure 2-4 show microscope photographs of a fully processed matrix pixel and of a pixel sensor.

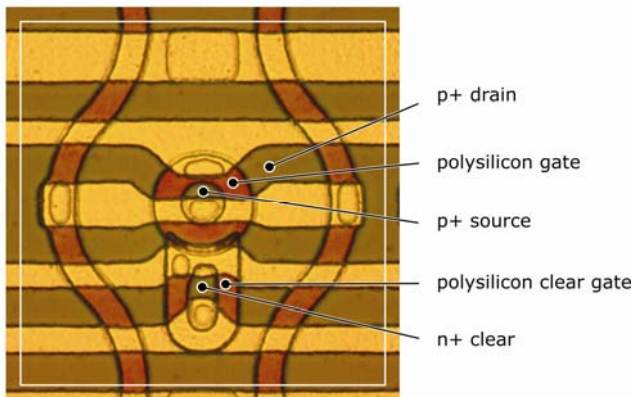


Figure 2-3: Microphotograph of a 75 μm pixel with a circular DEPFET in the centre and the ClearFET structure below. At the periphery, column-separating structures are visible. The gate length of the DEPFET is $< 5 \mu\text{m}$, the gate width is $\sim 45 \mu\text{m}$.

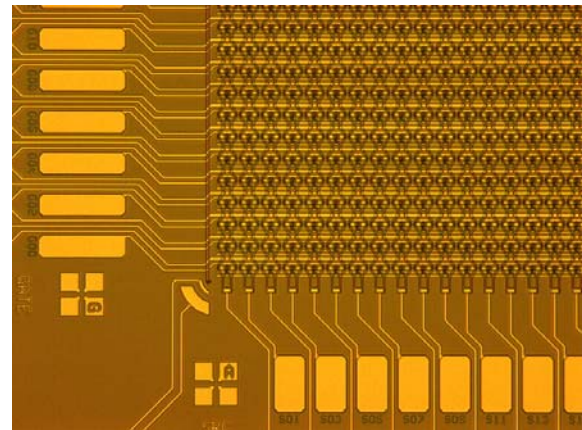


Figure 2-4: Corner of a 64 x 64 pixel sensor composed of DEPFETs as shown in figure 1.3. The bright rectangles are bond pads for the connection to readout and control chips.

Various options exist for the integration of a matrix of DEPMOSFET pixels. Basically, every pixel could be individually addressed and read out at arbitrary times. For the sake of speed and simplicity and considering the accommodation of the HXI behind the WFI, a simple interconnection scheme was chosen, which provides for a row-wise readout in a “rolling shutter” like readout mode (Figure 2-5). In spite of its simplicity, this mode still allows for a large variety of useful readout modes.

Each X-ray photon is measured by detection in a single pixel, of photoelectrons liberated on X-ray absorption. The pixel size is smaller than the optics resolution element, giving good spatial resolution. The energy resolution is limited by silicon photoelectron statistics and timing resolution according to readout speed. The field of view is about 18 arcmin (active detector area is $\sim 100 \times 100 \text{ mm}^2$).

The benefits taken from using a DEPFET based sensor are listed below.

- The DEPFET is a fully depleted device, the full Wafer thickness of 450 micron helps to increase the quantum efficiency in the range around 15 keV.
- DEPFET based devices are sideways depleted devices, which provides for an unobstructed, homogeneous entrance window with 100% fill factor and excellent QE in the low energy range.
- The local charge storage capability allows for a large variety of flexible readout modes, which allow observing objects in a large range of brightness without being limited by pileup.
- The very low readout capacitance of the DEPFET allows for very low readout noise and thus excellent energy resolution even at high speed.
- The sensor is area efficient compared to CCD based sensors, as no frame store area is needed.
- The sensor has an extremely low deadtime compared to CCD based sensors, as no charge transfer is needed.
- The sensor is radiation hard and power efficient, as the pixels are turned on only during readout.

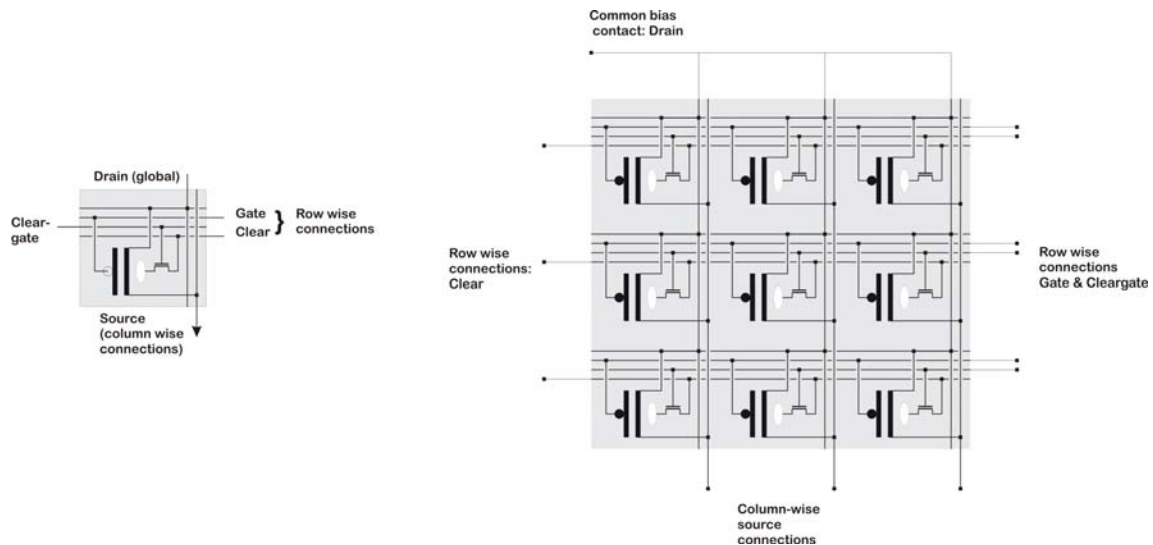


Figure 2-5: Matrix arrangement of DEPMOSFET pixels to form a large area focal plane detector. Row-wise connections of Gate, Clear, and Cleargate contacts allows for simultaneous addressing and readout of all pixels within one row. Column-wise connection of e.g. the sources allows for column-parallel amplification and filtering of the pixel signals. One bias contact, usually the drain, is common for all pixels.

2.1.2 Instrument performance specifications

According to the preliminary Science requirements, the following scientific objectives are to be met by the WFI:

- Detection, location and broad band colours of faint AGN counterparts down to a flux level of few 10^{-18} ergs cm^{-2} s^{-1} .
- Spatially resolved spectra of extended objects
- Spectral investigation of moderately bright point sources to time resolution \sim millisecond

The resulting performance requirements derived from these objectives have been listed in Table 2-1. The numbers given are the current baseline, wherever changes are possible, the decision drivers are indicated. Main open issues are the pixel size and array geometry, which are driven by the PSF size of the mirrors. Currently, a pixel size of $\sim 100\mu\text{m}$ is proposed. For this size, an array of about 1024×1024 pixels can still be integrated monolithically.

Table 2-1: Preliminary IXO-WFI performance requirements

Requirement	Specification	Comments
Device dimensions		
Area	10 x 10 cm ²	Integrated on monolithic 6" wafer
Thickness	450 μm	For good QE at high energies
Pixel size	100 x 100 μm ²	PSF size incl oversampling
Array dimension	1024 x 1024	Largest array dimension suitable for monolithic integration
Spectroscopy		
Energy resolution		
@ Mn-Kα 5.9 keV	125 eV FWHM	
@ C-Kα 282 eV	50 eV FWHM	
Readout noise	3-5 e ⁻ ENC	
Readout timing		
Readout time / frame	1.28 - 2.56 ms	Depends on FE performance
Processing time / row	2.5 – 4 μs	
Raw data rate	1.6 GByte / s	Final data rate depends on pre-processing.
Quantum efficiency		
Fill factor	100 %	No dead areas
QE @ C-Kα (282 eV)	33 %	Depending on implementation of filter (70nm Al Filter + dielectric layer system assumed as described in Section 2.6)
QE @ Si-Kα (1.74 keV)	93 %	
QE @ Cu-Kα (8.05 keV)	100 %	
QE @ 10 keV	96 %	
QE @ 20 keV	35 %	

2.1.3 Instrument configuration

Figure 2-6 shows an overview over the instrument configuration. The overall payload is divided into two compartments, the camera head and the electronics boxes. While the camera head is connected to the radiator and designed to keep the APS sensor at operating temperature, the thermal management requirements for the electronics boxes are much less strict. In the following, the various compartments of the instrument are discussed.

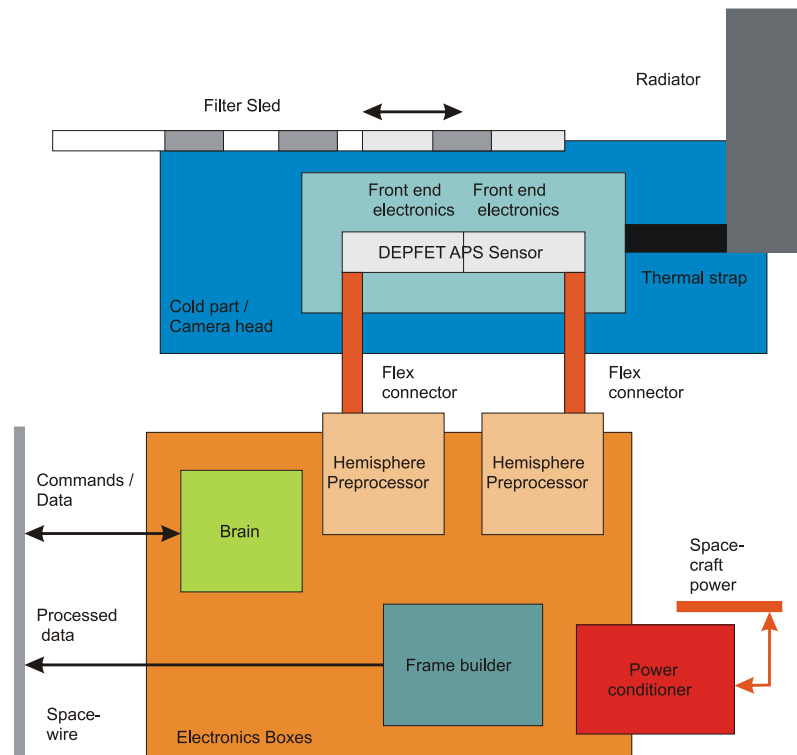


Figure 2-6: Overview over the instrument configuration. The FPA is divided into two units: The camera head and the Electronics Box(es). While the Camera head, which is mounted to the payload fixture, has to be operated at the required sensor temperature, the temperature of the components within the Electronics boxes is at Spacecraft ambient temperature. The two Hemisphere Preprocessor Boxes are situated in close proximity to the FPA, connected to the FPA by flexleads. Location of the rest of the electronics boxes is uncritical, as they are connected by a cable harness of up to 4 m length. A filter sled is part of the design. Suitable baffling has to be provided in front of the filter sled.

2.1.3.1 Filter sled / baffle

A baffle with suitable geometry is assumed to be present in front of the access point to the camera head for stray-light shielding and diffuse background rejection ($1/e$ at 28 keV). Access to the camera head with the APS is controlled by the filter sled. The details of the mechanism are still TBD. The filter sled can e.g. be implemented as a panel with different positions on it that can be moved into the optical field of view with a motor. Although the system is likely not to be launched in an evacuated state, the filter sled has a closed position to protect the APS sensor, e.g. during periods with excessive radiation. This position also serves as instrument door and for background observations. Safety operations may be required autonomously or via ground control to prevent excessive charged particle fluence (solar flare or local magnetospheric storms), micrometeorite protection or spacecraft attitude loss.

In total, the filter sled will have 4 positions: CLOSED, OPEN, FILTER and CALIBRATION. The FILTER positions may be selected per observation according to the necessity for additional optical light-blocking. For the FILTER position, a filter with transmissions similar to the XMM filter configurations will allow observations in case of high optical background. As a very thin optical filter is already integrated on the sensor entrance window, observations in OPEN position, where the incident photons have a clear path, already have a certain degree of optical background suppression. In CALIBRATION position, calibration

sources are used to expose both the WFI and HXI sensors to radiation of known energy. The CALIBRATION position will be equipped with 2 sources, Fe55 with an Al fluorescence target for the WFI and Am241 for the HXI, thus providing lines from 1.5 keV to 59 keV.

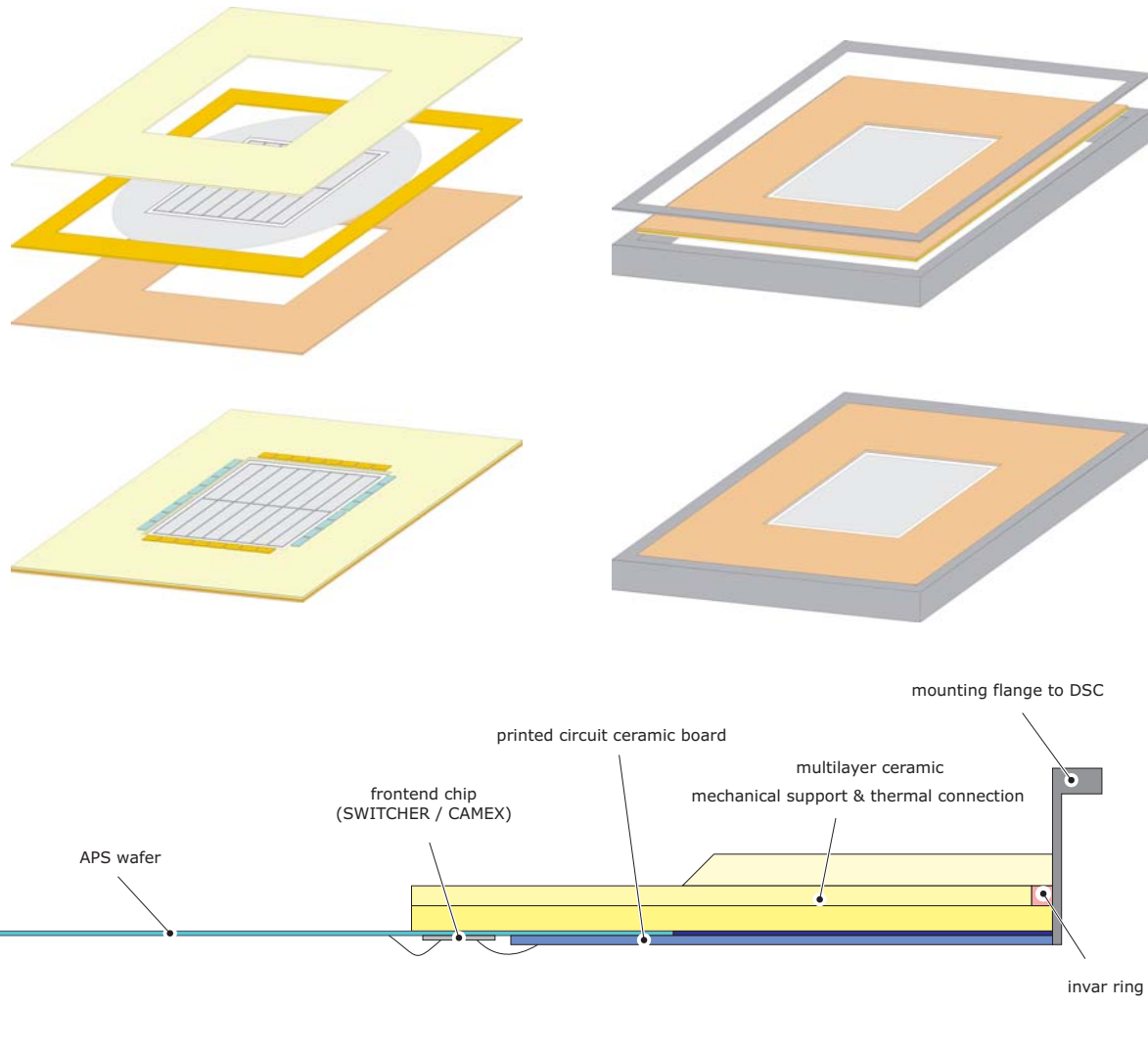


Figure 2-7: View and cross-cut through the preliminary mechanical design of the camera head. The wafer-scale APS device is integrated within a suspension-mount type assembly consisting of several multilayer ceramic boards also holding the front end electronics within an invar fixture, providing the interface to the radiator. The camera head is rectangular; the width of the camera head is 32 cm, the length still needs to be determined depending on the actual system design; a value of > 60 cm is likely. The height of the invar mounting structure is 22 mm. Attached are the Flexleads interfacing to the peripheral electronics.

2.1.3.2 Camera head

The camera head holds the FPA and its front end electronics, provides the required structural stability and the required cooling resources. The Camera head mount is connected to the radiator via the invar mounting frame. The camera head will also include a passive radiation shield consisting of a Cu sheet.

A conceptual drawing of the mechanical layout of the detector head is provided in Figure 2-7. The central gray square represents the APS. It is mounted onto a multi-layer ceramic board that contains the front end electronics. The thin assembly is mounted in a suspension mount type arrangement in a rectangular detector body frame which also provides the interface to the radiator and the spacecrafts payload fixture. The Hard X-ray camera resides on a similar assembly below the WFI, and within an extension of the frame. Several challenges have been identified with such a configuration and need to be resolved. The filter sled will be mounted in front of the frame. The cross-section is also shown in Figure 2-7. A filter between the APS and the potential position of the HXI blocks fluorescence radiation from the HXI and helps to decouple the systems thermally.

2.1.3.3 Radiator

The cooling of the FPA is intended to be performed by one single passive radiator. The thermal connection between radiator and camera head can be made either by heatpipes or by passive thermal straps. The temperature of the FPA will be kept at operating conditions by heater elements controlled by instrument housekeeping.

The radiator design needs to be investigated further within the overall spacecraft accommodation, and could feasibly be implemented as a flat panel. Due to the very different thermal requirements of WFI and HXI, esp. the HXI's need to be thermally cycled to positive temperatures, the thermal management concepts should be regarded separately, and the systems should be decoupled thermally as far as possible.

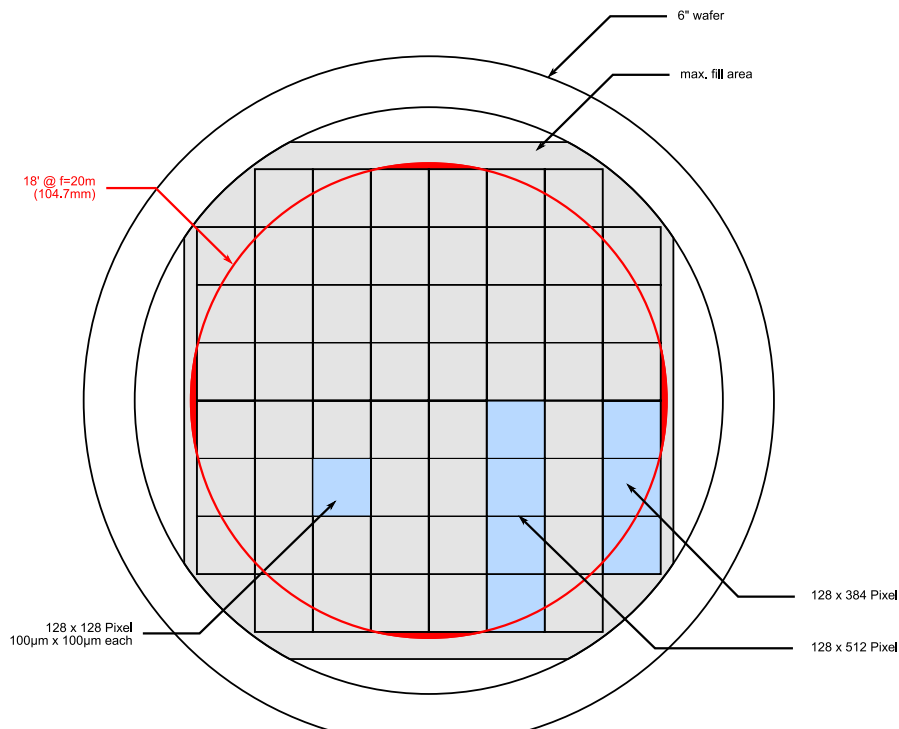


Figure 2-8: APS wafer. The sensor is integrated monolithically on a single 6' wafer. The 1024 x 1024 pixels are organized in two “hemispheres” and a total number of 16 sectors, 8 per hemisphere, of 128 x 512 pixels each. The baseline design foresees a pixel size of 100 x 100 μm^2 . In order to facilitate monolithical integration onto a 6 inch wafer, an option is being evaluated, in which one 1282 pixel sector per corner is left free. The resulting edge length of the sensor array of 102.4 mm defines a circular FoV of approximately 17.6 arcmin (at a focal length of 20 m). Assuming a nominal circular FoV of 18 arcmin (red circle), an area of 0.16 % at the extreme edges of the FoV is not covered (red area).

2.1.3.4 APS sensor

The baseline design assumes a pixel size of $100 \times 100 \mu\text{m}^2$ in order to provide a modest oversampling of the optics' Point Spread Function (PSF). With a 20 m focal length, and a 1024×1024 pixels organization (see Figure 2-8) the field of view is approximately 18 arcmin square. However, as the 18 arcmin diameter of the circular nominal FoV corresponds to 10.47 cm at 20 m focal length, whereas the quadratic WFI FPA has an edge length of 10.24 cm, approximately 0.16 % of the area of the nominal FoV is not covered (see Figure 2-8). Note that present limitations to wafer sizes (6 inch) lead to a preferred design with a $10.2 \times 10.2 \text{ cm}^2$ format.

The sensor pixels are organized in two hemispheres of 1024×512 pixels each, which can be controlled and read out redundantly. Moreover, each hemisphere is divided into 8 sectors of 128×512 pixels. These divisions are purely electrical and do not affect the entrance window, which stays homogeneous and unobstructed. However, the demonstration of representative matrix operation still has to be completed; prototype devices of 256×256 pixels have been produced as well as devices with 128×512 pixels, corresponding to the size of a full sector.

A silicon wafer thickness of $450 \mu\text{m}$ defines the detection efficiency at high energies (97 % at 10 keV). The detector entrance window is located on the opposite side of the wafer from the pixel structure, to ensure a minimum dead layer, allowing good low energy detection efficiency. It may have an integrated aluminium light shield deposited on the surface to block light from medium brightness targets. Currently, an entrance window configuration featuring a Silicon Nitride / Oxide layer system together with an Aluminium layer providing attenuation in the optical of $\sim 10^5$ and ~ 100 in the UV range is planned. For observations in presence of even brighter optical background sources, an additional filter with larger attenuation is available on the filter sled.

2.1.3.5 Front end electronics

The WFI FPA requires two different frontend ASIC devices (Figure 2-9): The so-called Control Front End (CFE) and the Analog Front End (AFE). Both frontends are present once for both hemispheres. The AFE ASIC is a member of the CAMEX family, a VLSI low-noise multichannel analogue signal amplifier/shaper circuit with integrated sequencer and serial analogue output. Each IC has 128 channels, one amplifier channel is required for every sensor column, and the signals of 64 channels are multiplexed on one output readout node; this yields one CAMEX and two analogue readout nodes per sector. Prototype ICs in combination with DEPFET Active Pixel Sensors (Figure 2-10) have already demonstrated that Fano-limited energy resolution over much of the energy range ($\sim 100 \text{ eV}$ FWHM) can be achieved.

The CFE ASIC is a derivate of the SWITCHER family. It consists of 128 channels with two output ports, each of which can be toggled between two output values. The SWITCHER controls the Clear, Cleargate and Gate terminals of the rows within the matrix. Only one row may be selected at a time, the sequence of rows, however, is controlled by an internal sequencer with in-flight programming capability. As three voltages need to be controlled to operate a row, two SWITCHER ICs are required to operate 128 rows, and 8 Switchers to operate all rows of a hemisphere, as shown in Figure 2-9.

The overall configuration on the FPA is shown schematically in Figure 2-11. The division of the sensor into two hemispheres is reflected in the redundant interconnection of the control signals and supply voltages for the hemisphere ICs. The hemispheres and sectors are named as indicated in the figure. The supplies for the Sensor IC itself, however, can not be made redundant, as the substrate is common and the hemispheres are designed to have a common backside contact in order to maintain a fill factor of 100 %.



Figure 2-9: Front end connection to the sensor. Each row of pixels requires 3 Switcher ports, and each column one CAMEX channel. The row connections are made to the respective SWITCHER devices at the left (Clear) and the right (Gate, Cleargate) respectively. A total number of 8 SWITCHER ICs is needed to operate one sensor hemisphere. The CAMEX IC has 128 channels, and every 64 channels are multiplexed to one serial readout node. This means 1 CAMEX and two readout nodes per sector.

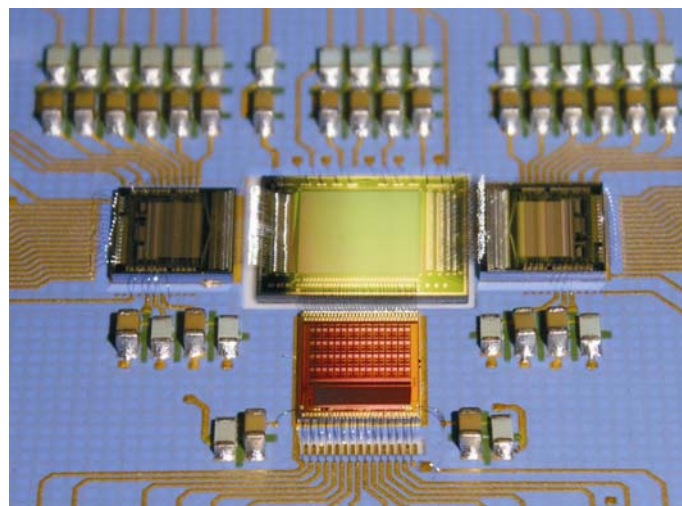


Figure 2-10: Photograph of a DEPFET APS hybrid with a 64 x 64 prototype sensor chip in the centre, SWITCHER control chips for readout/reset selection of one pixel row (left and right), and the 64-channel CAMEX readout chip at the bottom.

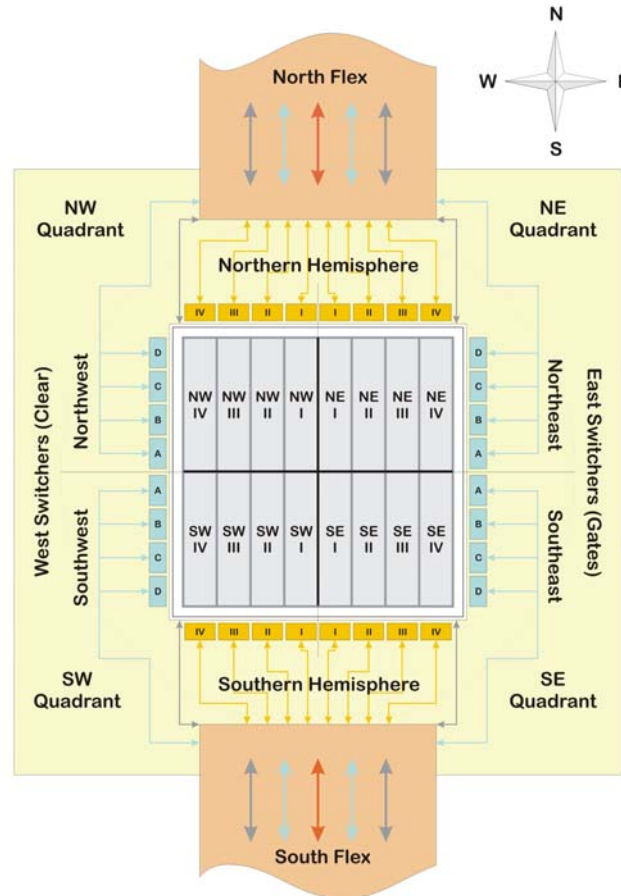


Figure 2-11: Overview of the FPA configuration. The sensor is divided into two hemispheres (“North” and “South”) with redundant frontends and connections to the readout electronics. Clear Switchers are located at the left (“West”) and the Gate Switchers at the right (“East”).

2.1.3.6 Flex connectors

The flex leads connect the Camera head with the Hemisphere Pre-processors (HPP). They carry all control and output signals as well as the supply and bias voltages. A width of approximately 10 cm and an overall pin count (including redundancies) of 156 has been estimated per flex. The flex itself consists of a flexible Kapton/copper based electrical interconnection, customized in sections for the respective kind of signal to be carried. The length of the flex leads depends on the overall design of the focal plane instrumentation. In no case the length of the flex leads should exceed a value of ~20 cm,

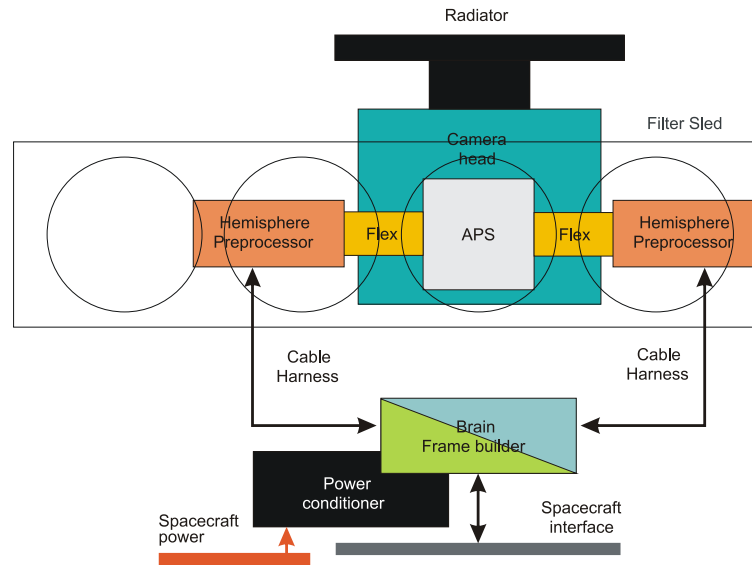


Figure 2-12: First sketch of the WFI compartments arrangement. The Modules requiring access to the spacewire interfaces are located in the frame builder / brain box in proximity to the power conditioner units. The hemisphere pre-processors are arranged symmetrically to the APS to ease access with the flex. The filter sled is located in front of the APS (greyed out).

2.1.3.7 Electronics boxes

The current concept foresees a total number of three types of electronic boxes of different complexity. The cards requiring spacecraft interfacing are combined in the brain / frame builder box. Two redundant units of each type are present in this box, connected via a backplane. Each hemisphere has its own hemisphere pre-processor box. Communication of modules within the hemisphere pre-processors takes place via a backplane, connection with the brain / frame builder module requires dedicated cable harness. Thermal requirements of the electronics boxes are less strict than for the APS, as their temperature can remain at spacecraft ambient. The power conditioner formats the spacecraft provided voltages. The instrument is made up of a total number of 5 boxes: The Brain/Frame Builder Box, two redundant Power Conditioners, and two Hemisphere Pre-processors.

2.1.3.8 Hemisphere pre-processors (HPP)

The serial analog data from the CAMEX ICs is digitized by one ADC each. As every CAMEX has 2 serial outputs, one hemisphere requires a total number of 16 ADCs. The digitization takes place in the so-called ADC clusters, four of which are required for one hemisphere. An ADC cluster is a card hosting 4 ADCs and one FPGA. The FPGA synchronizes the data and performs simple preprocessing tasks that can be conducted serially. The output data is then transferred to the framelet builder, which collects all data from the ADC clusters and performs the first step of pattern recognition as a precondition for further data reduction. The HPP is connected to the camera head by a short (< 20 cm) flexlead. The HPP contains suitable drivers to facilitate a long cable connection (< 4 m) to the Frame Builder.

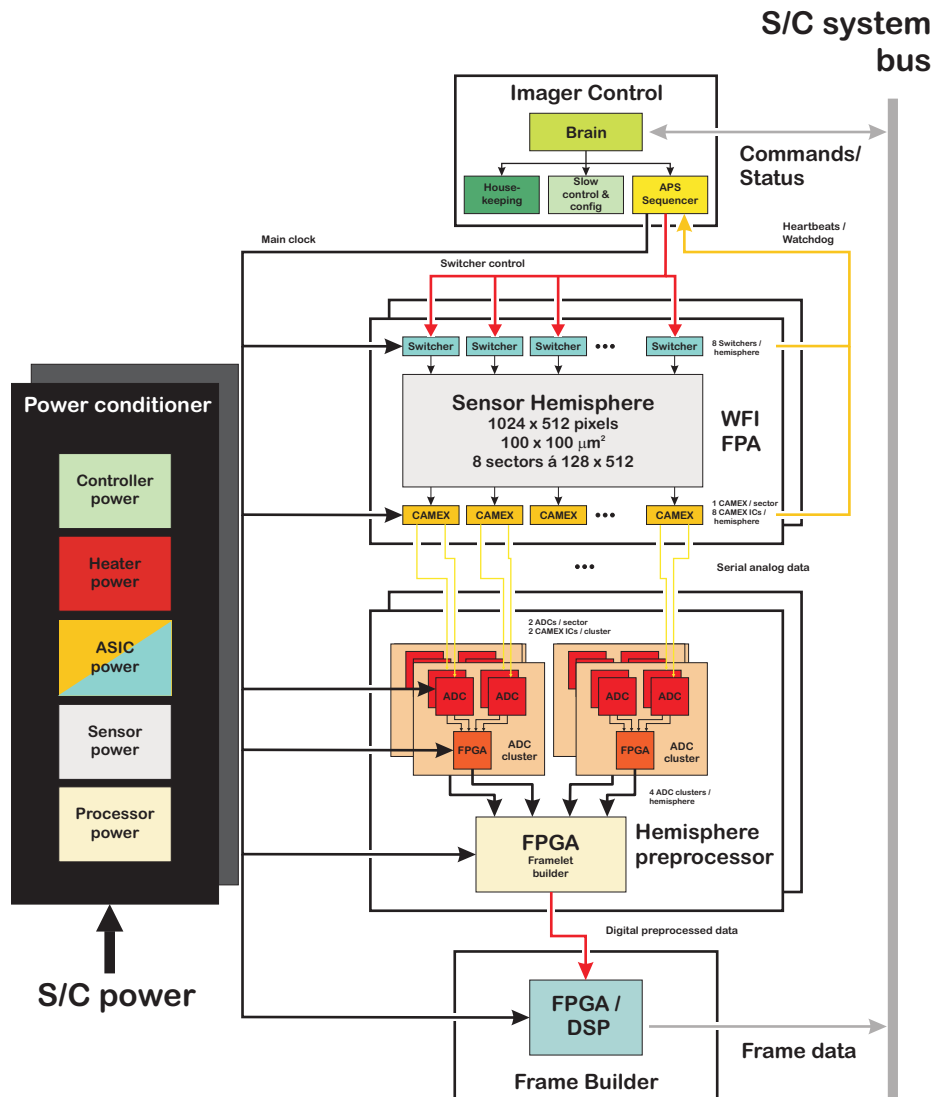


Figure 2-13: Overview over the instrument fast data flow. The fast APS sequencer provides control signals for the AFE and CFE and configures and synchronizes digitization and pre-processing of the data in the various downstream modules. In addition, correct functioning of the APS is controlled using watchdog circuitry on the FE heartbeats.

2.1.3.9 Frame builder

The data from the hemisphere pre-processors is then consolidated in the Frame builder, which detects and recombines photon patterns in the pre-processed data also at the inter-hemisphere border, performs further corrections to the data and data compression for telemetry, before the data is handed to the S/C interface for telemetry.

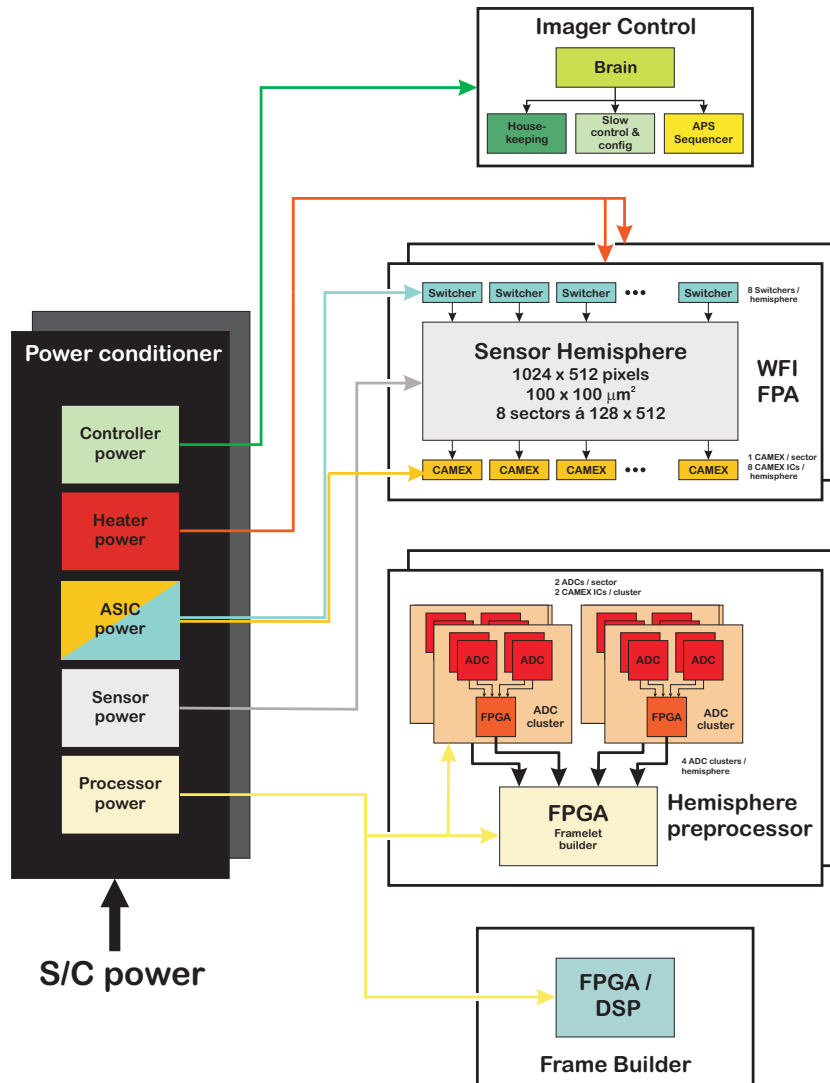


Figure 2-14: The power conditioner generates the supplies for the WFI subsystems from the S/C power. All currents can be monitored via housekeeping. All the voltages are commandable via slow control; some of the voltages are also adjustable within a certain predefined range.

2.1.3.10 Power conditioner

The power conditioners generate the required power for the various WFI subsystems from the S/C provided supplies. In addition, it switches power supplies on demand. Hereby, it has to be distinguished between adjustable voltages and commandable voltages. Commandable voltages can be commanded in states “on” and “off”, while adjustable voltages can also be adjusted in a certain range, which is important to e.g. compensate radiation damage effects in oxides. All voltage channels can be read back via slow control for housekeeping purposes.

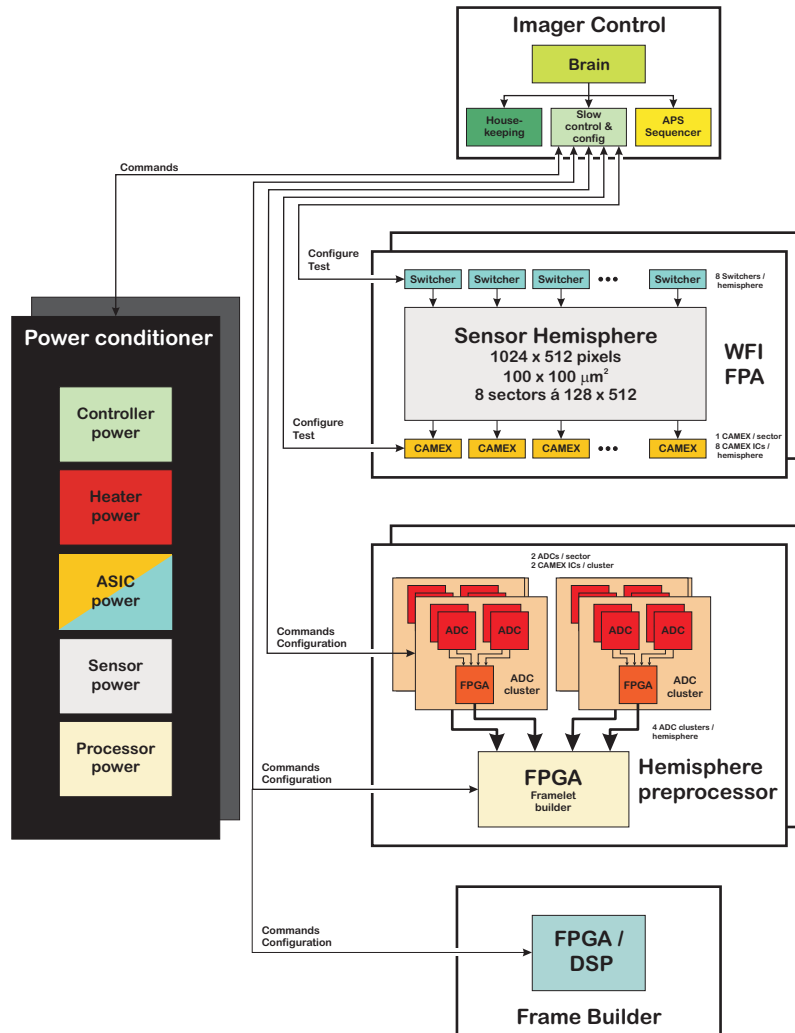


Figure 2-15: Overview over the instruments slow control chains. The slow control configures all the units and prepares the system for the requested data acquisition modes. The power conditioner is controlled via slow control, and many of the systems test features are initialized and used with the slow control.

2.1.3.11 Brain

The brain module contains three control blocks for the WFI. The fast APS sequencer drives the entire data acquisition chain (see Figure 2-13). It distributes all fast control signals to the front end electronics and also synchronizes the pre-processor modules via one single fast clock driving the entire data acquisition chain. In addition, it hosts the watchdog timer function, which is responsible for the supervision of the heartbeat signals from the various ICs, which is a continuous health check of the acquisition state of the system.

The slow control & config block (see Figure 2-15) is responsible for configuration and synchronization of the respective operation state of the system, voltage setting, configuration of ICs and pre-processor stages and frame builder via a serial 3 or 4 wire interfaces. As e.g. the selection of the ROIs on the sensor can be changed on-the-fly, the slow control path is separated from the fast data acquisition and can be operated

simultaneously. The slow control also controls the filter sled. The term slow control is, by the way, a traditional term, as the data rate and the time required for command execution is quite fast. Finally, most of the systems test facilities are configured and operated using the slow control interface. The housekeeping stage is responsible for all monitoring functions; temperature, currents etc. The housekeeping circuit is responsible for the temperature control by controlling the power drawn by the heaters. This is done via a slow serial interface, as most of these functions are not time critical.

2.1.3.12 Instrument configuration overview

An overview about the most important system components, the component count and the distribution of the respective tasks is shown in Figure 2-16. The filter sled control and the heaters for FPA temperature control are not shown in this figure.

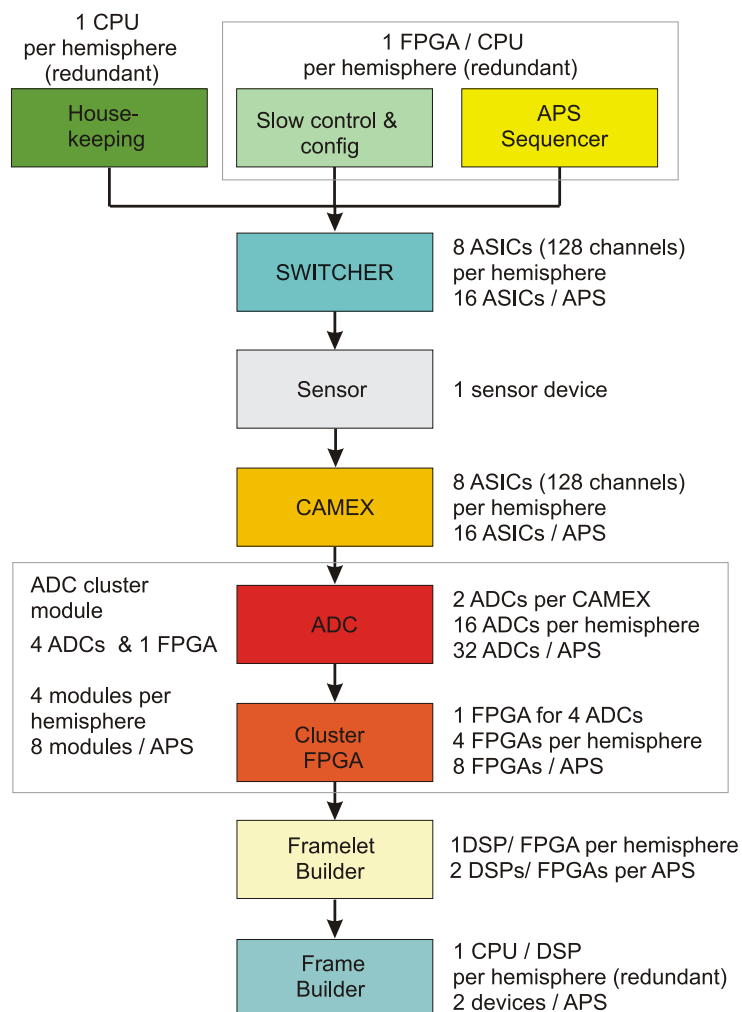


Figure 2-16: Overview over the instrument configuration. Shown are the data flow, the respective stages and the required component count and the respective assignment of tasks power conditioner units. The hemisphere pre-processors are arranged symmetrically to the APS to ease access with the flex. The units required by the filter sled are not shown.

2.1.4 Instrument optical design - filters

2.1.4.1 Baffle

The first requirement is that the instrument FOV has free and unobstructed view to the rear aperture of the mirror in case the filter sled is in *open* position. Secondly, the entire sensitive area of $\sim 10 \times 10 \text{ cm}^2$ must not be loaded with optical photons or diffuse X-ray background from the sky. To shield these background sources, a baffle is required. Suitable internal baffling outside the nominal circular FOV of 18 arcmin will be provided internally. As the minimum optical attenuation of the integrated filter is aimed to be 10^5 , a total photon rate of 10^{12} photons per square centimeter and second leads to one photon per pixel and frame for the targeted frame rate of 1 kFrame/s. This leads to a tolerable deterioration of energy resolution. Thus, the requirement of the optical baffling is to reduce the optical photon flux to a level of 10^{12} photons per square centimeter and second on the detector surface (i.e. behind the mirrors). In case of the X-ray background, the main requirement on the baffle is that the diffuse X-ray background should be reduced to a level of 1×10^{-3} photons per square centimeters and second in the energy range 0.2 – 20 keV, which should not be exceeded. In this case, the instrument can operate background limited.

2.1.4.2 Filters

For the WFI, an Al-filter together with an Silicon Oxide / Silicon Nitride layer system is placed directly on the entrance window of the focal plane detector, which would block IR/VIS/UV light to a level sufficient for most observations without deterioration of the low energy QE. The envisaged thickness values of the respective layers achieve attenuation in the optical of $\sim 10^5$ and 100 in the UV range. The current baseline is 70 nm Al on top of 35 nm SiN and 35 nm SiO. An additional filter on the filter sled allows for observations in presence of varying optical background. The FILTER position may be selected per observation according to the necessity for additional optical light-blocking. For the FILTER position, a filter with transmission similar to the XMM filter configurations will allow observations in case of high optical background. The current baseline for this filter is 100 nm Al on top of 300 nm PP. A detailed assessment is underway.

Stray light paths to the detector array, other than along the line of sight, should also be avoided. The filter sizes are expected to be only slightly larger than the detector sensitive area.

Table 2-2: Performance of IXO-WFI Filter positions as expected from XMM filter configuration.

Filter position	QE @ 282 eV (C-K α)	QE @ 1.74 keV (Si-K α)	QE @ 8.05 keV (Cu-K α)	QE @ 10 keV	QE @ 20 keV
CLEAR	33 %	93 %	100 %	96 %	35 %
FILTER	6 %	84 %	100 %	96 %	35 %

2.1.5 Instrument units' mechanical design and dimensions

At the present state of instrument development, no detailed mechanical design is available. Instead, estimation values of the envelope sizes of the respective components will be given as a basis for design evaluation on mission level. A summary containing the instrument units' masses and dimensions can be found in Table 2-8.

2.1.5.1 Component sizes

The focal plane assembly including cold finger, APS sensor body, detector body and shielding would have a volume of about $32 \times 32 \times 13 \text{ cm}^3$ (including Flex Brackets and HXI). One Hemisphere Pre-processor would have a volume of about $35 \times 25 \times 20 \text{ cm}^3$. Two devices are needed for the instrument, one for each hemisphere). The frame builder unit and imager control unit share a common box with a volume of $35 \times 40 \times 20 \text{ cm}^3$. The power conditioning unit has a volume of $35 \times 25 \times 20 \text{ cm}^3$. Current estimates of the masses and sizes of the respective components are listed in Table 2-7, a schematic overview of relative locations can be found in Figure 2-24.

2.1.6 Mechanisms

The WFI will most probably not be launched with the experiment body in vacuum conditions. Thus, a vacuum suitable instrument door is not required. Contamination is prevented prior to launch by purging and environmental contamination control. In addition, the FPA is protected during launch by the filter sled in its closed position. If the arrangement of the instruments in the focal plane permits, a circular eccentric filter wheel could also be considered.

The filter sled can, for instance, be made as a panel with different filter positions on it, oriented perpendicularly to the movement direction of the Moveable Instrument Platform (MIP). This is also its direction of movement. Its respective positions can be moved into the optical field of view with a motor. The filter sled position may be selected per observation according to necessity for additional optical light-blocking, for calibration source deployment or for safety. Safety operations may be required autonomously or via ground control to prevent excessive charged particle flux (solar flare or local magnetospheric storms), micrometeorite protection or spacecraft attitude loss. The filter sled is foreseen to have 4 positions; an open position in which incident photons have a clear path; a closed position for shielding against excessive radiation flux, for checking background noise and for protection during launch and ground testing; a calibration position (^{55}Fe and ^{241}Am , tbc by HXI); and a light blocking filter for high optical background observations.

2.1.7 Instrument units' thermal design

The most critical temperature for the WFI is the temperature on the focal plane detector. Currently, no detailed system design exists. Figure 2-17 shows a preliminary thermal schematic. A homogeneous temperature has to be achieved over the whole area to keep the leakage current contributions to the system noise on a level identical for all pixels. Additionally, the temperature of the AFE ICs has to be kept at the same level for all ICs. Figure 2-6 shows the concept of the focal plane assembly.

The wafer (whose shape has been adapted to the mount) is placed and glued in between two ceramic boards, and clamped by a suspension type mounting. Thermal modelling on the FPA for SIMBOL-X, which is also stacked onto a high-energy detector and is very similar to the IXO WFI mechanical concept, show, that a homogeneous temperature can be achieved in this way. The interface to the radiator / thermal straps consists of the surrounding invar frame. The entire cooling is intended to be made by one single passive radiator. The thermal connection between radiator and camera head can be made either by heatpipes or by passive thermal straps. Depending on the operating state and the respective power dissipation, heater elements placed on the free spaces of the multilayer ceramics will be used to keep the sensor temperature on operating level by keeping the overall power dissipation and distribution constant. The heaters are controlled by the instruments slow control loop. In this way, a minimal return-to-operation time is ensured.

The detectors will be cooled to 210°K by connection to the passive radiator and be stabilized to $\pm 0.1^\circ\text{K}$ by the internal heaters. The temperature should be within $\pm 0.5^\circ\text{K}$ of absolute value determined from ground calibration tests.

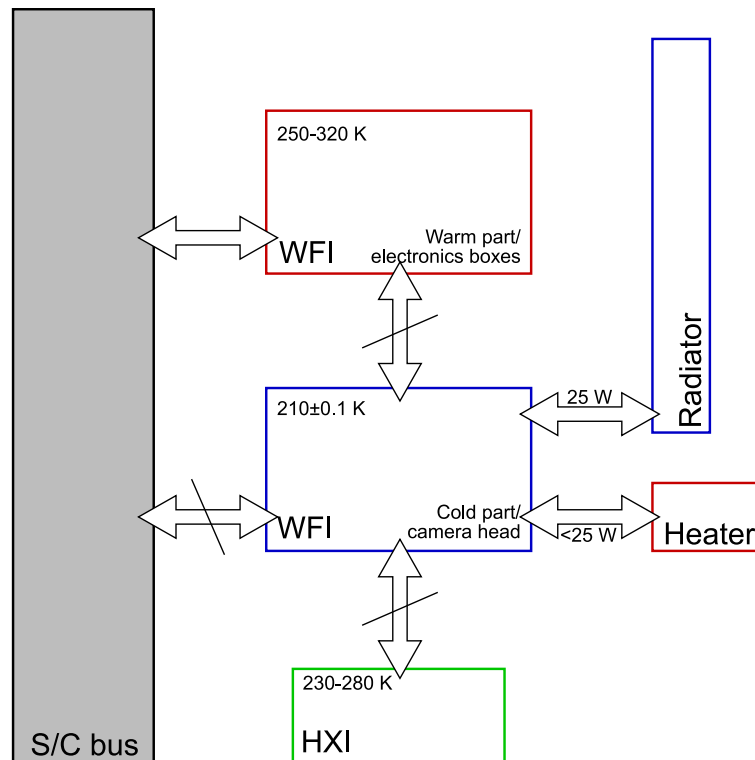


Figure 2-17: Preliminary thermal schematic including the HXI interface

Estimates of active power dissipation of the APS sensor, Switchers and CAMEXs give about 22 W including a 20% margin. The estimate also depends on temperature input from the Camera Head surroundings. The power dissipation will also be different depending on what operating mode is being used. Estimating an overhead power dissipation due to the heaters of ~25 %, the overall maximum power dissipation on the cold part of the WFI is 30 W. If parts of e.g. the ICs are turned off, the heaters will provide additional heat load to maintain constant temperature.

2.1.8 Electrical design

For block diagrams describing the electrical interconnection structure, refer to Figure 2-11 to Figure 2-16.

2.1.8.1 Sensor organisation

Figure 2-5 shows the interconnection of the pixels in the matrix. Every column of 1024 pixels is divided into two hemisphere columns. The row terminals, Clear, Cleargate and Gate, are connected row wise. Depending on the readout scenario, either the Drain or the Source serve as global biasing contact, while the other one is connected row wise and tied to the terminal of the respective column-readout channel of the readout ASIC. The two suggested readout schemes are shown in the Figure 2-18 and Figure 2-19. The drain readout is faster and more likely to be capable of meeting the speed requirements, while the source follower is capable of compensating large interpixel variations.

The final operating scenario is not yet decided upon although it has some impact on the sensor design; it will depend on the performance of the prototype ICs.

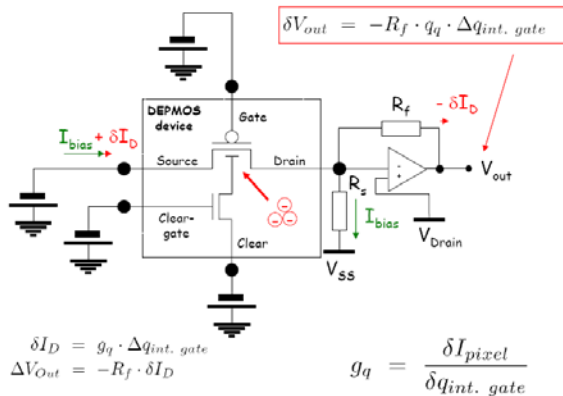


Figure 2-18: Schematic of the drain based current readout scheme. The current signal if the DEPFET is evaluated directly, but the FE electronics has to accommodate the differences in bias currents between the pixels.

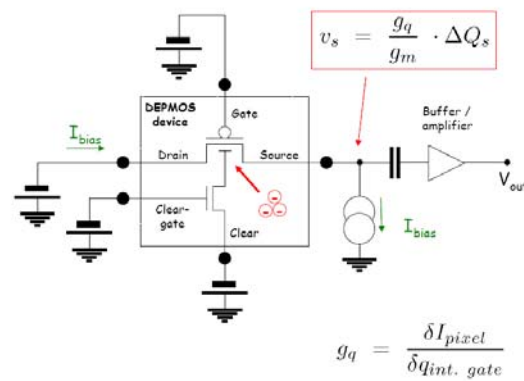


Figure 2-19: Schematic of the source follower readout scheme. The constant bias current is provided by a column-individual current source. The “floating” source allows for elegant compensation of pixel to pixel variations.

Figure 2-20 shows the scheme of data acquisition in the pixels. When the pixel is turned on, the FE electronics measures the signal level. Then the clear process is performed, and afterwards the signal level is measured for the empty pixel. The FE electronics calculates the difference, which is then proportional to the amount of charge integrated during the integrating period within the pixel. This process takes place simultaneously for all pixels in the currently selected row. When the acquisition is finished, the row is deselected and the next row is turned on. A row is sensitive to radiation all the time it is deselected, and even if it is selected, there is only a small period of time where it is actually insensitive.

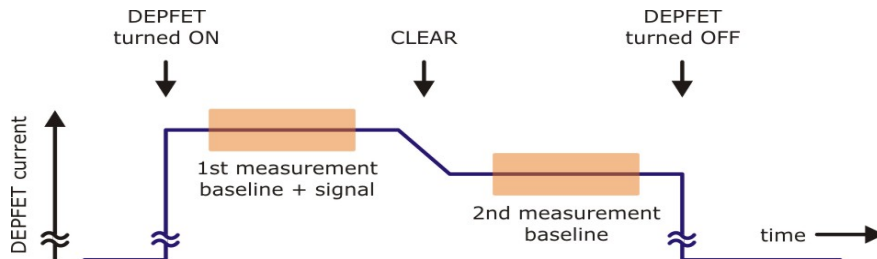


Figure 2-20: Signal evaluation scheme for the APS readout. The device is turned on, and the signal level (current or voltage) acquired before and after the clear. The difference signal is then proportional to the removed charge during the clear.

2.1.8.2 Analogue front end

Within the FE ICs, the signals are filtered. Currently two filtering schemes are discussed, n-fold CDS filtering, which has successfully been demonstrated with prototype CAMEX ICs (Figure 2-21), and trapezoidal shaping, which is superior compared to CDS in terms of series noise. Prototype ICs featuring trapezoidal shaping are currently being developed for both source follower and drain based current readout (Figure 2-22).

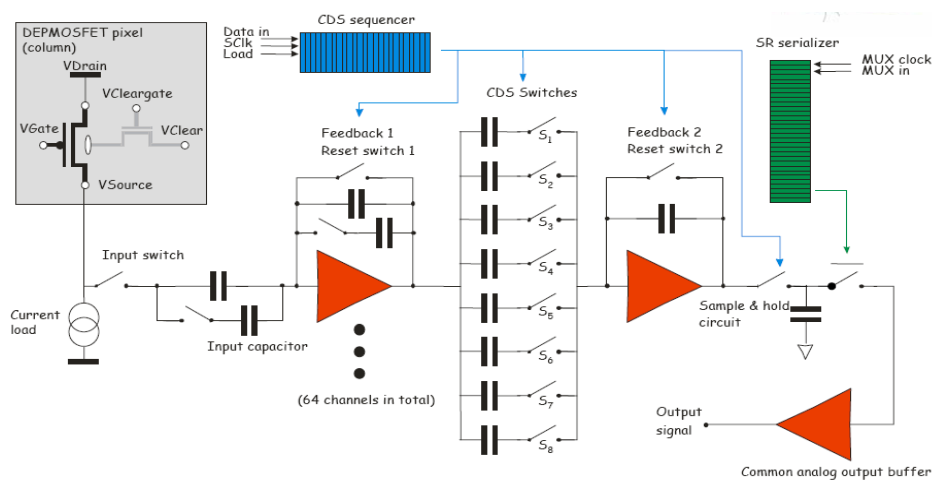


Figure 2-21: Schematic of the CAMEX IC. The AC coupled voltage preamplifier is followed by a 8fold CDS filtering stage, a sample & hold circuit and a serializer buffer. Both CDS filtering stage and output multiplexer are controlled by chip-internal sequencers. The output signal of the chip consists of a stream of analogue output signals.

All chips have in common, that they process all sensor columns in parallel and use an analogue readout buffer for serialization of the output signal. The final version of these ICs used for IXO is likely to follow the same concept. To meet the required frame rate, the 128 channels of this IC will be serialized to two outputs with a speed of ~16 MHz. The chips have an internal programmable sequencer for the control of the processing. The current generation of chips has a straight serial output with which windowing is not possible, but in the next IC generation the serializer will permit selection of arbitrary readout modes.

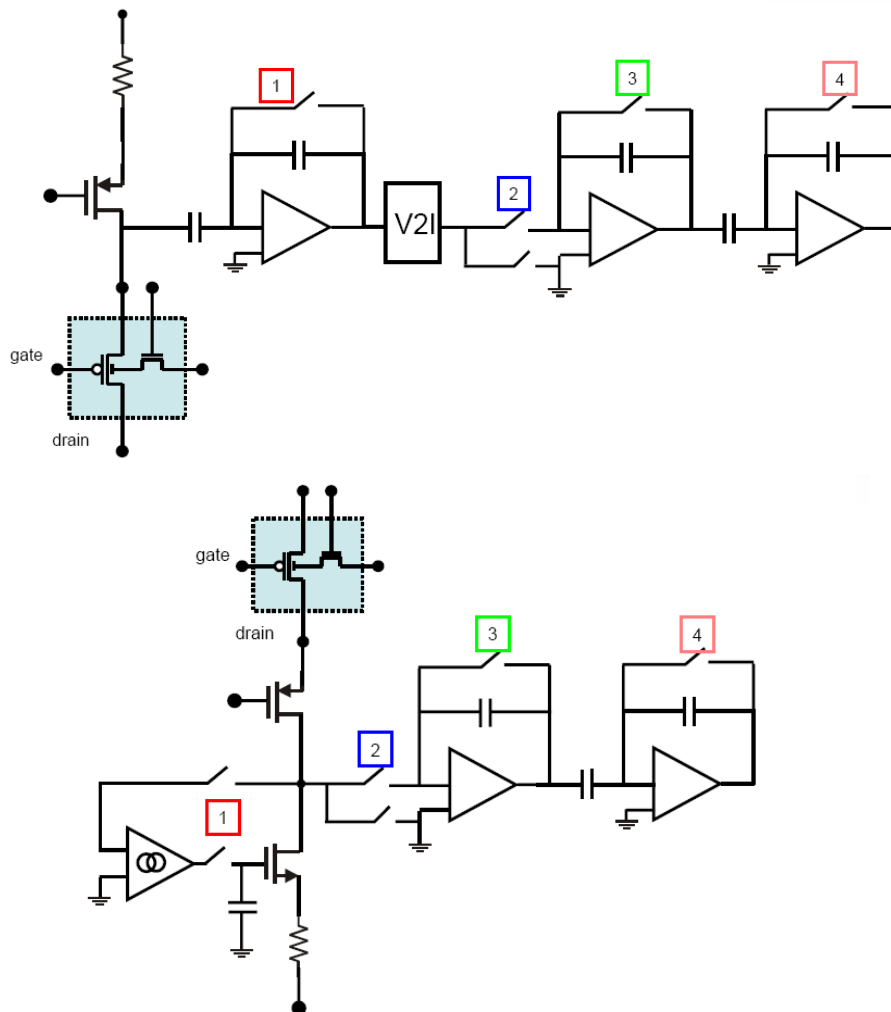


Figure 2-22: Schematic of the ASTEROID (upper image) and the VELA (lower image) ICs. Both ICs use a trapezoidal filtering stage for analog signal processing, which consists of an integrator / de-integrator stage. While the VELA IC, designed for drain-based current readout, directly subtracts the bias current and uses the pixel current for integration, the ASTEROID IC is made for source follower readout and requires an additional I2U converter for the integration current.

2.1.8.3 Control front end

The Control front end consists of 8 128 channel SWITCHER ICs. Every IC has two ports, each of which can be toggled between two voltages. The polarity of the voltages can be chosen, as well as their reference with respect to ground. Figure 2-23 shows a schematic of the current SWITCHER IIB. The chip in its current version is capable of row-wise switching of the channels, while for the next generation the chip will get an internal row sequencer, which allows for arbitrary selection and switching of channels.

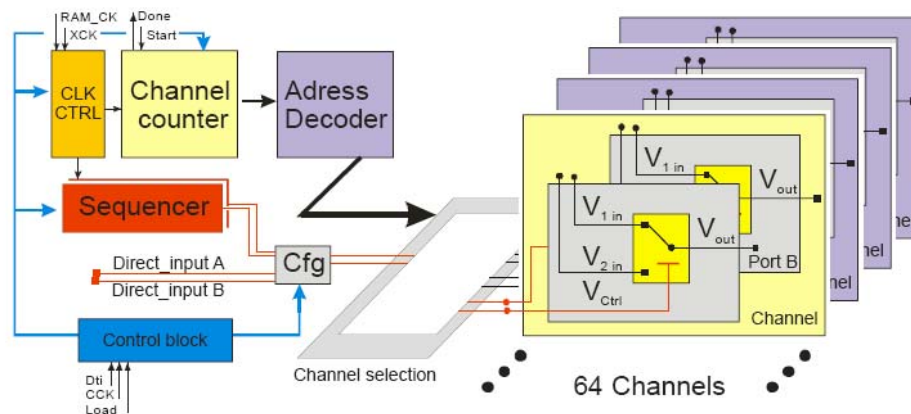


Figure 2-23: Schematic of the SWITCHER IC.

In consequence, the current version restricts ROIs in size and position to the size of one SWITCHER ICs, while later versions will allow on-the-fly selection of arbitrary ROIs and operation modes. The Switcher ICs can handle voltages as high as 20 V.

2.1.8.4 ADC clusters

The serial analog data is received on the ADC clusters. These are modules consisting of 4 ADCs and 1 Cluster FPGA. In addition to the analog data, the ADC clusters also receive timing signals from the main sequencer to synchronize the digitization. The Cluster FPGA captures the ADC data from the 4 ADCs and performs a couple of simple corrections to it. Depending on the available FPGA resources, additional memory and / or FPGA resources may be required here.

2.1.8.5 Framelet builder

The framelet builder collects the data from the ADC clusters and performs pattern detection to the data as a precondition for readout sparsification. The frame builder modules also receive timing signals from the main sequencer.

2.1.8.6 Hemisphere pre-processor

The hemisphere pre-processor, located in one electronics box, combines 4 ADC clusters and one framelet builder. The inter-communication between these cards inside the box takes place via a backplane.

2.1.8.7 Frame builder

The frame builder collects the data from the hemisphere preprocessors and does the final pattern recognition, event identification and data compression, and prepared the data for the transmission to ground. Hemisphere preprocessors and Frame builder communicate via fast serial links. The frame builder also receives timing signals from the Main sequencer. The Frame builder has access to the SpaceWire interface for the data transmission. This link needs to be capable of transferring the maximum overall data rate (455 kbit/s) after preprocessing to Spacecraft mass memory for downlink.

2.1.8.8 Main Sequencer

The main sequencer generates the sequence data for the operation and readout of the camera head and the timing signals for the digitization and the preprocessing in the respective required formats / logical standards. It also controls the correct functionality of the various ICs by supervision of the ICs heartbeat signals.

2.1.8.9 Slow control

The slow control configures the entire system via a relatively slow serial link. It also commands switching of power supplies for the respective operating modes.

2.1.8.10 Housekeeping

The housekeeper is responsible for the slow, timing uncritical tasks: power supply monitoring, temperature regulation of the FPA etc.

2.1.8.11 Brain module

The brain module combines Housekeeper, Slow control and Main sequencer on a common card with interface to the S/C data bus. Currently, three different concepts on how to implement these three functionalities within one module are discussed. Most promising is the solution with one FPGA for sequencer and slow control and one microcontroller for the housekeeping tasks.

2.1.8.12 Brain / Frame builder box

Brain module and Frame builder are located in a common electronics box and share a common SpaceWire interface.

2.1.8.13 Power conditioner

The power conditioner is responsible for generating the voltages required for the operation of the Camera head and the Electronics boxes from the Power provided by the spacecraft. All voltages are supposed to have measurable currents. Voltages for the FPA are foreseen to be adjustable, while all voltages are supposed to be commandable except slow control / SpaceWire interface power.

2.1.8.14 Cable harness

The APS is connected to the Hemisphere Pre-processor with a Flexlead. This must not be longer than 20 cm. The interconnection between the cards within the electronics boxes is done via a dedicated customized backplane. The interconnection between the Hemisphere preprocessors and the Brain module is done via the dedicated data harness (DH). The SpaceWire interface is located in the Brain box. The power harness (PH) is kept separately from the DH and distributes the power to the Brain box and the two hemisphere preprocessors independently. Within the hemisphere preprocessors, the power for the camera head is distributed to the flexleads. An optional heater cable can provide power to the heaters in the camera head directly. A separate slow control connection exists between Brain box and power conditioner. The interconnection length between HPPs and the Brain/Frame builder and between the HPPs and the Power conditioner Units should not exceed 4 m.

A summary of the expected number and gauge of the wires in the Data & Power Harness (DH & PH) and optional Heater Cable (HC) is given in Table 2-3, Table 2-4 and Table 2-5, respectively. Figure 2-24 and Table 2-7 give an overview over all interconnections of the various modules.

Table 2-3: Preliminary overview of the Data Harness (DH) leads

Purpose	Lead type	Number of leads
Analog/Digital Voltage/Signal	AWG 28, PVC/PTFE Insulator 1.27 mm	138
LVDS / Differential Cable	AWG 28, PVC Insulator 1.27 mm, twisted pairs	129

Table 2-4: Preliminary overview of the Power Harness (PH) leads

Purpose	Lead type	Number of leads
Standard Power	AWG 22, PVC/PTFE Insulator 2.6 mm	83
Analog/Digital Voltage/Signal	AWG 28, PVC/PTFE Insulator 1.27 mm	8
Shielded HV Cable	LEMO HV (outer sheath 2.9mm)	3
Shielded Power Cable	LSM 95 (outer sheath 1.5mm)	6

Table 2-5: Preliminary overview of optional Heater Power Cable (HPC) leads

Purpose	Lead type	Number of leads
Heater Power	AWG 22, PVC/PTFE Insulator 2.6 mm	16
Filter sled motor	AWG 22, PVC/PTFE Insulator 2.6 mm	8

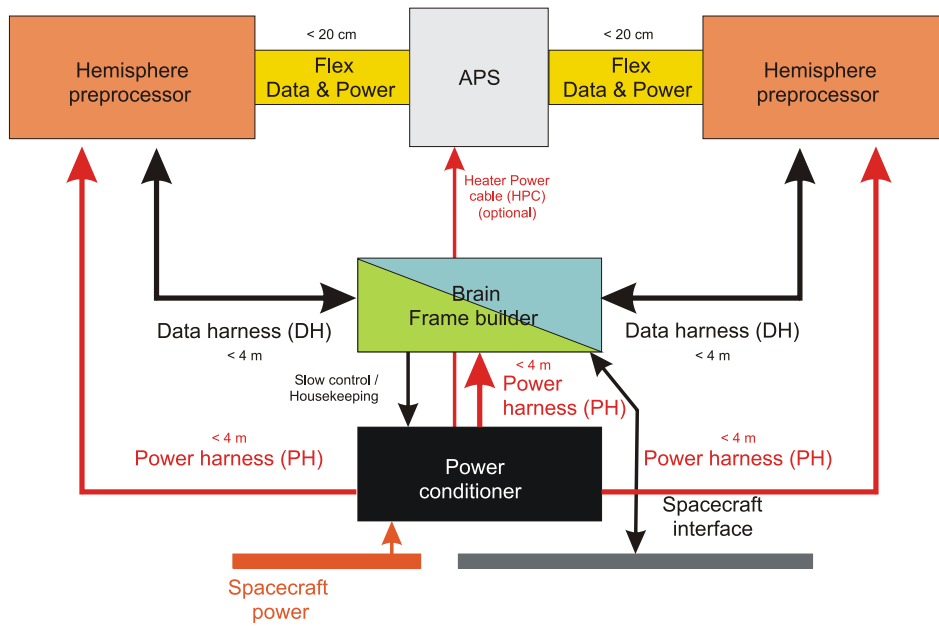


Figure 2-24: Cable harness and module interconnection. Data Harness (DH) and Power Harness (PH) lengths should not exceed 4 m. The Data & Power Flexleads need to be short ~20 cm.

2.1.9 On-board Software

Several functionalities have to take place by the on-board software. In the ICU/Power and Processing Box the onboard software has the tasks listed below. Hereby, it is to be noted that part of this software is to be implemented as FPGA firmware or dedicated ASICs. Implementation details are still to be assessed, but implementation within power budget is expected.

- Spacecraft interface software
- APS Sequencer software (FPGA firmware)
- Slow control software (FPGA firmware)
- Housekeeping software (Microcontroller)

Inside the various data pre-processor modules, framelet builder, cluster FPGA and frame builder most tasks are, for speed reasons, going to be implemented into an FPGA firmware.

Cluster FPGA:

Includes mostly simple DAQ tasks which can be executed serially.

- Offset subtraction: The offset value for each pixel is subtracted from the actual ADC value.
- Offset calculation (running average): Regularly and for special observation modes, for instance in case of observations with high optical background, the offset values have to be updated. This can either be done during a couple of “offset” acquisition (~100 frames) in advance. Additionally, the Offset values can be kept updated all the time by applying a “running average algorithm, which can account for e.g. optical background changes. A selectable number of offset values is summed up and the mean value is calculated, which then is going to be used as new offset value. Care has to be taken not to unintentionally include event charge in the offset value.
- Noise & threshold calculation: Every pixel has its individual primary and secondary threshold, which are determined as multiples of the pixel noise. The latter is determined as the variance of the pixel offset determination.
- Gain correction: Every pixel has an individual gain value, which is determined during the calibration measurements.

Framelet builder:

Includes further processing steps, relying on the availability of “area data”:

- Seed detection: Application of the primary thresholds to the data stream, and flagging events exceeding the primary threshold.
- Neighbourhood filter: All pixels in the seed neighbourhood (and all pixels at the hemisphere borders) are flagged for transmission.
- Addressing & zero suppression: All pixels which are not flagged for transmission are discarded, all flagged pixels are addressed for transmission.

Frame Builder:

Includes tasks for the final zero suppression, reduction of data volume and preparation of data for transmission:

- Border pattern reconstruction: Seed detection at the hemisphere border, neighbourhood filtering
- Secondary threshold: Detection of pattern type and shape, classification and (optionally) rejection of invalid pixels.
- Zero suppression: Pixels not containing pattern constituents are discarded.
- Pattern recombination: (optional) Recombination of pattern energy and pattern energy distribution.

- Corrections: Algorithms for corrections of Sensor / FE specific properties.
- Frame building / integration: Patterns for one or alternatively a selected number of frames are integrated within one data packet with timestamp etc.
- Compression: Compression algorithms are applied to reduce the telemetry data volume.

These algorithms will have different modes and settable parameters under control of the instrument control unit software. Figure 2-25 shows an overview over the various major data pre-processing steps and their assignment to the respective modules. Whether the calculation of the calibration dataset is to be done in the frame builder or offline on ground is to be studied.

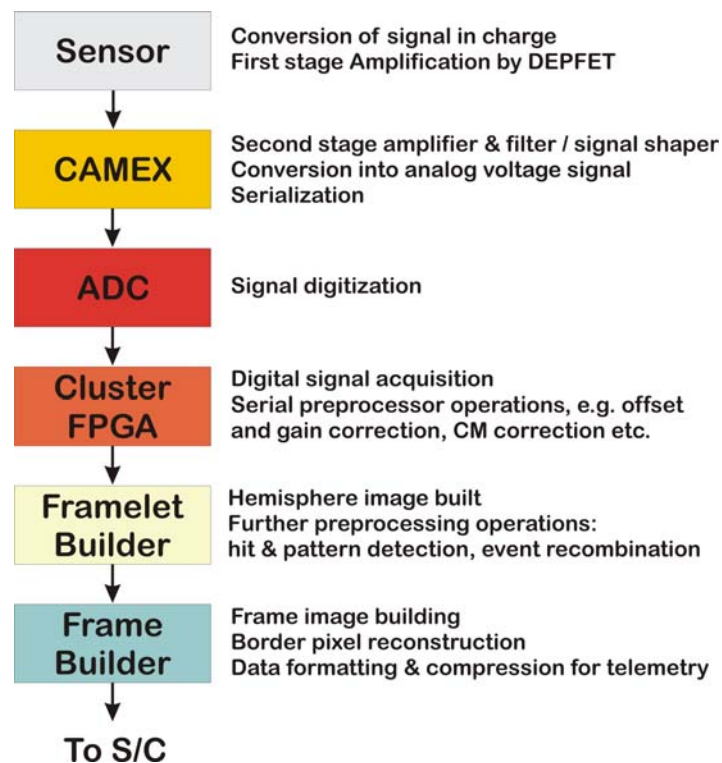


Figure 2-25: Overview over the various data processing steps.

2.1.10 Ground support equipment

Although the instrument is still in an early stage of development, representative samples have been produced and are going to be tested. The GSE developed for these prototypes will be the basis for the GSE of the Final camera head.

2.1.10.1 Electrical ground support equipment

The EGSE consists of a modular system, which can be used for successive replacement of the lab components with the flight components. The laboratory components are also the development basis for the respective flight hardware. In an early version, the Camera head itself will be operated by the standard sequencer with an adapter PCB, which will allow for more test features and flexible operation modes than the later Brain module. The characterisation of the sensor will be done in first place by full, direct sampling ADC modules. The data thus acquired can be analyzed and compared with the pre-processed data acquired with the flight hardware modules, which will be successively integrated to the system and replace the software tasks from the analysis software. The same process will take place for the power supplies as well. Once the system is fully integrated and ready for pre-flight operation, only a S/C interface simulator computer is required for the DAQ and the simulation of the S/C command access.

2.1.10.2 Mechanical and optical ground support equipment

In the laboratory, the Camera head will be operated within the test chambers of the CaliFa and PANTER facility. The cold finger will be substituted by a Stirling cooler / Pulse tube cooler of representative performance. A representative mount will have to be developed, too. Tests with prototype mirror modules at the PANTER facility are possible with representative prototypes as well.

2.1.11 Instrument mode description

2.1.11.1 Operating modes

All operating modes have in common, that the sensor is at operation temperature, the heaters are operated by the housekeeper only to keep the temperature constant. All analogue voltages are on and in set position. The sequencer is running, as well as all relevant parts of the data pre-processing. The row processing time T_{row} is constant. An overview over the different operating modes is shown in Figure 2-26.

Full frame

The full frame operation mode is the standard operation mode. The sequencer is operating all pixels within a row and successively all rows within the matrix. All rows see the same integration time, i.e. the time between two readouts. The integration time in this operation mode corresponds to the time needed to read out the entire pixel matrix, i.e. $512 \times T_{row}$. For the targeted integration time of $\sim 2.5 \mu\text{s}$ per row, the integration time is 1.28 ms, which yields a frame rate of ~ 800 Hz, at a raw data rate of 800 Mbyte/s per hemisphere, or 1.6 Gbyte/s total.

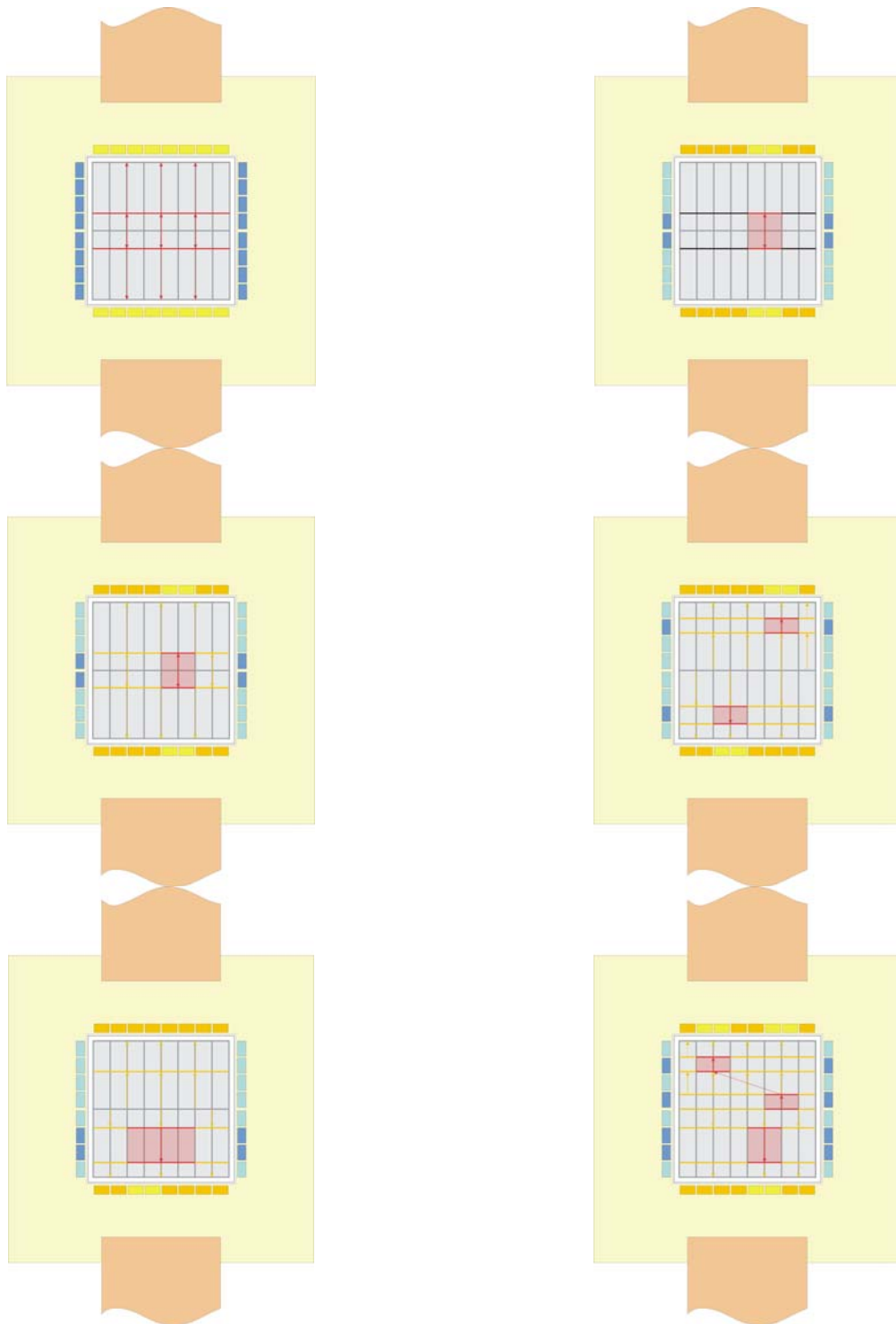


Figure 2-26: Schematic overview over the different instrument operating modes:

- Top row:** Full frame (left), framelet (right).
- Middle row:** Symmetric window (left), windows at different locations (right).
- Bottom row:** Asymmetric window (left), different ROI count (right).

Window mode

The window mode is a readout mode for the observation of the FOV with one or more bright objects or objects where a higher time resolution is required. It allows circumventing the pile-up limit to a certain degree. In the window mode, one or more well-defined ROIs are read out with a higher frame rate, without losing the information of the rest of the FOV. A window strip containing the ROI, the image area of the bright object, is read out repetitively, and a full frame acquisition follows with a certain duty cycle, e.g. for every 6th window acquisition. The integration time for a Window strip of width n is then $n \times T_{\text{row}}$, while the integration time for the full frame is $(d \times n + 512) \times T_{\text{row}}$. For a window strip of width 128 a duty cycle of 6 and a 2.5 μs row readout time, the integration time of the window is 320 μs , and for the full frame acquisition it is 3.2 ms. The next generation of Control front end ICs will allow arbitrary sizes and positions of the ROI windows on the FPA, overlapping with sector and hemisphere borders is possible. Reading more than one ROI on one Hemisphere is possible, but in case they have column overlap, they have to be read sequentially.

The row processing time of the AFE remains the same for windowing and full frame mode, as well as the speed of the data acquisition and the raw data rate, but the overall data rate depends heavily on size and brightness of the observed sources.

Framelet

The framelet acquisition mode is an additional operating mode in case bright objects are going to be observed and the data from the surrounding area is to be discarded. A window strip of a width in units of SWITCHER ICs is defined, which repetitively read out. The rows outside the ROI are switched to permanent clear. To reduce the telemetry to the absolute minimum, the information of the columns outside the ROI are discarded. In this way, an effective reduction of the FOV / APS sensor size is achieved. Within this framelet, window modes can be applied just like for the full frame mode, with the corresponding consequences for the integration times and time resolution.

2.1.11.2 Non-operating modes

For the non-operating modes, selected units are turned off, and the overall power consumption is reduced. The operating modes for the camera head and the digital parts have to be distinguished. It must be noted, that switching from one operating state to another has to be in agreement with the power up cycle guidelines.

Camera head operating states

- **Operation-ready** The instrument is operating and can take data at any time. All analogue and digital components are powered & configured. Heaters are controlled by housekeeping to keep temperature constant. Also used for calibration etc.
- **Hot shutdown** All operating voltages for the Camera head are turned off, the heaters compensate for the loss of power dissipation to keep the temperature at operation level, to allow for quick startup.
- **Cold shutdown** Complete shutdown of all Camera head voltages. Temperature of the FPA drops.

Digital part operating states

- **Active** Corresponds to the active state, sequencer is up and running.
- **Configured** All FPGAs are configured, the sequencer is quiet.
- **Off** Supply voltages for FPGAs are shut down, except for the components of the S/C interface and the housekeeper, which remain powered all the time.

The following table lists possible operation scenarios / combinations of operating modes for both digital section and camera head. The OFF condition is a possible scenario in times in which the S/C needs to enter a safe mode, and cuts power to the instruments. Consequently, there is no control over Housekeeping and PSU. The FPA temperature in the camera head will drop, and it will take some time (Value tbd pending thermal study. Expected value of order of few hours) to heat up again. Survival temperature ranges need to be observed by the S/C. The Sleep scenario is useful in cases where power must be saved, e.g. when the WFI will not be used for an extended period of time. The Standby mode is useful e.g. during re-targeting of the telescope system, together with the filter sled being in closed position. The Active state is the normal operating state; power dissipation is independent from the various operating scenarios described in the operating mode section above

Table 2-6: Summary of WFI operation modes power. These figures do not include the operation of the filter sled.

Instrument mode	Camera head	Digital part	Purpose	Power (cold, no margin)	Power (cold, incl 20% margin)	Power (warm, no margin)	Power (warm, incl 20% margin)
Off	Cold shutdown	Off	S/C launch & safe mode No instrument HK, no PSU control S/C must guarantee compliance with survival temperature ranges	0 W	0 W	0 W	0 W
Sleep	Hot shutdown	Off	Power save	25.1 W	30.1 W	36.5 W	43.8 W
Standby	Hot shutdown	Configured	Standby	25.1 W	30.1 W	193.6 W	232.4 W
Active	Operation ready	Active	Data taking	25.1 W	30.1 W	193.6 W	232.4 W

Additionally, the (rare) occasional filter sled operation of 20.6 W peak power has to be taken into account.

2.2 Mechanical Interfaces and Requirements

2.2.1 Location requirements

The instrument consists of several parts having various location requirements. These are summarized below:

2.2.1.1 Camera head

The Camera head has an interface to the ESA supplied passive radiator. The Radiator area and performance should be such, that an operating temperature of the APS sensor of not higher than 210 K can be maintained over the entire mission lifetime. The power dissipation in the cold part is 30 W (including 20% margin). Detailed requirements at the S/C cold-finger interface necessitate a thermal design study, which is still pending.

The location of the instrument should be such that its optical axis is aligned with the spacecraft Z-axis, and it is watching into the +Z direction. Furthermore its detector array should be in the focal plane of the telescope. An important boundary condition for the WFI camera head mechanics is arising from the requirement of the HXI detector to be within a Z-distance of not more than 3 cm behind the WFI sensor.

2.2.1.2 Electronics

The electronics circuitry shown in this document is divided up in a total number of 5 electronics boxes, 2 Hemisphere Preprocessors, one Frame Builder / Brain box containing two redundant frame builder / Brain units and two redundant Power conditioners. The HPPs are connected to the camera head via short (< 20 cm) flexleads. The HPPs are connected to the rest of the electronics via a cable harness of up to 4 m length. In order to enable EMC the electronics boxes should be electro-statically coupled to the camera head itself by low-ohmic connections / grounding strings being part of the cable harness, so that Camera head enclosure and electronics boxes form a single Faraday cage with exits only for the harnesses. Additionally, the Electronics boxes should be mounted thermally decoupled as much as possible from the APS to avoid unnecessary load to the radiator. The location requirements for the Brain / Frame builder box are less strict, requirements are good EMC shielding and equal cable lengths for the Data Harness (DH) branches to the different HPP modules. The DH length, i.e. length between the HPP modules and the Brain / Frame builder, should not exceed 4 m.

Table 2-7: Summary of module interconnections

	Hemisphere preprocessor	Brain / Frame builder	Power Conditioner
APS	Data & Power Flex <20 cm	N/C	Heater Power (HPC) <4 m (optional)
Hemisphere preprocessor		Data Harness (DH) <4 m	Power Harness (PH) <4 m
Brain / Frame builder			Power Harness (PH) <4 m

2.2.2 Alignment requirements

In order to keep the diameter of the circle of confusion below two pixels (i.e. $\sim 1/2$ PSF), the APS should become aligned to ± 1 mm along the Z-axis and orthogonal to the Z-axis with an accuracy of 0.35 arcmin. Alignment in the X and Y-axis should be ± 1 mm. It has to be made sure that the baffle is designed such that it accommodates the potential misalignments.

2.2.3 Pointing requirements and performance goals

TBD

2.2.4 Interface control drawing

At the present state of development, an ICD of the interface does not exist. Figure 2-12 and Figure 2-24 give an overview of relative positioning of the individual components. Very preliminary estimates on the sizes and masses of the respective units have been made. The focal plane assembly including filter sled, cold finger, camera head and shielding would have a volume of about $32 \times 70 \times 20 \text{ cm}^3$. The Hemisphere pre-processors would have a volume of about $35 \times 25 \times 20 \text{ cm}^3$ ($\times 2$, one for each hemisphere). The frame builder / Brain unit has a volume of $35 \times 40 \times 20 \text{ cm}^3$. The power conditioning unit has a volume of $35 \times 25 \times 25 \text{ cm}^3$. Current estimates of the masses and sizes of the respective components are listed in Table 2-8.

Table 2-8: WFI expected mass and volume budget (estimated outer envelopes).

Component	Height (cm)	Width (cm)	Depth (cm)	Mass per unit (kg)	No. of units re-quired	Margin (%)	Total Mass (kg)	Comments
Filter Sled	1.5	20	60	11.4	1	26	14.4	Including mechanisms, drivers and filters
Camera head	8	32	32	6.6	1	31	8.6	Including support, shielding, cables & interfaces to radiator
Radiation shield	10	32	32	11	1	55	17.1	Cu shield around APS within camera head
Hemisphere preprocessor (HPP)	35	25	20	2.5	2	30	6.5	2 modules, one for each hemisphere, several cards, backplane
Box for HPP	35	25	20	4.2	2	15	9.7	Shielding, support & enclosure for HPP
Brain / Frame builder module	35	25	20	1	2	30	2.6	2 redundant modules (one operated at a time) for both hemispheres,

								Backplane
Box for Brain / Frame builder	35	40	20	6.7	1	15	7.7	Common electronics Box for the two Brain / Frame Builder Modules
Power conditioner	35	25	20	2.5	2	30	6.5	2 redundant modules for instrument
Box for Power conditioner	35	25	20	4.2	2	15	9.7	One Box for each module
Flex Leads				0.1	2	55	0.3	Connecting camera head and HPPs
Total				64.7		28	83.0	Excluding external harnesses
Data harness (DH)				4.8	2	30	12.5	2 Harnesses, one for each hemisphere Busses carrying fast digital signals, length ~4 m
Power harness (PH)				3	2	30	7.8	2 Harnesses, various power supply connections
Heater Power Cable				0.8	1	30	1	1 Harness, carrying heater & filter wheel motor power
Total				81.1		29	104.3	Including external harnesses
HXI	30	30	8.5	25.0	1	30	32.5	See Section 4.2.4
Total WFI+HXI							115.5	Excluding external harnesses. Detailed combined WFI / HXI study pending.

2.2.5 Instrument mass

The most recent estimates on mass of the components are shown in Table 2-8.

2.3 Thermal Interfaces and Requirements

2.3.1 Temperature limit in space environment

The temperature of the Camera head is to be kept at 210 K during operation. In operation mode, the temperature will be stabilized to ± 0.1 K by an instrument-provided heater and an ESA provided radiator. The detailed specifications at the S/C cold-finger interface are pending a detailed thermal study of the WFI. In order to assure long term stability of all operational parameters, the temperature on the APS should not drop below 200 K and should not exceed 230 K in sleep mode. During launch, and if the S/C enters safe mode in an emergency, the S/C has to guarantee observation of the absolute maximum ratings of the survival temperature ranges.

For the electronics part, the standard MIL temperature specifications of -40 °C to $+85$ °C are applicable and should be kept. An operating temperature of around 300 K is desirable. Table 2-9 gives a summary of the operational and survival temperature ranges.

Table 2-9: Temperature ranges.

	Survival Range (absolute maximum ratings)		Long Term Stability Range		Operational Range		
	Minimal	Maximal	Minimal	Maximal	Minimal	Nominal	Maximal
Camera Head	170 K	350 K	200 K	230 K	209.9 K	210 K	210.1 K
Electronics Boxes	230 K	360 K	250 K	320 K	250 K	300 K	320 K

2.3.2 Temperature limits in laboratory environment

In laboratory environment the same temperature requirements as applied for the space environment are applicable.

2.3.3 Temperature sensors

The multilayer ceramic of the camera head is to be equipped with a total number of 4 temperature sensors of type PT 1000. In addition, integrated temperature diodes on the FPA help to monitor the APS temperature. The data of all these sensors is to be taken into account for heater control to ensure homogeneous temperature distribution on the APS within the required specifications.

For the digital electronics, temperature sensors for every module included in the housekeeping chain monitor the temperature within the electronics boxes.

2.3.4 Heaters

Heater elements are foreseen only for the APS to actively control the sensor temperature and to keep the camera head at operating temperature in case the FE electronics is shut down. Maximum power dissipation is expected to be ~ 30 W.

2.3.5 Thermal schematics

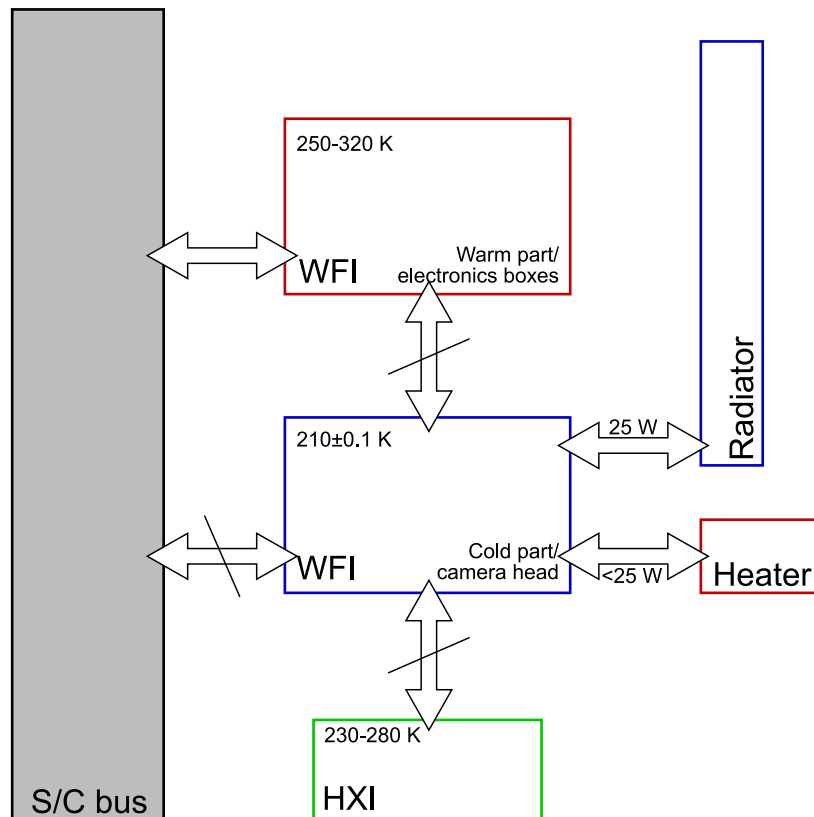


Figure 2-27: Preliminary thermal schematics. A detailed study of the thermal concept is pending

2.3.6 Thermal control requirements

As mentioned above, thermal control is required only for the APS. This will be achieved via a feedback between the housekeeper and the temperature sensors on the sensor itself (thermal diodes) and other temperature sensors (e.g. PT1000) on one side and the heater elements controlled via the housekeeper on the other side.

2.4 Electrical Interfaces and Requirements

2.4.1 Electrical resources requirement summary

The system requires access to the spacecraft provided power bus. It is assumed, that the power delivery is done via the spacecraft power bus. The delivered power is then converted into

- Digital supply voltages (~3.3 V) for the Brain module and the various stages of data preprocessing and frame building (commandable).
- Analog supply voltages (~3 - 5 V) for the ASICs of the AFE and the CFE units (commandable).
- Analog bias voltages (~3-5 V) to bias the AFE and CFE ASICs (adjustable)
- APS switching voltages (~20 V) for the operation of the APS (adjustable)
- HV bias (~200 V) for providing appropriate bias voltages to the APS (adjustable)
- Heater power for the APS heaters (adjustable)
- Operating power for the filter sled (commandable)

by the instrument provided power conditioner. Conversion is expected to be done mostly via high-efficiency DC/DC converters. The S/C is expected to be capable of delivering enough power to provide the respective power consumption in peak mode including the conversion loss of the converters.

2.4.2 Instrument power distribution block diagram

The power is distributed in a centralized way from the power conditioner via the power harness (PH) to the instrument subsystems. A representative block diagram, excluding heater power (which is also connected to the APS) and filter sled power, is shown in Figure 2-14.

2.4.3 Power budget

An overview over the instruments' required power resources is given in Table 2-10. Please note the following comments :

- The filter sled design is not yet fixed. The estimated value is based on the design for XMM
- The overall required heater power depends on the thermal design and the radiator. Part of the power is required to keep & regulate the temperature during normal operation and different pointings, but the peak value (in brackets) is required to replace the FE power on the APS in hot shutdown mode. So the power consumption is mutually exclusive. Overall power dissipation in the « cold » part is 30 W.
- « Cold » power dissipation of the ASICS during operation is only the 22 W to be delivered to the Camera head, the remaining 8 W are default heater dissipation for regulation purpose.
- Base for ADC clusters is 2 W / ADC, 3 W / FPGA
- Base for Hemisphere preprocessor power is 4 ADC clusters plus 1 FPGA consuming 3 W of power.

Table 2-10: WFI power resources. A constant total power dissipation in the cold part of the Instrument of 30.1 W can be assumed. Selective power off of redundant devices is not considered, all devices are considered to be powered.

Item	Assumption / notes	Number of units in Instrument	Power per unit w/o margin(W)	Total power w/o margin (W)	Margin %	Total Power (W)
Filter Sled	Design not yet fixed, estimation based on XMM	1		2.5 (av.) 12 (peak)	20	14.5
Camera head	210 K	1		18	20	22
Heaters	Temperature control At 210 K. Dissipation mutually exclusive with camera head	1		7 (typ.) 25 (max.)	20	8 (typ.) 30 (max.)
Temperature sensor array	4 different locations on focal plane	1		0.1	0	0.1
Hemisphere preprocessors	4 ADC clusters, 1 FPGA	2	49	98	20	117.6
Frame builder	FPGA module	2	6	12	20	14.4
Imager Control Unit (including temperature control)	1 FPGA / state machine, 1 microcontroller	2	6	12	20	14.4
Power Supply	Control part	2	3	6	20	7.2
System				165.1	20	198.2
System total	Incl. dc-dc converter efficiency of 70%			235.9	20	283.1

The following power consumption values result for the different instrument operation modes:

Table 2-11: WFI power at different operation modes including margin. The respective DC/DC converter losses of 70% are accounted for in the warm part power dissipation. Filter sled operation is not included.

Instrument mode	Camera head	Digital part	Purpose	Power (cold, no margin)	Power (cold, incl 20% margin)	Power (warm, no margin)	Power (warm, incl 20% margin)
Off	Cold shutdown	Off	S/C launch & safe mode No instrument HK, no PSU control. S/C must guarantee compliance with survival temperature ranges	0 W	0 W	0 W	0 W
Sleep	Hot shutdown	Off	Power save	25.1 W	30.1 W	36.5 W	43.8 W
Standby	Hot shutdown	Configured	Standby	25.1 W	30.1 W	193.6 W	232.4 W
Active	Operation ready	Active	Data taking	25.1 W	30.1 W	193.6 W	232.4 W

Additionally, the (rare) occasional filter sled operation of 20.6 W peak power (including DC-DC conversion efficiency) has to be taken into account.

2.4.4 Instrument modes' duration

2.4.4.1 Instrument continuous mode duration

As the data acquisition of the instrument runs continuously and the observed photon rate has impact only on the data volume, but not on the power consumption, the continuous data acquisition will be used 100% of the time, corresponding to the Active mode in Table 2-11.

2.4.4.2 Instrument peak mode duration

There is no instrument peak mode which differs from the continuous mode in terms of power. The peak power consumption occurs when the filter sled is moved while the system is in Standby or Active state. The phases of filter sled movement are short, and their frequency is not yet defined.

2.4.5 Telecommands

At the present state of instrument design, the following preliminary set of telecommands is defined:

- Power on and off commands
- Change of Instrument mode
- Filter sled position
- Start and Stop commands for System
- Definition of ROI and operation mode commands

These commands transfer only a small amount of data and trigger the respective configuration processes within the slow control circuit, so that the instrument is configured automatically.

Besides these high-level commands, other commands relying on the transfer of larger amount of data can be executed on special occasions:

- Transfer and verification of FPGA configuration data
- Adjustment of adjustable operation voltages
- Request & transmission of self-procured calibration data (offset / gainmap)
- Housekeeping commands
- Transfer of configuration data for AFE and CFE

2.4.6 Telemetry

2.4.6.1 Telemetry requirements

Table 2-12: Summary over telemetry data rates

	Minimum	Average	Maximum
Bit rate	1 kbit/s (HK)	45 kbit/s (normal src)	450 kbit/s (bright src)
Data volume	10 MByte (10 ks obs)	375 MByte (70 ks obs)	50 GByte (1Ms obs)

2.4.6.2 Telemetry description

At the present state of development, a precise definition of the command set etc. can not be provided.

Housekeeping telemetry

The Housekeeping circuitry will acquire housekeeping data autonomously within tbd. time intervals and keep a log by itself. The housekeeper will alert the brain module in case something is out of order and user action is required. The normal housekeeping data acquired will be transferred to ground in TBD intervals. Housekeeping At the present state of development, the housekeeping data consists of the following list of items:

- Sensor temperature (diodes)
- Camera head temperature (sensors)
- Heater condition
- Current values from power conditioner
- Status information of the sequencer
- Status information of the various pre-processor modules

Besides these regular checks, on-demand housekeeping commands can be given by the user, which will be executed with high priority.

Science telemetry

For each observation the WFI requires TBC commands to define operating modes, window configurations, filter sled position etc.

Science telemetry is sized according to the following assumptions:

- x-position: 10 bits
- y-position 10 bits
- energy: 12 bits
- time-label: 10 bit
- photon quality label 3 bits
- total: 45 bits /event.

In window mode for relatively bright objects, the count rate of 10^4 cts/sec can be accommodated, leading to a peak telemetry rate of 450kbit/s, but normally a rate is <1000 /sec so ~ 45 kbit/s.

During periods of high background, data could be dominated by soft protons indistinguishable from X-rays. Then a maximum rate of ~ 100 k counts/sec might result with a bit rate of 4.5Mbit/s. The instrument shall be programmed to recognize inappropriate data rates and truncate this transmission to order of 0.5 Mbit/s. If necessary, data compression could be achieved with a sparse transmission of the time bit and/or applying standard lossless compression.

2.4.7 Electrical interfaces

In the current concept, the sensor is connected to S/C power via the S/C power bus and the power conditioner. In addition, the connection to the S/C computer systems is done via the SpaceWire connection in the brain box. Reliable ground connection is required for the mechanical parts.

2.5 Electromagnetic Compatibility and Electrostatic Discharge Interface

2.5.1 Susceptibility requirements

The WFI does not need any magnetic field to operate. The instrument can withstand rather high magnetic field strengths and as such the requirements on ambient magnetic field levels are not foreseen to be very strict. A field of 10 G in the telescope focal plane as discussed due to, e.g., particle deflector magnets (tbd) would not pose a problem. However, be noted that the WFI system is not yet tested in strong magnetic/electrostatic field conditions.

2.6 Optical Requirements

2.6.1 Straylight requirements

Straylight from the X-ray sky has to be fully suppressed by suitable baffling. Optical straylight is stopped to a large extent by the entrance filters of the instrument. By nature straylight can be attenuated to any degree but it cannot be extinguished completely. The requirement is that it doesn't degrade the instruments energy resolution. For the WFI, an optical and UV-filter is deposited directly on the focal plane assembly and blocks IR/VIS light. The effect of the on-chip filter is strongly depending on the Al-thickness (Figure 2-28). Using an Al-thickness of 70 nm the IR/VIS load would be damped by a factor of 10^5 . By combination of the Al-filter with dielectric layers also UV-photons can be filtered effectively. An UV attenuation of 100 is envisaged. The current baseline for the UV/optical filter is 70 nm Al on top of 35 nm SiN and 35 nm SiO. Figure 2-29 shows the tradeoff in terms of reduced efficiency at low X-ray energies.

The on-chip filter will gain experience with similar detectors (pnCCDs, DEPFET Macro Pixel Sensors) to be used in the eROSITA, Simbol-X and BepiColombo missions. The integrity of the on-chip Al layer can be checked by high-resolution profiling and flat field optical illumination. In addition, a filter on the filter sled also contributes to blocking unwanted light of high-intensity optical sources.

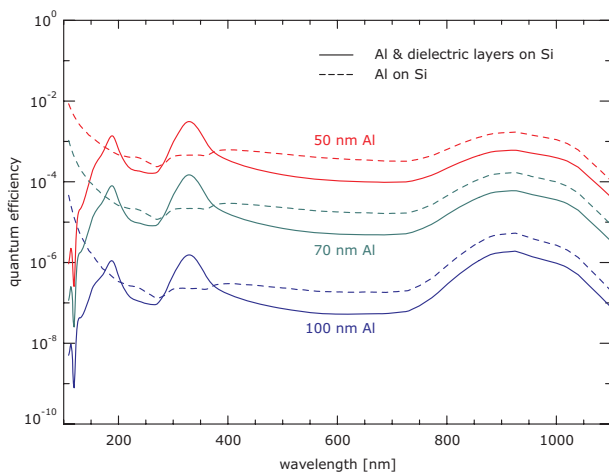


Figure 2-28: Filter effect of thin Al and dielectric layer system deposited on the WFI sensor entrance window in the UV and optical.

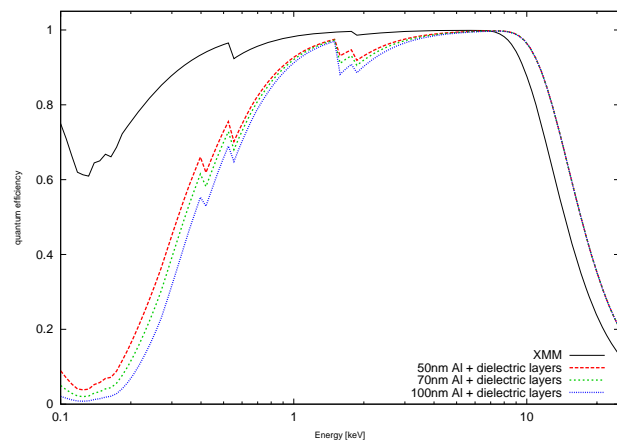


Figure 2-29: WFI quantum efficiency for different Al filter thickness. XMM (300 μ m sensitive bulk, no UV/optical blocking filter) shown for comparison.

2.6.2 Baffling requirements

In order to baffle stray X-ray and other stray light, a baffle system forward of the instruments will ensure that the field of view minimizes unwanted light to the focal plane. As the HXI will use the same baffle rather thick and heavy material is required to shield the cosmic X-ray background from reaching directly the HXI instrument. For the WFI, the first requirement is that the instrument FOV has free and unobstructed view to the rear aperture of the mirror in case the filter sled is in *open* position. Secondly, the entire sensitive area of $\sim 10 \times 10 \text{ cm}^2$ must not be loaded with optical photons or diffuse X-ray background from the sky. As the minimum optical attenuation of the integrated filter is aimed to be 10^5 , a total photon rate of 10^{12} photons per square centimeter and second leads to one photon per pixel and frame for the targeted frame rate of 1 kFrame/s. This leads to a tolerable deterioration of energy resolution. Thus, requirement of the optical baffling is to reduce the optical photon flux to a level of 10^{12} photons per square centimeter and second on

the detector surface (i.e. behind the mirrors). In case of the X-ray background, the main requirement on the baffle is that the diffuse X-ray background coming from outside the telescope's field of view should be reduced to a level of 1×10^{-3} photons per square centimeters and second, which should not be exceeded. In this case, the instrument can operate background limited.

The shape of the baffle will need to be optimized for optical straylight. The inside of the baffle would be coated black for straylight reasons. One open issue is the amount of outgassing by the baffle. Mitigations for minimizing the outgassing in the baffle are needed.

2.6.3 Charged Particle Rejection Requirements

Most events induced by charged particles focused onto the detector can be tagged as not resulting from a photon due either the track signature in the pixel array, or the total energy deposited. Most difficult to distinguish from photon detections are events induced by charged particles in the nominal WFI energy range. Therefore, WFI requires the charged particle deflector to deflect particles of energies in this band.

When observing using the optical filter position of the filter sled, charged particles lose a part of their energy on passing through the filter material. Therefore, the deflection requirement has to be extended to higher energies. The dominant species of charged particles is expected to be solar wind protons. Protons entering the filter with an energy of 75 keV, lose roughly 60 keV in the filter bulk and the UV/optical blocking filter on the detector. Electrons in the 15 keV regime lose only about 1.25 keV. Therefore the charged particle deflector should deflect protons up to 75 keV and electrons up to 17 keV.

2.7 Transportation, Handling, Cleanliness and Purging Requirements

2.7.1 Transportation requirements

When transporting the camera head, care has to be taken not to expose the sensor to strong shocks and vibrations, to humidity or corrosive gases. Thermal shocks have to be avoided. As the sensor will not be launched in an evacuated state, purging also during transportation is desirable, but not mandatory. The Sensor needs to be protected against contamination.

2.7.2 Handling requirements

The sensor has to be handled with appropriate care. It must not be exposed to strong shocks. Assembly and handling instructions, especially for the power connections, cycling of power supplies or the connection / disconnection of cooling equipment, have to be followed strictly. Handling personnel has to be trained accordingly and must wear protective clothing to prevent unintentional contamination of the device.

2.7.3 Cleanliness requirements

Any contamination of the entrance window has to be avoided, especially with organic contaminants. Personnel handling the devices and the area in which handling takes place have to be prepared accordingly. Personnel must wear appropriate clothing. Clean room class 10000-1000 or better is required.

2.7.4 Purging requirements

As the sensor will be launched in a non-evacuated state, constant purging with clean nitrogen is required, wherever possible.

2.8 Ground and flight operations requirement

2.8.1 Ground and pre-flight operation

When the sensor is operated on ground, it is required to operate either in vacuum or within purging gas atmosphere. The sensor must not be operated with cooling without being exposed to a vacuum environment. During all ground and pre-flight testing, the requirements in section 7 have to be kept. When operated, the sensor must not be exposed to direct or indirect light

2.8.2 Flight operations

While operating the sensor during flight, the sensor must not be exposed to direct sunlight without appropriate filters applied. Whenever redirection of the spacecraft is occurring, the sensor should be put to at least hot shutdown mode, and the filter sled moved into the CLOSED position. In order to ensure long term stability of all operational parameters, heating of the sensor to temperatures higher than -40°C or cooling below -70°C should be avoided. Operating the sensor in cold shutdown mode should be avoided, as contamination of the entrance window might occur.

2.9 Deliverable Models and GSE

2.9.1 Structural Thermal Model

The Structural Thermal Model (STM) is a mechanical model of the WFI focal plane assembly and electronics boxes. It includes

- flight-equivalent mechanics,
- a representative prototype of the ceramic board,
- a representative mechanical dummy of the sensor,
- representative dummies of front end chips,
- a special harness for validation of electrical connections and temperature control.
- a representative dummy of the brain / frame builder box
- representative dummies of the hemisphere pre-processor boxes
- representative dummies of the power conditioner boxes

The STM will be integrated according to flight standards. For the thermal test the power dissipation of the sensor, the frontend chips and the electronics boxes will be emulated by heaters. The STM will be used to validate the WFI mechanical structure with respect to vibration, shock, and thermal properties on a sub-system level before delivery for integration in the satellite STM. The thermal and mechanical properties of the STM will be nominal or near-nominal.

2.9.2 Engineering Qualification Model

The Engineering Qualification Model (EQM) is as representative as possible to the flight model in terms of mechanical and thermal properties and electrical functionality. It includes

- flight-equivalent mechanics,
- a flight-equivalent ceramic board,
- an electrically flight-equivalent sensor, potentially with reduced quality or cosmetic defects,
- electrically flight-equivalent front end chips,
- a flight-equivalent harness for validation of electrical connections and temperature control,
- electrically equivalent prototypes of the electronics boxes
- electronic Ground Support Equipment (GSE).

The EQM will be integrated according to flight standards. All components will be flight-equivalent, possibly with lower quality grade. The EQM will be used to validate the design concept in terms of electrical properties (system noise, readout speed, power dissipation) and to qualify the mechanical and thermal design. In addition it can be used for electromagnetic interference and compatibility (EMI/EMC) measurements. The GSE will have the same functionality as the spacecraft electronics but use different components. Over the course of electronics development the GSE will evolve from a local test unit at the PI lab to a flight-equivalent electronics assembly (section 1.10).

2.9.3 Flight model

The Flight Model (FM) is the detector assembly with all parts manufactured, integrated, and qualified to flight standards. The FM will be calibrated on a sub-system level in a dedicated calibration campaign before delivery for integration in the S/C.

2.9.4 Flight spare model

The Flight Spare model (FS) is a duplication of the full flight detector assembly with mechanical structure, fully populated ceramic board, front end electronics, and calibrated detector. Possibly, components of the EQM will be reused to build up the FS.

3 X-RAY MICROCALORIMETER SPECTROMETER (XMS)

3.1 Introduction

The purpose of the XMS is to provide spectra with an energy resolution of typically 2.5 eV in the energy range .2 – 10 keV for the central detector and 10 eV for the wider field outer section, simultaneously with images of a modest (several arcmin) field of view and with time resolved photon counting. The design presented here is likely to be proposed in case there is an Announcement of Opportunity for instruments on IXO, but in no way excludes that alternative technologies can provide better performance at the time of the selection.

The current specifications are based on the following approach:

An array of absorbers read out by Transition Edge Sensors (TES). For the readout of the array there are two options: time domain multiplexing (TDM) or frequency domain multiplexing (FDM). For the required spacecraft resources the differences between these options are small and the current specifications cover both read-out schemes.

There are a number of potential approaches for the *cooling chain* which are pursued in different institutes/industries. Typical examples include:

- a) five stage ADR pre-cooled by a pulse tube or pulse tube/4He Joule Thomson cooler, which provides a base temperature of 6 K
- b) a double stage ADR which is pre-cooled by Stirling or pulse tube cooler and a Joule-Thomson cooler which provides a base temperature of 2.5 K
- c) a combination of a 3He sorption cooler with an ADR precooled by a system which provides a 2.5 K base temperature
- d) a dilution fridge which is pre-cooled by a system ((Stirling or pulse tube) which provides a base around 1.8 K

Clearly it is not possible to include all these different options in the spacecraft related studies. Therefore we have selected as **baseline** the concept which is based on the system under development for the Japanese Astro-H mission but imposed additional requirements on its reliability: it should maintain its functionality even after failure of one of the mechanical coolers. The system, based on astro-H has a good Technical Readiness Level and has been studied in a fair level of detail. The system consist of a double ADR (dADR) pre-cooled by Stirling and Joule-Thomson coolers. The required spacecraft resources for this system are probably the most demanding and other solutions, with clear advantages and disadvantages, exist. In this PDD we give 3 alternative approaches and describe another system for the large stage cooler to indicate the range of options available. It is expected that over the coming period a detailed comparison of the different options will be carried out but it is expected that a final selection will be made at the time of the AO.

In addition it has, as yet, not been decided if the instrument team will have responsibility up to and including the last stage cooler or alternatively, including the full instrument cooling chain. As this does not directly influences the system studies, the current PDD includes the full cooling chain.

3.2 Instrument description

3.2.1 Introduction

The X-ray Micro-calorimeter Spectrometer (XMS) is an imaging X-ray spectrometer based on a pixel array of micro-calorimeters. Each pixel in the array consists of an absorber of which the temperature is read-out by a normal-to-superconducting phase transition thermometer with a critical temperature $T_c \approx 100$ mK, generally called Transition-Edge-Sensor (TES) (see Figure 3-1). The absorber-thermometer combination is weakly coupled to the 50 mK base temperature of the cryostat.

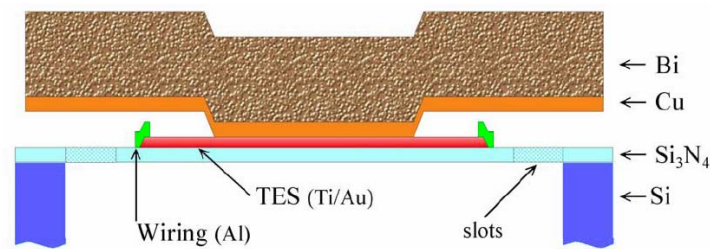


Figure 3-1 Schematic of a micro-calorimeter pixel (as developed at SRON), consisting of an X-ray absorber (in this case Bi/Cu), a phase transition thermometer (in this case Ti/Au) and a weak link (Si_3N_4 -membrane) to the base temperature of the cooler

The temperatures are read-out by a superconducting-to-normal phase-transition-thermometer, generally called Transition Edge Sensor. In these sensors a bi-layer will be biased in its transition between superconducting and normal resistance (see Figure 3-2). Usually these devices are operated in a voltage bias mode, keeping the resistance at its set point (typically 20% of the normal resistance). When a photon is absorbed, the temperature increases which will result in an observable change of resistance. The resulting change in current is read-out by a Superconducting Quantum Interference Device (SQUID), acting as a current amplifier. As SQUIDs are highly a-linear (see Figure 3-2) it is necessary to increase the dynamic range of the SQUID by means of feed back. Feedback for SQUIDs means that the flux through the SQUID loop is kept as small as possible (large loop gain). Such a SQUID feedback is generally called flux-locked-loop (FLL).

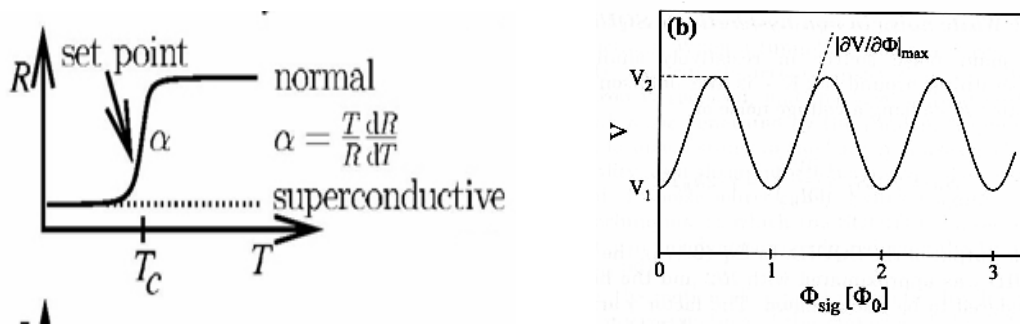


Figure 3-2 Operating principle of a Transition Edge Sensor (left) and its read out by a SQUID

To read-out a large number of pixels, the signals need to be multiplexed as otherwise the number of wires and thermal load on the cooler would become too large. Different approaches are being studied including the Time Domain Multiplexing (TDM), Frequency Domain Multiplexing (FDM, and Code Domain Multiplexing (CDM). The topology for the TDM and FDM read-out schemes is shown in Figure 3-3. The spacecraft resources (mass, power, volume) for these solutions are similar. The best performing read-out system will be selected for the XMS.

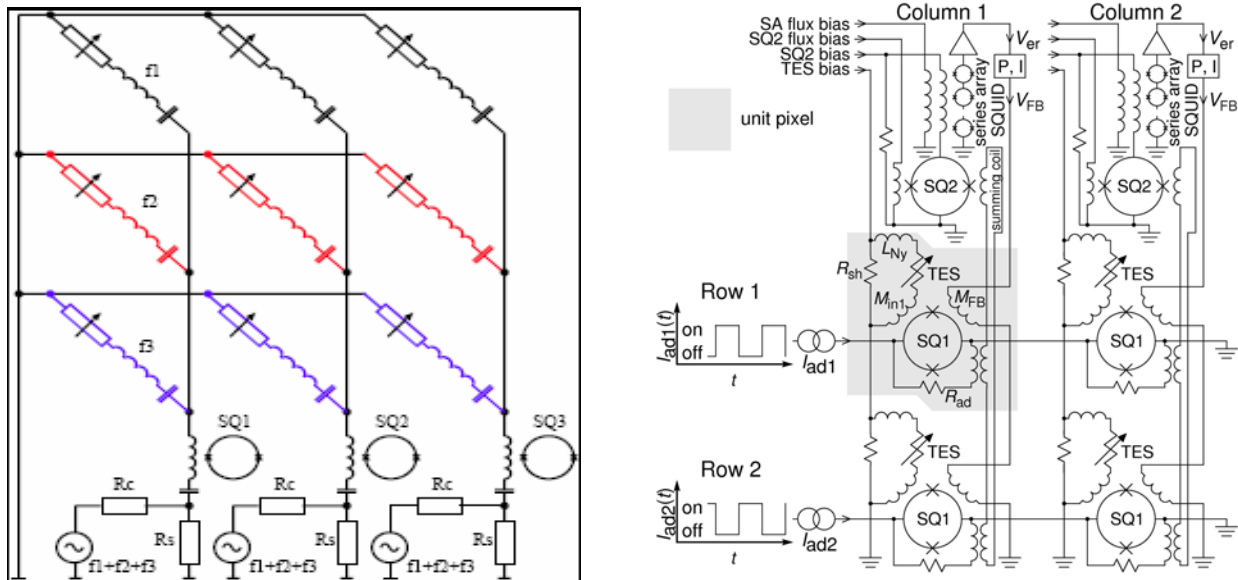


Figure 3-3 Topology for the read-out of an array. Left: the schematic topology for FDM shows that the pixels in each row are biased at a different frequency. Subsequently the pixels in each columns are summed onto one SQUID amplifier, so that the information of each pixel is separated in frequency space. Right: Schematics for TDM showing that the information of many pixels attached to one amplifier is sampled at different times, so that the information is separated in time space. In the NIST design SQUIDs are used as switches and the common amplifier is a 2-stage SQUID amplifier (adapted from Doriese, et al., NIMPR A 559, p808-810 (2006)

To operate the cryogenic detector at 50 mK a complex, heavy and power consuming cooling train is required. Main components of such cooling chain are a combination of various mechanical coolers and/or sorption coolers, a dewar with different temperature stages and a large stage cooler which provides the cooling capacity below a few K (typically an Adiabatic Demagnetization Refrigerator). A 3-D drawing of such a system is shown in Figure 3-4 but many different implementations can be considered.

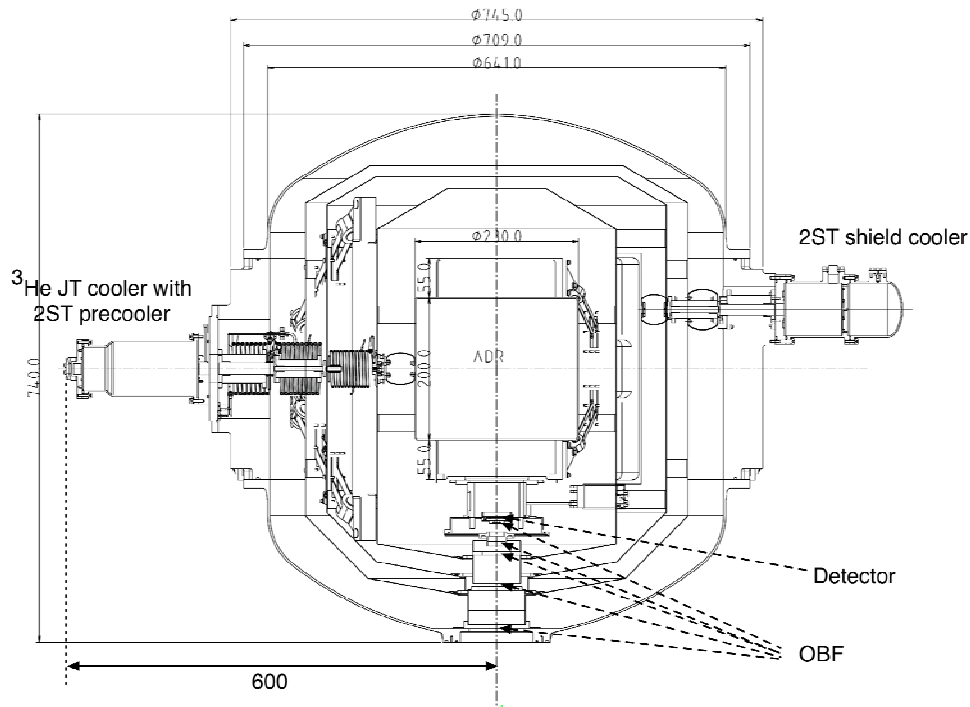


Figure 3-4 drawing of the cooler showing some basic components: the detector, the last stage cooler (ADR, the optical blocking filters (OBF) and two mechanical coolers coupled to different heat shields in the dewar. The actual implementation will have more cryo-coolers and the position is still TBD.

More detailed descriptions of TES micro-calorimeters can be found in literature (see RD04).

3.2.2 Instrument performance specifications

The scientific performance of the XMS is summarized in Table 3-1. As the number of pixels for a cryogenic array is limited, the detector is split into two parts: a central region with the optimal energy resolution and a fair match with the angular resolution of the mirrors and an outer array with degraded spectral and angular resolution but increasing the Field of View considerable. This is shown in Figure 3-5. Clearly, if technology improves beyond the current expectations, either the Field of View can be increased or the area of the detector with an optimal spectral resolution (the inner array) can be increased. Such change will follow a detailed scientific trade-off but, for the time being, the current requirements and design is a realistic prediction of the capability of the instrument. As can be seen in the figure, it is desirable to cover a FoV of 6.5 arcmin (provided that the spacecraft resources allow this) leaving the 4 corners for monitoring the particle background.

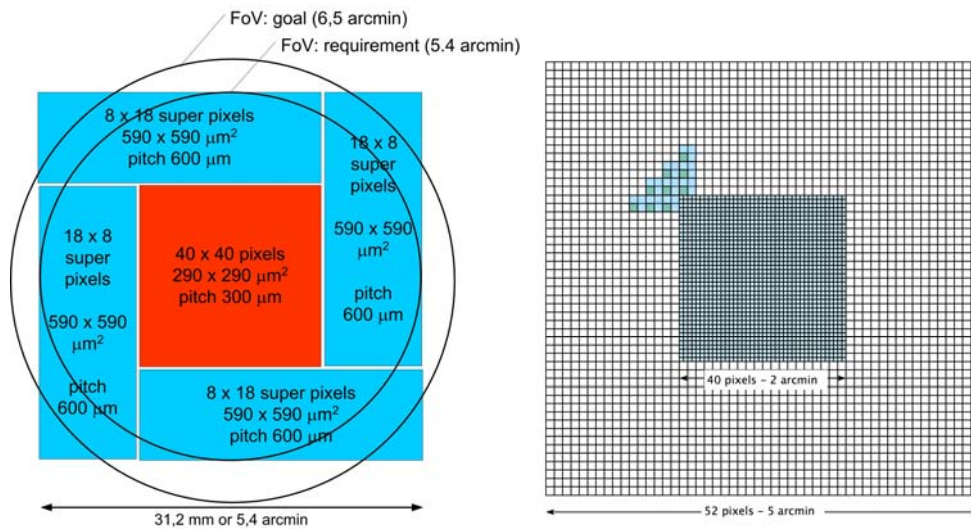


Figure 3-5 Two potential options for the layout of the Field of View showing the difference between the inner and outer array clearly. The outer pixels are twice as large and 4 pixels are read-out by a single TES.

Table 3-1 Instrument scientific requirements

Parameter	Requirement	Comment
Inner array		
Energy range	0.3 – 10 keV	Goal: 0.1 – 12 keV
Energy resolution ($E < 6$ keV)	2.5 eV	
FoV	2 arcmin	Corresponds to 40 x 40 pixels
Pixel size	300 μ m	The PSF (5 arcsec) corresponds to 0.5 mm and as such the pixel size is a compromise between FoV and undersampling of the PSF
Signal decay time (1/e)	300 μ s	Goal: 200 μ s
Outer array		
Energy range	0.3 – 10 keV	Goal: 0.1 – 12 keV
Energy resolution ($E < 6$ keV)	10 eV	Possibly this will be difficult to achieve and, for the large FoV, a value of 15 eV is more realistic
FoV	5.4 arcmin	Corresponds to a detector size of 31.2 x 31.2 mm ²
Pixel size	600 μ m	4 pixels will be read-out by a single TES with different thermal conductance between each pixel and the TES (so-called hydra's)
Signal decay time (1/e)	2000 μ s	Due to larger pixel size
Full array		
Absolute Time	50 μ s	
Time resolution	10 μ s	
Maximum count rate input on instrument	120.000 cts/sec	Observation of the Crab (120.000 cts/s) will be feasible using a diffuser (reduction > 0.15)
Maximum output from the instrument	20.000 cts/sec	Capability of backend processing for full detector array. At these rates the energy resolution could degrade (see requirement on the good grade events)
Typical count rate good grade events	500 cts/sec 50 counts/sec/pixel	During a typical observation (4 mCrab) $>80\%$ of the events will provide the nominal energy resolution (see 3.2.3.8). For bright point sources with > 100 cts/s/pixel a diffuser (see 3.2.4) can be included in the beam. This will introduce a reduction in the effective area.
Event size	42 – 64 bits	Depends on the user defined accuracy, spacecraft should be able to handle 64 bits/event
Quantum efficiency @ 1 keV	$> 60\%$	Entire instrument efficiency (e.g. blocking support structure in filters result in a QE ~ 0.7 and packing efficiency ($\sim 95\%$))
Quantum efficiency @ 7 keV	$> 80\%$	Defines absorber thickness
Energy resolution uniformity (FWHM)	1 eV	Fit by a Gaussian distribution
Detector dead area	$< 5\%$	Pixels with E-resolution $> 3 * \text{nominal}$ or QE $< 0.5 \text{ nominal QE}$

Straylight at main shell filter at 0.5 μm at 10 μm	$< 2.5 \cdot 10^9 \text{ ph/cm}^2/\text{s}$ $< 10^{17} \text{ ph/cm}^2/\text{s}$	Straylight will degrade the energy resolution of the detector. The specified levels are indicative and correspond to a degradation of the spectral resolution of less than 1 eV. More details are given in section 3.7.1.
Micrometeorites	< 38 pinholes of 100 μm diameter in OBF	Corresponds to a degradation of the energy resolution of 0.2 eV
Effective area change due to contamination over lifetime	$< 10\%$ over $0.2 < E < 1 \text{ keV}$	Depending on the contaminant (water) or hydrocarbons
Transmission fixed optical filters at 0.25 keV at 1.0 keV at 6 keV	0.1 0.7 0.9	Corresponds to 5 filters similar to those planned for astro-H (see section 3.2.4). The goal is to Si mesh filters with 20 nm Al and 45 nm parylene, increasing the transmission at low energy by a factor 2
Magnitude of early bright stars	$\text{mv} > 2$	Some objects (e.g. O, B stars are intrinsically very bright and to obtain a proper spectral resolution it will be required to attenuate the component so the energy resolution degrades by less than 0.5 eV A filter wheel with optical filters will be implemented
Non X-ray background	$2 \cdot 10^{-2} \text{ counts/cm}^2/\text{keV/s}$	This number is 4 times the background measured in Suzaku (due to the different orbit). In narrow lines this contribution is negligible. To obtain this level an anti-coincidence detector is required.
Continuous observing time	> 31 hour	Dimensions the cooling system
Instrument setup time	1 hour	1 hour to stabilize the instrument response such that, after corrections, the nominal resolution is achievable
Regeneration time	< 10 hr	Could be considerably shorter (1 hr)
Energy scale stability	1 eV / h	The non correctable drifts are part of the energy resolution. Drifts in the order of 1eV/h can be corrected. This requires: - a stable environment of the electronics - the capability to monitor the energy scale using onboard calibration sources (either on the filter wheel or electronically controlled)
Relative uncertainty in QE between pixels	$< 3\%$	This will be achieved by a combination of measures: - ground calibrations - in orbit verification on chosen sources - onboard calibration sources - dithering (to disentangle QE variations from source variations)

3.2.3 Instrument configuration

3.2.3.1 Instrument overview

The configuration of the instrument includes the electronics for the detector, the electronics to operate the cryo-coolers and control electronics. The detector is located inside a dewar, which is cooled by a set of cryo-coolers with its dedicated drive electronics. The Front End Electronics (FEE) is galvanically well connected to the detector. The amplified signals from the FEE are passed to the Digital Electronics where the data is digitized, the feed back signal is generated and the (demodulated) triggered event data, including triggers from the anti-coincidence detector are fed to the event processing electronics. In the Event processing unit the relevant event parameters (e.g. energy, time stamp, and event grade) are determined. The Instrument Control Unit (prime or redundant) is responsible for operating the instrument with the desired settings and also monitors the health of the instrument. It uses SpaceWire for its communications. The Power Supply Unit distributes the raw power over the cooler drives and provides regulated power for the electronic boxes. Some units are cold redundant whereas in other cases parallel signal chains are implemented (warm redundancy). This is shown in Figure 3-6.

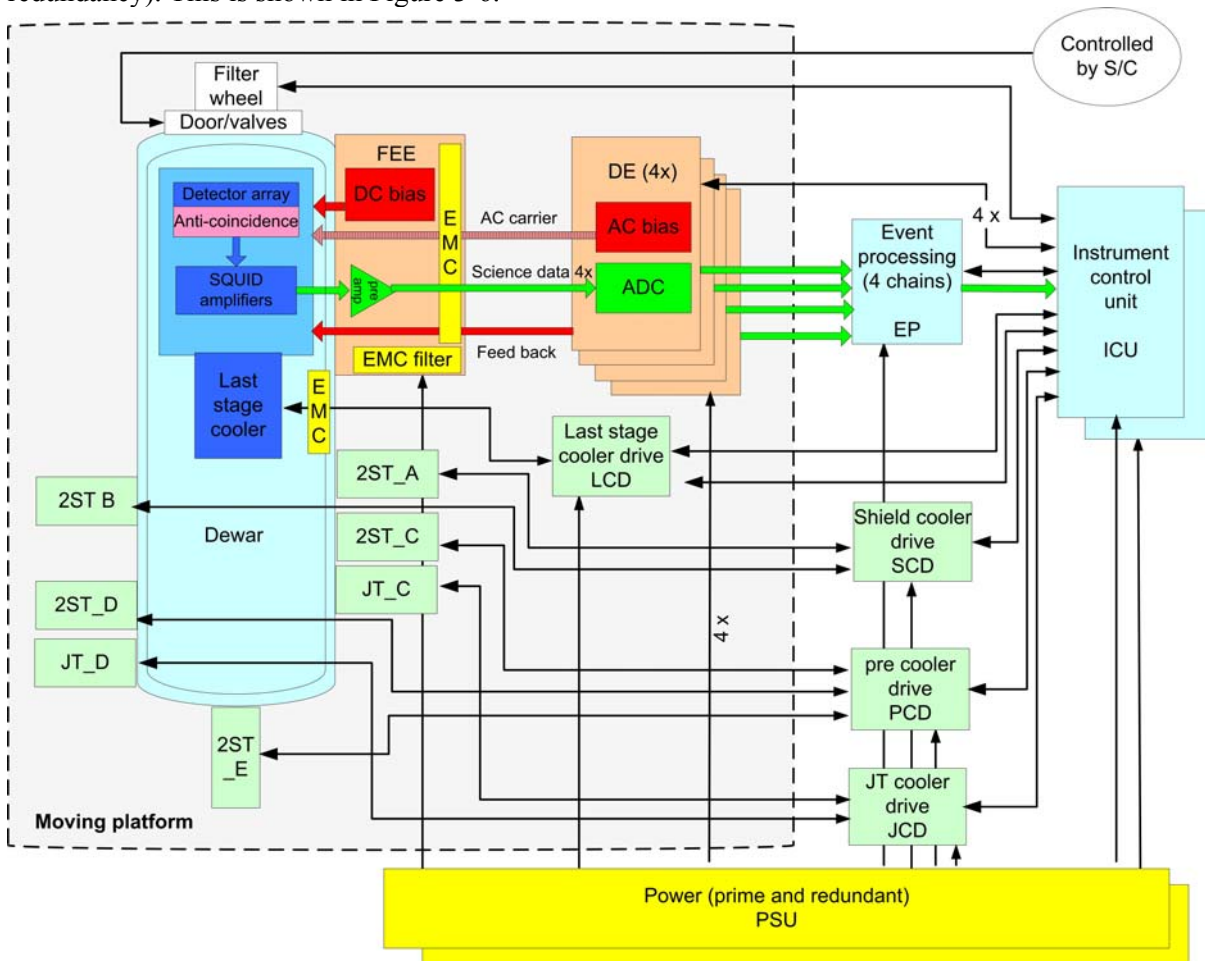


Figure 3-6 XMS configuration; the moveable platform is supposed to be provided by the spacecraft. Some optimization in the cabling is feasible (see text)

Potentially some of the cabling between the moving platform and the units at the fixed platform can be routed through a single SpaceWire router (e.g. all commanding.....). Typically all cabling for commanding and housekeeping for the filter wheel, the 4 DE boxes and the LCD can be routed through such SpaceWire router reducing these cables by a factor 6 (from 12 to 2) at the cost of two additional small boxes on the moving platform.

Table 3-2 Units for the XMS instrument

Unit	Number of units	Redundancy	Description
FEE	1	Warm	The Front End Electronics accommodates the low-noise-amplifiers (LNA) used to amplify the SQUID outputs. This box also contains the DC-bias sources for the SQUIDS. A separate card is foreseen for the low-noise amplifiers and DC-bias sources for the anti-coincidence SQUIDS. The box is galvanically (<better than 1 mΩ) integrated with the cryostat (either by bolting directly on the cryostat or by a < 0.5m cable) to form a Faraday cage with the focal plane instrumentation. The harness (if any) between this box and the dewar should be stiff (e.g. both units should be on the same platform)
DE	4	Warm	The digital electronics contains the following functionality: <ul style="list-style-type: none"> - digitization of the continuous datastream - generation of a feedback signal to linearize the SQUID amplifier response - generate the VETO signal from the anticoincidence detector - selection of events (trigger) to feed to the Event Processor box <p>The main components in this unit include ADC's, DAC's, and FPGA's (ASIC). The DE units can be located at a certain distance (typically 1 – 2 m) from the FEE-box.</p>
Dewar	1	n/a	The dewar provides the low and stable temperature (about 50 mK) for the detector and includes a combination of passively and actively cooled shields. It contains the following sub-units: <ul style="list-style-type: none"> - detector array - Anti-coincidence detector: a detector in the close vicinity of the detector (directly attached) which will detect charge particles. In the event logic this signal will be used to reject or flag non X-ray events onboard - Helmholtz coil allowing to tune magnetic field perpendicular to the detector array - Multiplexed read-out electronics: This is the system of fast switches (TDM) or LC-filters (FDM) with the very sensitive SQUID-based read-out amplifiers for the detector array and the few SQUID-amplifiers for the anti-coincidence detector - Cryogenic harness for detectors and housekeeping - Thermal shielding and shielding against magnetic fields (cryoperm

			<p>and superconducting shields)</p> <ul style="list-style-type: none"> - Thermal sensors to facilitate thermal stabilization of several (TBD)temperatures - optical blocking filters. These are needed for thermal control of the detector and also provide attenuation of any stray light. Heating of the outer filter will be provided by the instrument for decontamination. Typical 5 filters, connected to the various thermal shields, will be used; - vacuum door, the dewar will be launched evacuated to reduce the acoustic load on the dewar filters - cryo-coolers: the dewar includes a number of shields (3 or 4), thermally isolated and cooled by a set of cryo-coolers (in the current concepts these are Stirling or pulse tube and Joule-Thomson coolers). These coolers will be attached at the outer skin of the dewar and require a separate system for dissipation of the generated heat (heat pipes with radiator)
FW	1	n/a	filter wheel with 6 (TBD) positions including an open position and a closed position to protect the detector
EP	1 + 1	Cold	In the event processing box the triggered events from the DE are processed to extract the event parameters (energy, time, position). In addition the events are flagged for, veto signal from the anti-coincidence detector, event grade (low resolution, high resolution, etc)
SWR	TBD	Cold	A SpaceWire router can be implemented on the Movable Instrument Platform hence reducing the cabling between this platform and the rest of the satellite. Currently this is not part of the baseline.
ICU	1 + 1	Cold	This instrument control unit can autonomously set-up and control the instrument. It will also autonomously take action if instrument HK parameters get out of limit. It interfaces with the S/C and performs critical health checks of the instrument.
PSU	1 + 1	Cold	The Power Supply Unit distributes the raw spacecraft power over the cooler drive electronics (PCD, SCD, JTD) and provides regulated secondary power for all other units.
SCD	1	Warm	Shield Cooler Driver drives a set of Stirling coolers (not required in the case of the pulse tube/JT option
PCD	1	Warm	The Pre Cooler Drive drives the pre-cooling of the Joule-Thomson coolers. This unit is identical to the SCD for the Stirling option and to the JTD for the pulse tube option
JTD	1	Warm	The Joule-Thomson cooler Drive drives the J-T cooler (providing the 2.5 K reference temperature for the last stage cooler
LCD	1	Warm	The last stage cooler (ADR) Drive drives the large stage cooler during observation and regeneration and ensures the required temperature and stability

Some items are not part of the instrument but critical for its proper performance. These are listed in Table 3-3.

Table 3-3 Spacecraft functions required for the XMS

item	Function/requirement
Radiator	Heat dissipation of the cryostat (especially the cryo coolers) and the relevant electronic boxes
baffle	protects the FoV of the instrument against direct radiation form the sky. The detector array only sees the inside of the opaque telescope tube and the back of the X-ray optics without vignetting the FoV. In addition this baffle will include an electron and proton deflector which avoids electrons up to 20 keV (TBC) to hit the detector entrance filters. It should be noted that the baffle should, preferably, allow the FoV to be 6.5 arcmin using a larger part of the detector for science.
Pyro control	It is assumed that the spacecraft will be able to control the pyros required for the instrument (< 4, TBC). One for the door mechanism and two for the venting valves on the dewar (one with a small opening to be used initially and one with a larger capacity).
Thermal control	Thermal control of all units will be done by the thermal control system of the spacecraft. It should be noted that maintaining the non-operational and operational temperatures is critical and should be achieved independently of the instrument status (including during its OFF stage when cruising to L2).
Ground access	For ground operations it is required to have access to the filling ports of the LN2 reservoir of the dewar, and to the evacuation port of the dewar.
Straylight	See section 3.7.1
Stray magnetic field	< 10 ⁻⁴ T at the position of the instrument, see section 3.6.1.2 for more details
Temperature dewar outer shell	< 300 K, see section 3.4.1
Temperature JT compressors	< 303 K, turn-on and operational temperature ranges of the JT compressors is relatively narrow, see section 3.4.1

3.2.3.2 Redundancy

Space missions require optimal reliability. For cryogenic instruments this is in particular a challenge as the introduction of redundant cooling capability also implies a considerable increase in complexity (and thus reduced reliability). The ultimate solution is to fly more than one cryogenic instrument (assuming that there are no design flaws these could be identical). Unfortunately this is not possible. Therefore we have chosen a design with the following main components:

- where possible we have implemented warm redundancy. Using four parallel control and data streams, failure in one stream would reduce the detector area by 25% but still a significant fraction will be operational
- cold redundancy for a number of units in which these signal chains are combined (e.g. the instrument digital control unit, the power distribution unit etc.
- over dimensioning of the cryo-coolers. The power levels of the cryo-coolers are dimensioned such that with the failure of a single cryo-cooling chain, the 50 mK level is still feasible.

Despite this approach there are some parts in which full redundancy is not possible as the extra complexity for this redundancy (in heat switches) not only introduces improved redundancy but also adds components

which may fail. Where possible the control of such switches will be implemented in a redundant way (e.g. driven by two independent parallel electrical circuits).

3.2.3.3 Detector

The detector consists of the following components:

- The detector consists of an array with absorbers read-out by transition edge sensors. This array is produced using micro-machining technology and is supported by the detector chip (which is an integral part of the detector). This array has an inner section with an energy resolution < 2.5 eV and an outer section with larger and slower pixels with an energy resolution of < 10 eV (see Figure 3-5). Four pixels of the outer array are connected to one TES each with a different thermal conductivity. These are called super pixels. Using the difference in thermal rise time the position of the event in a super pixel can be determined. This is illustrated in Figure 3-9.
- For the read-out multiplex electronics is used. One element of this multiplex electronics are the SQUID current amplifiers. The current baseline for both TDM and FDM is two have a 2-stage SQUID amplifier. For TDM the current baseline is to have both the 1st stage SQUIDs and the 2nd stage array SQUIDs at 50 mK. For FDM the approach is to have the 2nd stage SQUID-arrays at a higher temperature (~ 1 K), thereby allowing a more powerful SQUID to drive a higher resistive cable. The other cold elements of the multiplexer chain are SQUID-based switches (TDM) or LC-filters (FDM). They consume virtually no power and are mounted at 50 mK. Precise mounting of the electronics has not yet been decided and can be just underneath the detector array or could be at the sides (rotated over 90 degree to increase the available space). The differences in the cooling systems between these options is small and can be neglected till a final selection of the read-out system is made,
- The anti-coincidence detector is mounted underneath the detector (to increase its effective solid angle). Currently it is assumed that this will be a Si detector read-out by a set of TES detectors.
- A set of Helmholtz coils is available to control the magnetic field in the detector. For the SQUIDS special shielding is implemented (see section 3.2.3.5)

This is illustrated in Figure 3-7 where the thermal connection to the cold finger (at 50 mK) is only schematically shown. Some relevant parameters for the detector are listed in Table 3-4.

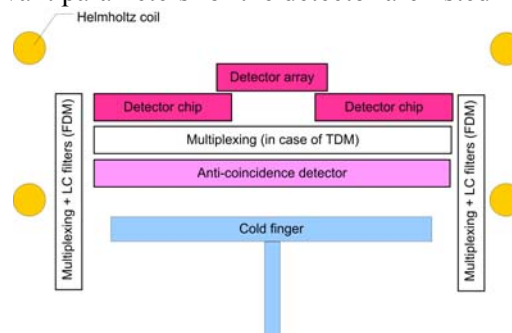


Figure 3-7 Schematic overview of the detector; the detector electronics can be placed directly underneath the detector proper or at the side.

A possible realization of the detector head for FDM is shown in Figure 3-8 (left). It contains the X-ray micro-calorimeter array, the LC-filter chips, the SQUID amplifiers, and the Helmholtz coils and the anti-coincidence detector together with the interconnection structure, the electrical interconnection harness, and the cryoperm/superconducting shields. In the design shown the TES-array, LC-filters, and anti-coincidence detector are at the 50 mK base temperature of the cryostat, while the SQUIDS and their shielding have been moved to 0.3 or 1K, depending the chosen cooler chain and its T-stages. At 2.5 K the overall Cryoperm/superconducting shield is situated. Depending on the SQUIDS finally used, and their power dissipation the SQUIDS could also be located at 50 mK.

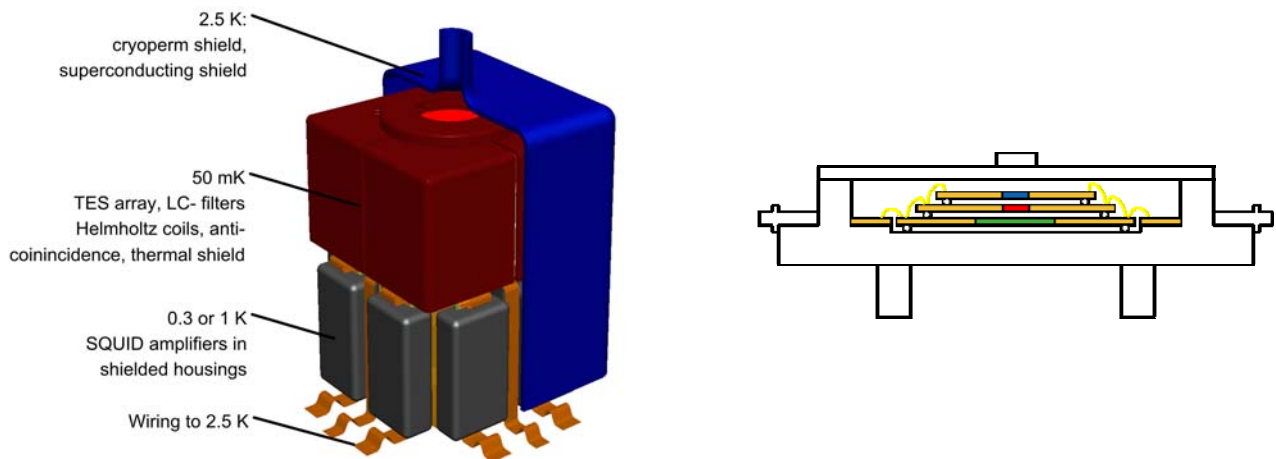


Figure 3-8 Detector head (left: possible layout in case of FDM requiring interconnections between components in two orthogonal planes (SRON); right: a possible alternative solution in case of TDM where potentially all components (detector, TDM and anti-coincidence detector) can be mounted in a configuration with all planes parallel to each other (TBC that this is feasible)

The read-out of the outer pixels (super pixels) (which are $600 \times 600 \mu\text{m}^2$) are multiplexed on a single TES (4 pixels onto one TES) using a variable thermal link. This is illustrated in Figure 3-9. This allows determining the event position by rise time determination.

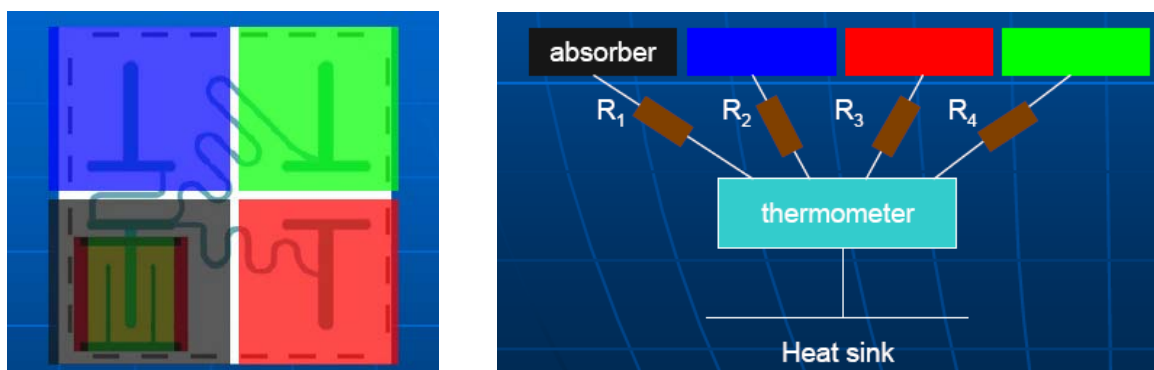


Figure 3-9 Schematic read-out of a super pixel illustrating the differences in thermal conductivity to the TES and bath temperature

The specifications of the detector are directly deduced from the science requirements.

Table 3-4 Some relevant parameters of the TES detector

Parameter	Value
Inner array	40 x 40 pixels of 300 x 300 μm^2
Outer array	4 sectors of 8 x 18 superpixels. Each superpixel includes a single TES connected to 4 larger (600 x 600 μm^2) absorbers
Read-out inner array	40 channels where each is multiplexing 40 detectors
Read-out outer array	4 x 8 channels where each channel is multiplexing 18 super pixels
Absorber thickness	7 μm Bi with a Cu thermalisation layer or 1.7 μm Au and 4-5 μm Bi

3.2.3.4 Read-out

For the read-out of a large array it is required to multiplex the detector elements at its bath temperature. This can be implemented in different ways:

- Time Domain Multiplexing where a set of pixels is connected to a single read-out channel and the signal of each pixel is multiplexed in time
- Frequency Domain Multiplexing where a set of pixels is connected to a single read-out channel but the pixels are separated in frequency space

a) *Time domain multiplexing*

Superconducting quantum interference devices (SQUIDs) are well matched to reading the current signals from these low-resistance (typically a few $\text{m}\Omega$ under optimal bias) sensors. Multiplexed readout is motivated by the need to reduce the number of wires running to the low temperature stages of the instrument for effective management of heat loads and design complexity. In the time-division multiplexing (TDM) concept, the outputs from the dedicated input SQUIDs of individual TES pixels are coupled to a single amplifier, and multiplexing is achieved by sequential switching of these input SQUIDs. Additional reduction in wire count is achieved by using common bias lines for multiple TES bias circuits; each bias circuit consists of a shunt resistor, the TES, the SQUID input coil, and additional inductance for filtering the detector response. Columns of individual bias circuits are biased in series with a common dc current. The reference design is based on 32-row multiplexing, with which the entire XMS focal plane array can be instrumented with 68 signal channels. Figure 3-10 is a schematic of the TDM read out.

amplifier. The electronics (digital) providing the feedback signal is outside the cryostat. Flux offsets for the 1st and 2nd stage SQUIDs are provided as well.

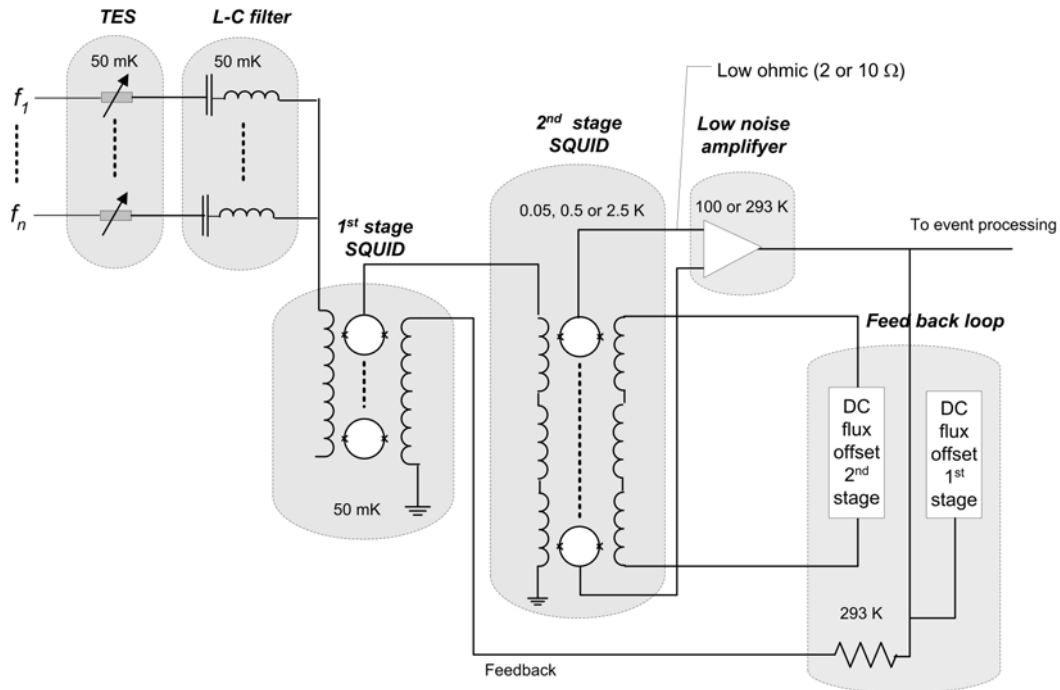


Figure 3-11 Array read-out scheme in case of FDM multiplexing

In the FDM topology the bias voltages to each column are supplied as a frequency comb, with each frequency centered at the LC-filter frequency for each pixel. This comb is transferred to a voltage bias by a divider network. Till now resistive divider networks have been used to create voltage bias. AC-bias allows however to use a capacitive divider network, which has the advantage to have no power dissipation. Such a bias layout is shown in Figure 3-12.

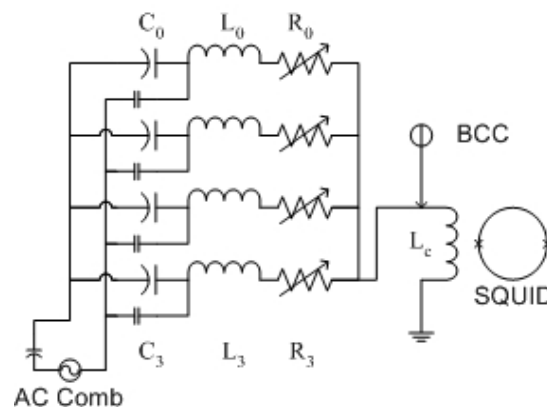


Figure 3-12 Bias configuration for one signal chain. Bias is accomplished by AC-bias comb with capacitive voltage divider. The comb is separated to the individual pixels by the pass band of each LC-filter. Bias-Current-Cancellation (BCC) is possible by feeding an out of phase bias comb to the SQUID input. Since Baseband Feedback has very high loop gain at each carrier frequency BCC is probably not required.

The current signals from each TES in one signal chain are summed at the input coil of the 1st stage SQUID, which therefore acts as the common impedance of the circuit. To keep crosstalk below $5 \cdot 10^{-3}$ the inductance has to be < 5 nH. For a single column up to ~ 45 detector elements can be multiplexed using a frequency band width between 1 – 10 MHz and a channel separation of 0.2 MHz.

Given the sinusoidal SQUID response the linear input range is restricted to $< \pm 1/8 \Phi_0$. To increase the dynamic range the SQUID will be operated in a feedback circuit, which is generally called a flux-lock-loop (FLL). Operation in FLL increases the dynamic range by a factor $(1+G_{FB})$ with G_{FB} the closed loop gain of the FLL. Furthermore it reduces the higher harmonics due the SQUID non-linear response by a factor $(1+G_{FB})^{n-1}$ for the nth order.

Baseband Feedback

The maximum gain-bandwidth of a feedback loop is limited by cable delay and phase rotation in harness and electronics. Such a system is not able to create significant gains $(1+G_{FB})$ up to the highest carrier frequency (10 MHz) intended to be used for FDM. The signal bandwidth is however only 10 kHz and the carriers are pre-determined. This allows creating feedback with sufficient gain-bandwidth for a signal (baseband) around each carrier frequency, so-called baseband feedback.

The technique is based on the fact that the information band of each signal is only about 10 kHz and that the 1 – 10 MHz AC-carriers are pre-determined, so that it is possible to compensate the feedback signals for delay by an appropriate phase-shift for each carrier. An overall block diagram of the "base band feedback" concept for the read-out of an X-ray spectrometer is shown in Figure 3-13. For each read-out column demodulation and subsequent filtering (integrator) of all M signals after amplification is required. The emerging baseband signals are re-modulated with their carriers and subsequently fed back to the summing point. The phases of the carriers used for re-modulation are adjusted such that the gain-bandwidth for each signal is centered around each carrier frequency. So the full 1 – 10 MHz bandwidth becomes available for multiplexing. The maximum gain-bandwidth around each carrier is approximately $\Delta f/6$, with Δf the carrier separation. For 200 kHz separation this results in a gain-bandwidth of 33 kHz, allowing for a loopgain G_{FB} of 3.3 x at the maximum signal frequency (10 kHz). The feedback gain at the carrier frequency is limited by calculation accuracies and noise. A value of 55 dB has been demonstrated.

The generation of AC-carriers and the baseband feedback calculations are all performed in the digital electronics, at present still FPGA-based, but for space applications ASICs are foreseen in order to reduce power dissipation.

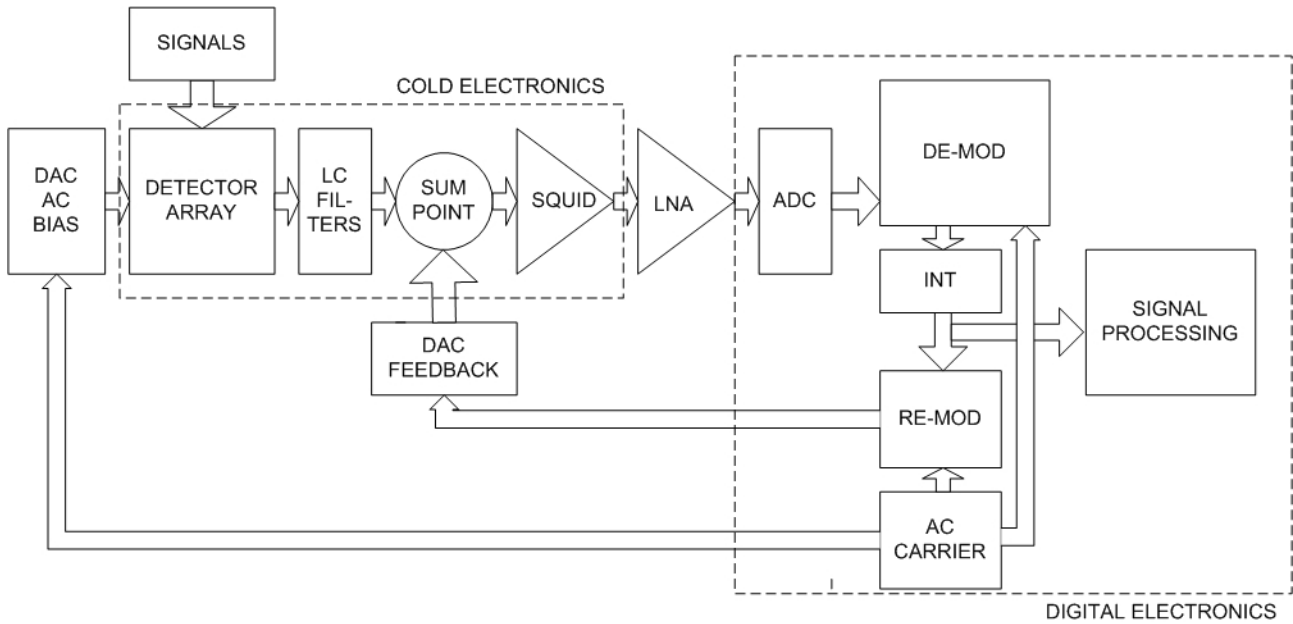


Figure 3-13 Block diagram of the Base band-FLL system

3.2.3.5 Helmholtz coils

The magnetic field and its stability have a major impact on the energy resolution. The presence of a magnet with a field perpendicular to the detector array allows tuning the field in which the sensors operate. Most often that is zero or a value quite close to that. The magnet also allows to compensate permanent fields at the detector, residues from external fields in the satellite or from the ADR-cooler. The stability of the field is extremely important as **0.1 – 0.15 mGauss variations changes the responsivity $\Delta S/S$ by about 10^{-4} .**

The other parameter of importance is the uniformity of the magnetic field over the TES-array. So far not a clear cut field uniformity specification does exist. At this moment we set it to 20% over the area of the device at the bottom end (see table 6-1). The magnet is designed to 2% uniformity.

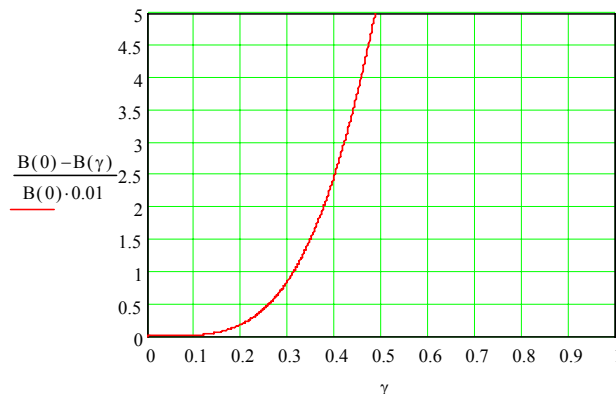


Figure 3-14 Helmholtz Magnetic Field uniformity

Figure 3-14 illustrates the uniformity of the magnetic field generated by a Helmholtz coil, actually consisting of two flat solenoids of diameter $2R$ separated from each other by a distance R . The graph shows the deviation from the on-axis field as a function of the off-axis distance $\varphi = x/R$. A uniformity of 2% can be met for a detector size equal to 0.38 of the coil diameter. This means that for a 3.2×3.2 cm detector we need coils with a diameter of $3.2/0.38 \cdot \sqrt{2} = 11.9$ cm. For the present moment we define the Helmholtz magnet as two flat coils with a diameter of 12 cm separated by 6 cm from each other. The on-axis magnetic field of a

Helmholtz coil is given by $B = \left(\frac{4}{5}\right)^{\frac{3}{2}} \frac{\mu_0 In}{R}$ with I the current through the coil, n the number of windings, R the coil radius, and μ_0 the permeability. If we chose to operate such that 1 Gauss is created by about 50 mA then the number of windings $n = 133$

3.2.3.6 Anti-coincidence detector

Due to the large surface of the TES-Array, a CryoAC detector segmented in 4 pixels (TBC) is the current baseline. Each pixel is employing a Silicon absorber with a TES microcalorimeter. Both the size and thickness values of each pixel, that define the rejection efficiency and the energy bandwidth of the detector, are based on the analysis of the expected particle background in IXO orbit that is now on going. From preliminary results, for each pixel an area of $18 \times 18 \text{ mm}^2$ (TBC) and a thickness lower than $300 \mu\text{m}$ (TBC) are adopted. Different configurations, with 2 or 3 pixels, slightly increase the bandwidth, while the dead time rises quickly for high count-rate.

From a phenomenological point of view from an event hitting the detector (silicon cooled down to sub-Kelvin temperature) two kind of merged pulses are expected, thermal and ballistic ones, whose rise time is quite different: some μs for thermal component and some hundreds of ns for ballistic component thus increasing the electric bandwidth. The ratio between the amplitude of the two components strongly depends on the distance between the TES and the incident particle and the surface-to-bulk ratio of the absorber. Since the CryoAC must be faster than the XMS calorimeter to efficiently reject particle events, the thermal component is used as baseline pulse to flag such events, but also the ballistic feature can be taken into account if higher timing is necessary. From the electrical point of view, the rising edge of the ballistic pulse must be taken into account for a correct design of the readout electronics

The electrical read-out of the TES CryoAC is based on standard FLL SQUID read out. We foresee 4 SQUID readout for 4 (TBC) TES sensors. Another part of the electrical design has to do with the non-linear response and limited dynamic range of the SQUID amplifiers. The commonly used way to linearize the response and increase the dynamic range of SQUIDs is by means of feedback. This feedback is generally called a flux-locked-loop, since it tends to zero the flux inside the SQUID loop. In the case of the CryoAC, the SQUID feedback can be closed in warm environment

Table 3-5 anti-coincidence detector specifications

Parameter	value
Number of Pixel	4
Pixel size	$18 \times 18 \text{ mm}^2$
Thickness	$< 300 \mu\text{m}$
Energy Bandwidth	10keV-1MeV (TBC)
Rise Time	$< 10 \mu\text{s}$
Effective Fall time constant (ETF)	$< 70 \mu\text{s}$

TES Material	Ir/Au
Absorber Material	Silicon
Transition Temperature	50-100 mK
TES normal resistance Rn	0.1-0.5 Ω
TES bias resistance	0.1 \times Rn
Bandwidth	Thermal: 50 kHz; Ballistic: 500 kHz
Slew Rate	< 50 A/s
Dynamic Range	$\sim 10^6 \sqrt{\text{Hz}}$
Max proton count rate (@5% dead time)	20-30 cts $\text{cm}^{-2} \text{s}^{-1}$
AC veto efficiency	> 97%

3.2.3.7 Harness

In this section we describe the harness between the units on the movable platform and on the fixed S/C deck. As can be seen in Table 3-6 this is a significant amount of harness as only units which need to be close to the detector (DE, FEE and LCD) have been placed on the movable platform and the power converter for the DE boxes is placed on the fixed platform. Clearly, from the harness perspective this is far from optimal and need detailed study during the spacecraft trade-off (e.g. trade-off between locating the power conversion on the movable platform (and less harness) or on the spacecraft platform (and significantly more harness))

Table 3-6 Instrument harness

Type	Number of cables	Description	comment
Power for DEE	8	Typical 8 x AWG15 + 8 x AWG26	For PSU prime and PSU redundant, max 16 wires/cable with AWG15 for power lines
Power for FEE, SWR, FW	8	typical 8 x AWG20 + 8 x AWG26	
Control/HK FEE/DEE	2	Spacewire	Cables has been reduced by interroducing a Space Wire Router (few kg) on the MIP (not shown in the diagram (figure Figure 3-6
Power, control and HK for SCD (5)	5	8 x AWG20	Assumes multiplexing of HK information on the compressor/cold head,
Power control and HK for JTD (2)	2	8 x AWG20	
Power/control FW		4 x AWG20	
Data stream FEE	36	Spacewire	Maximum datarate per spacewire cable is 400 Mbitps. With the large datarate between the DE (4x) and the EP we need 9 cables each
Control electronic units	2	Spacewire	Control of all electronic units (FE, DE, FW) will be done via a prime and redundant Space Wire Router

The cryo-harness is described in section. 3.4.5

3.2.3.8 Count rate capability

The relaxation time of each pulse is a critical for the energy resolution: if two subsequent pulses are too close in time the resolution will degrade and this depends heavily on the signal decay time. This is illustrated in Figure 3-15. With a typical event decay time (τ) of 150 μsec and a 10 τ pre-trigger and 40 τ post trigger this results in a decrease of high-resolution events and an increase of low-resolution events with increasing countrate. An estimate of this effect is shown in Figure 3-15.

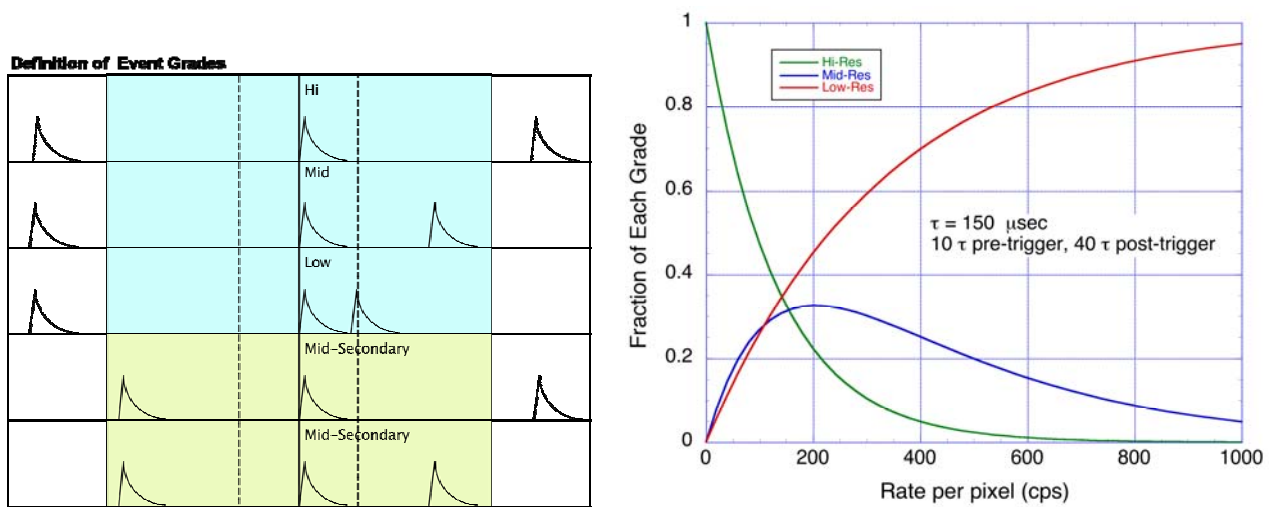


Figure 3-15 Fraction of events with the specified spectral resolution as function of the countrate For this example we have used 10 τ and 40 τ as selection criteria corresponding in high-resolution events with a resolution better than 2.7 eV and the low-resolution events with a resolution worse than about 3.5 eV. Using the diffuser (see section 3.2.4) the PSF can be spread over a number of pixels and hence affecting the ratio between events grades.

3.2.3.9 Onboard calibration

With a spectral resolution of $> 10^3$ it is extremely important to be able to monitor the stability of the instrument. In order to do this a set of measures are taken:

- Various electronic units and the detector require a very good temperature stability.
- The filter wheel will include radioactive sources which can be moved in and out of the beam
- Inside the detector there might be some pixels positioned outside the FoV and these might be directly illuminated by an Fe55 source
- The detector door will include a Be window which allows for ground testing with other radioactive sources
- An electrically controlled X-ray source (pyro-electrical or an electron impact source) is under study.

- A LED source could be implemented to verify the integrity of the optical blocking filters

3.2.3.10 Cryo-cooler

The detector has to be cooled to an operating temperature of 50 mK. To achieve this temperature over a mission duration > 5 year a cryogen free cooling system is required. There is a large set of potential solutions. We have selected three systems of which one is based on the Astro-H design, the second on the JWST-MIRO design, and the last one on the original XEUS-NFI2 design.

- A fully redundant design based on Astro-H
- B partially redundant design (electronics only) based on Astro-H
- C design based on JWST/MIRI cooler (similar reliability to JWST, > 5 year)
- D. Design based on JWST/MIRI cooler with reduced redundancy (only electrical)
- E. fully redundant design based on European pre-coolers with He3 sorption+ADR as last stage
- F. same as E, but only electrically redundant

Other designs with different advantages and disadvantages can be considered as well and a detailed trade-off, including an assessment of their technological readiness and reliability, is planned during the next phase.

Requirements on the cooling system are summarized in Table 3-7. Requirements allocated to the spacecraft system from the cooling system are listed in Table 3-8.

Table 3-7 Top level requirements on the cooling system. cooler characteristics (load only by detector electronics, related harness and the harness for the last stage cooler but excluding losses due to suspension and radiation)

Parameter	Value	Comment
Operational lifetime	> 5 years, with 10 year goal	Most likely a cryogen free system is required.
Reliability	> 95% (TBC)	Likelihood the cooling system will survive the mission lifetime (TBC by the agencies!)
Detector bath temperature	50 mK	The conducting/super-conducting transition will be around 100 mK
Temperature stability 50 mK	2 μ K/h	rms
Heat load from the detector system at 50 mK (sensor harness, detector, and front-end electronics)	1,5 μ W	In addition, parasitic heat loads from higher temperature stages must be considered, e.g. support wires, heat switch etc. The value includes contingency of 0.5 μ W.
Last stage cooler type	Single shot type is acceptable	In case of a continuous system the stability of the second temperature levels will be critical
Hold time of the last stage cooler	31 hr	30 hours + 1 hour setup time
Regeneration time of the last stage cooler	< 10 hr	Time needed to recycle the cooling system, is probably in the order of 1 hr
Heat load to the 2 nd stage at 0.5 K from detector electronics at 0.5 K	40 μ Wx2	From the ADR design this number is relatively large and preferred is 1.5 μ W*(500mK/50mK) ~

		15 μ W. A factor 2 is for design contingency
Stability of 2 nd stage	1 mK/h	Justification to be provided
Heat loads at 4 K or 2.5 or 1,7 from the detector Harness.	1.5 mWx2	In addition, parasitic loads from higher temperature stages (radiation and conduction), and from ADR (saltpill, magnet, and heat switch) must be considered. A factor of 2 is for design contingency.
Cooling power for last stage cooler at 2.5 K (TBC)	8.5 mW	This is the power available at the last stage cooler excluding the 1.5 mW required for the detector and its electronics
Heat load at 20 K from detector system (detector harness)	140 mW x2	In addition, parasitic loads from higher temperature stage must be considered. It is a nominal value, A factor of 2 is for design contingency
Heat load at 100 K from detector system (wire haress)	400 mW x 2	In addition, parasitic loads from higher temperature stage must be considered. It is a nominal value, A factor 2 is for design contingency
First resonance frequency	40 Hz (TBR)	The value will be updated after coupled load analysis with spacecraft and launch vehicle.
Requirements for ground tests. Outer shell temperature Time to reach 50 mK from room teperature	275 – 300K < 2 weeks	It is required to obtain 50 mK within 2 weeks, starting from room temperature
Magnet currents of the last stage cooler	< 5 A	
Magnetic fields at detector stage		See section 3.6.1.2
Redundancy	TBD	A system with redundancy in all mechanical coolers (i.e. excluding ADR), and a system without redundancy in mechanical coolers are considered.

The corresponding thermal schematic is shown in Figure 3-16. Part of the internal harness will be superconducting. The different temperature stages will be connected via CFRP and/or glass fiber reinforced plastic support straps which give an as low as possible thermal conductance while keeping the first resonance frequency during launch (at room temperature) above 40 Hz.

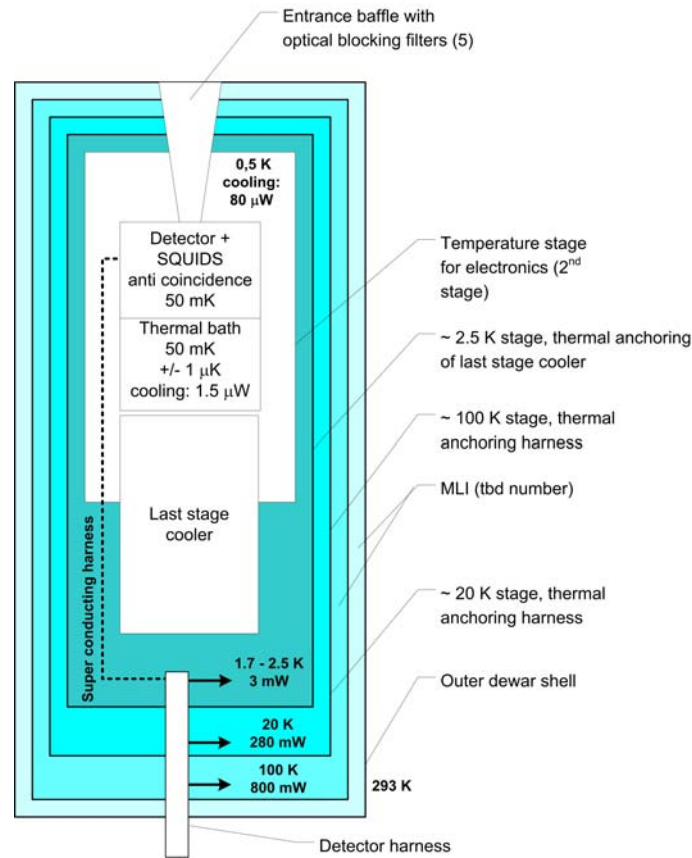


Figure 3-16 Thermal design of the cryo-cooler. The cooling power indicated is given for the detector electronics and its read-out harness (not the mechanical support of all stages or temperature sensors to control these stages). The cooling power of 10mW at 2.5 K includes parasitic loads. Heat load from detector harness is 1.5mW (2x)

Whereas the cryo-cooler is an item which is currently considered to be part of the instrument some cooling stages might be provided by one of the agencies. The specified cooling power at the different stages is indicative but, depending on the design, different intermediate temperatures (and hence corresponding cooling power) can be considered.

Table 3-8 Requirement allocation from the cooling system to the spacecraft system.

Parameter	Value	Comment
Temperature of the outer shell	≤ 290 K	Lower temperature is preferable and can reduce electrical power consumption of mechanical coolers.
Temperature of JT compressors	< 300 K	Turn-on and function temperature ranges of the JT compressor is relatively narrow. See Table 3-20. However, this is not the case for the JWST cooler

3.2.4 Instrument optical design

The optical design of the instrument is simple: the detector plane, which is inside the dewar on the central axis, should be within the specified accuracies from the focal point of the X-ray mirrors. Some components which have effects on the optical design include:

- a) The *filter wheel* is a disc with different slots in which different filters can be inserted. By rotation of the filter wheel different filters can be selected. The filter wheel position may be selected per observation according to necessity for additional optical light-blocking, for calibration source deployment or for safety. Safety operations may be required autonomously or via ground control to prevent excessive charged particle fluence (solar flare or local magnetospheric storms), micrometeorite protection or spacecraft attitude loss. The filter wheel is foreseen to have 6 positions (TBC) and the following filters are under consideration:
- beam diverter to reduce the countrate per pixel in case of strong point sources (a bended multi-channel plate, which needs to be properly aligned and has its own specific energy response is being studied). The basic principles of such diverter (courtesy Dick Willingale) are shown in Figure 3-17.
 - polarization sensitive filters (preferably these could be continuously rotated around the optical axis but this is probably too demanding)
 - optical filters (to suppress light from the objects which are observed).
 - a closed position to protect the instrument in case of emergencies and periods of high radiation
 - an open position (which gives the best sensitivity)
 - a position which includes an on-board calibration source (being either a radio active source or an electronically controlled electron source with a target)

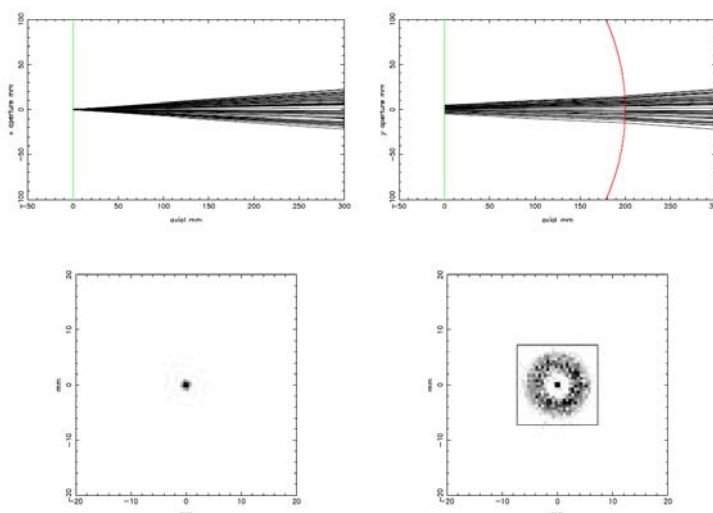


Figure 3-17 Effect of a beam diverter (bended multi channel plate) on the PSF. Left: nominal case: right after insertion of the beam diverter. Clearly the beam is spread over a larger number of pixels but at the expense of a limited efficiency of the beam diverter itself (order 30-40%)

In order to observe bright stars it will be necessary to reduce the optical light of such objects by inserting an additional optical blocking filter in the beam (as this also reduces the X-ray throughput this filter will only be used for optical bright objects). Accepting a resolution degradation of 0.2 eV and assuming a 10^{-5} transmission through the fixed optical blocking filters in the dewar we require a $2.5 \cdot 10^5$ suppression for O stars ($M_v = 2$), $5.2 \cdot 10^4$ for B0 stars ($M_v=2$) and $1.4 \cdot 10^3$ for A stars. Hence we reserve two positions in the filter wheel for additional filters with a suppression of 10^5 and $5 \cdot 10^2$. Typical the thickness will correspond to 10^5 and $5 \cdot 10^2$ suppression of optical photons (the thick filter is 200 nm polyimide with two layers of Al (total thickness 120 nm, TBC))

The filter wheel will be mounted on the dewar. Typical dimensions of a filter are 60 mm assuming a mirror diameter of 3.8 meter (maximum) and the distance between the detector and the filter wheel of < 0.3 m. The filter wheel is a disk of 400 mm (diameter) by 100 mm but at the location of the motor (diameter < 100 mm) the height will be 150 mm. The vacuum door of the dewar will be integrated with the filter wheel.

- b) Secondly the instrument requires fixed *light blocking filters* in the dewar to reduce the optical loading of the micro-calorimeter array by the sky and the thermal loading from the warm environment together with its inherent photon noise. In the optical regime those filters will require a rejection ratio of at least 10^5 (TBC), while thermal infrared radiation from a 300 K background must be attenuated by a factor of $\sim 10^9$ for wavelengths between 2 μm and 2 cm or it will degrade the detector performance. Light leakage of the satellite tube for solar photons is an additional concern and the intensity at the instrument entrance should be kept low (see section 3.7.1 for more details)

Notwithstanding these blocking filters we would like to observe soft X-rays down to the 100 eV range with good efficiency, but no material exists with a sufficiently high ratio of absorption coefficients between 0.5 eV and 100 eV. We instead make use of the very large real index of refraction of aluminum in the infrared to reflect away the long wavelength radiation. It is advantageous to divide the aluminum into several thin layers, since infrared has large reflection losses at each surface, while X-rays are relatively unaffected by surfaces. In general several of these filters are distributed over the entrances of the various heat shields in the cryostat. The filters are slightly tilted (\approx few degrees) with respect to each other in order to minimize multiple reflections. As a baseline we take 5 filters with a total of 280 nm polyimide and 210 nm Al with an integrated grid. The goal is a set of 5 filters with a total of 100 nm Al and 225 nm polyimide with a support grid per filter of 8 μm thick Si (97.2% open per filter). These filters have been developed for a Wisconsin rocket experiment and fulfill the background rejection requirements. Its diameter should be enlarged by a factor of about 2 (from around 4 cm diameter to about 9 cm). The X-ray transparency of the baseline and goal filter combination is shown in Figure 3-18. Heating of the filters is possible to evaporate possible condensable on the filters.

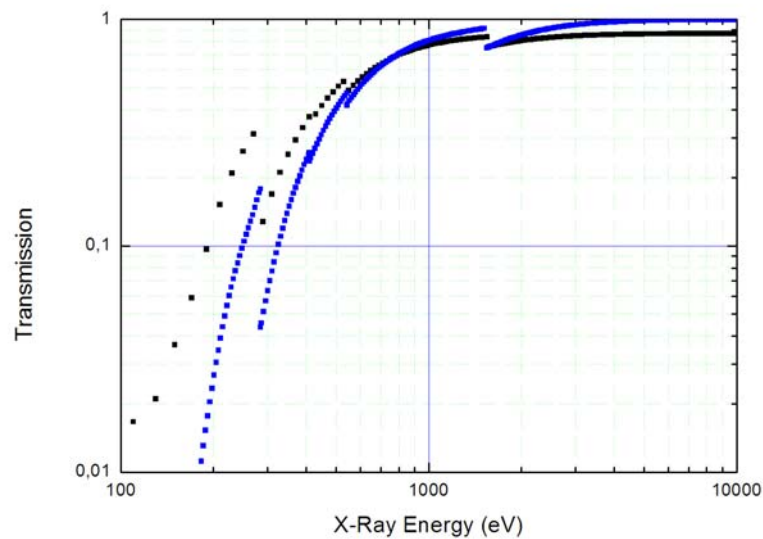


Figure 3-18 Transmission of baseline (blue) and goal (black) optical blocking filters (note that in case of the black curve the maximum transmission at high energies is underestimated (we simply used 97.2% transmission and neglected the fact that Si is transparent at these energies))

- c) In addition X-rays up to 10 keV from outside the FoV have to be suppressed by a factor 10 (TBC). With this suppression the contribution of this component over the field of view of the detector (< 0.2 sr) will be a factor 2 to 4 below the particle background of $2 \cdot 10^{-2}$ counts/cm²/s/keV. The satellite tube structure together with an instrument baffle will have to provide the required shielding.
- d) Charged particles will deposit energy in the detector. We adopt a limit of 20 keV for the energy deposit of the charged particles in the detector, well above the energy range of the detector. As charged particles loose energy in filters the most demanding condition is the situation where the thick filter in the filter wheel is in the beam. As this filter will be used for bright point sources only, in these cases a somewhat higher background is acceptable and this condition is therefore listed as goal only (see Table 3-9)

Table 3-9 charged particle deflector requirements

	Material	Electro n	proton
Requirement (only fixed optical blocking filters)	210 nm Al and 280 nm polyimide:	21 keV	78 keV
Goal (including thick optical filter in filter wheel)	+ 120 nm Al and 200 nm polyimide	21 keV	112 keV

- e) Micro meteorites: Initial estimates indicate that up to about 40 pinholes of 100 μm diameter, even if co-aligned, do not affect the energy resolution significantly (< 0.2 eV). These pinholes typically result in a 10% overall transmission increase due to the pinholes (and thus increase in the optical loading in the IR). If a micro meteorite will hit the detector array the effect is damage to a single pixel or to one read-out chain (if contacts would be damaged). Further analysis should translate this requirement in the need to have a highly transparent very fine mesh in the filter wheel or in front of

the filter stack to protect the filter stack against the impact of the larger particles. This clearly depends on the expected particle flux (frequency, size and velocity of the micro meteorites).

3.2.5 Instrument units mechanical design

The instrument mechanical design is driven by the requirement to operate the detector at 50 mK. To provide this temperature over the required lifetime a cryostat with shields at various temperature stages between 300 K and 50 mK is required. Mechanical coolers will be used to cool down these various shields and the focal plane, currently we assume a combination of Stirling coolers or pulse tube and Joule-Thomson coolers combined with an Adiabatic Demagnetization Refrigerator. These coolers and the detector have dedicated electronic boxes. Some of these boxes have stringent conditions on the distance to the detector (and cryostat) and will therefore be positioned at the same platform (moving) as the dewar with the detector (see Figure 3-6).

The mechanical design should also result in low enough vibration levels to prevent microphonic degradation of the instrument performance. Preliminary values from “warm” measurements on a microphonics free (not much margin) laboratory cryostat indicate that the typical acceleration levels on the 4K shield equals $< 3.5 \mu\text{g}/\sqrt{\text{Hz}}$ (see section 6.2). More work has to be done to transfer that to the detector stage (50 mK) and to extract requirements.

3.2.6 Mechanisms

The instrument mechanisms are given in Table 3-10.

Table 3-10 Mechanisms for XMS

Parameter	Controlled by	Comment
Filter wheel/door	Instrument/spacecraft	The filter wheel includes 6 positions and the door of the dewar is integrated. It is assumed that the initial opening (door function) will be performed by the spacecraft pyro system whereas the selection of the filter is under instrument control.
Main shell valve	spacecraft	Up to 2 valves to be opened by the spacecraft to equalize the pressure inside and outside the dewar

The XMS will be launched with the experiment body in vacuum conditions to avoid acoustic loads on the optical filters and a closed front-covering door which will be opened and remain open once a suitable out-gassing period has completed. The design of the door must be made such that it does not give rise to additional stray-light issues or becomes a source of fluorescence X-rays. To prevent single point failure, the opening mechanism needs to be designed with redundancy in mind.

3.2.7 Instrument units thermal design

The dissipation of the heat produced by the electronic units and the cryo-coolers on the dewar will be the responsibility of the spacecraft. The thermal design for a detector at a temperature of 50 mK is a major issue.

Although this can be achieved using different technology (see section 3.1), we have selected one cooling system which is representative for the various options using the Astro-H design as reference configuration (a fully redundant version and a version with only electronic redundancy is presented). In addition a lighter version based on the JWST/MIRI cooler, and a version based on the XEUS-NFI2 design are presented to indicate the range of options available.

3.2.7.1 Astro-H baseline design

- the operating temperature is achieved by a set of cryogen free cryo-coolers: the first step in the cooling train is realized by 2-stage Stirling coolers (providing a 100 and 20 K reference temperature), the second step is achieved by a 3He Joule-Thomson cooler which is pre-cooled by its own Stirling coolers (providing a reference temperature of < 4 K?) and the last stage cooler is realized using an Adiabatic Demagnetization Refrigerator (providing the 50 mK temperature)
- The system is a one shot system implying that all intermediate temperatures for anchoring the harness are stable. The typical operational time is about 30 hours with a regeneration time for the ADR of less than 10 hour (typically 1 hour)
- The system includes a high degree of redundancy: all cryo-coolers are fully redundant in the sense that in nominal conditions they will run at half of their power and in case of failure of one cooler, the corresponding cooler will be operated at full power. This is not completely feasible in the sense that there is a single ADR with single heat switches. Control of the heat switches is, however, warm redundant.
- The cooling system includes 3 thermal shields (100 K, 20 K and 1.7-4 K) and the isolation between these shields is optimized using MLI.
- The system will be launched under vacuum (~ 0.1 bar, TBC) which requires a pump down a few weeks before launch. Following launch the system will be opened to allow outgassing before it is switched on.
- Inside the dewar there is a baffle with optical blocking filters. The purpose of this component is to provide the required thermal insulation while still allowing for maximum transmission of the X-rays. A set of 5 thin filters is applied.

3.2.7.2 Astro-H reduced design

This design is essentially identical to the baseline design with the exception that the number of mechanical coolers has been reduced whereas the electronics is fully redundant. In this case we will have:

- 2 two-stage Stirling coolers to cool the shield
- 2 two-stage Stirling coolers to pre-cool the JT cooler
- One JT cooler

Detailed calculations are required to confirm the reliability of this (lighter) solution.

3.2.7.3 JWS/MIRI design

In this section we provide some background on the JWST/MIRI design:

- the operating temperature is achieved by a set of cryogen free cryo-coolers: the first step in the cooling train is realized by a single 3-stage Pulse tube cooler (providing precooling for the lower temperature JT cooler as well as for the dewar shields). Unlike the ASTRO-H concept, no cold radiator or ground support LN2 is required. The second step is achieved by a 3He Joule-Thomson cooler to 2.5K or to 4.4K with the same cooler filled with 4He. The JT cooler is pre-cooled by the lowest stage of the precooler (~15K). The last stage cooler is realized using an Adiabatic Demagnetization Refrigerator (providing the 50 mK temperature)
- The system is a one shot system implying that all intermediate temperatures for anchoring the harness are stable. The typical operational time is about 30 hours with a regeneration time for the ADR of less than 10 hour (typically 1 hour)
- A 5-stage continuously operating ADR based on the ADR developed by NASA-GSFC will also be considered.
- The system includes a high degree of redundancy: In order to meet the reliability requirements, the pulse tube/JT precooler for the ADR can be configured similar to JWST as a single string precooler with redundant electronics or alternatively for very high reliability as fully redundant. The ADR is not redundant and is a single ADR with single heat switches. Control of the heat switches is, however, warm redundant.
- The cooling system includes 4 thermal shields (120 K, 45, 15 K and 1.7-4 K) and the isolation between these shields is optimized using MLI.
- The system will be launched under vacuum (~0.1 bar, TBC) which requires a pump down a few weeks before launch. Following launch the system will be opened to allow outgassing before it is switched on.
- Inside the dewar there is a baffle with optical blocking filters. The purpose of this component is to provide the required thermal insulation while still allowing for maximum transmission of the X-rays. A set of 5 thin filters is applied

For this design we will consider a system with fully redundant electronics and mechanical coolers and a system with redundant electronics only.

3.2.7.4 XEUS/NFI2 design

In this section we provide some background on the design for IXO based on the XEUS/NF2 study:

- the operating temperature is achieved by a set of cryogen free cryo-coolers: the first step in the cooling train is realized by two-stage Stirling cooler providing a 150K stage and cooling the coldest shield and the JT cooler down to 15K. An additional cooling stage at 100K will be provided by either a cold radiator or a single stage Pulse Tube/Stirling cooler as a backup solution. The second step is achieved by a 3He Joule-Thomson cooler to 2K, similar to the design of the Planck 4K JT cooler taking advantage of new compressor developments currently ongoing. The JT cooler is pre-cooled by the lowest stage of the precooler (~15K). The last stage cooler is realized using a hybrid sorption cooler/ADR cooler currently under development for the SPICA/Safari mission. The system is a one shot system implying that all intermediate temperatures for anchoring the harness are stable. The typical operational time is about 30 hours with a regeneration time for the Sorption cooler/ ADR of less than 10 hour.
- A two stage ADR based on the previous developments will also be considered.

- The system includes a high degree of redundancy: A fully redundant system for the Stirling and JT cooler can be implemented. The 50mK cooler is not redundant, but some internal redundancy is implemented in the cooler itself (as implemented on Herschel).
- The cooling system includes 3 thermal shields (150 K, 15 K and 2 K) and the isolation between, these shields is optimized using MLI or low emissivity coating for the lowest temperatures.
- The system will be launched under vacuum which requires a pump down a few weeks before launch. Following launch the system will be opened to allow outgassing before it is switched on.

For this design we will consider a system with fully redundant electronics and mechanical coolers and a system with redundant electronics only.

3.2.8 Electrical design

The multiplexed read-out of the cryogenic detectors is a major challenge and details have been given in section 2.3.4. In addition to the read-out and multiplexing of the detector elements the electrical design of the instrument keeps the following starting points:

- adequate shielding and filtering to enable operation of the very sensitive TES and SQUID amplifiers in a dirty laboratory and satellite environment.
- Adequate shielding of the SQUIDs and TES from magnetic fields (from ADR, compressors, and spacecraft)
- a good grounding philosophy and use of differential signal handling with good common mode rejection.
- separation of sensitive analogue electronics from digital electronics
- The stringent temperature stability requirement should be part of the design, and could require stabilization algorithm, automatic gain adjustments, and temperature stabilization of critical units
- To meet the stringent EMC requirements the FEE-box has to be situated close to the cryostat (< 0.5 m) and have a galvanic connection with a resistance < 1 mOhm.

3.2.9 Onboard software

The instrument is controlled by the ICU. This is a real-time operating system with a number of tasks to control the instrument. The full onboard software can be loaded from ground but it will also be present in EPROM. In addition the Event Processor is based on a DSP on which the applied numerical filters (but also the software) can be uploaded. Some units will have firmware (ASICs/FPGA) for which the relevant parameters can be set.

Table 3-11 Typical size of uploadable code and commands

Unit	Uploadable	Size [Mbyte]	Function
IDC	Yes	1	<ul style="list-style-type: none"> - interface to satellite - control/command of instrument - trigger safe mode in case defined housekeeping parameters go out of limit - collection of housekeeping data - packing of science data, bulk storage is assumed to be part of the spacecraft
EP	Yes (optimal filters)	14	<ul style="list-style-type: none"> - optimal filters to extract event parameters and assign quality flags require 125 kbyte/pixel and it is assumed that for the full array (2176 pixels) we need 100 different templates (TBC). This need to be uploaded after full switch on or after change in detector performance (assume typically once per month)
DE	No, firmware but controlled by user defined levels	-	<ul style="list-style-type: none"> - generate bias voltages, - control multiplexing and de-multiplexing of data (feedback loop) - set triggers to extract data - apply triggers using anti-coincidence filters
Other boxes	No, firmware	-	<ul style="list-style-type: none"> - the condition of each unit (e.g. power level for the cryo-coolers) will be set by the users

3.2.10 Ground support equipment

The instrument ground support equipment (see also section 3.10.5) includes the following items:

- handling tools
- tools to test at instrument level (including the required tools to operate the cooler)
- electrical ground support equipment
- vacuum pumps
- Liquid Nitrogen fill equipment

3.2.11 Instrument mode description

The basic modes and their transitions are listed in Table 3-12 and shown in Figure 3-19. Depending on the science goals the internal instrument settings will be optimized but these do not affect the satellite resources at a significant level. Typical durations and power levels are given in 3.5.4.

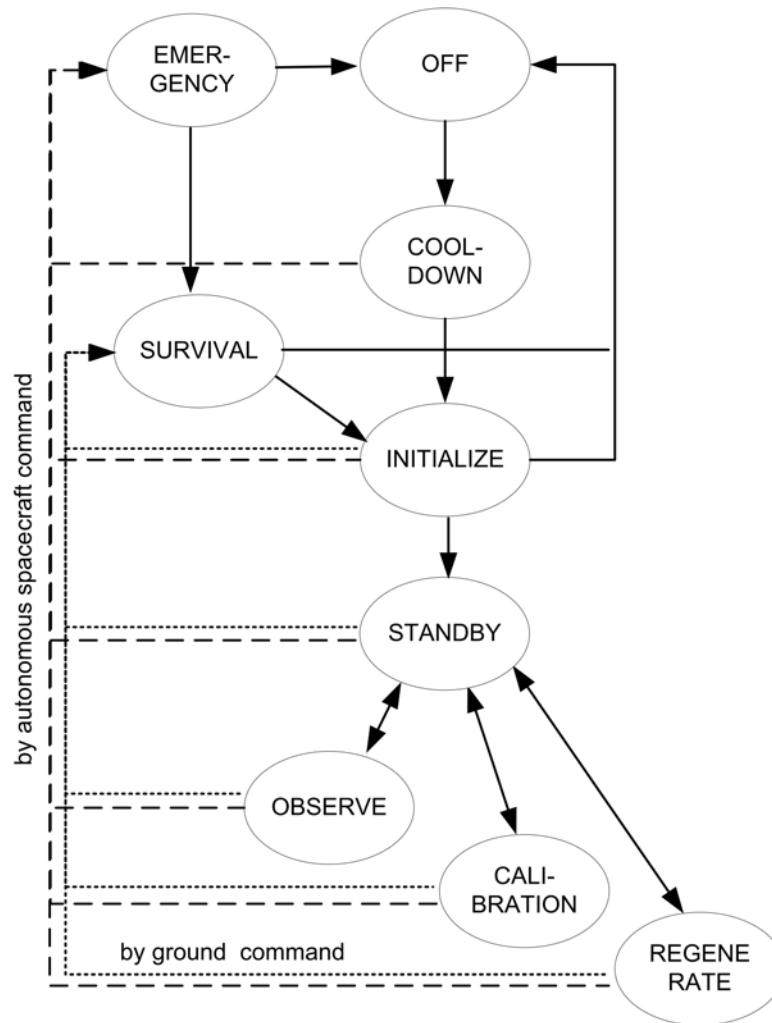


Figure 3-19 Instrument modes

Table 3-12 Instrument modes

Mode	Condition	Comment
OFF	During and following launch	Preferably this condition is avoided in orbit. If it nevertheless occurs one has to restart the whole instrument
COOL-DOWN	Cooling from room temperature to cold detector	Note that during ground operations this mode for the baseline Astro-H option will be different from the in-orbit conditions. Using a LN2 reservoir the cooling is speeded up on ground. Possibly the cryocoolers can be operated at higher power
INITIALIZE	After full or partial instrument switch-off.	Start setting up the instrument step-by-step with sufficient status verification and

		health probing. This contains setting of TES bias voltages, setting of SQUID bias voltages, and flux offsets, locking feedback loops, etc
OBSERVE	Nominal condition during data taking	
CALIBRATION	Normal condition during data taking	Although the conditions are equal to OBSERVE, no science data is taken (e.g. closed filter wheel with calibration sources on)
REGENERATION	Condition during regeneration of the Last Stage Cooler	In the current baseline design the dADR is being recycled. All electronic units will stay operational to maintain a stable condition for the instrument
STANDBY	During periods when one of the other instruments is prime	During these times it will be advantageous to perform calibration measurements with the XMS: 50 mK
SURVIVAL	Power is minimized while keeping the cryo-coolers on	The advantage of this mode is that the mechanical cryo-coolers stay in a stable condition and resumption of the instrument can be relatively fast (< 24 hours)
EMERGENCY	Minimal power usage	Only some housekeeping information will be collected
Alternative		In case of failures of a unit (e.g. one of the cryocoolers) the power requirement remains similar but the distribution of the units can be different (in case of a fully redundant system)

3.3 Mechanical Interfaces and Requirements

The total mass of the instrument is 324 kg excluding a design margin and the radiators to dissipate the heat generated by the cryo-coolers and by the electronic boxes. An option with reduced redundancy in the cooler chain will reduce the mass to 253 kg (reduced Astro-H) or to 199 and 166 kg in case the JWST/MIRI solution is adopted. With the XEUS-NFI2 cooler solutions the instrument masses are 293 and 241 for the fully redundant and reduced redundant options, respectively.

3.3.1 Location requirements

The instrument consists of several units with different accommodation requirements. These are summarized in Table 3-13.

Table 3-13 Position and alignment requirements of the various XMS units

Unit	Location/length cable harness	Comment
Detector	In mirror focus	Detector is located on the central axis of the dewar 265 mm above the mounting plane on the spacecraft.
FEE	< 0.5 m from dewar	The distance between the FEE and the dewar should be minimized and will be galvanically coupled (< 1 mΩ), distance driven by pick-up of noise, not by delay
DE_1, DE_2, DE_3, DE_4	< 1 m from FEE	
LCD_prime, LCD_redu	< 1 m from dewar	The last stage cooler drive should be close to the dewar as well (TBC)
All other units	< 3 m from dewar	In case of the pulse tube coolers its drive electronics can be placed on longer distance (8 m) but 3 m is suggested as a not too demanding requirement

3.3.2 Alignment requirements

The alignment of the cryostat with the micro-calorimeter relative to the mirror focus is important. In Table 3-14 we give the alignment requirements which are split into two components: the internal alignment of the dewar (as this system will cool down) and the alignment of the mirror with respect to the detector position as defined by its interface with the spacecraft. For these parameters we specify the alignment accuracy (where should the unit be located), the accuracy with which the position is known (could be determined in orbit using flight calibration data) and a stability which could not be corrected.

Table 3-14 Alignment requirements for the XMS

Axis	Instru- ment [mm]	Space- craft [mm]	Comment
X, Y (lateral)			The plate scale is 0.5 mm/PSF (5 arcsec)
Accuracy	1	1	Mirror vignetting over 20 arcsec is estimated to be 1%. Under this assumption these accuracies only affect the baffle design and the summed misalignment (20 arcsec) is small compared to the FoV (5.4 arcmin)
Knowledge	0.05	0.05	The sum of the knowledge at any point in time should be significantly less than the PSF and at the most comparable with the accuracy of the star tracker (1 arcsec). This translates into knowledge of the position of better than 50 micron.
Stability	0.05	0.1	The sum of these accuracies should be less than 0.3 x PSF. The budget assigned to the spacecraft is somewhat larger to consider thermal expansion of the telescope tube
Z (focal length)			The scale factor is 2.5 mm / PSF (5 arcsec)
Accuracy	0.5	0.5	Assuming this can not be actively corrected
Knowledge	1	1	Knowledge about this parameter is of little use and therefore this is relaxed compared to the accuracy and stability requirements
stability	0.5	0.5	Small (< 1/3) contribution to the PSF

3.3.3 Pointing requirements and performance goals

With a pointing accuracy/stability of 1 arcsec, the contribution to the PSF due to the pointing will be small. A 1 arcsec requirement can be easily met by a standard star tracker.

In addition to the pointing requirements **dithering of the spacecraft** is required to disentangle detector features from true features in the observed objects. The requirement is that a typical long observation, which is used to observe weak features, is split into a number of different pointings. As minimum a raster scan with 9 observations is required which are separated by 2 PSFs (10 arcsec). Alternatively a more continuous dithering pattern (a Lissajous figure as used by Chandra) could be used as long as a typical region of 20 x 20 arcsec is covered.

3.3.4 Interface control drawing

No full set of interface drawings is given. All electronic boxes are defined by their width, length and height. In addition we provide interface drawings for the dewar options:

3.3.4.1 Baseline Astro-H design

The position of the cryocoolers can depend on the spacecraft design and two configurations are shown in Figure 3-21 and Figure 3-22.

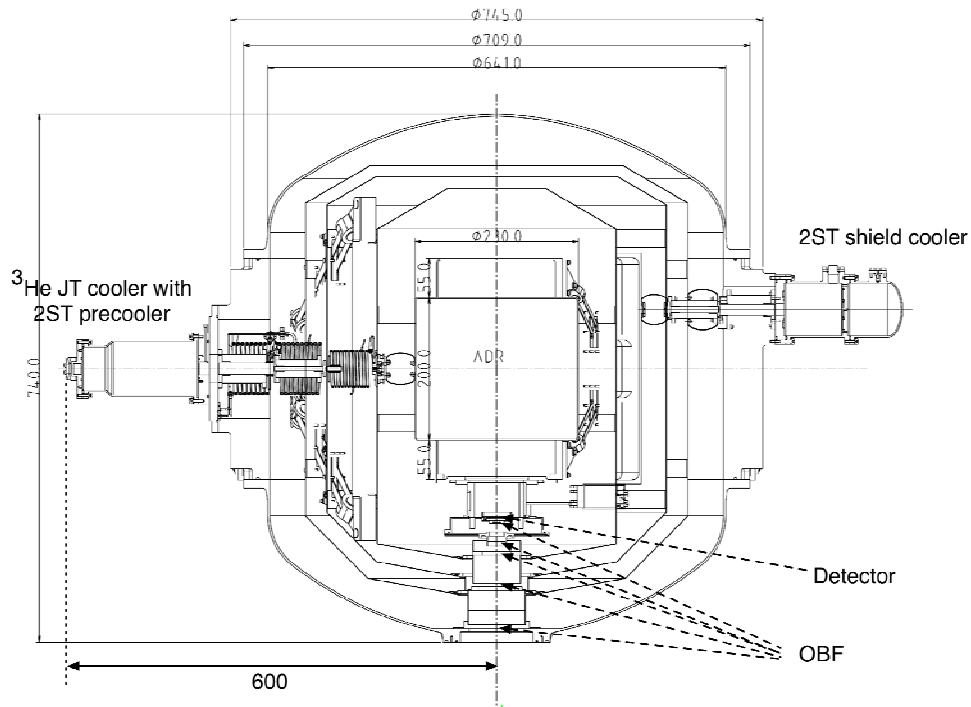


Figure 3-20 Interface drawing for the outer envelope of the dewar showing one 2ST and one JT cooler only. In this drawing all mechanical coolers are mounted on side of the Dewar. Different allocation is also possible are shown in Figure 3-2 and 3.3. A JT cooler is drawn on the left, and 2ST shield cooler is drawn on the right to show their sizes in comparison with dewar. The phase angles of these two coolers will not be 180° in actual Dewar design (see Figure 3-2).

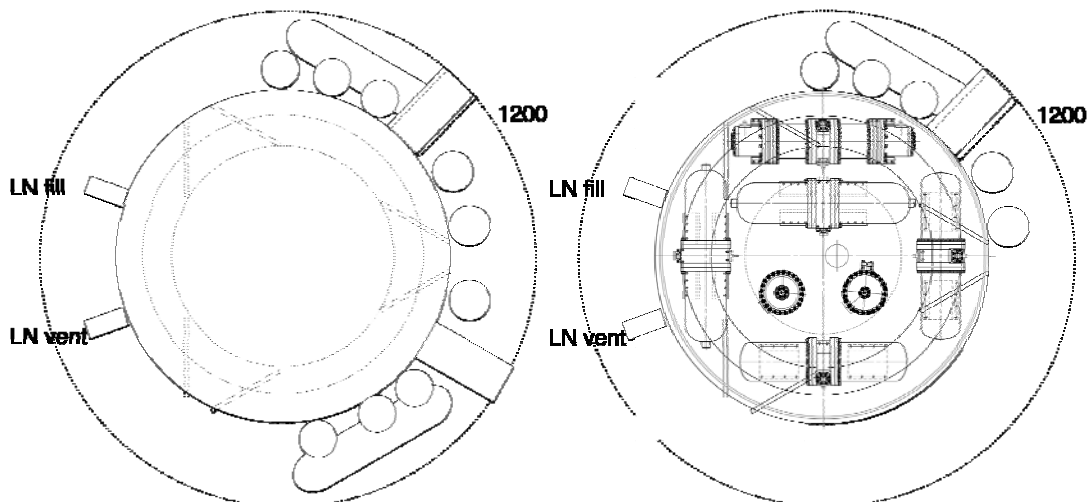


Figure 3-21 Position of mechanical coolers on side of the dewar (phase angle can be optimized) in case of a fully redundant design (option A, left) and the option with reduced redundancy (B, right)

3.3.4.2 Cooler based on JWST/MIRI

In Figure 3-22 we show the design based on JWST with the reduced redundancy (only electronics redundant). This unit can accommodate the same last stage cooler and detector. The height of the unit is 700 mm (includes compressors).

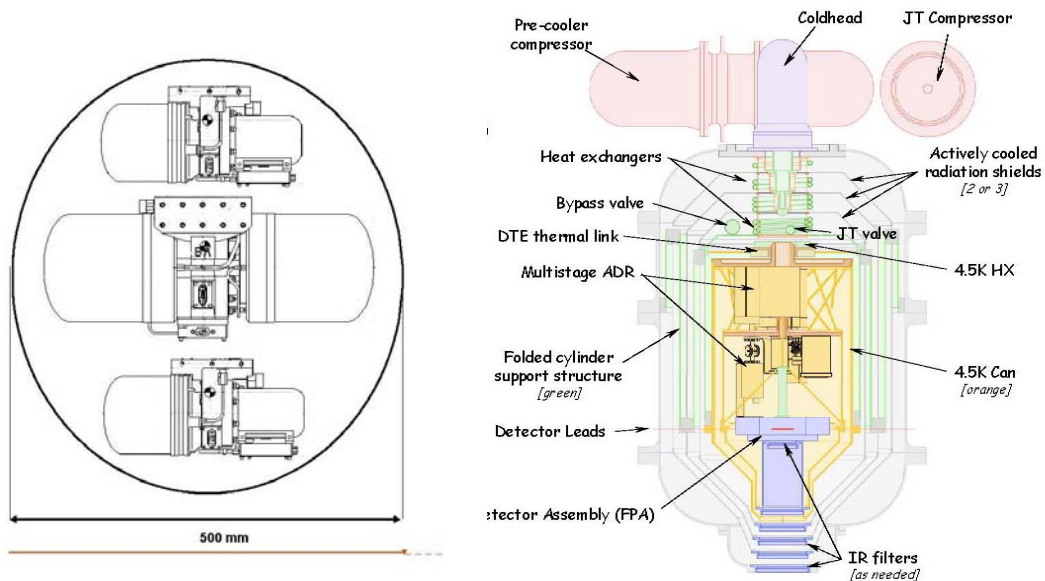


Figure 3-22 View of the cooler based on JWST/MIRI (the large unit is the pre-cooler compressor for the pulse tube)

3.3.4.3 Interface between last stage cooler/detector and the cryostat

In addition we specify the volume for the detector head and the last stage cooler, enabling separate optimization of the different cooler stages (see Table 3-15). In Figure 3-23 we give an example of such last stage cooler and detector

Table 3-15 Dimensions of last stage cooler and detector

Unit	Size	Comment
Last stage cooler	230 mm Ø by 310 mm height	Defines the volume at 1.7-4 K within which the last stage cooler will be suspended. Depending on the selected last stage cooler (and its TRL levels), we hope to reduce this size
Detector head	200 mm Ø by 80 mm height	Includes space for the electronics on 50 mK and 0.5 K. The height can be increased by a factor 2 without the need to modify the outer dimensions of the dewar

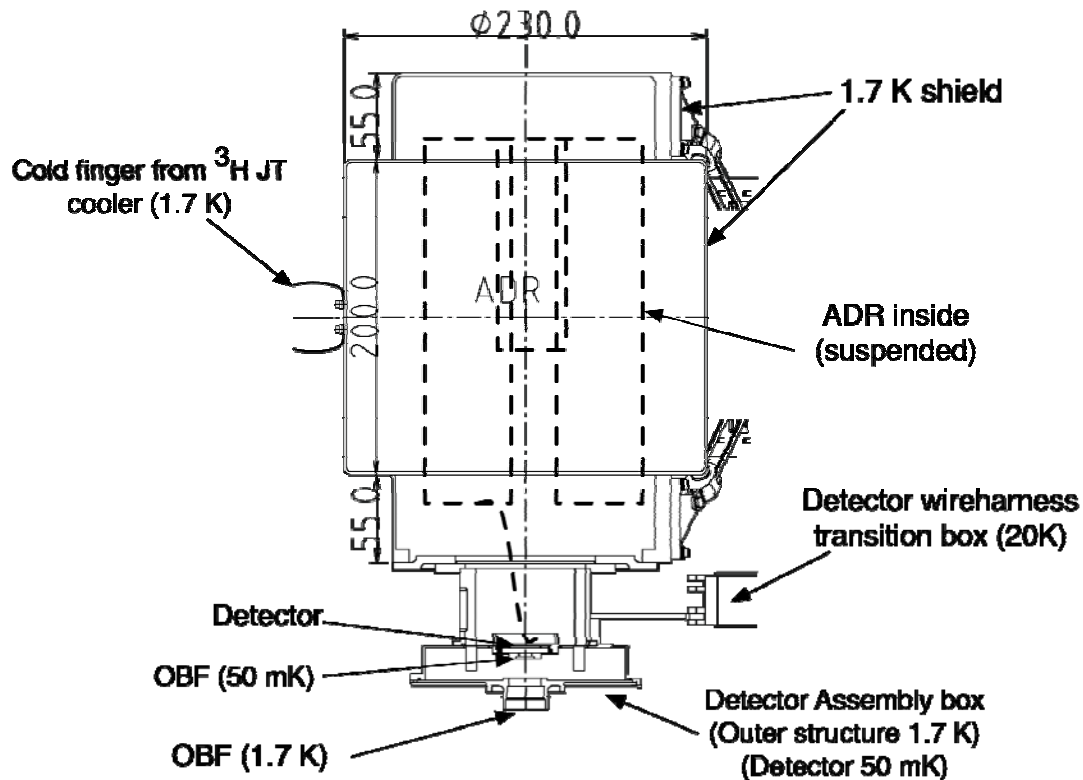


Figure 3-23 An example of the Interface control drawing for the last stage cooler, the detector head, and 1.7 K shield. The envelope of the double stage ADR is 200mm diameter x 310mm height. The size of detector assembly box in the figure is about 80 mm in height and 200mm in diameter. The height can be about a factor of two larger, because there is a room between the 1.7 K and 20 K shield in the opposite side (top side in the figure).

3.3.4.4 A He³ sorption/ADR combination as last stage cooler

Whereas the first two presented cooling chains include either a dADR or a cADR as last stage, various different options for the last stage exist as well. Below we indicate the performance of a He-3 sorption cooler in combination with a single stage ADR and a 2.5 K base temperature (under development at CEA in France for IXO, and baselined in the XEUS-NFI2 cooler options). In this approach the most demanding stage in terms of mass (first ADR stage) is replaced by a ³He sorption cooler, which can weigh less than 300 grams (heat switches excluded). A major advantage of such system is the reduced magnetic field strengths required to order the paramagnetic salt. This translates into power and mass savings. This is further aggravated when considering the support structure: a heavier component to be mechanically held certainly requires a substantial support structure. And the support structure has a direct impact on the parasitic thermal loads and thus on the performance.

The thermal architecture takes advantage of all available cooling resources and a variable thermal path is provided to the 15 K stage. In fact due to the limited cooling power at 2.5 K, the 15 K stage will be used to evacuate a large fraction of the enthalpy and heat capacity associated with the sorption cooler recycling phase. Because the system will be alternatively coupled to one stage or the other, several heat switches are required (see Figure 3-24).

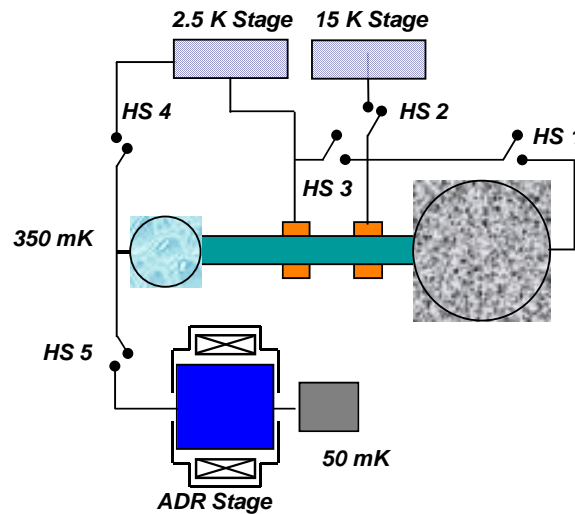


Figure 3-24 Schematic of the thermal architecture of the last stage cooler

The primary advantage is thus a significant mass saving. A second advantage is that stray magnetic fields within the instrument from the ADR magnet are weak and do not necessitate any complex or heavy magnetic shielding.

Based on the main specifications, i.e. $1 \mu\text{W}$ and $10 \mu\text{W}$ respectively at 50 mK and 300 mK for a stand time of 30 hours (+ 1 hour to tune the instrument), a preliminary sizing has been carried out (note that the cooling requirements have increased due to the larger detector size). It turns out that a HERSCHEL type sorption cooler fulfil the need, pending the pumping line is redesigned. The main characteristics of the cooler are reported in the Table 3-16. A current of 5 A has been assumed for the coil. Obviously this current has a direct impact on the size and thus the mass of the coil (reducing to 2 A increases the mass of the coil by roughly 700 grams).

Table 3-16 Size and mass of the sorption/ADR cooling system meeting the basic cooling requirements

Parameter	Value
Size last stage cooler + cold head	15 cm \varnothing x 33 cm height
Mass last stage cooler	< 6 kg*
Mass cold head	< 3 kg
Detector position (cm from top)	3 cm
Stray magnetic field at detector position	0.05 Gauss
Stray magnetic field at detector position during regeneration	0.5 Gauss
Stray magnetic field outside cooler measured from the center of the cooler at	
– 50 cm distance	< 0.1 Gauss
– 100 cm distance	< 0.01 Gauss
Maximum current for large stage cooler	2 or 5 A (TBC)
Power to the cooler during regeneration (< 10 hr) at cooler interface	< 1W

(*: the operating temperature (50 mK) has a strong impact on the mass. A 10 mK increase could lead to a substantial reduction (in the range 0.5 – 1 kg))

3.3.4.5 European pre-cooling chain for He3 sorption/ADR

Considering the He3 sorption/ADR as a final stage, the following pre-cooling chain based on the 10K Stirling development currently ongoing and the soon to be issued development for a 2K JT cooler can be considered. The 2K JT cooler will be based on the compressor developed for the 10K Stirling cooler and take maximum heritage of the Planck 4K cooler. A schematic of the architecture of such a chain is shown in Figure 3-25.

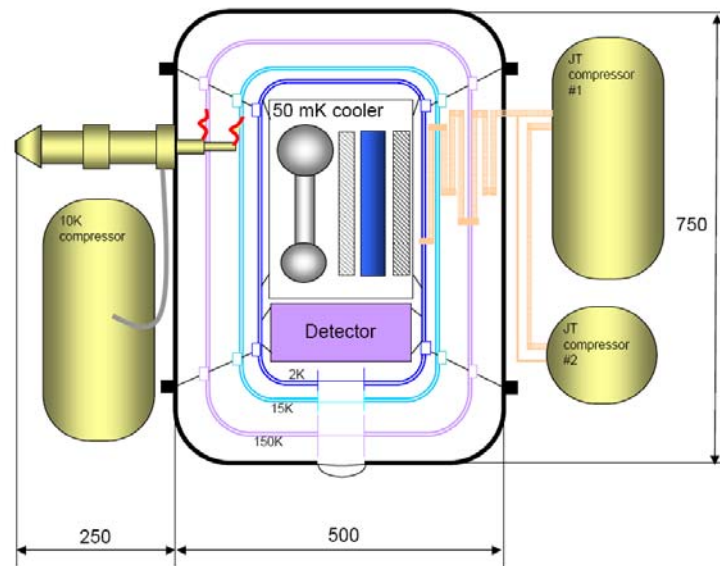


Figure 3-25 Schematic of the thermal architecture of the European chain for the He3 sorption/ADR cooler

3.3.4.6 Spacecraft accommodation

In Figure 3-26 we provide some preliminary ideas about the accommodation of the instrument on the satellite. We assume that the instrument is launched upside down (looking downwards). The detector is 265 mm from the interface to the platform on which the instrument is mounted. The filter wheel/door combination is directly attached to the cryostat. The dewar is supported by 12 struts. Space has been allocated for the cryocoolers. Alternatively one could lower the instrument provided that a sufficiently large hole in the MIP can be made. In this case shorter struts (or no struts) will be required or the instrument can be mounted directly on the lower part of the grith ring. The exact location will depend on the satellite requirements but they can be placed at a side (as is shown) or at the top (not shown). The cryocoolers can be placed as much as possible in opposing directions to allow for the other instruments on IXO to be located as closely as possible to the XMS instrument (note our thermal requirement of the outer dewar shell temperature). We also indicate the position of the instrument harness (lower interface of the central grid ring) and the required distance to the FEE is measured from this interface (phase angle can be chosen).

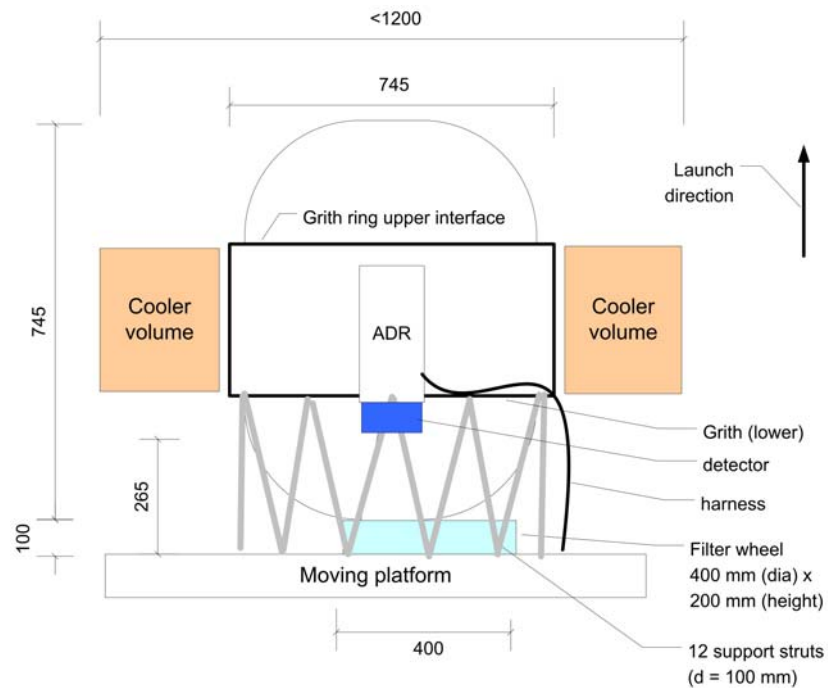


Figure 3-26 Possible configuration of the XMS on the focal plane moving platform for option A including typical dimensions.

3.3.5 Instrument mass

The total estimated basic for the Astro-H dewar option is given in Table 3-17 where clearly the dewar is the main component. For completeness we also provide the mass of the unit with no redundant cryocoolers (but only with redundant drive electronics).

Table 3-17 Resource requirements¹⁾ for the XMS (basic mass). A generic design margin and an allocation for harness is given at the end

	box mnemonic	# of boxes	# sub- units	Unit [kg]	Total [kg]	Total baseline [kg]	Total Option B [kg]	Length [cm]	Width [cm]	Height [cm]
filter wheel + door	XMS-FW		1	8	8	8	8	∅ 40		20
dewar assembly¹⁾	XMS-DA	1	1		200,3	200,3	159,8	∅ 120		74
Detector + SQUID			1	1,4	1,4					
sensor internal harness			1	5						
50 mk dADR			1	18,75	18,75					
20 K shield cooler (2ST)			2	9,5	19					
JT precooler (2ST)			3	9,5	28,5					
JT cooler			2	22	44					
shields/MLI			1	13,248	13,248					
structure			1	59,562	59,562					
ground operations (LN)			1	7	7					
struts			1	4,44	4,44					
Aperture (optical baffle inside dewar)			1	2,2	2,2					
outer covers			1	2,2	2,2					
Last stage cooler drive	XMS-LCD	1	1	10	10	10	10	13	25	38
front end electronics	XMS-FEE	1	1	3,8	3,8	3,8	3,8	15	23	20
Digital electronics	XMS-DE	4	4	4,8	19,2	19,2	19,2	23	28	20
Fixed spacecraft platform										
instrument control unit	XMS-ICU	2	2	4	8	8	8	27	14	18
power supply unit	XMS-PSU	2	2	7,5	15	15	15	25	38	20
event processor	XMS-EP	1	1	13,6	13,6	13,6	13,6	28	28	20
pre cooler drive	XMS-PCD	1	3	6	18	18	9	32	32	13,5
Shield Cooler drive	XMS-SCD	1	2	6	12	12	6	32	32	13,5
Joule Thompson drive	XMS-JTD	1	2	8	16	16	8	38	27	32
total units / total mass (best estimate)		15				324	252,4			
Estimated/tentative instrument harness						16				
total units						340				
Design contingency + margin (NASA)						1,3				
Margin ESA						1,2				
grand total NASA						421				
Grand total ESA						408				

1. note that, for example, the introduction of a SpaceWire Router (SWR) will increase the mass of the electrical units by a few kg but reduces the mass of the harness. This will be studied in detail during the next phase
2. the mass of the XMS-FEE is possibly underestimated in view of the increased number of read-out channels
3. the dimensions of the cooler depend on the selected option, see, for example [Figure 3-20](#) and [Figure 3-21](#).

In [Table 3-18](#) we provide the corresponding information for the solution based on JWST/MIRI. Clearly this approach has a mass advantage but detailed comparisons should confirm the validity of this approach (e.g. do all solutions reach the same level of reliability). Similarly, [Table 3-19](#) shows the total masses for the solutions based on the XEUS-NFI2 cooler.

Table 3-18 resource requirements for the XMS mass based on a JWST/MIRI design (only basic mass)

	box mnemonic	Fully redundant mechanical cooler + redundant electronics				Single mechanical cooler + redundant electronics				Comment
		# of boxes	# sub-units	Unit [kg]	Total [kg]	# of boxes	# sub-units	Unit [kg]	Total [kg]	
filter wheel + door	XMS-FW		1	8	8	1		8	8	No Change
dewar assembly	XMS-DA		1			1				
Detector + SQUID			1	1,4	1,4	1		1,4	1,4	No Change
sensor internal harness			1	5	5	1		5	5	No Change
50 mk dADR			1	18,75	18,75	1		18,75	18,75	No Change
20 K shield cooler (2ST)			0	0	0	0		0	0	Item Deleted. Precooler cools shield
JT precooler (PT)			2	16,5	33	1		16,5	16,5	High capacity PT precooler
JT cooler			2	13,1	26,2	1		13,1	13,1	2 compressors per JT cooler + recuperators
shields/MLI structure			1	17,5	17,5	1		17,5	17,5	Additional Shield
structure			1	38,5	45,5	1		38,5	38,5	Scaled for smaller size
ground operations (LN)			0	0	0	0		0	0	High capacity PT precooler used for precooling
struts			1	3,5	3,5	1		3,5	3,5	Scaled for smaller size
aperture			1	2,2	2,2	1		2,2	2,2	No Change
outer covers			1	2,2	2,2	1		2,2	2,2	No Change
Last stage cooler drive	XMS-LCD	1		10	10	1		10	10	No Change
front end electronics	XMS-FEE	1		3,8	3,8	1		3,8	3,8	No Change
Digital electronics	XMS-DE	4		4,8	19,2	4		4,8	19,2	No Change
fixed platform										
instrument control unit	XMS-ICU	2		4	8	2		4	8	No Change
power supply unit	XMS-PSU	2		3,5	7	2		3,5	7	Precooler and JT drive include power conditioning
event processor	XMS-EP	1		13,6	13,6	1		13,6	13,6	No Change
pre cooler drive	XMS-PCD	2		12,1	24,2	2		12,1	24,2	JWST MIRI electronics
Shield Cooler drive	XMS-SCD	0		0	0	0		0	0	Item Deleted. Precooler cools shield
Joule Thompson drive	XMS-JTD	2		3,3	6,6	2		3,3	6,6	JWST MIRI (ACE) electronics
Relay Switch assy	New item	0		4,9	0	1		4,9	4,9	JWST MIRI
Estimated/tentative instrument harness					4			0,4	2,8	Only internal cooler harnesses counted
total units or mass		15	23		198,5	16	19		165,6	

Table 3-19 XEUS/NFI2 option

	box mnemonic	Fully redundant mechanical cooler + redundant electronics				Single mechanical cooler + redundant electronics				Comment
		# of boxes	# sub- units	Unit [kg]	Total [kg]	# of boxes	# sub- units	Unit [kg]	Total [kg]	
filter wheel + door	XMS-FW		1	8	8		1	8	8	No Change
dewar assembly	XMS-DA		1				1			
Detector + SQUID			1	1,4	1,4		1	1,4	1,4	No Change
sensor internal harness			1	5	5		1	5	5	No Change
50 mk dADR			1	9	9		1	9	9	Scaled Sorption-ADR cooler
20 K shield cooler (2ST)			0	0	0		0	0	0	Item Deleted. Precooler cools shield
JT precooler (10K Stirling)			2	15	30		1	15	15	10K Stirling precooler
JT cooler			2	30	60		1	30	30	2 compressors, heatexchanger, fluid management and cleaning (based on Planck)
shields/MLI structure			1	12	12		1	12	12	
ground operations (LN)			1	58	58		1	46	46	
struts			0	0	0		0	0	0	10K Stirling precooler used for precooling
aperture			1	4,2	4,2		1	4,2	4,2	Scaled from Herschel
outer covers			1	2,2	2,2		1	2,2	2,2	No Change
Last stage cooler drive	XMS-LCD	1		10	10	1		10	10	No Change
front end electronics	XMS-FEE	1		3,8	3,8	1		3,8	3,8	No Change
Digital electronics	XMS-DE	4		4,8	19,2	4		4,8	19,2	No Change
fixed platform										
instrument control unit	XMS-ICU	2		4	8	2		4	8	No Change
power supply unit	XMS-PSU	2		3,5	7	2		3,5	7	Precooler and JT drive include power conditioning
event processor	XMS-EP	1		13,6	13,6	1		13,6	13,6	No Change
pre cooler drive	XMS-PCD	2		11	22	2		11	22	Sentinel 3 Stirling electronics scaled
Shield Cooler drive	XMS-SCD	0		0	0	0		0	0	Item Deleted. Precooler cools shield
Joule Thompson drive	XMS-JTD	2		8,7	17,4	2		8,7	17,4	Planck 4K JT electronics
Relay Switch assy	New item	0		4,9	0	1		4,9	4,9	Same as JWST
total units or mass		15	23	293		16	19	241		

3.4 Thermal Interfaces and Requirements

In this section we provide the thermal interfaces and temperature limits assuming the full cooling chain is being delivered by the instrument team. In case only the last stage cooler is delivered an additional interface specification is required (cooling power and stability at the interface).

3.4.1 Temperature limit in space environment

The micro-calorimeter detector array is sensitive to exposure to high temperatures. Therefore its temperature should be kept at or smaller than standard room temperature, i.e. < 300K. For shorter periods temperatures (< 12 hour) up to about 325 K are allowed.

Temperature limits for the electronic boxes are the usual standard with the exception of the Front End Electronics. To avoid drifts in the gain we require a smaller variation of the temperature over time.

Table 3-20 Temperature requirements for the Astro-H option (sometimes it is allowed to start a unit while it is still somewhat colder than its operational range)

Unit	Operating	Short term variations [K/min]	Long term variations [peak/valley]	Non-operating
Dewar	200 / 300 K			190 / 300 K < 12 hr: 190 / 325 K
JT cryocooler (suction valves)	0 / 30 C			-40 / 60 C
Stirling coolers	- 70 / 30 C			-70 / 60 C
FEE	-20 / 50 C	0.1	4	-30 / 70 C
DE	-20 / 50 C	0.2	4	-40 / 60 C
Electronic boxes: DE, EP, ICU, PSU, LCD, SCD, PCD, JCD	- 20 / 50 C			- 30 / 70 C

Table 3-21 Temperature requirements for JWST cooler option (sometimes it is allowed to start a unit while it is still somewhat colder than its operational range)

Unit	Operating	Short term variations [K/min]	Long term variations [peak/valley]	Non-operating
Dewar ¹⁾	200 / 300 K			190 / 300 K
JT cryocooler	-5/ 45C			-25/55 C
PT cooler	- 5/45 C			-25/55 C
FEE	-20 / 50 C	0.1	4	-30 / 70 C
DE	-20 / 50 C	0.2	4	-40 / 60 C
Electronic Boxes: PCD, JCD	-5/45C			-25/55C
Electronic boxes: EP, ICU, PSU, LCD, SCD,	- 20 / 50 C			- 30 / 70 C

1) non-operational maximum temperature dewar can be up to 325 K for < 12 hours

3.4.2 Temperature limits in laboratory environment

On ground the same requirements as in orbit apply (see Table 3-20 and Table 3-21)

3.4.3 Temperature sensors

The thermal control inside the dewar is part of the instrument. The spacecraft has to control the thermal environment by:

- substitution heaters for the electronic units if these are switched off
- thermal control of the dewar environment if the cryo-coolers are switched off during longer periods (to keep these in their non-operational range). This could be achieved by electrically controlled (loop) heat pipes
- accurate control of the temperature of the cryo-coolers (especially the JT to ensure that the relevant suction valves stay in their limited operational range in case of the Astro-H option)

Table 3-22 temperature sensors and heaters

Unit	Heating	Temperature read-out
electronic units	Spacecraft thermal control	Spacecraft thermal control as desired
JT cooler	Active control by spacecraft	Spacecraft, critical in case of the Astro-H option
Dewar outer shield	Heating of the decoupling of the thermal link to the radiators is under control of the spacecraft (e.g. dewar should remain in its non-operational temperature range with all cryo-coolers off.	spacecraft
Radiators	No	spacecraft

3.4.4 Heaters

See Table 3-22.

3.4.5 Thermal schematics

In this section we give the thermal schematics of the instrument for the selected baseline cooling chains (options A, B and C). Clearly this will change if a different set of mechanical coolers is selected but its boundary conditions (cooling to 50 mK down from room temperature) remains unchanged. Depending on the selected cooling chain and potential failures the power dissipation on the dewar will also vary (see tables Table 3-23 to Table 3-26). In the various options it is required that the stages up to the last stage cooler can handle the dump of the last stage cooler if this is in the REGENERATE mode (in case of the dADR).

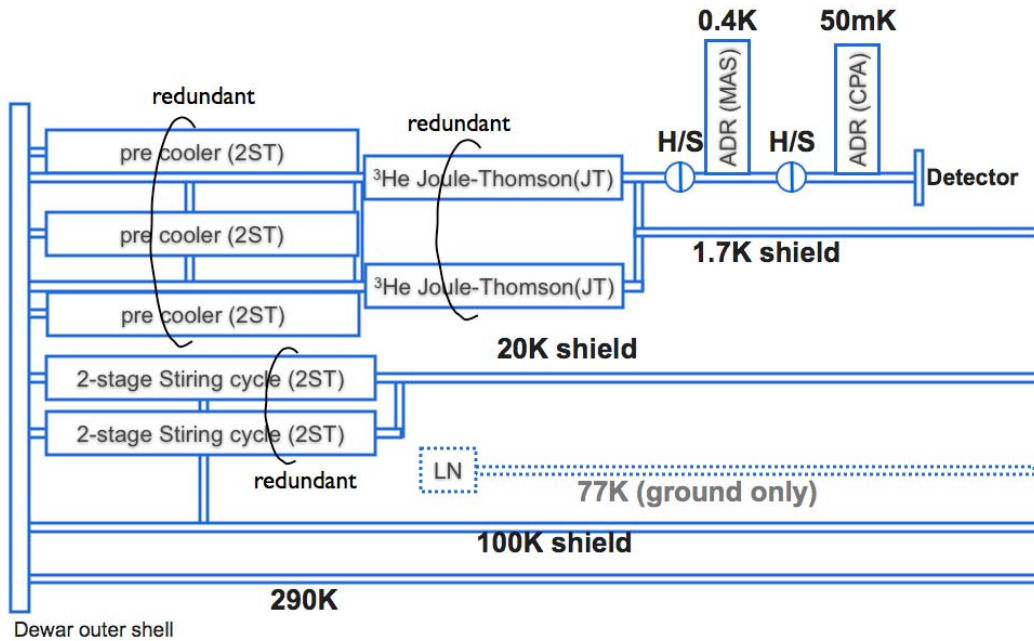


Figure 3-27 Thermal schematics of cooling chain from room temperature to 50 mK for option A (redundant design) (thermal link between 100 K shield and outer shell should be removed)

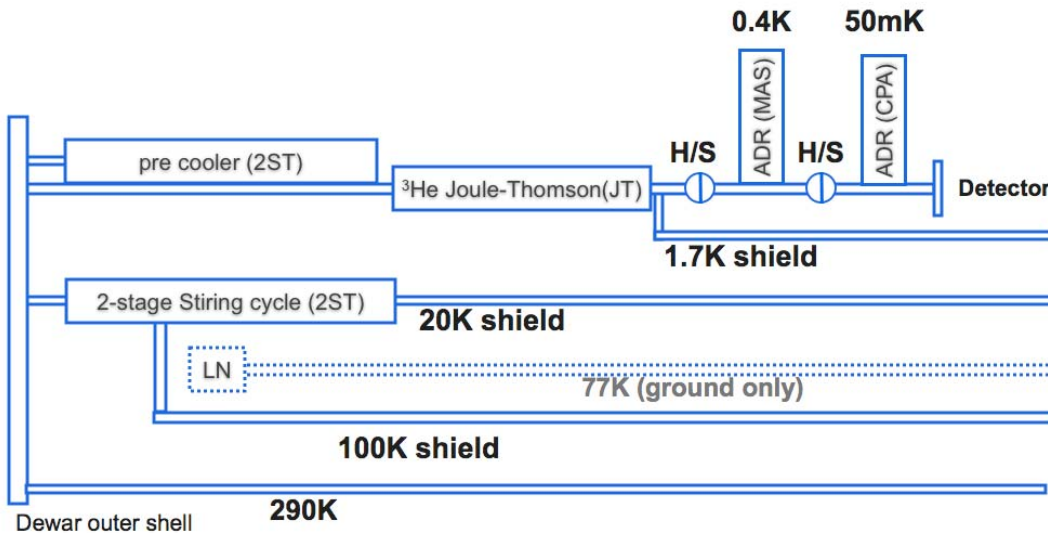


Figure 3-28 Same as Figure 3-28 but for option B (reduced redundancy)

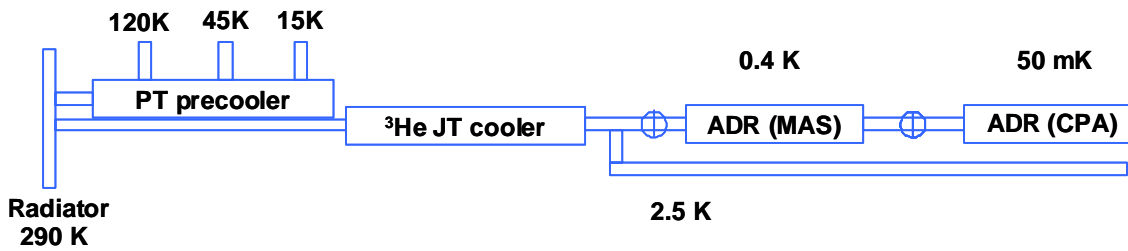


Figure 3-29 Thermal schematic of the JWST cooler option

Table 3-23 Power dissipation from the coolers mounted on the Dewar for option A for normal operation and for failure modes

Component	Normal	Failure in a shield cooler	Failure in a pre cooler	Failure in JT circuit
JT1 compressors	50W	90W	50W	0
JT2 compressors	50W	90W	50W	90W
Pre cooler 1 compressor	35W	35W	0	35W
Pre cooler 1 displacer	15W	15W	0	15W
Pre cooler 2 compressor	35W	35W	60W	35W
Pre cooler 2 displacer	15W	15W	30W	15W
Pre cooler 3 compressor	35W	35W	60W	35W
Pre cooler 3 displacer	15W	15W	30W	15W
Shield cooler 1 compressor	35W	0	35W	35W
Shield cooler 1 displacer	15W	0	15W	15W
Shield cooler 2 compressor	35W	60W	35W	35W
Shield cooler 2 displacer	15W	30W	15W	15W
Total on dewar	350 W	420 W	380 W	340 W

Table 3-24 Power dissipation from the coolers mounted on the Dewar for option B

Component	Power dissipation
JT compressors	90W
Pre cooler compressor	90W
Pre cooler displacer	30W
Shield cooler compressor	90W
Shield cooler displacer	30W
Total on dewar (nominal)	330 W

Table 3-25 Power dissipation for coolers mounted to dewar for the JWST cooler (option C/D)

Component	Electronics Redundant	Fully Standby Redundant
	Watts	Watts
PT Precooler 1	140	164
JT Compressor 1-1	44	45
JT Compressor 1-2	44	45
PT Precooler 2	NA	0
JT Compressor 2-1	NA	0
JT Compressor 2-2	NA	0

Total on dewar	228	245
PT drive 1	43	47
JT Drive 1-1	29	30
Switch Relay Assembly	0	NA
PT drive2	0	0
JT Drive 2-1	0	0
JT Drive 2-2	0	0
Total Power from PSU	300	331

Table 3-26: Power dissipation for coolers mounted to dewar for the ESA/XEUS cooler (option E/F)

Component	Electronics Redundant (average/recycling) Watts	Fully Standby Redundant (average/recycling) Watts
Stirling Precooler 1	113/150	155/200
JT Compressor 1-1	80/80	80/80
JT Compressor 1-2	80/80	80/80
Stirling Precooler 2	NA	0
JT Compressor 2-1	NA	0
JT Compressor 2-2	NA	0
Total on dewar	273/310	315/360
Stirling drive 1 (76% eff)	36/47	49/63
JT Drive 1-1	25/25	25/25
JT Drive 1-2	25/25	25/25
Switch Relay Assembly	0	NA
Stirling drive2	0	0
JT Drive 2-1	0	0
JT Drive 2-2	0	0
Total Power from PSU	359/407	414/473

The harness between the room temperature electronics and the focal plane has a clear impact on the thermal design. The harness will be made up from twisted wire pairs and includes the following components:

- In case of a single stage SQUID amplifier each of the channels requires 3 twisted pairs to operate the SQUIDS, in case of a double stage SQUID amplifier 5 twisted-wire pairs are required. Two pairs require quite low impedance (depending on the design both $< 10 \Omega$ or even one as low as 2Ω), and 3 pairs with an impedance of about 100Ω . In addition 2 wire pairs (FDM) are planned for each signal chain to bias the pixels with an AC-comb. These pairs can have an impedance of 100Ω .
- The harness to apply a field in the Helmholtz coils. This harness has a prime and redundant channel and has to handle up to 50 mA (see section 3.2.3.5). Therefore we have selected a low Ohmic line (10Ω).

- The harness to read-out the relevant temperatures. Currently we expect to have up to 5 sensors at the 50 mK level (detector chip, SQUID, LC filters, salt pill, ...) and 3 at the 0.5 K level and 3 at the next higher level (or if cold electronics is applied the temperature can also be monitored. Temperature sensors for the proper performance of the full cooling chain is NOT included in this table and has to be considered as part of the cooling chain..
- The last stage cooler may, depending on the chosen system, require large currents during regeneration. The current specification is that a current up to 5 A is acceptable. The thermal leak of this is not included in table Table 3-27 where we only give the thermal dissipation for electronic components of the detector and its related cabling.

To minimize the heat load onto the cryostat the harness has to be anchored at the various temperature stages. Between 300K and 1.7/2.5/4K use will be made of normal conducting wire looms, while for temperatures < 4K superconducting looms will be used. The thermal load of the detector, its read-out electronics and the wires of the different stages has been calculated and is summarized in Table 3-27. The corresponding electrical wiring is shown in Figure 3-30.

Table 3-27 Calculated power dissipation at the different temperature stages

Tempera- -ture stage	Item	Power	number	Total [μ W]	Comment
50 mK	TES	10 pW	2176	0.022	
	SQUIDs	10 nW	40 + 32	0.720	Consistent with a 4 SQUID design, if more SQUIDs are used this increases (15 SQUID ~ 30 nW)
	CryoAC TES	3 nW	4	0.012	
	CryoAC SQUID	0.14 nW	4	0.0006	TBC, number is low
	Harness from 50 mK to SQUID array at 0.5 K	3 twisted pairs	40+32+4	0.096	Array SQUID is assumed to be at 0.5 K (TBC that this is really needed).
	TES-bias harness from 50 mK to 0.5 K	2 twisted pairs	40+32+4	0.064	Harness will be anchored at all temperature levels (0.5, 2.5, 20 and 100 K)
total 50 mK				0.92 μW	
0.5 K	Array SQUID	500 nW	40+32+4	38.000	Assumes the array SQUID of a 56 x 4 SQUID system (expected 470 nW)
	Harness from array SQUID to 1.7 K	5 twisted pairs	40+32+4	3.116	5 twisted pairs for array SQUIDs and 1 st stage SQUIDs, the twisted pairs for biasing the 1 st stage SQUIDs are thermally anchored at the 50 mK level
	TES bias	2 twisted pairs	40+32+4	1.246	10 Ω over all temperature stages
	Harness for	Twisted	2x1	0.016	10 Ω over all temperature stages

	Helmholtz to 1.7 ¹⁾	pair			
	Harness for temp. sensor to 1.7 ¹⁾	2 twisted pairs	2x11	0.180	All 100 Ω over all temperature stages
Total 0.5 K				42.6 μW	

				[mW]	
1.7 K	Harness for detector to 20 K	7 twisted pairs	40+32+4	1.440	Assumes resistances as shown in the caption of Figure 3-30
	Harness for Helmholtz to 20 K	Twisted pairs	2x1	0.032	
	Harness for temp. sensor to 20 K	2 twisted pairs	2x11	0.045	
Total 1.7 K				1.5 mW	Only electronics excluding loads due to last stage cooler and suspension

20 K	Harness for detector to 100 K	7 twisted pairs	40+32+4	130.000	Assumes resistances as shown in Figure 3-30
	Harness for Helmholtz to 100 K	Twisted pair	2x1	6.230	
	Harness for temp. sensor to 100K	2 twisted pairs	2x11	0.217	
Total 20 K				136 mW	

100 K	Harness for detector to 300 K	7 twisted pairs	40+32+4	368.000	Assumes resistances as shown in Figure 3-30
	Harness from Helmholtz to 300 K	Twisted pair	2x1	0.002	
	Harness from temperature to 20 K	2 twisted pairs	2x11	17.200	
Total 100 K				375 mW	

¹⁾ Harness for the Helmholtz coils and temperature sensors has a prime and redundant channel, for each temperature 2 twisted pairs are needed

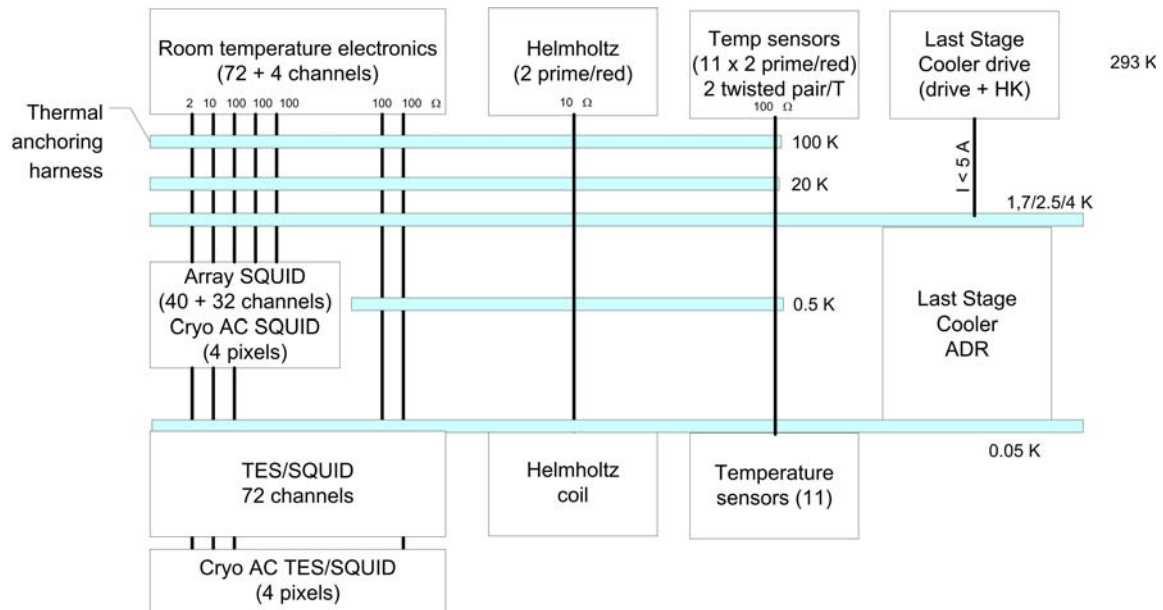


Figure 3-30 Electrical wiring including the thermal anchoring of the wires for FDM, Time Domain Multiplexing will give similar loads. For the calculations we assume for the 2, 10 and 100 W lines a distribution of (0.5, 0.17, 0.33), (2.5, 0.83, 6.67) and {71.43, 23.81 and 4.76} for the difference stages respectively (1st, 2nd and 3rd stages respectively for 300 – 100 K, 100 – 20 K and 20 – 1.7 K)

3.4.6 Thermal control requirements

The thermal control of the detector is carried out by the instrument itself and will be based on relevant HK parameters collected by the ICU. In addition the following aspects could affect the thermal control at satellite level:

- after a certain observation time the last stage cooler needs to be regenerated. In the current concept the instrument will do this autonomously or under ground control. This will result in an increase of the required power. In the instrument status HK (to be supplied to the spacecraft control system) the instrument mode will be reported.
- in addition it will be possible to heat the outermost optical blocking filter of the dewar in case this has been contaminated. This will be done following ground commanding only and has no significant impact on the satellite (except that this command should not be given during an observation).

3.5 Electrical interfaces and requirements

3.5.1 Electrical resources requirement summary

The instrument has its own power converters and power conditioning unit and will require about 1000 W from the satellite bus in the standard operational mode.

3.5.2 Instrument power distribution block diagram

The instrument power distribution block diagram for nominal operations is given in Figure 3-31. Essentially there are two approaches:

- the cooler drives receive the raw bus power through the PSU and provide any necessary conversion in the unit itself
- the electronic units (DEE, DE, EP and ICU) receive regulated power from the PSU at the required voltages. These secondary voltage lines are well (TBD dB) separated per box, per voltage, and for analogue and digital use.

The power lines should be floating to allow for single point grounding of the instrument. Sufficient (TBD) filtering to avoid noise will be required for the most sensitive parts of the electronics (FEE).

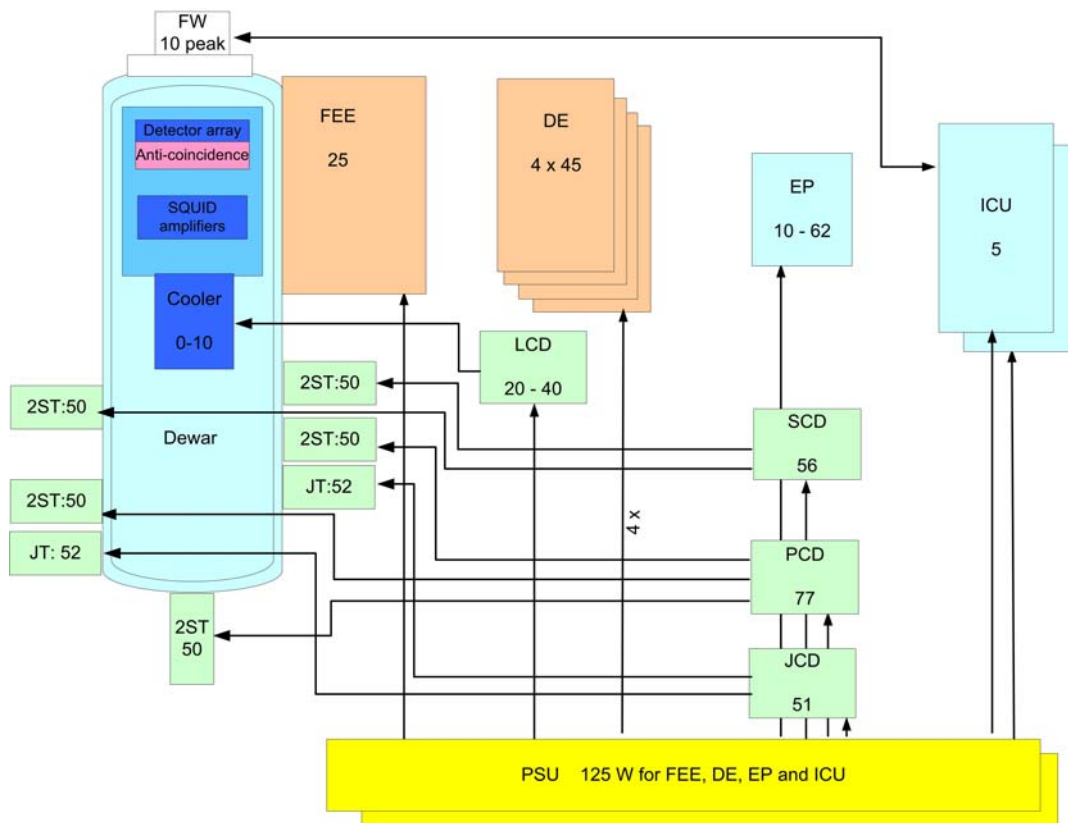


Figure 3-31 Power distribution diagram for the nominal case (see section 3.4.5 for power levels in case of the failure of one of the cryo-coolers)

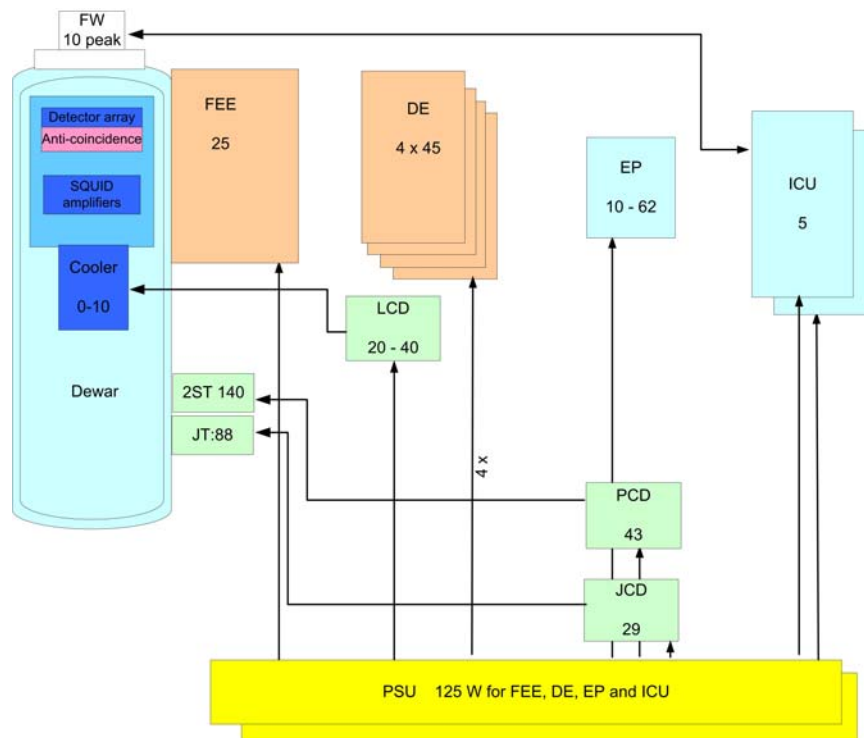


Figure 3-32 Power block diagram for JWST cooler option

3.5.3 Power budget

The power budget for instrument using the baseline cooling option (A) is given in Table 3-28. It should be noted that the numbers are for nominal conditions only. In case of the failure of a 2ST cooler or a JT cooler the power in one of those will be zero whereas the other will run approximately at double of its power. Only during rotations of the filter wheel, this unit requires power. The duration of this is expected to be less than a few minutes. Furthermore the power consumption of the Event Processing (EP) box will be strongly correlated with the event rate on the detector. The value indicated in the table is the maximum. Typical values will be significantly smaller.

Table 3-28 Power budget for XMS excluding design margins (DC-DC conversions are included assuming a 70% efficiency (for the detector electronics this conversion loss is included in the PSU, for the cooler units it is part of the relevant drive electronics

mnemonic	name	# units	off	cool-down	observe/calibrations/initialize	high count rate	Regene rate	standby	survival	Emergency	□ peak
XMS-FW	filter wheel	1	0	0	0	0	0	0	0	0	10
XMS-FEE	pre-amp/FEE ¹⁾	1	0	0	24,8	24,8	24,8	24,8	0	0	
XMS-DE	Digital Electronics	4	0	0	180	220	20	20	0	0	
XMS-EP	event processor ²⁾	1	0	0	62	62	10	10	0	0	
XMS-LCD	Last stage cooler drive	2	0	0	20	20	40	20	0	0	
XMS-SCD	Shield Cooler drive	1	0	87	56	56	56	56	56	0	
XMS-PCD	Pre-cooler Drive	1	0	56	77	77	77	77	77	0	
XMS-JTD	Joule-Thomson cooler drive	1	0	0	51	51	51	51	51	0	
XMS-ICU	instrument control unit	2	0	5	5	5	5	5	5	5	
XMS-PSU	power supply unit	2	0	5	125	142	43	34	5	5	
XMS-DA	dewar assembly	1	0								
XMS-DA/SC	2 stage Stirling shield coolers	2	0	100	100	100	100	100	100	0	
XMS-DA/PC	2 stage Stirling pre-coolers	3	0	150	150	150	100	100	100	0	
XMS-DA/JT	JT cooler	2	0	0	105	100	95	95	95	0	
XMS-DA/LSC	last stage cooler	1	0	0	0	0	10	0	0	0	
total power (nominal)				403	956	1008	632	593	489	10	
total peak power (nominal)				403	966	1008	632	603	489	10	
Additional power in case of failure (max)				70	70	70	70	70	70	0	
typical duration [hr]			n/a	1 wk	10	10	1	30	1 wk	short	
maximum duration				2 wk	30	30	2	long	?	?	
fraction of time					86%	5%	4%	5%			

1. This number needs further justification and depends on the exact drive capacity of the 2nd stage SQUID
2. Power of the event processor depends on the count rate. The given number is the maximum

In case of the JWST cooling option the total power in the OBSERVE mode is 748 W (detector control = 417, cooler = 331 W) (for the coolers we used 82% conversion efficiency (measured) in stead of the 70% in case

of options A and B. For the XEUS/NFI2 cooler option the total power in OBSERVE mode is $417+414=831$ W.

3.5.4 Instrument modes' duration

In Table 3-29 the typical duration of the different modes is given.

Table 3-29 Instrument modes' durations

Mode	Duration	Comment
COOL-DOWN	2 weeks	Cool down from room temperature to the 2.5 K level (in orbit, during ground operations an additional LN2 reservoir is used to speed this up to 1 week)
INITIALIZE	Few hr	Time needed to check out of the instrument electronics and its detector related units
OBSERVE	Few to 31 hr	A small (typically 60 W) variation in power is possible depending on the source intensity
CALIBRATION	Few to 31 hr	Same as OBSERVE with closed door. Will be executed when one of the other instruments is prime
HIGH COUNTRATE	Few to 31 hr	In a fraction of the observation (< 5%) the source intensity will be large and additional processing power in the DE and especially the EP is required
REGENERATE	1 - 2 hr	During regeneration no data taking is feasible (e.g. an other instrument could be selected. The requirement is that regeneration will take place within < 10 hr, but we expect to reach a generation time of 1 – 2 hours.
STANDBY	Few to many hours	When one of the other instruments is prime, the XMS can either be in the CALIBRATION mode collecting calibration data from the onboard calibration sources or can be in its STANDBY model. One hour before switching to the OBSERVE mode the last stage cooler should be regenerated.
SURVIVAL	Weeks	It is possible to save power by switching off the detector and the last stage cooler. By keeping the other mechanical coolers operational the dewar will maintain the condition to start regeneration immediately
EMERGENCY	Preferably < hours	When the mechanical coolers are off for a few hours it will be possible to restart the cooling system without much delay. If this period prolongs for longer periods a new COOL-DOWN might be required and this should be minimized

3.5.5 Telecommands

It is foreseen that the instrument operational modes will run by software located in the instrument controller, and that they can be started by an uplinked or time-tagged command containing the variables to be set.

Obviously the uplink should allow for uploading of calibration information to the instrument with a significant volume. Typical numbers for other cryogenic instrument missions are about 5Mbits monthly.

For each observation the XMS requires a small number of commands to define operating modes, door position etc. The maximum number of commands is typically 25 (of 255 bytes each (TBC)) but in general it will be restricted to a few commands only.

3.5.6 Telemetry

The dataflow of the instrument is continuous and analogue for the focal plane array, the SQUID amplifiers, and the low noise amplifiers in the FEE. Digitization of the analogue dataflow will take place by ADC's in the DE. The sample speed has to be consistent with the used multiplex scheme and is about 200 Msa/s for TDM and 50 Msa/s for FDM. The algorithms to create feedback to the SQUID amplifier chain are also running on the continuous datastream.

From there on we get data streams per pixel, that can be decimated to an amount of samples commensurate with the signal bandwidth of about 10 kHz. Subsequently trigger algorithms will search for events (X-ray or background generated) in that datastream and send only events with a length of 20 ms (TBV) to the Event processor box. From there on the data processing is dependent on the number of events, i.e. the instrument countrate. The processing should extract the event parameters, e.a. energy, time, position, etc.

The telemetry requirements are summarized in Table 3-30 and more details are given in the subsequent paragraphs.

Table 3-30 Telemetry requirements

Type	Max rate	Duration
Science data	64 kbit/s	Typical observation (< 500 counts/s) with properly working anti-co detector and maximum event size (64 bits) including a margin of a factor 2
	840 kbit/s	Maximum countrates (10.000 counts/s) possibly during periods of high background but at moderate event information (42 bits/event) including safety factor 2
	200 kbit/s	During dedicated calibrations of the instrument
Housekeeping	4 kbit/s	Continuously, also when one of the other instruments is prime. This rate is an upper limit and includes no safety factor
Telecommand acknowledge		As appropriate, infrequent

3.5.6.1 Housekeeping telemetry

The instrument generates housekeeping data of a 256 (TBC) number of variables measured at a 1 Hz (TBC) sampling frequency with 16 bits accuracy. This number is an upper limit as some parameters can be sampled at a lower frequency or with reduced accuracy.

3.5.6.2 Science telemetry

The telemetry structure is defined in Table 3-31 and the typical and maximum telemetry rates in Table 3-30. It is assumed that, when operational, the instrument can generate a science data stream at the indicated level and that the satellite will have memory for buffering this data before transmission to the ground.

Table 3-31 XMS event size

Parameter	Bits	Comments
Event position	12	X, Y information for all (2176) pixels, a more simple system would require 6 bits for X, 6 bits for Y and 3 bits for the segment (central, + 4 outer)
Energy	16	0,25 eV binning op to 16 keV,
Time stamp	8 – 16	
Rise time	0 - 8	
Event type	4 - 10	Flag to indicate event grade
Anti coincidence type	2	Flag to indicate anti-coincidence grade
Total	42 – 64	

During periods of high background, data could be dominated by soft protons indistinguishable from X-rays. These might not pass into the anti-coincidence system and therefore avoid rejection. Then a maximum rate of ~300 kcounts/sec might result with a bit rate of 10Mbit/s. However at such sustained rates, the thermal recovery time likely prevents useful spectroscopic data being retained, so that the instrument likely inhibits at some predetermined rate the transmission at such high data rates to circa 1Mb/s. If necessary data compression could be achieved with a sparse transmission of the time bit and/or applying standard lossless compression.

3.5.6.3 Detector calibration data

During the calibration mode the instrument will generate either proper X-rays or all kind of other datasets, including TES I – V data, SQUID I – V and Φ – V data, energy of test pulses, etc. Those datasets will have various formats. There should at least be 10 kbit/s available for typical transmission rates, but in case of debugging of problems a telemetry rate of 100 kBit/s is requested. In the calibration mode the data packages will be quite different from those described in table 5 – 4.

3.5.7 Electrical interfaces

The instrument will use spacewire for all its interfaces. The different interfaces are given in Table 3-32.

Table 3-32 XMS electrical interfaces

Interface	Unit	Type	Comment
Command/houskeeping	ICU prime/redundant	Spacewire	
Power	PSU prime/redundant	custom made	See section 3.2.3.7 for more details
Pyro		TBD	Up to 4 pyro's will be accommodated. These will be prime/redundant
Grounding	Dewar (TBC)	Custom made	The instrument will use a single ground point on the cryostat. So all the regulated secondary power from the PSU should be floating. It is expected to use the shields of the cables to define the common ground

3.6 Electromagnetic Compatibility and Electrostatic Discharge Interface

3.6.1 Susceptibility requirements (EMC cleanliness and grounding)

A schematic design for EMC cleanliness is given in Figure 3-33. The instrument itself is a Faraday cage. The instrument is separated from the ADR both electrically and magnetically inside the cryostat. The focal plane (TES, LC-filters, SQUIDs and magnet) is surrounded by a double shield made up of a Cryoperm and a superconducting layer. Harness from room temperature to focal plane runs through the cryostat, which should also be laid out as a Faraday cage, which means that the harness for thermometry and potential ADR current leads will have to be filtered (clean). Room for a filter box at 2.5 K should be foreseen. From there on the harness could be run in a superconducting tube (shield) into the focal plane faraday cage (included in harness mass). So in this set-up external radiation fields (both electrical and magnetic) will reach the detector through the front baffle (where also the X-rays enter) and through the connection to the cold finger. For now we will assume tubes with a sufficient length to diameter ratio to suppress these fields. A superconducting grid at the radiation entrance to the detector is under consideration.

The Front End Electronics box containing the SQUIDs electronics is integrated with the cryostat or connected with a short harness in order to make it part of the cryostat's Faraday cage.. It contains only analogue read-out electronics and generators for the sensitive DC-bias signals for SQUIDs and magnets. The connections to the other electronic units (and power supply) are properly filtered.

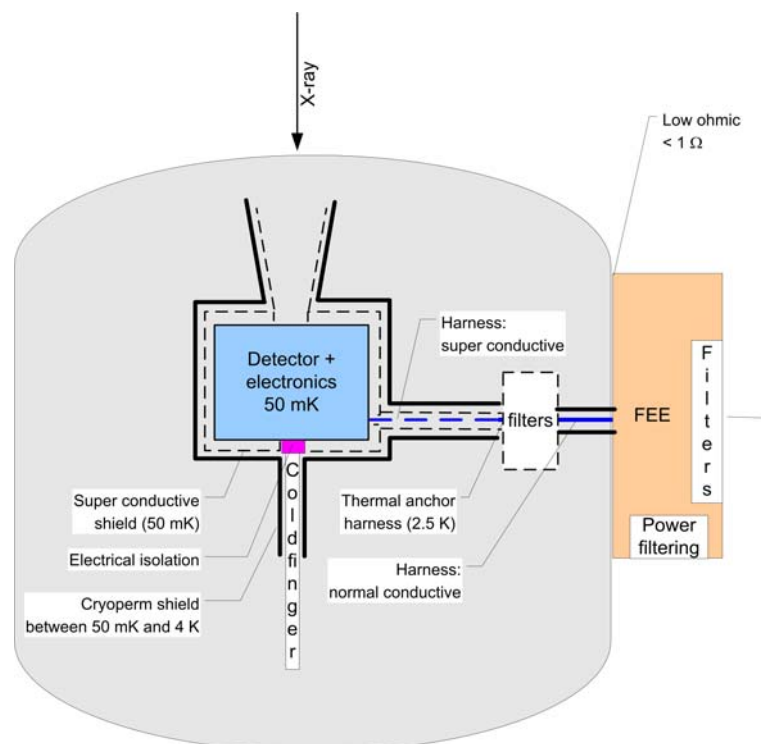


Figure 3-33 Schematic design of EMC related shielding of the detector. The FEE should be mounted within < 0.5 m of the cryostat and have an Ohmic connection (harness) to it with a resistance < 1 m Ω .

A summary of the important points to EMC cleanliness is:

- Twisted wire pair harness and differential electronics for common mode rejection.
- Faraday cage around the entire focal plane instrument with double-walled magnetic and electrical shielding inside the ADR.
- Cryostat acting as Faraday cage as well through careful filtering of all lines entering the cryostat
- Openings in the double-walled shield(s) made such (tubes with sufficient length to diameter) that the fields can not enter the instrument volume
- Filtering of all harness at 2.5 or 4 K stage and at entrance to FEE.
- Single point grounding on the cryostat.
- Only low frequency analogue electronics inside FEE.

3.6.1.1 Conducted susceptibility

There are no specific requirements on the conducted susceptibility on the signal and the power lines. The signal lines will meet the spacewire requirements and the Power Supply Unit will meet the susceptibility requirements of the spacecraft power system (e.g. rms on power line)

3.6.1.2 Radiated susceptibility

The TES detector is very sensitive to power absorption from external EMI sources, which could cause degradation of energy resolution. EMI from the cryo-coolers and the stray magnetic field from the ADR have to be suppressed. These are discussed in some detail below.

Magnetic field susceptibility

Both the TES as well as the SQUIDs are quite sensitive to external magnetic fields. Typical sensitivity values are given in table 6 – 1. For this table it has been assumed that the SQUIDs do have an additional shielding layer with respect to the TES focal plane array, so that the susceptibility of the instrument is driven by that of the TES.

The stability of the bias field perpendicular to the TES is very important. A change in the field strength of 0.1 – 0.15 mGauss changes the responsivity $\Delta S/S$ by about 10^{-4} . This will require significant reduction of the ADR magnetic field by shielding of the ADR magnets, and potential use of buckling magnets, together with shielding of the focal plane array. The present design of magnetic shield includes a cryoperm shield and superconducting shield (Pb/Sn).

Table 3-33 magnetic field susceptibility requirements

Parameter	Value	Comment
Static B-field at TES and SQUID (inside the shield)	$< 1 \mu\text{T}$	During cooldown the static field outside the superconducting shield and inside the mu-metal shield should also be $< 1 \mu\text{T}$
Non-uniformity in static field over TES (independent from each other)	$< 0.2 \mu\text{T}$	To allow same offset B-field for all pixels. Additional magnet add settable field with 2% uniformity
B-field drifts over TES (0 – 1000 s)	$< 5 \text{ nT}_{\text{rms}}$	Responsivity change $-\Delta S/S \sim 10^{-4}$ for 10 nT
B-field drifts over SQUID (0 -1000 S)	$< 0.77 \text{ nTrms}$	
B-field noise over TES	$< 10 \text{ pT}/\sqrt{\text{Hz}}$	To allow same B-field for all pixels
B-field noise over SQUID	$< 2 \text{ pT}/\sqrt{\text{Hz}}$	

B-field (static) outside instrument shielding consisting of mu-metal shield and superconducting shield	$< 10^{-4}$ T	Less than 1 μ T acting on superconducting shield when it is cooled through its transition.
Non-uniformity of permanent external (non-attenuated) field over TES	$< 2 \cdot 10^{-5}$ T	Similar to the < 0.2 μ T variation over the calorimeter surface
B-field drifts outside instrument shielding	< 0.12 mT _{rms}	
B-field noise outside instrument shielding	< 0.3 μ T/ $\sqrt{\text{Hz}}$	
B during non-operational periods (recycling, others) after the superconducting instrument shielding has cooled down.	$< 10^{-3}$ T (TBC)	When larger fields occur this could be trapped in the superconducting shield and a full warm up (very undesirable taking a long time) will be needed to restore the required conditions

With proper shielding (cryoperm + superconducting shield) the external magnetic field can still reach the detector by:

- Fkux vortices trapped in the superconducting shield during cooldown. Since the requirement is 10^{-6} T, and the cryoperm shield reduces the field by about a factor 100x the static magnetic field outside the cryostat during cooldown should be $< 10^{-4}$ T. Care has to be taken that also the conical parts of the superconducting baffle are shielded by about this factor by the cryoperm.
- The detector and SQUIDs can still be reached by magnetic fields through the openings in both shields required for the detector entrance to the sky, the detector cold finger, and harness. Attenuation of these leaks will be essentially achieved by a long conical shaped super conducting baffle for the X-ray side and a long cylindrical shaped super conducting baffle for the cold finger. Of these two the front baffle is the most difficult for a detector of 3.2×3.2 cm² and a cone angle of 5.4 degree (a mirror radius of 1.9 m and a focal length of 20 m). Assuming conical shaped structures with a length equal to about twice the average diameter we get an attenuation of about $8 \cdot 10^5$ and $1.6 \cdot 10^3$ for fields parallel and perpendicular to this tube structure.

Given the complexity of the focal plane and shielding geometry we for the moment assume the worst case attenuation for the perpendicular field, i.e. 64 dB. Since we estimate a attenuation of 40dB for the cryoperm shield we get a total attenuation of 104 dB.

This number has been used to calculate the requirements onto the satellite as given in Table 3-33. The maximum permanent field in the satellite is limited by cooldown requirements. In case this is truly limiting external (warm) shielding could be considered.

Electrical field susceptibility

An important cause of EMI disturbances is the absorption of variations in the high-frequency radiation at levels of 1 fW, which already give rise to unacceptable degradation of the energy resolution in the order of a few eV. Approximate sensitivity levels are given in Table 3-34.

Table 3-34 Electrical field susceptibility

Victim	Sensitivity	Frequency dependent behaviour
TES	40dBpV 1)	DC – 15GHz
TES	80dBpT	0-50 kHz
TES filter inductance		Sensitive at resonant frequencies
Squid 1	31dBpT 2)	0 – 100MHz
Squid 2	31dBpT 3)	0 – 100MHz
Cable loop BCC, DC Bias Squid 1	17dBpA 4)	0 – 100MHz
Loop TES, Shunt, LC-filter, Squid 1	17dBpA	Sensitive at resonant frequencies
LNA input	50 dBpV 5)	0 – 100MHz
ADC input Demux board	97dBpV 6)	0 – 100MHz

1) Noise level $2eV = U^2/R$, $R=30m\Omega$, $\Rightarrow 100pV$

2) Noise level Squid = $0.2\mu\Phi_0$, $\Phi_0 = 2.068 \cdot 10^{-15}$, area = $13 \cdot 10^{-12} m^2$, $B=31 dBpT$

3) Larger area of array Squid compensates gain in first Squid

4) Noise level input squid used as threshold, $7pA_{eff}$

5) LNA input noise $0.3nV_{eff}$

6) ADC input /dynamic range used as threshold, $2V_{tt}$, $10^7 \Rightarrow 70nV_{eff}$

So far experience has shown that with a careful design (single ground, differential electronics, separated and filtered power lines, etc) the instrument works within specification in our research laboratory environment. Obviously detailed sensitivity levels and an extensive system analysis would be required to get adequate specifications for the satellite.

For the moment we ask from the satellite on environment with a field strength $< 2 V/m$ (TBC) for 10 kHz – 4 GHz. This number includes adequate margin with respect a standard 10 V/m laboratory environment.

3.6.1.3 Electrical Discharge

There are no special requirements with respect to electrical discharge once the instrument is integrated. The instrument does however component (SQUIDS, LC-filters, TES-interconnection leads) that in itself are ESD sensitive and will have to be handled with care during integration in the instrument.

3.6.2 Susceptibility for microphonics

The TES and its read-out system are sensitive to microphonics introduced by either the cryo-coolers themselves or by the spacecraft (e.g. reaction wheels). The instrument design will include balanced compressors running at slightly different frequencies. Similar precautions are required for spacecraft units which may induce microphonics during observations (e.g. reaction wheels but not the unloading of the reaction wheels).

In our laboratory environment it has been shown that a TES can be operated in a dry-cooler environment (Cryomech pulsetube) without suffering from microphonics. The typical vibration levels at the cold-stage (measured warm) are about $0.3 - 3 \mu g/\sqrt{Hz}$ for $30 < f < 300 Hz$. We know that not very much margin does exist in our present measurement set-up. These numbers are similar to those measured on the Suzaku XRS detector and should be used as requirements for the design.

3.6.3 Susceptibility to radiation

The SQUIDS have been tested with regards to radiation hardness. The results show tolerance levels up to at least 100 kRad. Currently, no radiation hardness data is available for the TES. Since it is made up of Au-Ti bilayer it should be able to withstand similar levels of radiation as the SQUIDS.

3.7 Optical Requirements

3.7.1 Stray-light requirements

Optical straylight will to a large extent be stopped by the entrance filters of the instrument, which have a transmissivity of $< 10^{-5}$ (TBV) in the optical and $< 10^{-10}$ in the IR wavelength range. The optical straylight should not add more power to each detector pixel than about 1% (TBV) of its bias power, provided it is stable. Furthermore the loss of energy resolution by photon induced noise should be kept < 0.2 eV_{rms}. The photon noise induced degradation of the energy resolution is given by $\Delta E_{rms} = \sqrt{P \cdot h \nu \cdot \tau}$ with P the optical power hitting the one pixel, $h\nu$ the photon energy, and τ the effective time constant of the detector, i.e. about 300 μ s. For a pixel of about 300 x 300 μ m² and an entrance filter with about 10^{-5} and 10^{-10} (TBV) transmission we can allow for straylight levels of about $2.5 \cdot 10^9$ at 0.5 μ m and $1.0 \cdot 10^{17}$ ph/cm²/s at 10 μ m, respectively. With regard to the maximum power level at one pixel these rates result in a power input of 1.6 fW, which is about 10000x lower than the bias power and therefore quite ok.

Table 3-35 Straylight requirements at the entrance of the instrument

Wavelength	Suppression by cryostat entrance filters	Allowed input flux at dewar entrance in photons/cm ² /s
0.5 μ m	10^5	$2.5 \cdot 10^9$
10 μ m	10^{10}	$1.0 \cdot 10^{17}$

Assuming this level is due to sunlight ($T_{eff} = 5770$ K, intensity is $1.38 \cdot 10^3$ J/m²/s) and an acceptable resolution degradation of 0.2 eV, the incident flux on the detector entrance filters, after applying a reduction due to the spacecraft structure of $5 \cdot 10^7$ is $1.26 \cdot 10^{10}$ photons/cm²/s. This is nicely consistent with the presented straylight requirements

3.7.2 Baffling requirements

The instrument will require baffling to:

- suppress the X-ray background (see section 3.2.4, items e). This could be realized by a tube in front of the detector or some blocking plates in the telescope tube.
- to protect the instrument for a too high particle background. Although it is expected that the detector proper (TES and SQUID) is radiation hard and possibly the electronics in the electronic boxes is the most critical, this needs to be proven by the appropriate tests (which haven't been carried out yet). Depending on the outcome some shielding around the entrance might be required (to ensure sufficient stopping power over 4π).

It is expected that the baffling implemented for the larger WFI will be sufficient for XMS.

3.8 Transportation, Handling, Cleanliness and Purging Requirements

3.8.1 Transportation requirements

The instrument dewar shall be transported in a temperature and pressure controlled container which will be supplied together with the instrument. The orientation of this container is not important (TBC). Following integration it is assumed that the prime spacecraft contractor will guarantee these conditions. No special requirements exist for shockloads. For all other units standard transport containers will be provided but during transportation the non-operational limits should be observed.

3.8.2 Handling requirements

At selected points in the program pumping of the dewar after integration on the spacecraft is required. For cooled operations it is required to have access to some of the dewar plumbing (to fill the LN2 tanks)

3.8.3 Cleanliness requirements

Molecular contamination must be guaranteed to be small compared with effects of X-ray transmission filter performance. For instance within the energy range a Carbon line at 275 eV will be affected by a hydrocarbon build up. An attenuation length of 0.1 microns implies a change in efficiency of 10% (already affects useful calibration) at end of life. Consequently the molecular contamination level should be below a few 10^{-7} cm²/g.

3.8.4 Purging requirements

No purging is foreseen.

3.9 Ground and flight operations requirements

3.9.1 Ground and pre-flight operation

In Table 3-36 the ground operations after delivery to the spacecraft are specified. At instrument level the different sub-units will be calibrated at the required level and instrument end-to-end tests will be performed using radio-active sources (the integrated instrument will not be tested at a synchrotron facility).

Table 3-36 Ground and pre-flight operations of the XMS

Test	Conditions	comments
Post delivery	Cooled dewar, X-ray from a few pixels	Cool-down cycle is less than 2 weeks
Post integration	Warm dewar, functional	Electrical connectivity will be tested but no X-ray measurements
mechanical acceptance	Warm dewar, functional	See above
EMC	Cooled dewar, X-ray from single pixel	Effect of external cooling equipment need to be controlled
Thermal Balance	Cooled dewar, X-ray from onboard calibration sources, verification of micro-physics due to AOCS system (reaction wheels) should be tested.	During the thermal balance test the system can be fully operated provided that the cryo-coolers are operated on 1.5 (TBC) times their nominal power. During these tests X-rays from the onboard calibration source will be observed by all pixels.
Pre-launch	Warm dewar, functional	Electrical connectivity will be tested but no X-ray measurements

3.9.2 Flight operations

A large variety of options exist for the flight operations. In this section we give some representative samples for typical cases. Many of the relevant characterizations can be performed when one of the other instruments is observing provided that the required telemetry rate and cooling power is available for the XMS (the main fraction of the cooling power is required in any case as the cryo-coolers will be operated at a stable level).

Table 3-37 Typical flight operations for the XMS (add plot with time of OBSERVE during WFI is main

Goal	
observe	<ul style="list-style-type: none"> - Prepare last stage cooler (eventually regenerate if needed) - Set relevant spacecraft parameters (telemetry allocation etc) - Perform 1 hour verification run with onboard calibration source - Move detector into focus - Choose instrument settings (filter wheel, readout of detector segments, etc) - Observe (typically less than 30 hours, if longer regeneration is needed) - Move detector out of focus - Perform 1 hour verification run with onboard calibration source
Standby	<ul style="list-style-type: none"> - Close filter wheel
emergency	<ul style="list-style-type: none"> - close filter wheel - switch off units which are not critical (FEE, DE, LCD) but leave other units on (at low power levels)
Initialize	<ul style="list-style-type: none"> - collect data for filter templates onboard (e.g. could be done when instrument is not selected for an observation using onboard cal sources)
internal calibration	<p>These calibrations require special settings of instrument parameters (and possibly some structure for the data format) but do not affect spacecraft resources. Typically these are performed during the performance verification phase and in case the performance is unexpected. During all these measurements we will have</p> <ul style="list-style-type: none"> - close filter wheel - set housekeeping rate at its maximum (1 Hz) <p>calibration of electronics:</p> <ul style="list-style-type: none"> - gain evaluation using electronic stimulus - electronic noise evaluation - characterization of SQUID amplifiers, and setting of bias point <p>Detector calibration</p> <ul style="list-style-type: none"> - IV-curves on individual TES (frequency: at least each time the instrument is cooled down from above 4K or has been switched off): - monitor critical current near zero bias to optimise magnetic field bias - noise measurements as a function of biaspoint <p>anti-coincidence detector</p> <ul style="list-style-type: none"> - At selected times the spectrum, time duration and shape of events of the anti coincidence detector will be transmitted to the ground. These can be used to check the health of this detector and its gain. Other important information is the energy deposit of the minimizing

	<p>ionizing particles.</p> <p>end-to-end characterisation</p> <ul style="list-style-type: none"> - select onboard calibration source - observe with the instrument and extract noise spectra and relevant parameters (on ground)
External calibration	<p>External calibrations are dedicated observations to monitor the instrument performance. Typically these will be carried out once every half year and include (typically 50 ks each):</p> <ul style="list-style-type: none"> - observation of stable extended source (e.g. SNR 1E0102) - observation of bright continuum source centred at 9 different positions (e.g. Mrk 421). This provides information about contamination (especially around ice on the detector) - observation of a stable soft source to verify contamination (e.g. RXJ 1856, vela pulsar) - observation of line rich source at 9 different positions (Capella, Ab Dor). Using the grating instrument the energy of the lines is exactly known and this information can be used to check the instrument response

Operating modes

The XMS will be operating by execution of a limited number of predefined set of time tagged commands executed by the spacecraft. Observation times will range from hours up to 30 hours. The modes are described in sections 3.2.11 and in 3.5.4

3.10 Deliverable models and GSE

3.10.1 Structural Thermal Model

A full STM will be delivered which is thermally and mechanically representative (90% of the dynamic mass).

3.10.2 Engineering Qualification Model

A qualification model will be developed being representative of the instrument (warm redundant parallel chains will not be implemented). A full instrument qualification including vibration in cold conditions (the stiffness of the straps inside the dewar is dependent on the temperature) is planned.

3.10.3 Flight model

A full flight model will be delivered

3.10.4 Flight spare model

A flight spare model will be produced but not integrated (e.g. cold head, last stage cooler separately). Depending on the spacecraft requirements fully integrated spare electronic boxes will be available or this will be provided on sub-system level (e.g. for a data processing unit with an equivalent channels it is probably sufficient to have 2 (or 3) spare channels and not the fully integrated system).

Unit	Flight spare	comment
Dewar	No	No integrated flight spare unit is planned (especially not for the large thermal shields inside the dewar and the outer structure). Instead flight spare sub-units will be maintained: <ul style="list-style-type: none"> - one Stirling cooler - one JT cooler - a second last stage cooler - a second detector (including SQUIDS and anti-coincidence detector) - a second set of internal harness - a second set of straps - 25% of the number of struts to mount the dewar on the satellite In case in a late stage the dewar has to be refurbished, this will have a major impact on the schedule. However, in case of a problem, a simple replacement will not be sufficient as the cause of the non-performance needs to be investigated first (which effectively means a disassembly of the unit).
FEE	No	Of all boards a fully tested flight spare will be maintained (e.g. for parallel chains only one/two spare will be maintained)
DE	1	One full DE (nominal 4 units are used)
PCD/SCD	1	One unit for the Pre Cooler Drive and the Shield Cooler Drive together

3.10.5 Ground Support Equipment

Although the list of ground support equipment is not complete some main parts include:

GSE	Function
Hoisting tools	Only for the dewar
Instrument control unit	Equipment to control the instrument in case there is no spacecraft to control the instrument
Instrument power supply	Equipment to provide power to the instrument
Instrument cooling	Equipment to connect the dewar to the LN2 supply and pumping system to operate the instrument in an ambient environment on the ground.
Cryo-cooler cooling system	Equipment to maintain the temperature control of the cryo-coolers under ambient test conditions

4 HARD X-RAY IMAGER (HXI)

The Hard X-ray Imager (HXI) is mounted beneath the WFI, to extend the energy coverage up to 40 keV. The two instruments share the same focal plane, and the same baffle structure, with heavy metal sheets added for hard X-ray coverage. The HXI detector is made up of three layers, 2-Silicon (Si) and 1 Cadmium Telluride (CdTe) detector, setting back from the WFI plane by about 20, 22.5 and 25 mm, or less, respectively. The set-back of 25 mm on the CdTe detector enlarges the PSF by 1.25mm in diameter because of the defocusing, which corresponds to about 13 arcsec, assuming an effective radius of 1 m at 30 keV combined with 20 m F.L.

4.1 Instrument Description

4.1.1 Introduction

From the scientific requirement, the HXI should cover from 10 keV to 40 keV with an energy resolution better than 1 keV (FWHM) at 40 keV and a field of view (FOV) of 12×12 arcmin². Since silicon becomes almost transparent in the energy band above ~ 30 keV, even with a thickness of two or three mm, semiconductor detectors with high mass absorption coefficient, such as Cadmium Telluride (CdTe), are crucial for the detection of hard X-ray photons. In order to obtain high spatial resolution that matches with the angular resolution of the IXO XRT, and to cover a wide FOV, we propose to use a newly developed Double-sided Strip CdTe detector (DS-CdTe detector) as the first option. Based on the rapid development of 2-D low-noise & low-power ASICs, we could envisage the use of a 2-D pixel array if we are able to operate the ASIC with sufficiently low power. By using 2-D pixel detectors, an improvement of energy resolution could be expected. A detector with a thickness of 0.5 mm provides 100 % detection efficiency for 40 keV hard X-ray photons. The position resolution of 220 μm (or < 600 μm in the pixel option) corresponds to a pixel size of 2.3×2.3 arcsec² (respectively 6.2×6.2 arcsec²). The detector field of view (FOV) is designed to be 70×70 mm² as a default referring to the existing detector technology. In addition, a 105×105 mm² device to cover the same FOV as that of the WFI is under consideration. To suppress background, an active anticoincidence shield is deployed around the imager. It is made of 2 cm thick BGO (Bi₄Ge₃O₁₂) crystals, read-out via avalanche photo diodes (APDs).

In addition, two layers of Double-sided Si Strip Detector (DSSD), with dimensions the same to those of the CdTe detector (i.e. 7 cm wide and with a thickness of 0.5 mm) will be mounted above the CdTe. Experience on the Suzaku hard X-ray detector clearly showed that the background of Si, actively shielded by BGO is pretty low in the orbit. Instead, background of GSO (Cd₂SiO₅) covering above ~ 40 keV is pretty high. This is due to cosmic ray activation. CdTe is a heavy material and therefore background due to activation could be high as well. If we only rely on CdTe, we may lose our sensitivity in the 10-30 keV band, in which the Si detector can still work. In order to avoid such risks, Si layers above the CdTe are useful. In the current stage, we assume a non-X-ray background of 5×10^{-4} cts s⁻¹ cm⁻² keV⁻¹. This value is about 2 times higher than the actual level observed in HXD-PIN onboard Suzaku. We set the margin because of the difference in the detector design and the fact that the orbit of Suzaku and IXO differs. Since the HXD-PIN background is affected by particles in SAA, which we do not need to care at L2 orbit, the current estimation of non-X-ray background is conservative.

HXI is contained within an extension of the WFI body, located behind the nominal focal position by about 25 mm. Soft X-rays will be absorbed in the WFI, while hard X-rays will penetrate through it and be absorbed in the HXI.

The IXO-HXI introduces the experiences of preceding missions, such as the ASTRO-H (former NeXT) HXI. Baseline design is based on the ASTRO-H design with some improvements. Therefore, the ASTRO-H-HXI is treated as one of the Engineering test model for the IXO-HXI. Lessons learned from Simbol-X and NuSTAR will also be adopted.

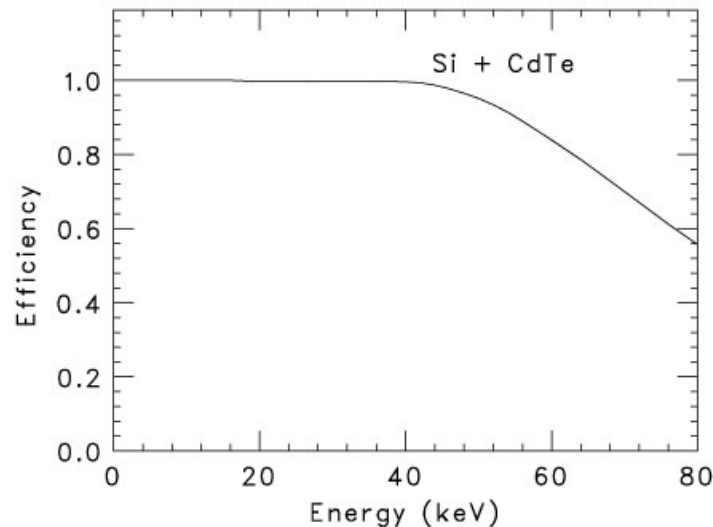


Figure 4-1: Efficiency of a combination of DS-CdTe detector and Si DSSDs.

4.1.2 Instrument performance specifications

The specific performance of the HXI is summarized as follows.

Table 4-1: HXI scientific specification

Characteristics	Strip design	2-D pixel array option
Detector Type	Si and CdTe Schottky Diode double sided strip	Double sided Si strip and CdTe Schottky Diode pixel devices
Strip pitch	220 μm (for both sides)	<600 μm (for CdTe pixel)
Number of strips	320 (for both side) total 1280 strips for CdTe Two layers of DSSD are placed in front of CdTe, with a total of 2560 strips	>13k / >31k+ channels for 70 mm wide CdTe pixel detector, and 2 layers of DSSD, in total 2560 strips
Array Size (mm^2)	70 \times 70	Idem
Field of View	12 \times 12 arcmin ²	Idem
Energy range	10–80 keV	Idem
Energy Resolution	$\Delta E < 1$ keV(FWHM)	Similar or better
Non X-Ray detector Background	5×10^{-4} counts $\text{keV}^{-1}\text{cm}^{-2} \text{s}^{-1}$ roughly flat	Idem
Count rate/pixel with 10% pile-up	20000 cts.s^{-1} independent of the position	Idem

Count rate/source with 10% pile-up	20000 cts.s ⁻¹ independent of the position (note Crab is expected to generate 100-500 cts.s ⁻¹ only)	Idem, Pile-up is significantly reduced with pixels if each channel is individually operated, depending on the ASIC detailed design.
Timing accuracy	10 μs	Idem
Typical/ Max telemetry	10 kbs ⁻¹ (1 Mbs ⁻¹ max for ground calibration)	Idem
Operating Temperature	Detector -40 or -30 (TBR) ± 2 °C Electronics 20± 20 °C	Idem
Thermo control to maintain temperature and raise temperature to +5°C, if necessary		
Instrument Power, excluding thermal control	41W	Idem
Total Mass	25 kg	Idem
Total Power	46 W; Additional 50 W (TBR) heater power will be temporary needed to heat up the device up to +5°C (see text for detail).	Idem

4.1.3 Instrument configuration

The HXI system composes of 3 boxes, the sensor part (HXI-S), the analog electronics box (HXI-E) and the digital electronics part (HXI-D). Baffle, door and filter sled with calibration source are shared with those of the WFI. Wire harness between the boxes will amount to less than 10 kg in total, depending on the distance between each of the boxes.

4.1.3.1 The Imager part

The HXI employs an array of compound-semiconductor double-sided strip detectors read out by front ASICs bonded to strip electrodes, orthogonally implemented on both sides of the semiconductor wafer. To obtain good imaging quality, the detector is based on highly uniform CdTe semiconductor and Si. In each of the DS-CdTe and DSSD layers, the current baseline design employs a 2 × 2 array of 3.5 cm large devices. Each detector has 160+160 strips with a strip pitch of 220 micron. These double-sided strip layers provide with a 12 arc-minute square field of view and an imaging capability of 2.3 arcsec with a 20 m focal length.

Another technology option is the CdTe 2-D pixel device, with a pixel pitch of < 600 micron or <6.3 arcsec resolution. Because of the reduced electrode area per channel, better energy resolution and higher throughput is expected in this case. Since the pixel pitch gets a bit larger, the pixel option with current technology is good in case the mirror PSF at the hard energy band is wider than 13'', which is expected from the set-back of the CdTe imager from the focal plane by 25 mm.

A thickness of 0.5 mm or 0.75 mm is considered for CdTe. Bias voltage is about 600 V. In the strip option, the signal from a photon absorbed in the detector is detected through the strip electrodes implemented on both sides of the layer, and fed into analogue chains implemented in the ASICs. In the pixel option, the signals from the pixel electrodes are fed into the ASIC. Either a combination of Charge Sensitive Amplifier and Shaping Amplifier or a Time-over-Threshold architecture will be used in the ASIC. According to the measurement with prototype detectors, an energy resolution of better than 1 keV (FWHM) can be achieved in the energy range from 10 keV to 80 keV when we operate the detector at or below 233 K. The DSSDs will also have a thickness of 0.5 mm. The read out system is the same to that of the CdTe detectors. Bias voltage

for the DSSDs are about 250 V. An ^{241}Am source will be mounted on the filter sled of the WFI, at the calibration isotope position.

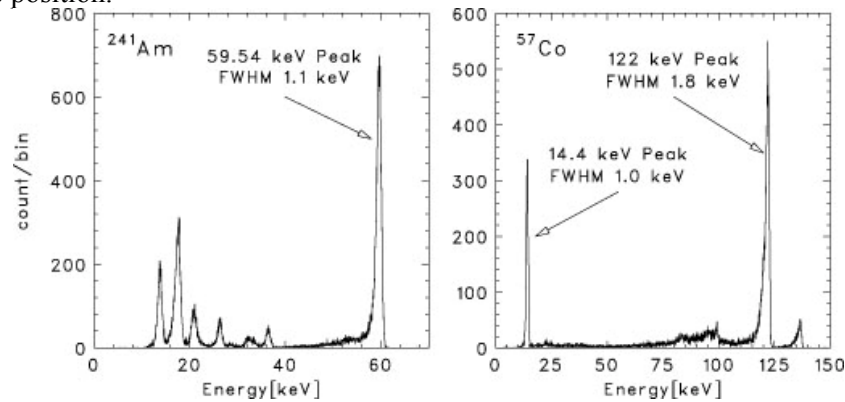


Figure 4-2. Energy spectrum obtained with a large-area CdTe diode pixel detector. A pixel size is $1.4 \times 1.4 \text{ mm}^2$. Operating temperature is -20°C . The signal from pixels is processed with specially designed ASIC, which will be used for the proposed CdTe strip detector.

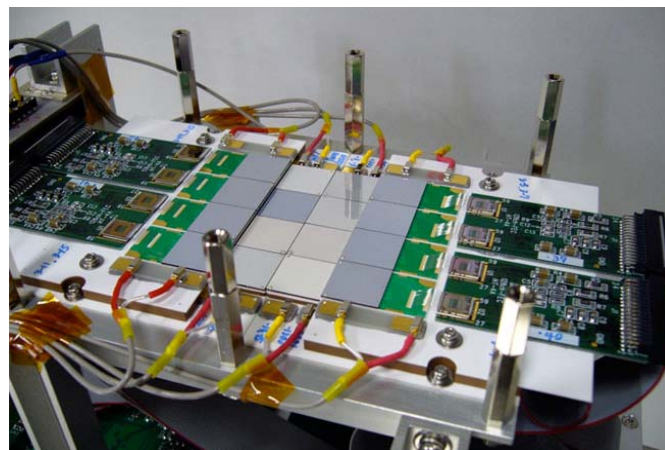


Figure 4-3. Large area CdTe diode Pixel Detector (8×8 pixel detectors tiled 4×4) and the interface electronics currently under test in JAXA. The IXO-HXI will use double-sided strip devices, which is the next generation technology to this detector.



Figure 4-4. Photo of a DSSD prototype layer. The DSSD size is $2.5 \times 2.5 \text{ cm}^2$. The IXO-HXI will use DSSDs with a similar design, but with a larger area of $3.5 \times 3.5 \text{ cm}^2$ (4 chips per layer) or larger.

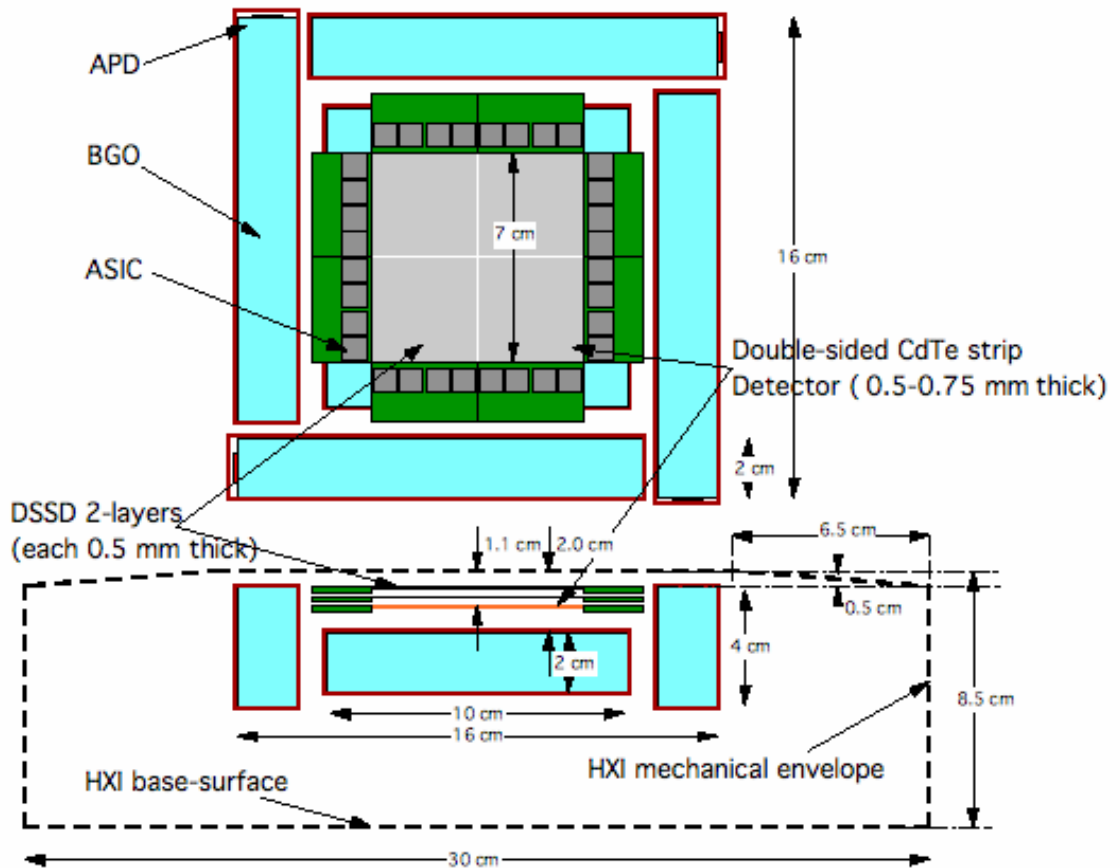


Figure 4-5. Geometry of the detectors in the HXI focal plane

4.1.3.2 Active shield

In order to obtain high sensitivity with the HXI, the DSSDs and DS-CdTe/pixel CdTe detectors are actively shielded by BGO scintillators. This shield is indispensable, as the non X-ray background is the dominant source of the background in the energy range of the HXI. A thickness of ~ 2 cm of BGO will be required, not only for shielding against background photons but also for reducing the number of particles that reach the CdTe detector and give rise to activation. In order to cope with the BGO shield, the detector should have fast timing resolution of 1 to 4 μ s, such that we can veto the events when there is a hit in the shield. Light from the BGO is read by APD. The APDs require a bias voltage of ~ 400 V.

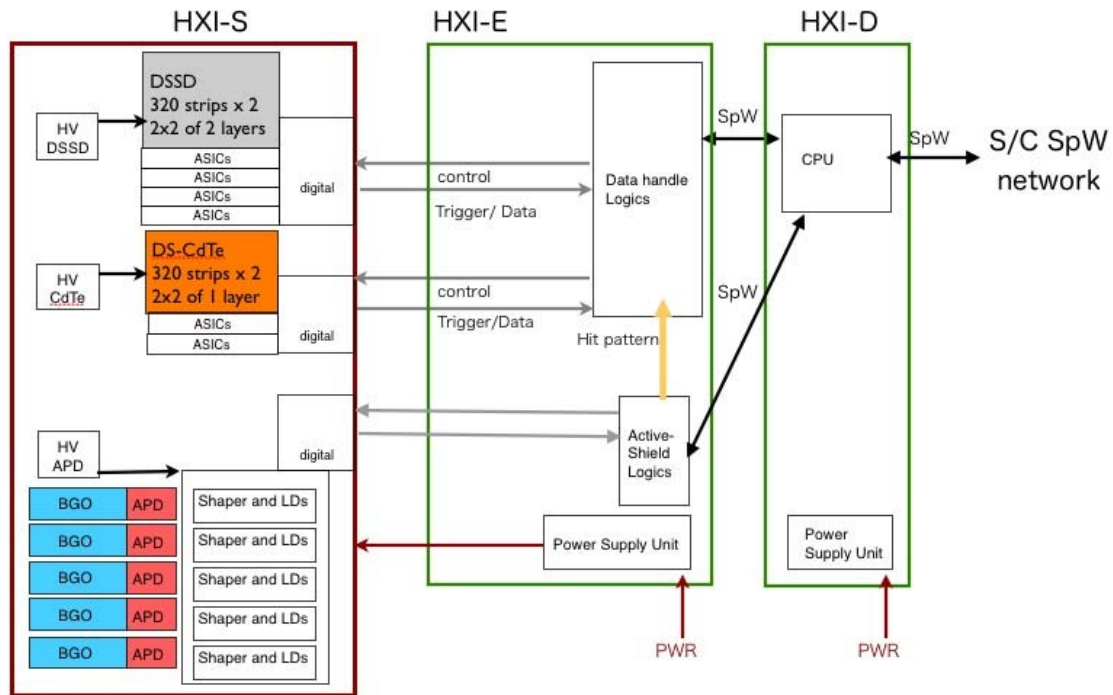


Figure 4-6. Overview of the sub-system of HXI

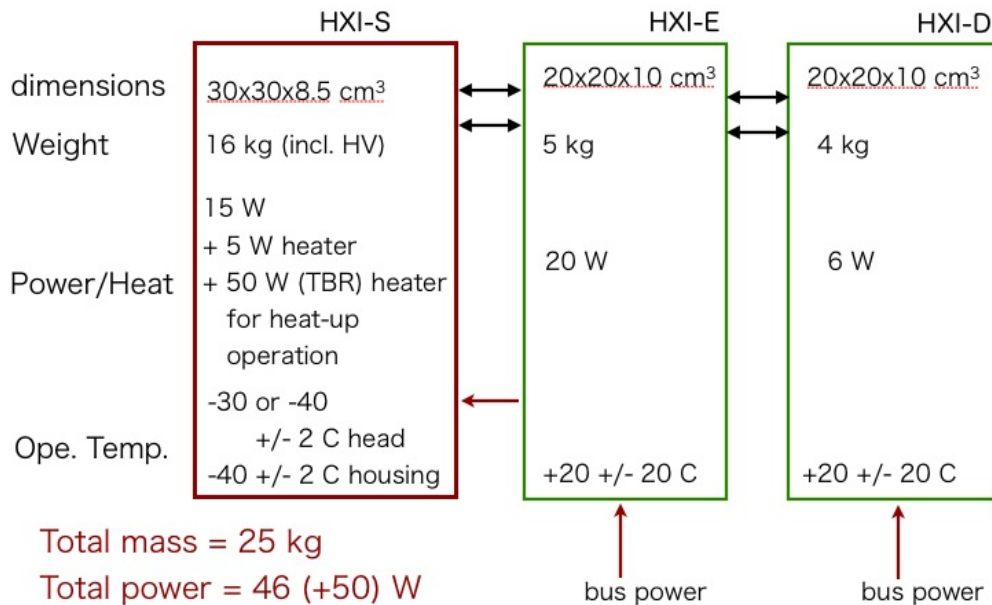


Figure 4-7. Mechanical block resource diagram of HXI. The three HV modules are physically attached to HXI-S, but thermally isolated from it.

4.1.4 Instrument Optical Design

The HXI is mounted right below the WFI. Thus most of the optical and alignment requirements are common to those of WFI. The Z-axis offset is to be minimized to reduce degradation in imaging resolution. Here, we assume that the focal plane is set at WFI surface. Since the effective radius of the mirror optics is about 1 m for X-rays above ~20 keV, the front surface of the HXI-CdTe imager must be mounted within 25 mm from the focal point to keep the defocusing effect smaller than 1.25 mm, i.e. 13 arcsec.

Cosmic X-ray background directly (e.g. not via the mirror) coming into the HXI imager is a major problem. To reduce it, baffling is required. Since the HXI is placed beneath the WFI, the baffle structure is common. The HXI specific requirement is to absorb photons up to 80 keV. From the absorption power calculation, a thin Gold layer with line-of-sight thickness of 200 μm is considered as baseline. An equivalent alternative is under consideration. This corresponds to 1/e attenuation energy of 70 keV.

Because of its location, i.e. beneath the WFI, there is no optical filtering requirement on the HXI. By similar reason, there is no requirements for the charged particle deflectors, since the WFI will effectively stop these particles in the energy range of interest (<80 keV).

A calibration source made of either a radio-active source (^{241}Am) or electrical X-ray generator is considered as an option. This requirement depends on the expected radio-activity in CdTe, and the line emissions observed in the DSSDs (e.g. within the coincidence window between the DSSD and the CdTe). Since the calibration source, if required, is irradiated, the HXI sensitivity will decrease significantly. Thus, it shall be able to be removed or powered off in case not used.

4.1.5 Instrument units' mechanical design and dimensions

HXI-S forms a rectangular box, 30x30 cm^2 wide and 8.5 cm in height. The box is light tight, but not vacuum tight. Refer to Figure 4-5, Figure 4-7 and Figure 4-8. Mechanical (and thermal) interface is defined on the base-surface at the bottom and the detector is bolted to a cold finger beneath. Detailed design is not completed.

Regarding the HXI-E and HXI-D, the box sizes and weights are defined. The mounting technique is not critical and may be adapted easily to the payload arrangement as long as HXI-S and HXI-E are located within 2 m (maximum harness length). On the other hand, HXI-D can be located anywhere within 10 m from HXI-E.

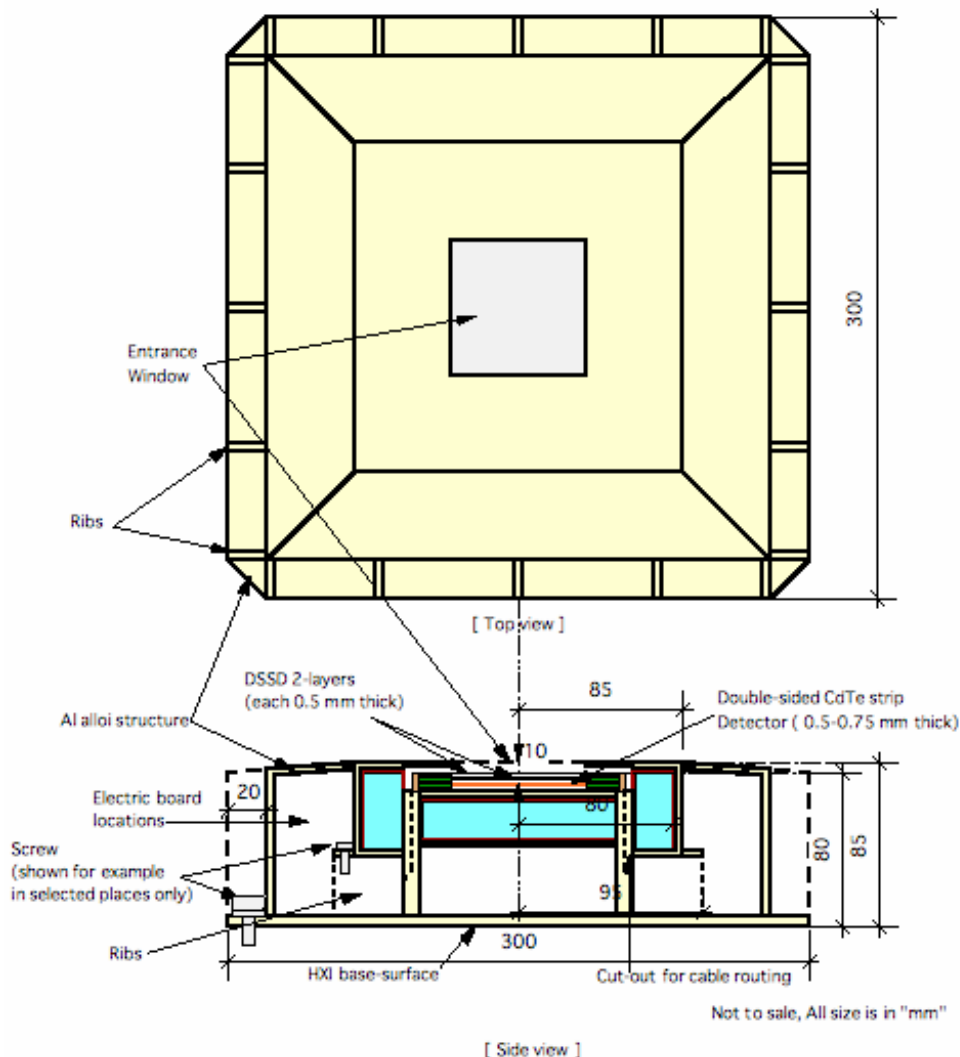


Figure 4-8. Mechanical design rough sketch of HXI-S.

4.1.6 Mechanisms

No moving part exists in the HXI system. Other mechanical requirements will be described elsewhere.

4.1.7 Instrument units' thermal design

The baseline HXI-S as a whole is operated at 233 K. Since it is mounted right below the WFI, which is operated at 210 K, a thermal de-coupling is required. Another requirement is to heat-up the CdTe detector material up to 278 K once a month (baseline). The CdTe and DSSD is not operating in this heat-up period, and no bias will be applied. The heat up and then cool down operation is required to be completed within 3 days, with <math><15\text{ C/hr}</math> temperature slope. The heat-up operation could be performed when other focal plane instruments are at the focus. To radiatively decouple WFI and HXI, a thin Aluminized Mylar foil will be used as the entrance window. Simple estimates show that the heat input from HXI-S to WFI-S through radiation is less than 1 W and 2 W in ordinal and heat-up operations, respectively. HXI-E and HXI-D can be operated at room temperature, i.e. $293 \pm 20\text{ K}$.

4.1.8 Electrical design

In the ASICs for DSSDs and CdTes, parallel ADC is built in to convert analogue signal to digital (AD conversion) in the chip without multiplexing. Note that the power budget already includes these ADC and associated digital circuits, based on the experience on the prototype ASIC with ADC already implemented. Since the progress of the ASIC development is rapid, we anticipate to adopt much advanced ASIC when it becomes available. The power dissipated by the ASICs is as low as $300\mu\text{W}$ per channel. There would be an option to use CdTe pixel detector, if low power and large area 2-D ASICs becomes available. The front-end ASICs are controlled via a specified logic board. High voltage power supply will be also connected to the ASIC boards. Dedicated analogue circuits for reading out APDs are required. They will be controlled by a specific logic board. In total 9~15 W will be dissipated within HXI-S, depending on the adopted technology.

Both the imager data and shield data will be fed into the data handling logic, responsible for raw event screening, such as anti-coincidence and so on. The logic will also provide with House Keeping data of the imager and the shield. For further data screening and event packet generation, on-board data histogram accumulation and House Keeping packet generation and so on, a CPU-based digital board will be required.

Electrical (as well as mechanical) system block diagram is shown in Figure 1.1-6. HXI-S contains the ASICs, its control electronics and high voltage bias suppliers. Bias supplier of the APDs are also mounted. HXI-E contains APD analog circuits and logics for 1st stage data screening. HXI-D controls the HXI-E, generate telemetry packets and receive commands from the bus-system. There are both digital and analog interface between HXI-S and E, only digital interface between E and D. The digital lines will be based on SpaceWire technology. Power is supplied from HXI-PSU to HXI-E and D, while that for HXI-S is supplied via HXI-E.

4.1.9 Onboard software

No detail specification is defined yet. There already exists a reference design for the software used in ASTRO-H and BepiColombo MMO. Note that the ASTRO-H-HXI software, with little modification, will be usable in all sense.

4.1.10 Ground support equipment

4.1.10.1 Electrical GSE

Power supply and computer supporting SpaceWire interface is required. Other GSE such as thermostatic chamber etc. can be shared with other projects and/or existing equipments.

4.1.10.2 Mechanical GSE

N/A. JAXA existing GSEs will be used for the vacuum test, thermal vacuum test, vibration test and EMC test. The same procedures taken in the ASTRO-H-HXI, with some updates regarding the IXO specification are considered as baseline.

4.1.11 Instrument mode description

4.1.11.1 Operating modes

There are 2 operating modes: the normal observing mode and the calibration mode. Former is in the normal operation. The latter is used in the calibration of ASICs and function check of the system, in which mode the imager is not observing celestial objects but the power consumption is the same to that of the normal observing mode.

4.1.11.2 Non-operating modes

There are 2 non-operating modes, as well: the power-off mode (including the safe mode) and the CdTe heat-up mode. In the former mode, all system power is off. Only the power to keep the instrument components within its required temperature is used. In the latter mode, only the HXI-S (and HVs) will be powered off. HXI-E and D will keep monitoring the instrument status. In addition, heater power is required to heat-up the HXI-S to 278 K.

4.1.11.3 Comments on the Safe mode

Safe mode, which will be used in emergency, is the same to the power-off mode. When asserting the safe mode, however, the HXI needs a few commands and 30 seconds (TBR) of time to safely reduce their HV levels, avoiding damage or stress on the analog inputs. Depending on the safe mode requirement, the HXI could be immediately powered-off, though some small stress is inevitable. In the latter case, the risk of malfunction is low, but non-negligible (TBR).

4.2 Mechanical interface and requirements

4.2.1 Location and alignment requirements

As already mentioned, HXI is mounted right below the WFI. Here, we define location requirements relative to WFI. Refer to Figure 4-5 for HXI geometry.

In the X-Y direction, the HXI alignment requirement is the same to that of the WFI. The imager center of HXI must be mounted right below that of the WFI, within 500 μm accuracy. Rotation accuracy must be < 5 arcmin as well. On the Z-axis, as specified in section 4.1.4, we require that the front surface of the HXI-CdTe imager be mounted within 25 mm from the focal point.

4.2.2 Pointing requirements and goal

Pointing requirements are the same to those of WFI.

4.2.3 Interface control drawing

Not yet specified. Refer to Figure 4-8.

4.2.4 Instrument mass

Table 4-2. HXI resource table.

Component	Location from FP	Mass (kg)	Mass margin (kg)	Power (W)	Power margin (W)	Temperature (operation)
Detector head	< 25mm (HXI-S CdTe top)	16	4.8	20	6	- 40 ± 2 ° C Detector head: -40 or -30 (TBR) +/- 2 ° C
Electronic unit	< 2 m	5	1.5	20	6	20 ± 20 ° C
Data processing	< 10 m	4	1.2	6	3	20 ± 20 ° C
Sums		25	7.5 kg	46 W	15 W	
Tot inc margins		32.5 kg		61 W		

4.3 Thermal interface and requirements

4.3.1 Temperature limit in space environment

Temperature requirements are summarized in Table 4-3 “HXI temperature requirements”. Temperature slope must be < 15 C/hr.

Table 4-3. HXI temperature requirements

Component	Operation	Non-operation	Safe Mode	Heat-up mode	Ground operation	Ground handling
HXI-S	-40 ± 2 ° C	-42 – +40 ° C	-42 – +40 ° C	+5 ± 2 ° C	-20 ± 2 ° C	-42 – +40 ° C
HXI-E	20 ± 20 ° C	-40 – +40 ° C	-40 – +40 ° C	20 ± 20 ° C	-20 – +30 ° C	-40 – +40 ° C
HXI-D	20 ± 20 ° C	-40 – +40 ° C	-40 – +40 ° C	20 ± 20 ° C	-20 – +30 ° C	-40 – +40 ° C

4.3.2 Temperature limit in laboratory environment

Specified in Table 4-3 “HXI temperature requirements”. Temperature gradients on time must be < 15 C/hr.

4.3.3 Temperature sensors

Internal temperature sensors are included within the HXI data acquisition system. However, we need several sensors to understand the HXI status, when the HXI system is off. We require 1 on the HXI-S structure, 1 on HXI-E and 1 on HXI-D. For contingency, 2 lines each will be preferred.

4.3.4 Heaters

Besides the 5 W heater required from the overall instrument thermal design to keep the imager head within the required temperature, HXI-S needs an additional heater with 50 W (TBR) power to heat-up the CdTe sensor of HXI-S to 278 K.

4.3.5 Thermal schematics

Figure 4-9 provides the thermal schematics of HXI-S. Here, we employ a cold-plate thermally connected to a radiator, and thermally controlled by a heater. HXI-S is thermally (and mechanically) connected to the cold-plate.

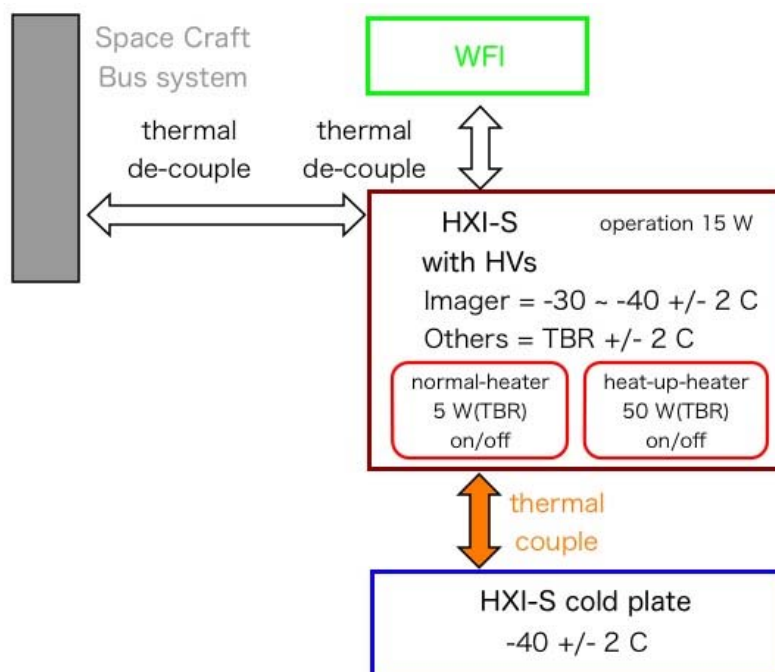


Figure 4-9: Thermal schematics of the HXI-S

4.3.6 Thermal control requirements

Specified in Table 4-3 “HXI temperature requirements”.

4.4 Electrical Interfaces and requirements

4.4.1 Electrical resources requirement summary

Electrical resource requirement is summarized in Table 4-2 “HXI resource table” and Figure 4-7 “Mechanical block resource diagram”.

4.4.2 Instrument power distribution block diagram

Described in Figure 4-7 “Mechanical block resource diagram of HXI”.

4.4.3 Power budget

Described in Table 4-2 “HXI resource table”

4.4.4 Instrument modes’ duration

4.4.4.1 Instrument continuous mode duration

Duration of the normal observation mode is variable, from 1 ks to 1 Ms. The calibration mode requires the same power condition as the normal mode. In this mode, two sub-modes will exist with no difference in power requirements, a test-pulse operation on the LSI and a calibration source irradiation from the filter sled of WFI as an option. Power-off mode spends no power, except for that used to satisfy thermal requirement.

4.4.4.2 Instrument peak mode duration

In the CdTe heat-up mode, power consumption in HXI-S is zero, while that in HXI-E and HXI-D is the same as in the normal observation mode. An additional 50W (TBR) heater power to heat up the CdTe sensor in HXI-S is needed, but will be off for most of the life time. The heat-up mode will last at most 72 hours.

4.4.5 Telecommands

TBD. HXI system requires dozens of commands to control itself. A parameter table upload will be needed to modify the operation parameters of HXI-S, E and D. For critical commands, such as HV up/down, power-off etc., a special care such as double command, command arming and so on will be required.

4.4.6 Telemetry

4.4.6.1 Telemetry requirements

TBD. In total 10kbs⁻¹ typical and 1 Mbs⁻¹ burst. SpaceWire packet transmission is assumed in this estimate.

4.4.6.2 Telemetry description

Housekeeping telemetry

HK data with 1 Kbyte size is needed for every 1 second. When the detector operation becomes stable, this period can be longer as 4 second or more.

Science telemetry

In total 10 kbs⁻¹ typical and 1 Mbs⁻¹ burst. Event data are 32 Byte each, with timing, position, pulse-height and flag and trigger grade digital pattern included. It will be wrapped up to form a event packet with a size of 4 KByte (TBR) to reduce overheads on telemetry transfer. In total, we require telemetry budget of 10 kbs⁻¹. With a typical 30 ks observation, 38 Mbytes of memory is required. The HXI will rely on the S/C mass

memory in baseline. However, HXI-D will have a memory with a size of 256 Mbyte or more, which could be used as a memory buffer as well. Decision will be made after the trade-off study of S/C telemetry system designing.

4.4.7 Electrical interfaces

TBD. SpaceWire will be the standard used for serial data transfer. Data/command lines are doubled up for redundancy. Required power and weight is included in the tables shown above. Power lines for the required voltages and current to both the HXI-E and the HXI-D are shown in Figure 4-6. No redundancy in power-lines is assumed.

4.5 Electromagnetic compatibility and Electrostatic discharge interface

4.5.1 Susceptibility requirements

HXI does not need any magnetic field to operate. The instrument can withstand rather high magnetic field strengths (of about 10 Gauss) and as such the requirement on ambient magnetic field levels are not foreseen to be very strict. However, be noted that the HXI system is not yet tested in strong (stronger than in laboratory) magnetic/electro static field.

Should it be necessary, shielding (μ -metal tapes, metal strips etc.) that can reduce magnetic fields will be used.

4.6 Optical requirements

4.6.1 Stray-light requirements

In principle, HXI requirements on stray-light are the same as those for the WFI, but within the energy band above 10 keV.

4.6.2 Baffling requirements

As already specified in section 4.1.4, HXI requires rather thick baffling to shield the Cosmic X-ray background directly (e.g. not via the mirror) coming into the HXI imager. The HXI specific requirement is to absorb photons up to 40 (or 80) keV. In the baseline, we require a thin Gold layer with a line-of-sight thickness of 200 μm on the baffle. If the incident angle of the line-of-site is 5 degree, the required mechanical Gold thickness is about 20 μm . This corresponds to a 1/e attenuation energy of 70 keV. Equivalent alternative is under consideration.

There are no specific requirements for charged particles which are ‘focussed’ by the mirror into the detector on the HXI side.

4.7 Transportation, Handling, Cleanliness and Purging requirements

4.7.1 Transportation requirements

(TBR) N/A. Follow standard space-born standards for electrical boxes.

4.7.2 Handling requirements

(TBR) N/A. Follow standard space-born standards for electrical boxes.

4.7.3 Cleanliness requirements

(TBR) N/A. Follow standard space-born standards for electrical boxes.

4.7.4 Purging requirements

(TBR) N/A. Follow standard space-born standards for electrical boxes.

4.8 Ground and Flight Operation requirements

4.8.1 Ground and pre-flight requirements

In addition to the full function test within the satellite thermal vacuum test, we require a simple operation test using weak radio-isotopes, in addition to the ^{241}Am source mounted on one of the four filter sled positions of WFI. In this simple operation test, the HXI-S can be at room temperature.

4.8.2 Flight operations

TBD

4.9 Deliverable Models and GSE

4.9.1 Structural Thermal model

(TBR) Prepare a model with mechanical and heat output the same to the real imager, without electronics but with thermometers.

4.9.2 Engineering Qualification model

(TBR) Prepare one unit.

4.9.3 Flight model

(TBR) Prepare one unit.

4.9.4 Flight spare model

(TBR) Prepare one whole unit, and a few backup of critical parts (DSSD, DS-CdTe etc.).

5 HIGH TIME RESOLUTION SPECTROMETER (HTRS)

The purpose of the HTRS is to provide spectra with resolving power $E/\delta E$ of 5-50 in the energy range 0.5 to 10keV, at very high time resolution (10 μ s) and with very high count rate capability (2MHz). The HTRS is based around an array of silicon drift diodes.

5.1 Instrument Description

5.1.1 Introduction

The High Time Resolution Spectrometer (hereafter HTRS) will provide the International X-ray Observatory (IXO) with the capability of observing bright galactic X-ray sources (e.g. X-ray binaries, magnetars). Those sources can generate up to 1 million of counts per seconds, equivalent to about 5 times the intensity of the Crab. The HTRS will further provide better than 200 eV spectral resolution at 6 keV, together with microsecond time resolution, for photons of energy between 0.3 and 10 keV. The HTRS is based on an array of 37 hexagonal Silicon Drift Diodes (SDD), placed out of focus, in a way that the focal beam is distributed over the whole array.

5.1.2 Instrument performance specifications

The HTRS will easily meet the top-level mission requirement of handling 1 Crab X-ray sources with a throughput larger than 90%. However, potential HTRS targets (e.g. X-ray bursters) often exceed the 1 Crab intensity level, reaching in some cases ten Crabs. Following the CDF run (November 17th, 2008), an HTRS response matrix was generated from which the Crab spectrum generates about 200 kcounts/s, assuming a thickness of 450 microns for the SDD. From this, the HTRS specifications are:

Table 5-1: Summary of the HTRS requirements

Maximum count rate	2 Mcounts/s (~10 Crab)
Energy range	0.3 to 10 keV
Time resolution	10 μ s
Energy resolution	<200 eV @ 6 keV (150 eV goal)
Deadtime @ 1 Crab	< 1 %
Pile-up @ 1 Crab	< 1 %
Data rate @ 1 Crab (full resolution)	~6.6 Mbits/s

5.1.3 Instrument configuration

The HTRS is a high-count rate instrument. Among the fastest X-ray detectors currently available, SDD are the most suited for the HTRS. The SDD is a completely depleted volume of silicon in which an arrangement of increasingly negatively biased rings drive the electrons generated by the impact of ionising radiation towards a small readout anode located on the backside and in the centre of the device. The time needed for the electrons to drift is much less than $1\mu\text{s}$. The main advantage of SDDs over conventional PIN diodes is their small physical size and consequently the small capacitance of the anode, which translates to a capability to handle very high count rates simultaneously with good energy resolution. To take full advantage of the small capacitance, the first transistor of the amplifying electronics is integrated onto the detector chip. The stray capacitance of the interconnection between the detector and amplifier is thus minimized and, furthermore, the system becomes practically insensitive to mechanical vibrations and electronic pickup.

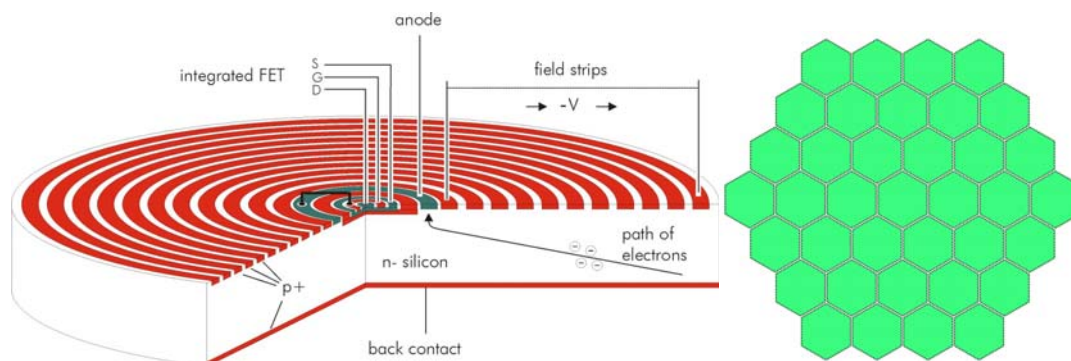


Figure 5-1: Concept of a single drift diode X-ray spectrometer (left). Layout of the HTRS comprising 37 closely packed SDDs (right).

In order to reduce the dead time and pile-up fractions, in the regime of extreme count rates to which the HTRS will be exposed, the detector will be placed out of focus, in such a way that the focal beam is distributed over several SDDs. In the current design, the HTRS is an array of 37 hexagonal SDDs (see figure above). Hence the detector will see an out-of-focus image of the mirror. The intensity as a function of radius is not constant (since the effective filling factor slightly depends on radius) and depends also strongly on energy (photons of higher energies are reflected from the inner parts of the mirror). As a consequence, the flux received by the detector will not be uniform: some SDDs will see more counts than other. A trade does exist between the SDD size and the out-of-focus distance, to make the focal beam spread as uniform as possible. In the current design, which assumes that all SDDs have the same size and an IXO focal length of 20 meters, a $5''$ Point Spread function, the optimum out-of-focus distance is about 12 cm for 4 mm SDDs (corresponding to a length of the hexagonal side of 2.3mm). The size of the SDDs will be adjusted when the final PSF is known, so that the distribution of flux is uniform and 100% of the source flux is intercepted by the SDD array (using slightly larger pixels and out-of-focus distance is possible and would smooth the distribution of counts), see Figure 5-2.

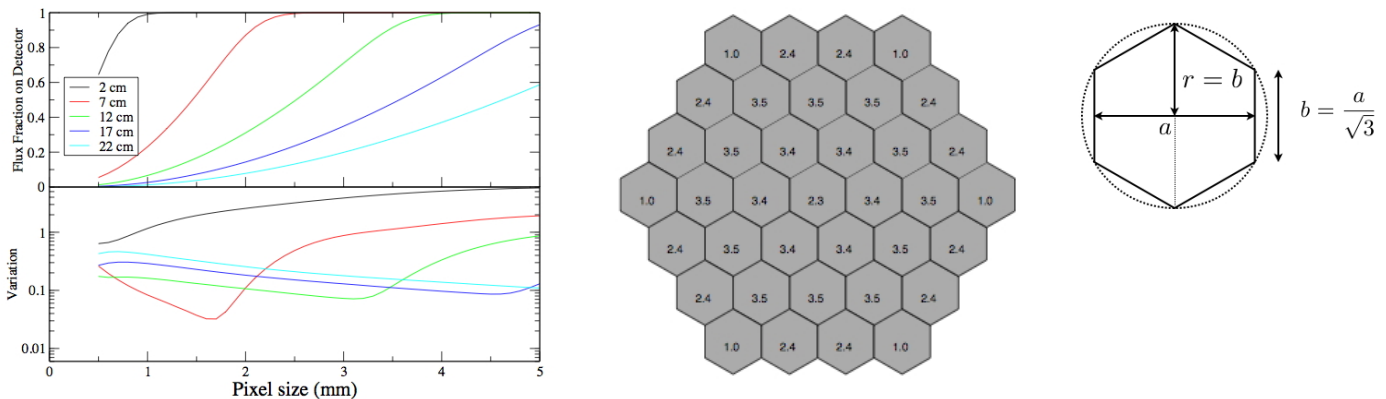


Figure 5-2: (Left) The fraction of the 1 keV flux captured by the detector array and the standard deviation of the count rates for the individual pixels. The smoother distribution is preferred. Different curves correspond to different out-of-focus distance. Centre) The percentage of 1 keV photons received on each of the 37 hexagons of 4 mm, located 12 cm out-of-focus. Courtesy of Tim Oosterbroek (ESA). Right) Hexagon definition, “a” is the pixel size used in the left figure.

In the above design, the most exposed SDD will receive about 3.5% of the total source flux. In the analogue electronics chain, dead time will include contributions from the signal rise time, the charge-sensitive pre-amplifier and the shaping amplifier. The first two of these can be very short, and the limiting contribution is that of the shaping amplifier, where a trade-off between speed and energy resolution is necessary. Shaping time constants as short as 50 ns have been found to be usable. This translates to a minimum feasible dead time of about 300 ns. Using currently available devices and pipelining techniques, the analogue-digital conversion stage is not a limiting factor at these speeds.

Monte Carlo simulations were performed to estimate the effect deadtime has on the efficiency of the HTRS. The simulations assume a point source illuminating the HTRS in its default configuration, i.e., 37 SDDs in the out of focus distance of 12 cm and with 4 mm pixel size, and distributing the source counts on the pixels according to the figure above. The source was assumed to have a constant count rate and a Crab-like spectrum. Photon arrival times onto the HTRS are generated according to Poisson statistics. The dead time and energy pile up are taken into account by discarding photons that hit a pixel within 300 ns of the previous photon.

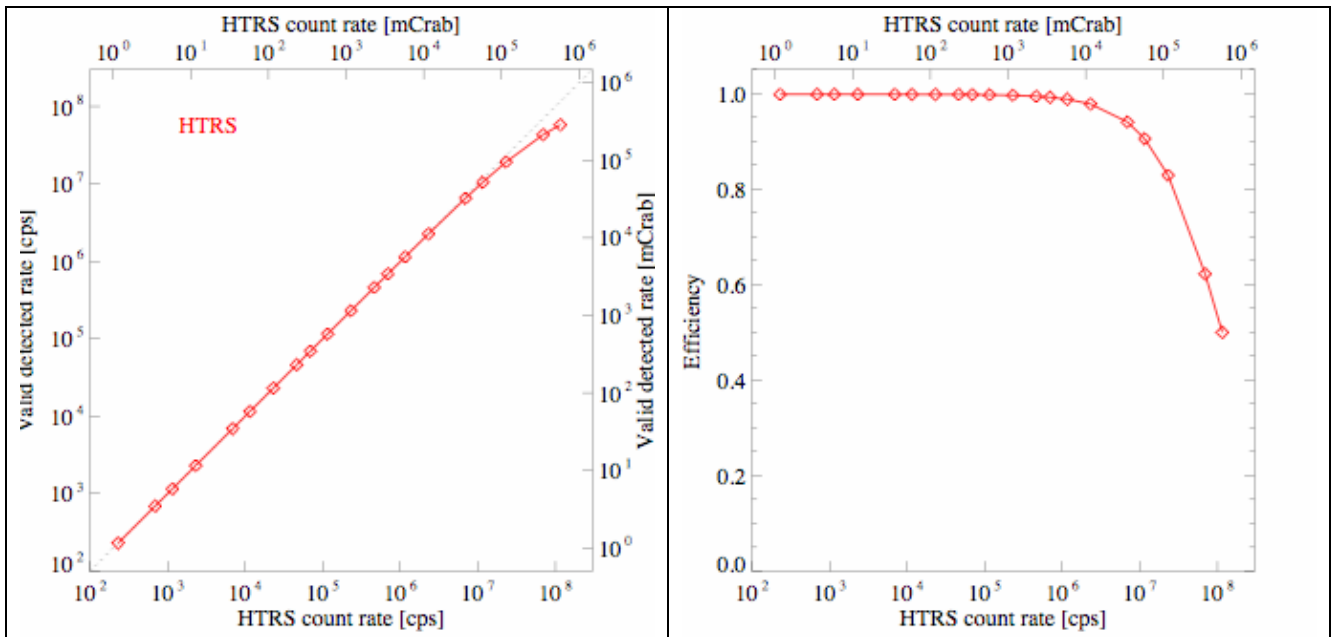


Figure 5-3: HTRS detection efficiency versus input count rate, considering photons hitting the sensitive area of the HTRS array. Courtesy of Joern Wilms and Mickael Martin.

When photons hit the SDD close to its edge, a fraction of the charge cloud produced can diffuse to the neighboring pixel. The effect such "split events" have is still under consideration. The occurrence of split events can be reduced by placing a blocking filter (or a collimator) on the outermost region of each SDD. The size of the region is not yet defined but will be somewhere between 50 and 80 microns. This will reduce the measured count rate by less than 7%.

The figure above shows the measured HTRS count rate as a function of incident HTRS count rate. From these simulations without the blocking filter, indicating that pile-up starts to affect the HTRS performance above 10 Crab. This fact is also illustrated in the same figure (right panel) where the efficiency of the detection process is illustrated. Here, the efficiency is defined as the ratio between the photons incident onto the sensitive area of the detector and the detected photons. Moderate pile up (a reduction of efficiency by 5%) is apparent only for source fluxes above 30 Crab.

Even for 1 Mcounts/s, using a very fast shaping time constant of 75 ns, energy resolution of less than 260 eV at 5.9 keV has been measured for a moderately cooled detector (-15°C). In the figure below, the energy resolution at 5.9 keV is shown as a function of count rate for two different shaping times. It indicates that, for a count rate of 100 kcounts/s (corresponding to the count rate received by the brightest SDD by a 15 Crab source), an energy resolution of better than 200 eV can be obtained.

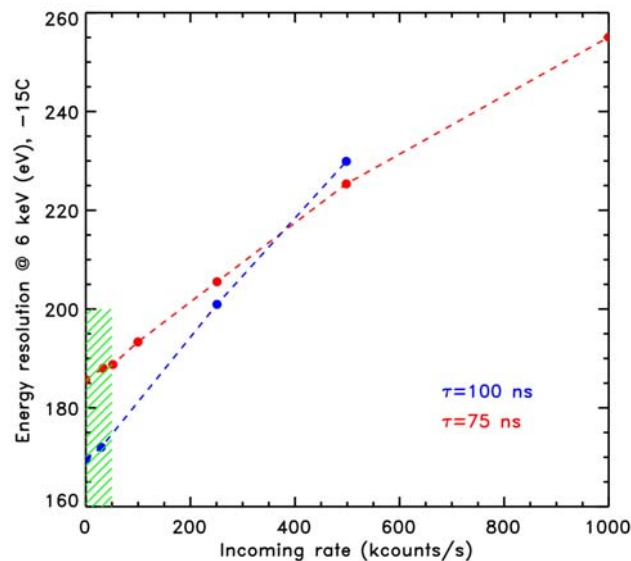


Figure 5-4: Energy resolution at 6 keV of a single SDD as a function of the incoming rate of photons for two shaping time constants. At the highest incoming rate an energy resolution better than 260 eV is achieved (courtesy of Peter Lechner). The dashed area corresponds to the count rate regime to which the individual diodes of the SDD will be exposed. Using today's technology (analog readout), this shows that the requirement of an energy resolution better than 200 eV is already met.

Table 5-2: The High Time Resolution Spectrometer in a nutshell

Detector type	37 silicon drift diodes
Diode dimension	Hexagon of 4 mm
Diode thickness	450 microns of Silicon
Diode sensitive area	13.9 mm ²
Total sensitive area	5.13 cm ²
Detector dimensions	28.7 mm × 21.9 mm
Operating temperature	-20 C
Cooler	Radiator
Bias voltage	150 V

The current HTRS design builds upon the heritage of both the MPE/MPI (+ PNSensor GmbH) and CESR, as well as its partners, such as the University of Tübingen and the University of Erlangen-Nuremberg. The MPI Halbleiterlabor, which is expected to build the SDD array is a common research facility of the Max-Planck-Institut für Physik in Munich and the Max-Planck-Institut für extraterrestrische Physik in Garching. It has a well-established world leadership for manufacturing silicon drift detectors. Silicon drift detectors are used in fast photon counting applications at synchrotron light facilities like EXAFS and X-ray holography, and for the optical light readout of scintillator crystals in medical imaging. The CESR, which will provide the front-end electronics has recently been involved in the building of a similar analog electronics for the ESA INTEGRAL/SPI spectrometer. The team around the HTRS is currently involved in the building of the analog and digital electronics for the Cadmium Telluride based semiconductor array (6400 individual detector cells) for the Chinese-French SVOM gamma-ray burst mission (currently ending a Phase A and targeted for a launch in 2014). Finally it is worth mentioning that SDD have already successfully flown on a NASA Mars rover mission. The option that the analog electronics is replaced by a digital electronics (after the pre-amplifier) is also being considered at CESR, as part of an R&D program funded by CNES (see figure below)



Figure 5-5: SDD test bench set-up at CESR. It enables analog and digital readout of the SDD.

5.1.4 Instrument optical design – filters

In order to reduce the heat load on the coolers and the photon induced noise on the detectors, IR and optical light blocking filters are required in the line of sight of the detectors. Apart from blocking IR/VIS/UV to a sufficient level, they should also not compromise the detection efficiency of the instrument. As the WFI, an Al-filter together with an Silicon Oxide / Silicon Nitride layer system is placed directly on the focal plane detector, which would block IR/VIS/UV light to a level sufficient for most observations without deterioration of the low energy QE. The envisaged thickness values of the respective layers achieve attenuation in the optical of $\sim 10^6$ and 100 in the UV range. The detailed composition of this filter, consisting of an Al / SiO / SiN layer system, needs to be assessed.

In addition to the light blocking filters discussed above, the filter wheel might have additional filters that can be placed in the optical line of sight, see Section 5.1.6

5.1.5 Instrument units' mechanical design and dimensions

The instrument itself comprises three units: the detector unit, the detector electronic unit and the control electronic unit. The detector unit comprises the SDD array as well as the 37 pre-amplifiers closely packed.

The HTRS Detector Electronic Unit (DEU) and Control Electronic Unit (CEU) can be assembled into one single box in a volume of $35 \times 20 \times 20 \text{ cm}^3$ located at a distance of less than 100 cm from the detector unit. These numbers are derived from scaling of the electronics chains of the 19 Germanium detectors, currently flying on the INTEGRAL spectrometer.

It is foreseen that the detector head will have a cylindrical shape with a diameter of 5 cm and a height of 2 cm. The FEE box located right next to the detector head is also of cylindrical shape with a diameter of 7 cm and a height of 5 cm (see figure below). The filter wheel and motor has an oval shape of 10.6 cm height by $27.0 \text{ cm} \times 20.4 \text{ cm}$. A CAD design of the HTRS with the filter wheel and associated electronics box is shown below: it shows the filter wheel, its motor, the detector unit is green, and the central electronic unit is maroon (this design is preliminary).

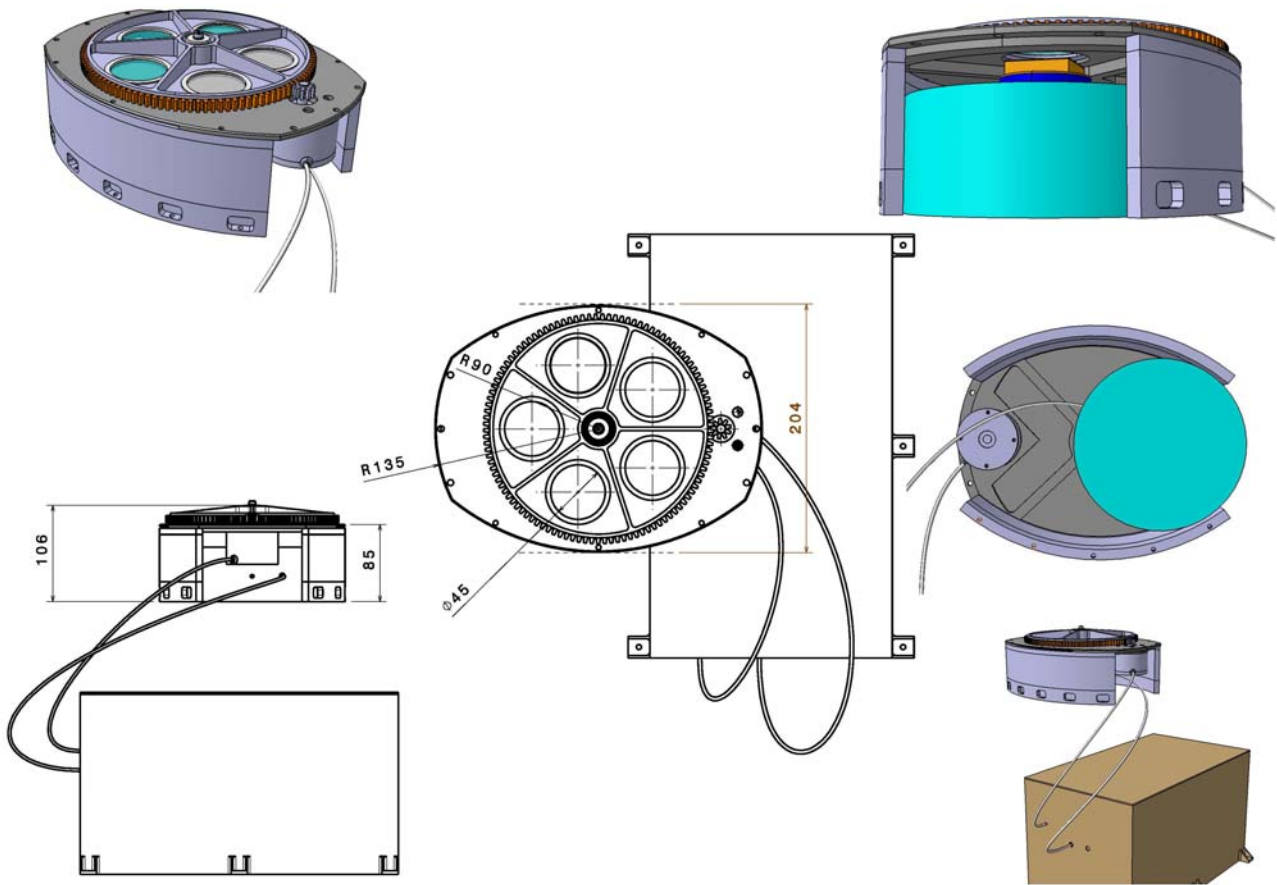


Figure 5-6: CAD model of the HTRS with the filterwheel, the detector unit and the electronic boxes.

5.1.6 Mechanisms

Instrument door

The HTRS is not expected to be launched with the experiment body in vacuum conditions and a closed front-covering door is therefore not needed. On the other hand, the instrument will be launched with the filter wheel in its closed position. Contamination is prevented prior to launch by purging and environmental contamination control.

Filter wheel

The filter wheel is a system to protect the detector, and to reduce the optical loading on the SDD array. It consists of a rotating disk perpendicular to the optical beam and controlled by a motor. The motor is commanded by a dedicated electronics, which allows us to select accurately a specific orientation of the filter wheel. A number of predefined orientations (hereafter, positions) are used in order to cover the HTRS detector with different filters. Filters may be selected on a per observation basis according to the necessity to reduce the optical loading of the detector, but specific positions are also needed for calibration source deployment or for instrument safety reasons. Safety operations may be required autonomously or via ground control to prevent excessive charged particle flux (solar flare or local magnetospheric storms), micrometeorite protection or spacecraft attitude loss.

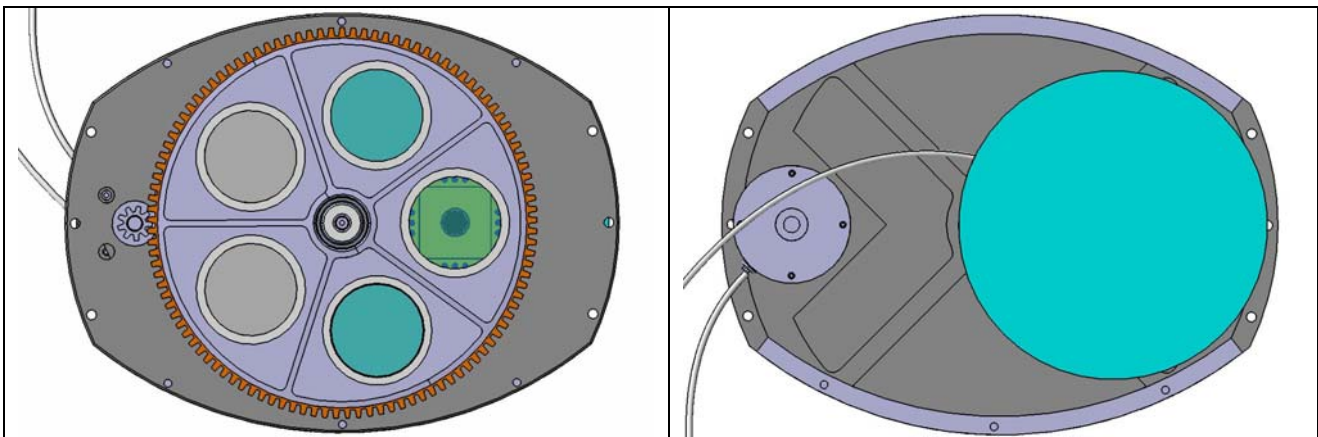


Figure 5-7: The top and rear view of the HTRS detector unit and its associated filter wheel (this is a preliminary design). Right) The filter wheel with its 5 positions. The SDD array is visible in green. Left) The detector unit is shown in green and the motor of the filter wheel in blue.

The filter wheel is foreseen to have 5 positions:

- Position 1) Closed (Operative mode: power-off, stand-by, electrical calibration, observation for calibration purposes)
- Position 2) Opened (Operative mode : Observation, normal rate)
- Position 3) With thin or medium transmission filter (Operative mode: observation, no optical loading).
- Position 4) With a thick transmission filter. (Operative mode : observation, very high optical loading)
- Position 5) With calibration sources (^{55}Fe and $\text{Ti}/^{109}\text{Cd}$ (TBC)). (Operative mode : calibration)

The filters in position 3 and 4 are still to be confirmed by scientific simulations. The thin filter or thick filter positions may be selected per observation according to the necessity for additional optical light blocking. For details on the envisaged thin/medium and thick filters (see L. Strüder et al., The European Photon Imaging Camera on XMM Newton: The pn-CCD camera, *Astronomy & Astrophysics*, Vol. 365, No. 1, pp. L18-L26, (2001) and K.H. Stephan et al., Optical filters for the EPIC CCD camera on board the XMM astronomy satellite, *Proceedings of the SPIE* Vol. 3114, p. 166-173(1997)).

The figures above show a preliminary analysis of the filter wheel configuration. The driving of the motor on the side of the wheel rather than along its axis allows the detector and the motor to be placed next to each other, therefore reducing the overall height of the system. The support structure consists in two circular structures. The baseline is to use a light material (e.g., NIDA). The detector module is directly attached to the wheel support plate. The support structure is directly fixed to the PIM.

The filter wheel will be equipped with a system of control of the position, so that the central unit receives an independent acknowledgment that the correct filter position has been reached. To this effect, holes encoding the position will be placed around each filter. A LED/sensor system will detect the proper location of the wheel: Two LED/sensors ensures the wheel is centered on an existing filter position, and three LED/sensors allow the identification of the filter number. This is described in Figure 5-8 below.

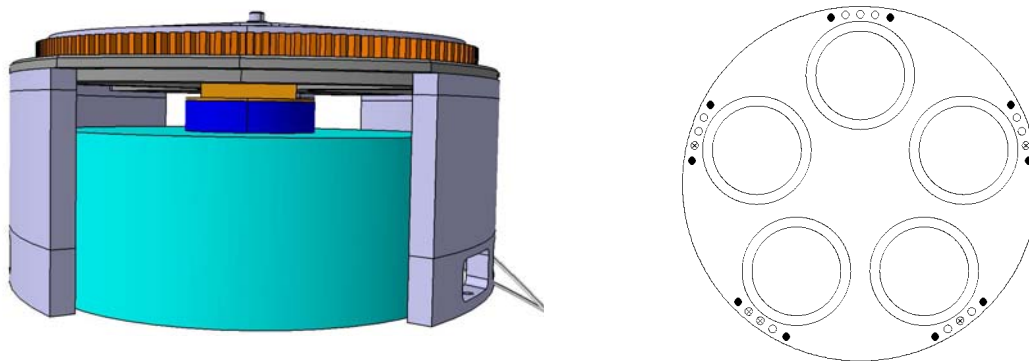


Figure 5-8: left) side view of the filter wheel and detector. Right) The black dots are holes used to ensure the filter wheel is in a valid position, which is the case if and only if the signal from both corresponding sensors is on. The empty dots indicate the location of filter identification holes. Only those marked with a cross are holes. The reading of the corresponding sensors encodes the filter number in binary form.

The filter wheel must not fail in a position, which would prevent any HTRS science operation (e.g., closed filter). The motor will have two wirings. The placement of the motor on the side of the filter wheel, as opposed to commanding directly the filter wheel's axis, could allow also a second motor to be positioned.

The baseline for the motor is a stepper motor, which simplifies the commanding electronics.

The mass budget for the filter wheel alone (without the electronics) is about 2 kg. The mass budget for the electronics, derived from a scaling of the Astro-E2 filter wheel electronics and our design work for Astro-H is about 2 kg. Based on estimates foreseen for Astro-H, the power budget for the motor, position readout and controlling electronics is < 7W idle and the peak power is about 16 W when the motor is turning. This is to be confirmed, since it depends on the specifics of the chosen motor. The power dissipated in the electronics itself is estimated at 4 W. This means that the peak power consumption due to the wheel is about 20 W.

5.1.7 Instrument units' thermal design

The thermal design of the instrument is not yet finalized, being part of an internal study, which is starting. The thermal interface to the instrument is assumed to be a cold plate, spacecraft provided, at $-50C \pm 2.5C$. A cooling system via passive radiator will allow the science operating temperature to be reached, i.e. $-20C$. The detector temperature **should be stabilized to $\pm 1C$** , across the SDD array, by an instrument provided thermal regulation system. The radiator design needs to be investigated further within the overall spacecraft accommodation, and could feasibly be implemented as a flat panel.

5.1.8 Electrical design

The general electrical design follows from the assumption that each SDD has its own charge sensitive preamplifier located as closely as possible to the diode itself (this is the detector unit). The detector electronic unit (DEU) contains 37 spectroscopy amplifiers and 37 high-rate analog to digital converters (ADC), as well as the high voltage power supply. The Control Electronic Unit (CEU) is responsible for the configuration of the SDD array, the data acquisition, compression and storage. It is also in charge of the power conversion and all interfaces with the spacecraft resources, such as commands, telemetry, power supply.

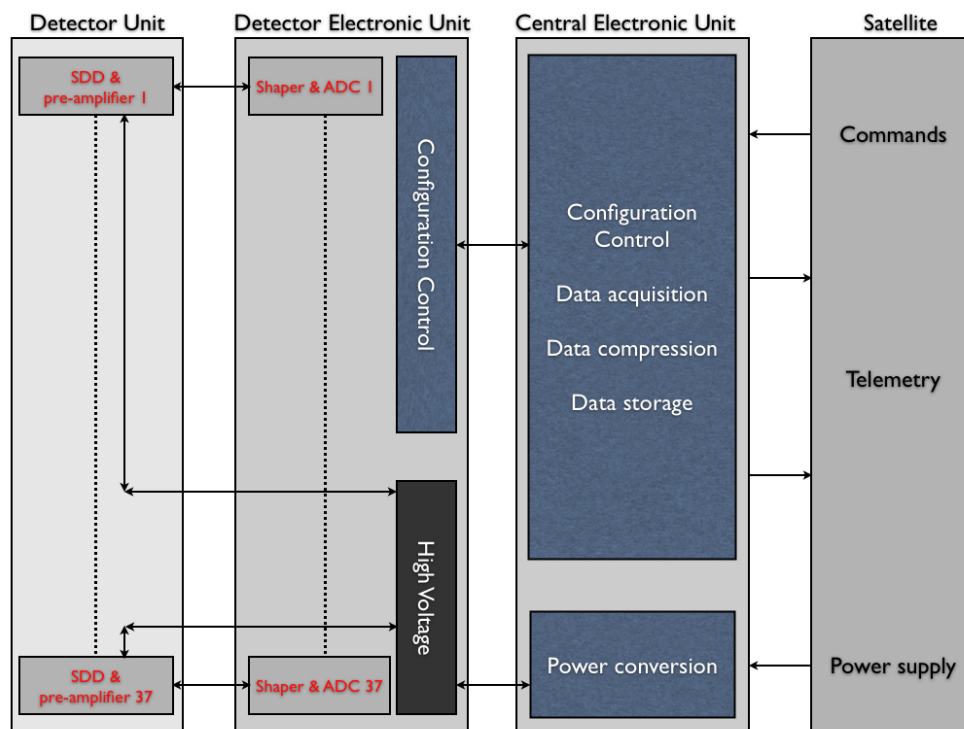


Figure 5-9: Overall electric design of the HTRS

The main part of the electronics lies in the Detector Electronic Unit. A preliminary design is shown below:

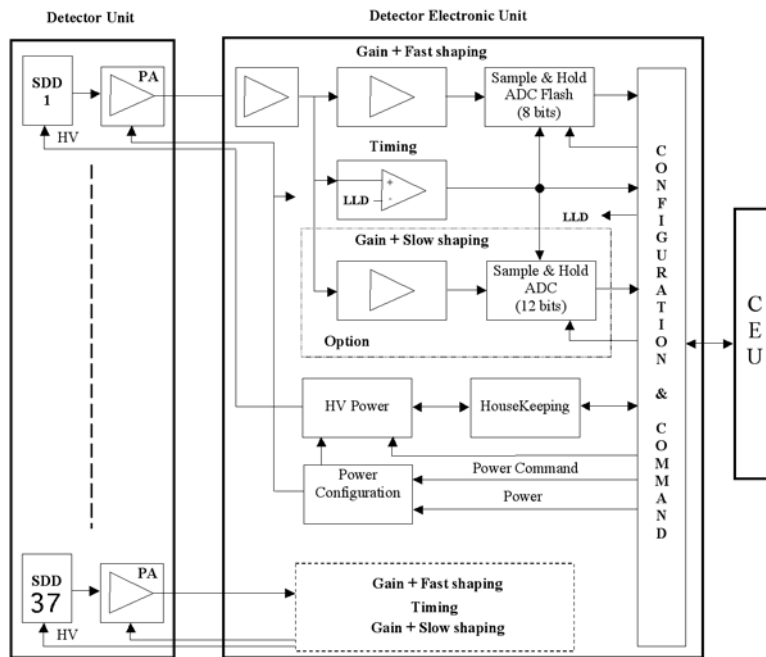


Figure 5-10: Detector Electronic Unit

5.1.9 On-board software

The on-board software will be responsible for four main tasks:

- Ensure the interfaces with the spacecraft (commands, housekeeping,...)
- Perform Instrument control and configuration
- Perform data acquisition, compression, and storage
- Provide the power conversion to the detector electronic unit

5.1.10 Ground support equipment

5.1.10.1 Electrical ground support equipment

EGSE and MGSE are integrated parts of the project and will be upgraded along the project lifetime. Among its first functionalities, one can list:

- end-to-end calibration of the SDD array selected for flight, under various conditions
- end-to-end tests of the electronics chains (DU and DEU)
- end-to-end tests of CEU software
- Spectral and timing calibration of the HTRS in flight conditions

5.1.10.2 Mechanical and optical ground support equipment

Specific elements of the MGSE will be developed to match the functionalities described above. In particular, a re-use of the test facilities developed for the SVOM-ECLAIRS instrument is planned.

The MGSE will include:

- The mechanical devices, the electronic chains and the software used to integrate, cool, test and select the SDD arrays to be integrated within the different models (flight, qualification, mechanical or thermal)
- The mechanical devices and supports, the electronic chains, the software, the thermal-vacuum chambers, the thermal control, to check the HTRS integration and validation.

5.1.11 Instrument mode description

5.1.11.1 Operating modes

The HTRS instrument will be operating by execution of a limited number of predefined observation sequences that the spacecraft receives at a previous communication window. The science modes will define both the instrument operating sequence and the data processing requirements. Different modes of operations can be considered; one is a photon-photon mode both with and without the diode information, another one is a binned spectral mode, where only the number of counts in a spectral channel is coded. The choice of the data mode will define the data rate (see below). Given the past experience with the RXTE Proportional Counter Array, it is likely that the **binned spectral mode** with sub-millisecond integration time will be used as **the default operation mode**.

The data could be stored temporarily in the HTRS mass memory (see overall electrical design, baseline of 16 Gbits) as a buffer for later transfer to the spacecraft memory. There is no requirement to download the data in real time. A high speed link will be available in the HTRS to transfer the data to the spacecraft memory for downloading. However for some particularly bright and new objects, it may be worth to send a subset of the data to the ground quickly enough, to assess the interest of the source.

The operating mode (binned spectral mode) and parameter configuration of the HTRS will be set by commands from the ground at the beginning of the observation. The operating mode and parameter configuration of the HTRS will be defined by the observer using prior knowledge of the target (e.g. maximum brightness from long term monitoring by X-ray all sky monitors, overall rms variability of the source).

The on-board software of the HTRS will be designed to control that the mass memory does not get overloaded, with the mode chosen by the observer. Although this will require a careful study, one possibility would be to switch automatically the HTRS to a degraded mode of operation, yet preserving the quality and integrity of the data.

The requirement for the absolute timing accuracy to be provided by the spacecraft (and ground segment) is better than 100 microseconds (TBC).

5.1.11.2 Non-operating modes

The most relevant non-operational mode is the one for which most of the instrument has been switched off. In the standby and safe modes, only the thermal control of the SDD array is running to maintain its temperature within safe range.

5.2 Mechanical Interfaces and Requirements

5.2.1 Location requirements

The main requirement is that the detector assembly must be located **in a defocused position** to smooth the photon distribution more or less equally across the SDD array. With a focal length of 20 m and a SDD hexagonal size of 4 mm, the optimum out of focus distance is about 12 cm (see above). These numbers will have to be consolidated when the PSF is known as to ensure that more than 99% of the focal beam is intercepted by the SDD array.

5.2.2 Alignment requirements

The location of the instrument should be such that its optical axis aligned to ± 1 mm along the Z-axis and orthogonal to the Z-axis with an accuracy of 0.35 arcmin. Alignment in the X and Y-axis should be ± 1 mm. It has to be made sure that the baffle is designed such that it accommodates the potential misalignments.

5.2.3 Pointing requirements and performance goals

As the HTRS is not an imaging device, it has no particular requirements for pointing accuracy. The size of the detector has been chose to allow the source to jitter within the observation by as much as $10''$, which corresponds to about 1 mm at the placement of the HTRS.

5.2.4 Interface control drawing

There is no ICD at the moment. The figure below gives an overview on how the instrument will interface with the spacecraft.

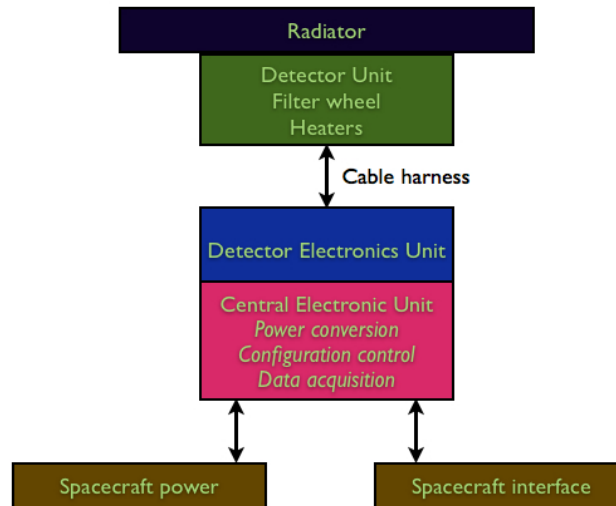


Figure 5-11: Interface to spacecraft concept

The flow diagram of the control electronic unit (CEU) is shown below. The CEU has two main functionalities: one is responsible for the processing and storage, and one for the power supply. The CEU FPGA is in charge of the interface with the spacecraft (TM/TC), of the configuration control and the data acquisition of the DEU, preprocessing, memory storage, and data packaging. The other functionality is linked to the power supply, DC-DC converters, which provide the various voltages for operating the DEU. Special care will be taken to all aspects related to EMI/EMC.

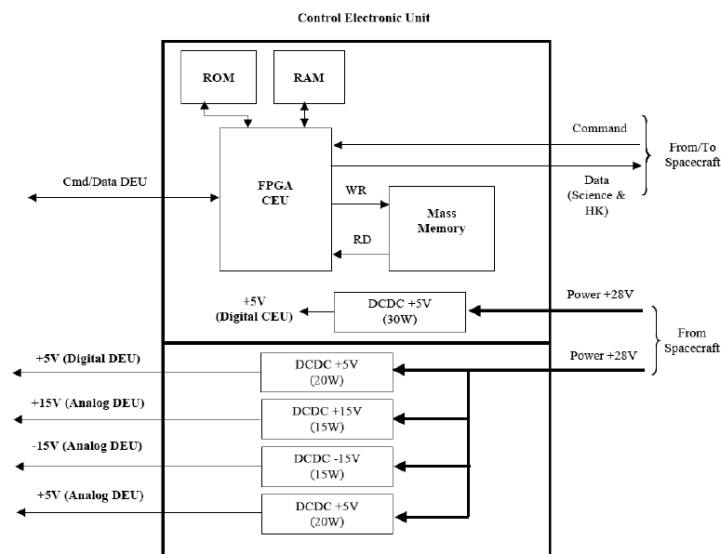


Figure 5-12: Overall design of the Control Electronic Unit providing the interfaces with the spacecraft

5.2.5 Instrument mass

The overall dimension of the HTRS is given in the table below (these numbers have to be consolidated, but include the margins):

<i>Filter wheel + Detector unit</i>	<i>Oval of length 27cm, width 20.4 cm and height of 10.6 cm</i>
<i>Detector Electronic and Control Units</i>	<i>Single Box of 35 x 20 cm and height of 20 cm</i>

The main constraint is that the detector head is not distant from its electronics by more than one meter. The mass budgets is shared between the filter wheel and the three units as indicated below.

	Unit	Mass	Total
Filter wheel			
Wheel - 5 positions	1	0.24	0.24
Wheel supporting plate	1	0.58	0.58
Motor	1	0.5	0.5
Mechanical structure	1	0.8	0.8
		Total	2.12
Contingency		20%	2.544
Detector Unit	Unit	Mass	Total
SDD array	1	0.1	0.1
Housing	1	0.5	0.5
Charge sensitive preamplifiers	37	0.05	1.85
Heaters	4	0.01	0.04
		Total	2.49
Contingency		20%	2.988
Detector Electronic Unit	Unit	Mass	Total
ADC boards (shaping, sample and hold)	37	0.1	3.7
Power configuration	37	0.05	1.85
Configuration control	2	0.4	0.8
		Total	6.35
Contingency		20%	7.62
Central Electronic Unit	Unit	Mass	Total
FPGA boards	4	0.5	2
DC/DC cards	4	1.3	5.2
Data Processing Unit	1	2	2
Configuration control	1	0.4	0.4
Power and filter wheel electronics	1	2	2
Detector Electronic and Central Electronic Unit housing	1	2	2
		Total	13.6
Contingency		20%	16.32
HTRS total mass			24.56
HTRS total mass + (20% margins)			29.47

Harnesses	Unit	Mass	Total
Harness (DEU to DU)	1	0.5	0.5
Data harness (from CEU)	1	0.5	0.5
Power harness (to CEU)	1	1	1
		Total	2
Contingency		20%	2.4

5.3 Thermal interfaces and requirements

5.3.1 Temperature limit in space environment

The optimum temperature of the SDD detectors is -20 C ($\pm 1\text{ C}$). In operating mode, the temperature will be stabilized to within 1 degree, by an instrument-provided heater and a spacecraft provided radiator. The detailed specifications at the S/C cold-finger interface are pending a detailed thermal study of the HTRS. The survival range for the SDD array is between -40 C and $+35\text{ C}$.

The electronics should be run at 30 C ($\pm 10\text{ C}$), with a survival range between -40 C and $+60\text{ C}$.

5.3.2 Temperature limits in laboratory environment

The same requirements, as described above, apply also to laboratory environment.

5.3.3 Temperature sensors

Temperature sensors will be provided as to monitor the detector temperature. 4 temperature sensors are foreseen over the whole SDD array.

5.3.4 Heaters

A thermal study of the whole HTRS is currently underway, but heaters will be needed to keep the detectors within its functional range. We assume that cooling via passive radiator will allow the science operating temperature to be reached. The maximum power consumption is not known with accuracy but is expected to be less than 10 Watts.

5.3.5 Thermal schematics

The figure below shows a picture of the detector housing without the cover and with the cover closed. It is assumed that a similar detector housing will be used for the HTRS.

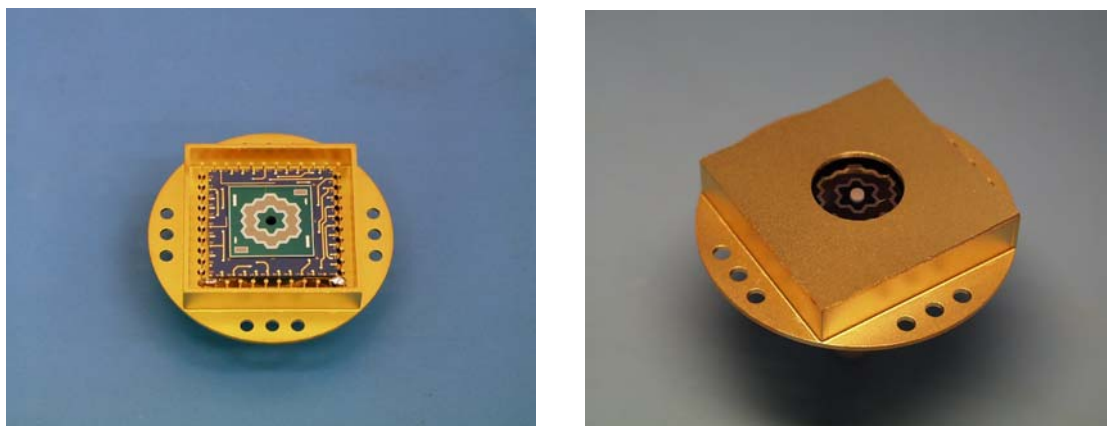


Figure 5-13: Picture of the SDD array and housing

Inside the housing the chip is mounted (glued) and wire bonded to a ceramic carrier. The ceramic is glued on the cold side of a cold plate and electrically connected by wire bonding to the pins of the housing. To dissipate the heat a copper bolt is inserted through the hole in the housing bottom part. A thermal study of the whole HTRS is currently underway, but the schematics below gives a preliminary thermal design.

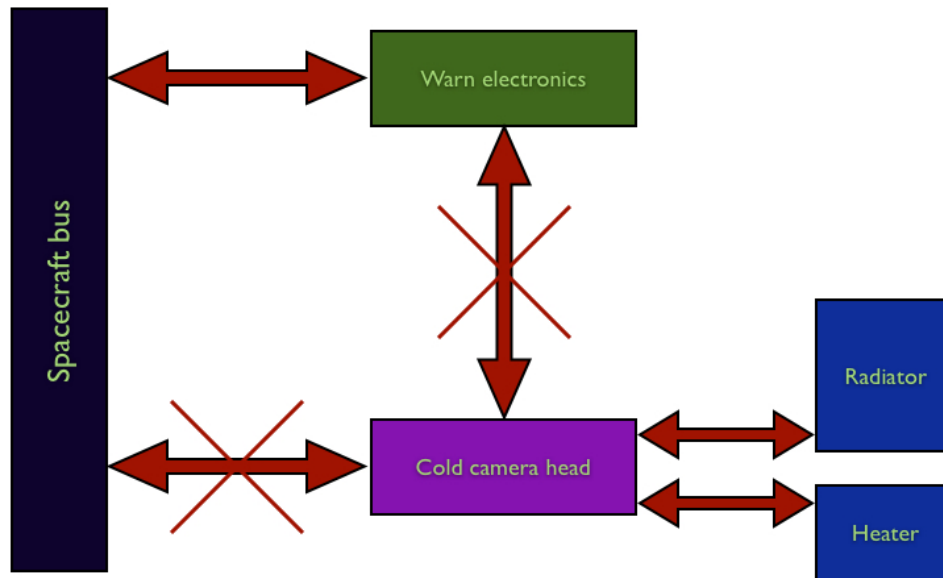


Figure 5-14: Preliminary thermal schematics

5.3.6 Thermal control requirements

Although they work safely at room temperature, the diodes reach the optimum performance at **-20C**. Such temperatures reduce the leakage current to acceptable levels. The temperature must not exceed **+35 C**, both at work and during quiescent phases. A lower bound to the operating temperature should be taken at **-40 C**. The temperature **should be stabilized to $\pm 1C$** , across the array by an instrument provided heater. The radiator design needs to be investigated further within the overall spacecraft accommodation, and could feasibly be implemented as a flat panel. A thermal study of the HTRS is currently underway, but in the baseline, only 12 Watts at the pre-amplifier level have to be evacuated, i.e. very close to the SDD array whose temperature must be kept at **-20C**. For instance, this could be easily achieved with a semi active system made of one radiator equipped with at least one variable heat conductance pipes (VHCP) connected to the plate with at least one constant heat conductance pipes (CHCP). Both would be actively commanded and regulated by a dedicated automaton, located in the Control Electronic Unit. This is to be investigated during the thermal study.

5.4 Electrical interfaces and requirements

5.4.1 Electrical resources requirement summary

The main requirement is that the Control Electronic Unit gets the +28 V from the spacecraft.

5.4.2 Instrument power distribution block diagram

The CEU has two main functionalities: one responsible for the processing and storage, and one for the power supply. The CEU FPGA is in charge of the interface with the spacecraft (TM/TC), of the configuration control and the data acquisition of the DEU, preprocessing, memory storage, and data packaging. The other functionality is linked to the power supply, DC-DC converters, which provide the various voltages for operating the DEU. Special care will be taken for all aspects related to EMI/EMC.

5.4.3 Power budget

The power budgets is shared between the three units as indicated below. This table includes however power needed for the heaters.

Table 5-3

	Peak	Standby	Off
Detector Unit + thermal control (10 W)	22	10	10
Filter wheel (at peak)	20	0	0
Detector Electronic Unit (DEU)	20	0	0
Central Electronic Unit (CEU) (4 W for the filter wheel electronics)	34	0	0
HTRS total power	96	10	10
HTRS total power + 20% margins	115.2	12	12
HTRS total power + 20% margins and 70% DC-DC conv. efficiency	164.6	17.1	17.1

The filter wheel power consumption has to be consolidated.

5.4.4 Instrument modes' duration

5.4.4.1 Instrument continuous mode duration

The HTRS will be operating by execution of a limited number of predefined observation sequences to be stored in the spacecraft DPU that the spacecraft receives at a previous communication window. The science modes will define both the instrument operating sequence and the data processing requirements.

A calibration measurement of a few 100s (TBD) of seconds with the calibration source on the filter wheel is foreseen before starting the observation (especially if the observations are distant in time). In addition, a pulsed astrophysical source (e.g. the Crab pulsar if available in the sky) will be required in order to measure the energy response and test timing accuracy of electronic chain. Such observation could be performed at a rate of once per year for instance.

Normal operations will consist of relatively short pointed observations (~ 25 kseconds).

5.4.4.2 Instrument peak mode duration

The peak mode duration is set by the filter wheel operation.

5.4.5 Telecommands

Once the HTRS is ON target, it is activated with the sequence of commands including:

- Power ON +28V CEU
- Reset CEU
- Autotest CEU
- Copy and run Application software
- Power ON DEU
- Reset DEU
- Autotest CEU & DEU
- HT ON SDD array
- Upload configuration
- Select configuration mode, either Calibration or Measurements
- Monitoring and regulation of operating parameters (e.g. temperature)
- Activate and run mode

To switch off the HTRS, the following sequence of instructions is needed:

- Select configuration mode
- HT OFF SDD array
- Power OFF DEU
- Power OFF CEU

5.4.6 Telemetry

5.4.6.1 Telemetry requirements

There are no specific telemetry requirements because we do not take as a requirement to download the data in real or near real time. Data will be stored in the mass memory of the instrument and transmitted for download to the spacecraft whenever telemetry becomes available.

5.4.6.2 Telemetry description

Housekeeping telemetry

The HTRS will generate housekeeping data of a few tens of variables (High voltages, temperatures, integrated count rates) measured at a one minute sampling frequency, with a 12 bits resolution. This should yield a bit rate of about 20 bits/s, continuously during the operating time.

Science telemetry

The HTRS will be run in binned spectral mode, with a binned time and number of spectral channels allowed to vary. In the following, we have assumed an integration time for the spectra of 1/4096 seconds (as used most of the time for the RXTE Proportional Counter Array), a uniform repartition of the counts over the number of spectral bins, and a ratio of the peak versus mean flux to be 20 (e.g. on-off pulse of the Crab pulsar, flares from Sco X-1). A 5% overhead has been added to the raw data rate for data stamping. For a 1 Crab source and 128 channels, the science data rate is about 2.2 Mbits/s.

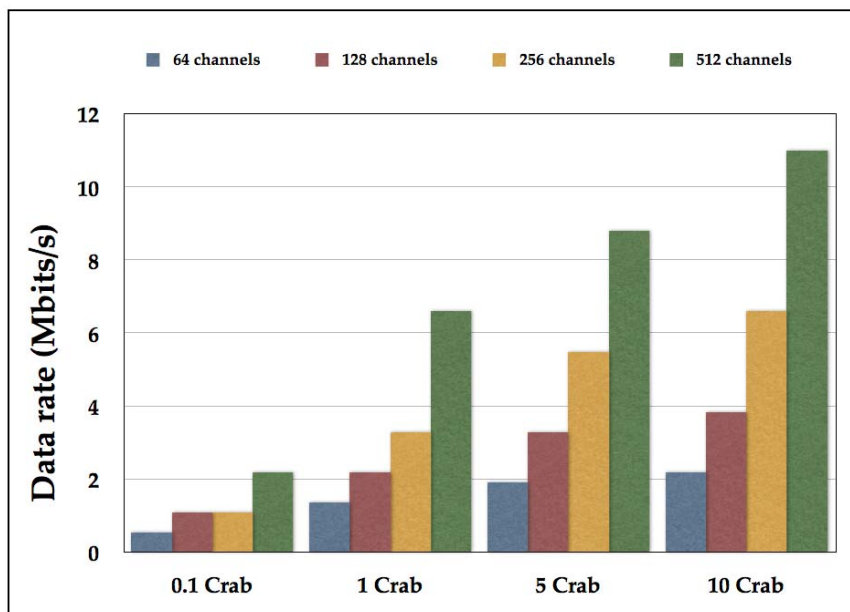


Figure 5-15: Instrument datarates

Spectral parameters:

Channels:	512
Assume 1 Crab corresponds to [cps]:	200000
max. flare amplitude:	20

Time resolution:

time resolution [bits]:	12
integration time [sec]:	2.44E-04
[musec]:	244
Nyquist freq [kHz]:	2.048

number of spectra/sec: 4096

packet size [bits]:	65536
packet header size [excl. time info; bits]:	128
total header size [bits]:	140

Source flux in Crab:	0.1	1	5	10
avg. source count rate [cps]:	20000	200000	1000000	2000000
max. source count rate [cps]:	400000	4000000	20000000	40000000
max. rate/channel [cps]	781.25	7812.5	39062.5	78125
avg max. photons/channel/integration time	0.19	1.91	9.54	19.07
Poisson 1 sigma:	0.44	1.38	3.09	4.37
max. photons + 2 sigma	1.06	4.67	15.71	27.81
required bits/channel:	2	3	4	5
channel capacity/integration time [ph]:	4	8	16	32
<i>total bits/spectrum:</i>	<i>1024</i>	<i>1536</i>	<i>2048</i>	<i>2560</i>
bits/1sec packet	4194304	6291456	8388608	10485760
raw science data rate [Mbits/s]:	4.19	6.29	8.39	10.49
spectra/packet:	63	42	31	25
packets/sec:	66	98	133	164
packet data rate [Mbits/s]:	4.33	6.42	8.72	10.75

The data could be stored temporarily in the mass memory of the HTRS (TBC) and transferred to the spacecraft memory for later download. Since there is no requirement to download the data in real time, this can be done at any time after the completion of the observation. The data will be transferred, using a SpaceWire type connexion at a rate TBD (likely over 100 Mbits/s).

5.4.7 Electrical interfaces

As shown for the overall electrical design of the instrument, the electrical interfaces with the spacecraft are limited to the satellite power towards the instrument control electronic unit (CEU), commanding to the CEU, and housekeeping and science data transport from the CEU to the spacecraft. A main and a redundant channel are foreseen. The connection to the spacecraft computer systems is done via the SpaceWire connection. Reliable ground connection is required for the mechanical parts.

5.5 Electromagnetic compatibility and electrostatic discharge interface

5.5.1 Susceptibility requirements

The cleanliness requirements are very similar to those of the WFI. As far as we can see at this early state of development, there are no specific constraints on the conditions for magnetic cleanliness and grounding which exceed the usual care to be taken while accommodating semiconductor based X-ray detectors within an experimental environment. The XMM-EPIC pn CCD accommodation study may be taken as a baseline. Special care has to be put on the cleanliness of the required detector voltages and operation voltages of the analog electronics from any HF pickup caused by the power supplies. A stable and solid ground connection must be provided. Ground loops must be avoided.

Radiation hardness is an important issue for the HTRS since it will be exposed to high radiation doses by observing bright X-ray sources. The total ionized dose on the JFET, connected to the collecting anode on the back of the device, imposes the main limitation. High-energy photons that are absorbed in the transistor region increase the amount of oxide charge and interface traps. This reduces the charge carrier lifetimes and contributes to increase of the leakage current. Laboratory measurements have shown that SDD survives 10^{13} photons above 12 keV, which is equivalent to a 3 year exposure of 10^5 photons per second. A single SDD, 5 mm², of the same technology and comparable layout as the HTRS was irradiated with Mo-K radiation at 17.4 and 19.6 keV at a Peltier temperature of 253 K (energy chosen because it poses most damage to the readout side of the chip). Damage effects from the radiation include silicon/oxide interface damage in the drift ring region. This leads to an increased leakage current.

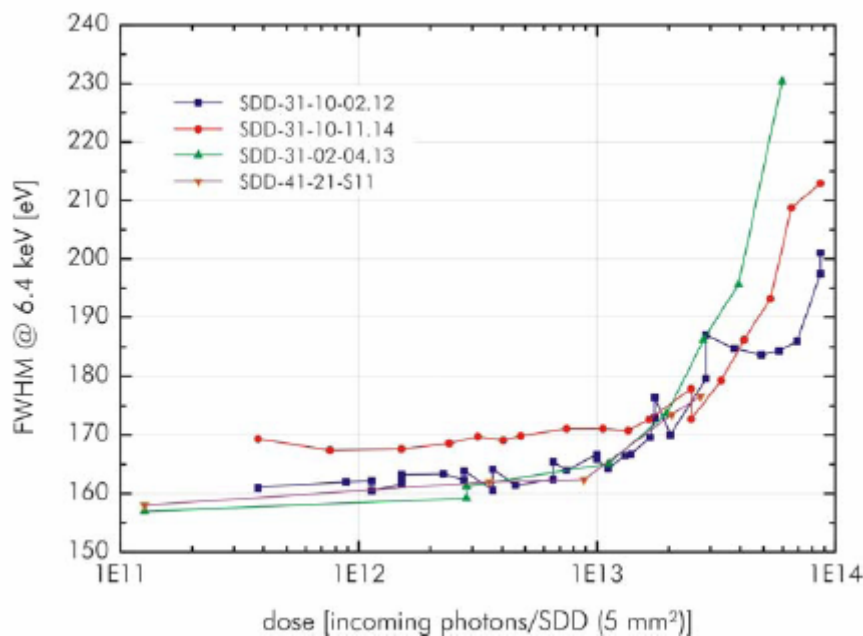


Figure 5-16: Degradation of energy resolution against dose of incoming photons.

From XMM pn CCD experience it is known the absorption of one 10 MeV proton causes an increase of leakage current by 10-17A at room temperature. At the L2 orbit, the proton flux is uncertain to some

degrees, but the HTRS shall be exposed to 10^9 protons/cm² in its 10 year lifetime. For an SDD-cell of some mm² this would roughly mean an additional leakage current 10 pA at Peltier temperature. In terms of noise this is only 1 el. ENC. Compared to the initial noise (150 eV at 6 keV corresponding to 18 el. ENC) the additional 1el. (to be added quadratic) can be considered as negligible. The above analysis is clearly simplistic, and a thorough radiation test campaign for the SDD is included in the instrument development plan (it should start in 2010).

5.6 Optical requirements

5.6.1 Stray-light requirements

Straylight from the X-ray sky has to be fully suppressed by suitable baffling. Optical straylight is to a large extent stopped by the entrance filters of the instrument. By nature straylight can be attenuated in any order but it cannot be extinguished completely. The requirement is that it doesn't degrade the instruments energy resolution. If we accept an average optical load of 1 photon per pixel and frame this translates to a photon flux of $3 \cdot 10^4 \text{ ph cm}^{-2} \cdot \text{s}^{-1}$ being absorbed in the detector (assuming a 4096Hz frame rate). For the HTRS, an Al-filter deposited directly on the focal plane assembly would block IR/VIS light. The effect of the on-chip filter is strongly depending on the Al-thickness. Using an Al-thickness of 100 nm the IR/VIS load would be damped by a factor of 10^6 allowing for a photon flux before the filter of $3 \cdot 10^{10} \text{ ph cm}^{-2} \cdot \text{s}^{-1}$. By combination of the Al-filter with dielectric layers also UV-photons can be filtered effectively. Figure 5-17 shows the tradeoff in terms of reduced efficiency at low X-ray energies. The on-chip filter will gain experience with similar detectors (pnCCDs, DEPFET Macro Pixel Sensors) to be used in the eROSITA, Simbol-X and BepiColombo missions. The integrity of the on-chip Al layer can be checked by high-resolution profiling and flat field optical illumination. In addition thick and thin filters on the filter wheel will also contribute to blocking out unwanted light of high-intensity optical sources.

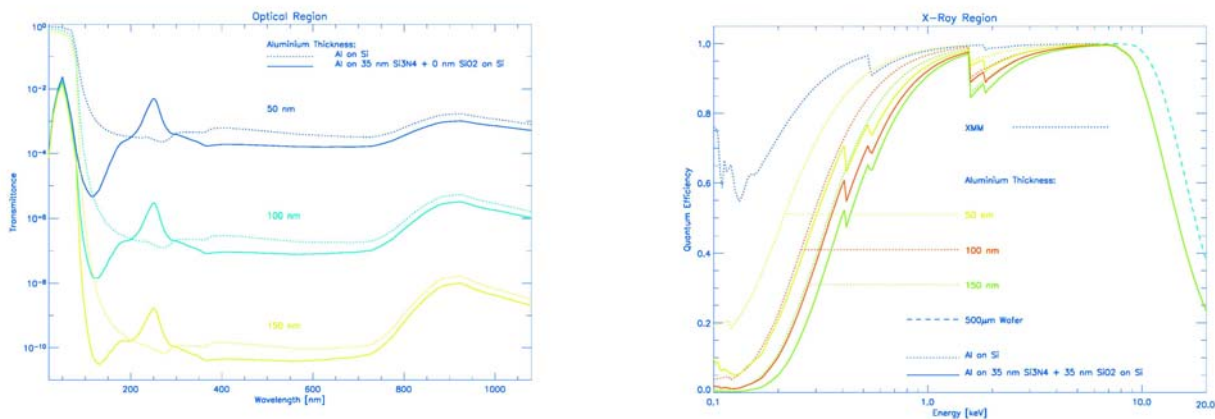


Figure 5-17: Left: Filter effect of thin Al deposited on the HTRS sensor entrance window. Right: HTRS quantum efficiency at different Al filter thickness.

5.6.2 Baffling requirements

In order to baffle stray X-ray and other stray lights, a baffle system forward of the instruments will ensure that the field of view minimizes unwanted light to the focal plane. For the HTRS, the first requirement is that the instrument FOV has free and unobstructed view to the rear aperture of the mirror in case the filter wheel is in open position. Secondly, the entire sensitive area of $2.8 \times 2.6 \text{ cm}^2$ must not be loaded with optical photons or diffuse X-ray background from the sky. As the minimum optical attenuation of the integrated filter is aimed to be 10^6 , a total photon rate of 3×10^{10} photons per square centimeter and second leads to one photon per pixel and frame for standard frame rate of 4096 Hz. This should lead to a negligible deterioration of energy resolution. Thus, requirement of the optical baffling is to reduce the optical photon flux to a level of 3×10^{10} photons per square centimeter and second on the detector surface (i.e. behind the mirrors). In case

of the X-ray background, the main requirement on the baffle is that the diffuse X-ray background should be reduced to a level of 1×10^{-3} photons per square centimeters and second, which should not be exceeded (note however that the HTRS will observe predominantly bright X-ray sources for which a background at this level will be absolutely negligible).

5.6.3 Charge particle deflection

Most events induced by charged particles focused onto the detector can be tagged by the total energy deposited in the SDD array. Most difficult to distinguish from photon detections are events induced by charged particles in the nominal HTRS energy range. Therefore, HTRS requires the charged particle deflector to deflect particles of energies in this band. When observing using the optical filters (thin and thick filters foreseen), charged particles lose a part of their energy on passing through the filter material. Additional losses will take place in the HTRS entrance window. Therefore, the deflection requirement has to be extended to higher energies. The maximum proton energy to be deflected will depend on the properties of the filters, but by analogy with previous mission, protons should be deflected to about 90-100 keV energies and electrons between 15-20 keV.

5.7 Transportation, handling, cleanliness and purging requirements

5.7.1 Transportation requirements

There are no specific transportation requirements, which exceed the usual care to be taken while transporting semiconductor based X-ray detectors within an experimental environment.

5.7.2 Handling requirements

There are no specific handling requirements, which exceed the usual care to be taken while handling semiconductor based X-ray detectors within an experimental environment.

5.7.3 Cleanliness requirements

Similar to the WFI, molecular contamination must be guaranteed to be small compared with effects of X-ray transmission filter performance, although *this is less of an issue because most sources observed with the HTRS will be subject to galactic interstellar absorption*, suppressing most of the source photons below 1 keV. Science simulations show however that a low-energy threshold around 0.3 keV would be highly desirable (in particular to dig out the disk contribution to the overall emission of galactic binaries). During all ground operations HTRS will be closed by a door mechanism that will allow purging with clean gas. Precautions adopted for XMM-EPIC seem to have been successful at this level, but trapped cryogenics between successive cold light filters must be avoided.

5.7.4 Purging requirements

During all ground operations HTRS will be closed by a door mechanism that will allow purging with clean gas.

5.8 Ground and flight operation requirements

5.8.1 Ground and pre-flight operation

In the laboratory, the instrument will be tested in conditions matching as closely as possible the conditions it will meet in flight, so that full testing and calibrations will be possible on the ground.

5.8.2 Flight operations

The HTRS will be launched with the filter wheel on its closed position.

The instrument in-flight management is done autonomously on board, or via ground control in case an exceptional event happens, e.g. excessive charged particle flux due to solar flares, micrometeorite protection or spacecraft attitude loss.

The filter wheel should be closable to prevent excessive charged particle flux (solar flare or local magnetospheric storms), or protect for micrometeorites or spacecraft attitude loss. Autonomous safe mode may be required in addition to pre-programmed commands.

Internal calibrations will occur frequently to ensure the stability of instrument calibration with respect to system X-ray energy-ADC gain function etc. This can be via special observation in appropriate filter wheel position, and most efficiently during spacecraft slew. The filter wheel positions foreseen are: open, closed, calibration (radioactive source, see gain monitoring calibration above), and 2 filter positions with TBD transmission.

Operating modes:

The HTRS will be operating by execution of a limited number of predefined observation sequences to be stored in the spacecraft DPU that the spacecraft receives at a previous communication window. The science modes will define both the instrument operating sequence and the data processing requirements.

A calibration measurement, either from calibration source (filter wheel) or on a pulsed astrophysical source (e.g. the Crab pulsar if available in the sky) will be required in order to measure the energy response and test timing accuracy of electronic chain. Normal operations will consist of relatively short pointed observations (~ 25 kseconds). Data is stored internally and downloaded when telemetry is available. Due to the brightness of the sources observed by the HTRS, damage to other instruments has to be avoided during HTRS observation.

Standby mode:

The High Voltage are switched off, only the thermal control of the SDD array is active.

5.9 Deliverable models and GSE

5.9.1 Structural Thermal Model

It is foreseen to develop and to manufacture a preliminary model or bread board for testing the performances of the Detector Unit (DU), the Detector Electronic Unit (DEU), the Control Electronic Unit (CEU) and the Thermal Control Unit (TCU) with the final electronic and thermal design. Then we shall develop a Engineering Qualification Model (EQM) with a representative set of detectors channels.

5.9.2 Engineering Qualification Model

Electronic architecture : 5 channels with electronic boards and 14 channels with thermal loads.

Electronic components MILITARY range (-40° to +85°C).
DC/DC converters for 5 modules

The Detector Unit includes :

- 5 measurement channels : 5 detectors SDD and 5 Preamplifiers
- 14 thermal loads
- HK Thermometers and heaters for thermal regulation

The Detector Electronic Unit which contains :

- 5 spectrometry boards
- 5 HVPS loads
- 14 thermal loads

The Control Electronic Unit which includes (1 processor board without REDUNDANT unit) :

- Housekeeping and heater control board
- Processor board (microprocessor + multiplexer interface FPGA + memories).

Full wiring and connectors of the DU, DEU and CEU boxes.

DU – CEU Harness

Mechanical architecture :

Full mechanical DU.

Full mechanical DEU.

Full mechanical CEU.

Full mechanical TCU which includes cold finger, heater pipes and radiator.

Test facilities :

Simulator equipment for SSD detectors, preamplifiers, coders, HVPS and modules.

Ground testing for the characterization of preamplifier and coder boards.

HTRS EGSE includes Quick-Look computer + Analysis computer + Data recording.

5.9.3 Flight model

Electronic architecture: 37 channels

Flight electronic components
DC/DC converters for 37 modules

The Detector Unit includes:

- 37 measurement channels: 37 detectors SDD and 37 PreAmplifiers
- HK Thermometers and heaters for thermal regulation

The Detector Electronic Unit which contains:

- 37 spectrometry boards
- 1 HVPS loads

The Control Electronic Unit which includes (2 processor units: NOMINAL and REDUNDANT) :

- Housekeeping and heater control board
- Processor board (microprocessor + multiplexer interface FPGA + memories).

Full wiring and connectors of the DU, DEU and CEU boxes.

DU – CEU Harness

Mechanical architecture:

Full mechanical DU.

Full mechanical DEU.

Full mechanical CEU.

Full mechanical TCU which includes cold finger, heater pipes and radiator.

Test facilities :

Simulator equipment for SSD detectors, preamplifiers, coders, HVPS and modules.

Ground testing for the characterization of preamplifier and coder boards.

HTRS EGSE includes Quick-Look computer + Analysis computer + Data recording.

5.9.4 Flight spare model

Electronic architecture: 4 channels

Flight electronic components
DC/DC converters for 4 modules

The Detector Unit includes:

- 4 measurement channels: 4 Pre-amplifiers
- HK Thermometers and heaters for thermal regulation

The Detector Electronic Unit which contains:

- 4 spectrometry boards
- 4 HVPS loads

The Control Electronic Unit which includes (1 processor board without REDUNDANT unit):

- Housekeeping and heater control board
- Processor board (microprocessor + multiplexer interface FPGA + memories).

Mechanical architecture:

4 modules recovered from CQM mechanical modules

Test facilities:

Simulator equipment for SSD detectors, preamplifiers, coders, HVPS and modules.

Ground testing for the characterization of preamplifier and coder boards.

HTRS EGSE includes Quick-Look computer + Analysis computer + Data recording.

5.10 Open issues for the HTRS

Energy response of the mirror: If a high-energy extension is foreseen for the mirrors, then the SDD array will have to be complemented in a similar way as for the WFI, with a higher Z semiconductor detector located underneath. Among the potential high-energy semiconductor detectors, CdTe schottky could be considered. Such detectors would both ensure the overlap in energy range with the SDD array, and provide a flat energy response up to around 70 keV and 10 μ s timing resolution. This will add some complexity to the detector design and associated electronics, but nothing critical at this stage, mostly because the HTRS is not an imaging device.

Digital processing: In the current design of the instrument, the baseline design for the electronics is a fast analog chain (there is a high level of confidence that this can be demonstrated at the TRL 5 level at the end of 2009). In the timeframe of IXO, it is however conceivable that truly digital processing electronics will be possible, even at the high rates encountered by the HTRS. This is going to be studied internally as part of an R&D program funded by CNES. A ASIC with the 37 pre-amplifiers and fast ADCs to digitize the signal would make the HTRS design more compact and lighter.

6 X-RAY POLARIMETER (XPOL)

6.1 Instrument Description

6.1.1 Introduction

The purpose of the XPOL is to provide, in the energy range 2 – 10keV, polarization measurements simultaneously with angular measurement (5 arcsec), spectral measurements ($E/\Delta E$ of ~ 5 @6 keV) and timing at few μs level. XPOL is based on a Gas Pixel Detector (using Dimethyl-Ether or DME), a counter with proportional multiplication and finely subdivided that is able to recognize tracks and thence to derive the ejection direction of the primary photoelectron. The track analysis also provides the impact point with a precision of $\sim 150 \mu m$ FWHM, largely oversampling the PSF. A major effect which decreases the position sensitivity is the blurring due to the absorption of photons from an inclined beam at different heights in the gas. The read-out chip has 105600 pixels with a $50\mu m$ pitch. The FOV is of 2.6×2.6 square arc minutes.

6.1.2 Instrument performance specifications

The basic performance specification for this instrument is to enable Polarimetric measurements to 1% Minimum Detectable Polarization (3σ) for a 1mCrab source. A further summary of the specifications is given Table 6-1 and Figure 6-1 for XPOL with He-DME 20-80, $50 \mu m$ Be window, 1cm drift region.

Table 6-1: Summary of performance specifications (assuming a Focal length of 20 m)

Polarization sensitivity	1% MDP (3σ) for a 1mCrab source
Detector size	$15 \times 15 \text{ mm}^2$
Energy range	2 – 10 keV
Energy resolution	20 % at 6 keV
Angular resolution	7"
Pixel size	$50 \mu m$
FOV	2.6×2.6 arcmin square
Timing resolution	5 μs
Efficiency	See Figure 6-1
Modulation factor	See Figure 6-1
Polarization angle resolution	~ 1 deg

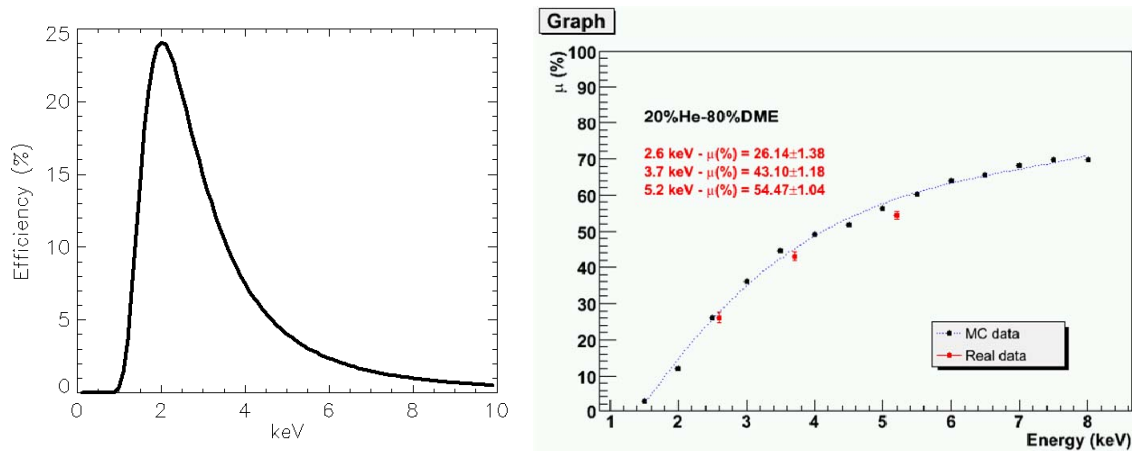


Figure 6-1: (Left) Efficiency. (Right) Modulation factor measured at 2.6 keV, 3.7 keV and 5.2 keV compared with the Monte Carlo previsions.

6.1.3 Instrument configuration

6.1.3.1 Baffle

A baffle is required to protect the X-ray background from the sky to impinge in the detector. Possible configuration with an instrument-provided pre-baffle should be considered.

6.1.3.2 Focal plane assembly

The Gas Pixel Detector is an advanced evolution of the Micropattern Gas Chamber where the multi-anode read out is fully pixellated. It is based on a gas cell with a thin entrance window, a detection/drift gap where the X-ray photon is absorbed with the ejection of a photoelectron that produces a ionization pattern in the gas (track). The track is drifted by a parallel electric field to a Gas Electron Multiplier (GEM) that multiplies the track without modifying the shape. At short distance a collection anode plane is covered of metal pads with a high filling factor distributed on a hexagonal pattern. Each pad has its own independent electronic chain to detect the charge collected from the conversion gap. The image of the track is analysed to reconstruct the point of impact and the original direction of the photoelectron. The reconstructed point of impact instead of the charge centroid gives to this detector an imaging resolution down to $150\mu\text{m}$. An additional blurring of the order of $700\mu\text{m}$ (diameter) should be accounted due to the inclined penetration of photons in the gas and absorption distributed along a gap of 10 mm (parallax error). The linear polarization is determined from the angular distribution of the photoelectron tracks. We will use a self-triggering CMOS analog chip. The top metal layer of the CMOS pixel array is patterned in a matrix of 105,600 hexagonal pixels with a $50\mu\text{m}$ pitch. Each pixel is directly connected to the underlying full electronics chain which has been realized in the remaining five metal and single poly-silicon layers of a $0.18\mu\text{m}$ VLSI technology. The noise of each chain is $50 e_{\text{rms}}$ only. With the moderate gain of 500 single electrons produced in the gas cell can be detected. The system has the capability to auto-trigger and only data included in a window around the pixels that triggered are fetched out for A/D conversion. Therefore notwithstanding the large number of pixels only sub-frames of 400 to 600 pixels, completely including the track are extracted in real time at each event.

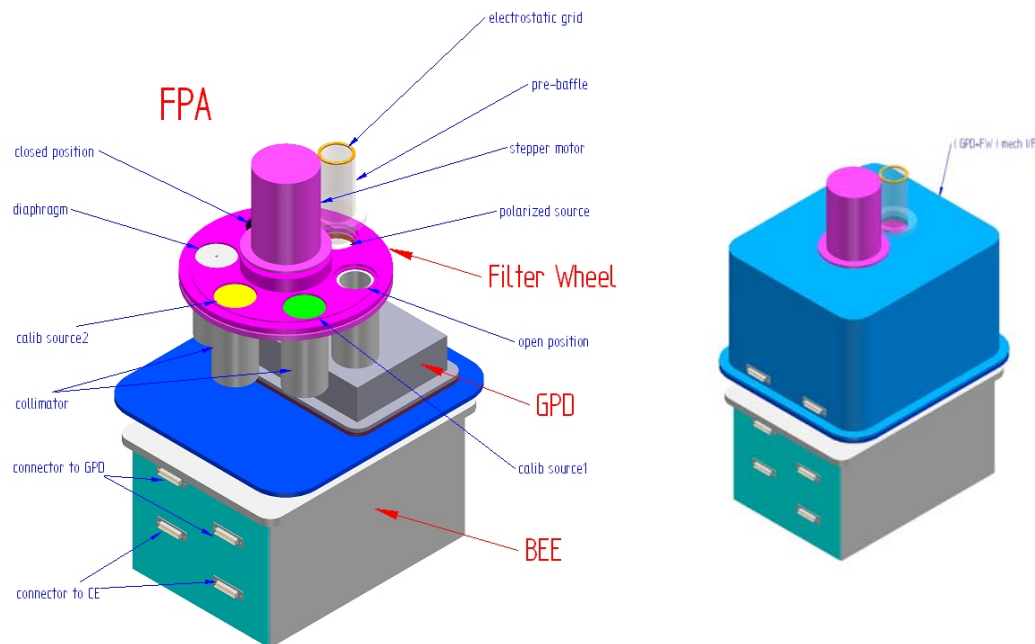


Figure 6-2: A possible configuration (FPA top-bottom layout) for XPOL on IXO

From the construction point of view the GPD is like a conventional proportional counter with anodic plane and front end electronics all included in a VLSI chip. According to all data on aging of mixtures based on noble gases with various quenching, included DME (Dimethyl-ether or $(\text{CH}_3)_2\text{O}$) (testing aimed to LHC experiments), XPOL gas mixtures can accommodate the radiation damage levels foreseen for IXO. The long experience on sealed gas counters, operated in space for years by the GPD manufacturer (Oxford Ltd), gives confidence that the long term pollution of the mixture is not a major problem. Actually a sealed GPD is working in laboratory since more than 24 months without showing any degradation of the performances. The procedures of the construction are all compatible with use for space. The GEM is a metal-coated Kapton film, similar to that used in Stellar X-ray Polarimeter (SXP) detectors. Long term stability in a sealed gas cell with Beryllium window was achieved not only for proportional counters (e.g. COS-B, HEAO-1, Einstein, GINGA, XTE) but also for GSPC (TEMNA, ASCA, SAX) which are extremely sensitive to pollution from out-gassing. Thus the detector is a sealed body with no gas refilling system.

The GPD is assembled together with a Filter Wheel (FW see paragraph 6.1.6) and eventually a pre-baffle into the FPA. If an external particle deflector is not provided, an electrostatic grid (such as the one flown on-board of the Beppo-SAX satellite), located on top of the FPA will avoid ions to impinge on the detector window which is polarized at 2 kV.

The total weight is few hundred grams, mainly due to potting of the HV distribution and connectors. The Gas Cell has as baseline a gas filling at 1 Atm He (20%) DME (80%) with 10 mm absorption/drift gap. Based on studies in progress the pressure could be increased to 2 Atm to improve the efficiency especially at higher energies. The mixture could eventually be replaced with other mixtures less sensitive to lateral diffusion during drift to allow for thicker absorption/drift gap. In this case the overall length could increase of 10mm. The baseline window is $50\mu\text{m}$ of Beryllium which provides a transparency of 64 % at 2.3 keV. In case technology shows that an improved performance can be achieved at energies below 1.5 keV a thin plastic window could be adopted.

The read-out ASIC chip, based on 0.18 μm CMOS VLSI technology, has been already successfully tested. The self-trigger download mode works perfectly. The noise for each pixel is around $50 e^-_{\text{rms}}$. All the major functions have been already tested and are compliant with the requirements for XPOL.



Figure 6-3: (Left) The sealed gas pixel detector currently working in laboratory. (Right) an exploded view. The window is 1.5 cm x 1.5 cm.

6.1.3.3 Back-End Electronics

The Back End Electronics (BEE, see Figure 6-2) is the assembly that contains the electronic boards placed between the Focal Plane assembly and the Control Electronics box. It consists of I/F Electronics (I/FE) boards and the HV Power Supply (HVPS).

6.1.3.4 Control Electronics

The Control Electronics (CE) is a data processing box which also controls the whole instrument. It interfaces both the instrument and the spacecraft, so it is the central node of XPOL. It can be located out of the focal plane interface plate until a distance of about 20m.

6.1.4 Instrument optical design – filters

The 50 μm thick Beryllium window is opaque to optical and infrared light, however as thermal shield and possibly to reject plasma the accommodation of a thin aluminised membrane can be studied.

6.1.5 Instrument units' mechanical design and dimensions

The XPOL instrument consists of the FPA and the CE unit. The FPA comprises the GPD+FW unit and the BEE unit.

At the present state of instrument development there are two possible configuration layouts: the first one with the BEE unit located alongside of the GPD+FW unit (side by side layout, Figure 6.1-4) and the second one with the BEE unit located on bottom side of the focal plane (top-bottom layout, Figure 6.1-2) provided that the HV connectors distance - between GPD and BEE - is less than 20 cm. The CE unit can be located anywhere outside the focal plane.

Table 6-2: XPOL units' dimensions

UNIT	Dimensions (L, W, H)	notes
GPD+FW (mech I/F included)	19 cm x 17 cm x 18 cm	see note below [†]
Back-end Electronics	19 cm x 14 cm x 10 cm	
FPA (side-by-side layout)		see Figure 6-4
on focal plane tray top side (+Z)	19 cm x 32 cm x 18 cm	see note below [†]
on focal plane tray bottom side (-Z)	- -	
FPA (top-bottom layout)		see Figure 6-2
on focal plane tray top side (+Z)	19 cm x 17 cm x 18 cm	see note below [†]
on focal plane tray bottom side (-Z)	19 cm x 14 cm x 10 cm	
Control Electronics	29 cm x 11 cm x 20 cm	see Figure 6-5

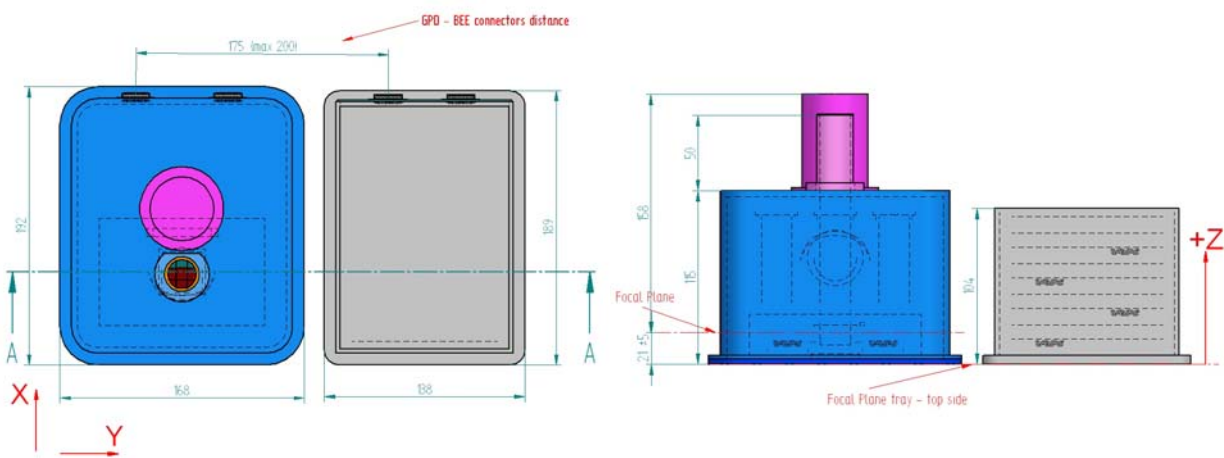


Figure 6-4: XPOL design and dimensions. GPD+FW and BEE in side-by-side layout

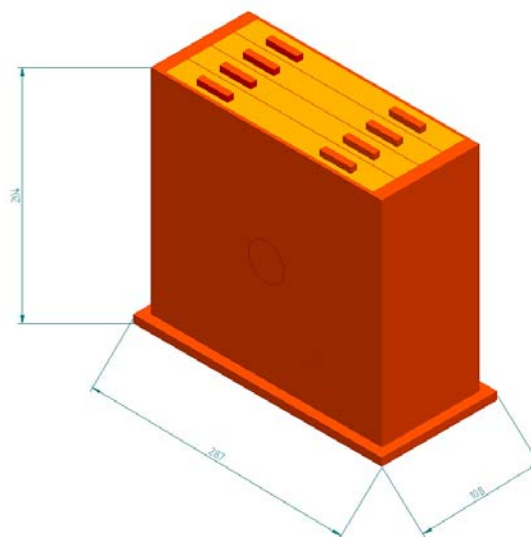


Figure 6-5: XPOL design and dimensions. CE

6.1.6 Mechanisms.

The filter wheel is a disc with different positions on it that can be rotated into the optical field of view with a motor. The Filter wheel position may be selected for observation, for calibration source deployment or for safety. Safety operations may be required autonomously or via ground control to prevent excessive charged particle fluence (solar flare or local magnetospheric storms), micrometeorite protection or spacecraft attitude loss.

The filter wheel is foreseen to have 7 positions:

- Position A) Closed. (Operative mode: power-off, stand-by, electrical calibration, observation*)
- Position B) Opened. (Operative mode: Observation, normal rate).
- Position C) With transmission filter. (Operative mode: observation, very high rate)
- Position D) With diaphragm. (Operative mode : Observation, small FOV)
- Position E) With calibration source I (Fe^{55}). (Operative mode : calibration)
- Position F) With calibration source $\text{Ti}/^{109}\text{Cd}$ (TBC). (Operative mode : calibration)
- Position G) With polarized source. (Operative mode : calibration)

* For internal background evaluation

For the sake of simplicity, it will be evaluated whether an open/closable instrument door could be used instead of a filter wheel. A calibration source would be inserted on a side of the detector.

6.1.7 Instrument units' thermal design (TBD)

The GPD optimal working temperature is 10° C. The stability will be +/- 2° C and will be maintained by a Peltier cooler managed by the XPOL associated electronics. All other units have wider operative range (-10 / +45 °C) so don't need any active control inside the instrument.

The units' mechanical interface plates act as thermal interfaces. The S/C Focal Plane structure should be thermo-regulated to maintain the units' temperatures within the operative and non-operative limits (see Section 6.3).

6.1.8 Electrical design

The analog output from ASIC will be A/D converted by the Back-End I/F electronics. The ASIC will be controlled by a dedicated FPGA, the A/D converted data will be zero-suppressed, a microprocessor will manage the telecommand and the housekeeping. The Back-end I/F electronics will also assign the time flag to each event.

The Control electronics will process the data from I/F electronics. It will format the data for the S/C computer, it will calculate, for each photon collected, the impact point and the photoelectron emission direction for bright sources. It will store the processed data in the local mass memory to be sent to the on board mass-memory. Data will be sent to telemetry when available to XPOL.

The critical High Voltage requirements for the HVPS (board located inside the BEE) are:

Table 6-3: High Voltage power supply for XPOL

ΔV	Nominal Volts	Range Volts	Current μA	Regul. bits	Stability % in the whole T range	Ripple mV	Ramp Up Volt/s	Ramp Down Volt/s
$V_{drift} = V_w - V_{Gup}$	1000	2000÷700	20	4	2	500 pk to pk	100	200
$V_{multiplication} = V_{Gdown} - V_{Gup}$	500	350÷600	1	8	0.5	100 pk to pk	10	10
$V = V_{Gdown} - V_{pad}$	300	100÷400	20	8	0.5	100 pk to pk	10	10

6.1.8.1 Back-End Electronics

The BEE is in charge of:

- Distribute and filter the low voltage power supply required to the ASIC;
- Supply the GPD with all the high voltages needed;
- Manage the ASIC analog and digital I/O;
- Implement a spectroscopy electronic chain for the GEM analog output;
- Digitally convert the analog output of the ASIC (ADC function);
- Store auxiliary information related to each event (e.g. X,Y coordinates of the ROI corner);
- Time-tag the events with at least 5 μs of resolution;
- Digitally perform some basic processing (pedestal calculation, suppression of not-fired pixels)
- Temporarily store the converted data (both from ASIC and GEM);
- Transmit to the CE the science data to be processed;
- Integrate some HK and Science Ratemeters related to the GPD activity (e.g. good event, rejected events, temperature...);
- Provide Instrument HK to the CE for active monitoring and telemetries purposes.
- Implement the Peltier Driver for the GPD temperature control

For analog signal integrity reasons, this BEE unit should be placed close to the GPD. A reasonable distance could be 10-20cm.

6.1.8.2 BEE - GPD Electronics Interface Description

The GPD is the core of the instrument since it carries the GEM and the readout ASIC.

It is provided with different electrical interfaces:

- Power: 2 x 1.8V (Analog and Digital ASIC core power supply) and 2 x 3.3V (Analog and Digital interface circuitry power supply)
- ASIC Analog Input Reference Voltages
 - 16 Trigger thresholds (one for each cluster) referred to Vref0 (generated internally to the ASIC)
 - Test Input Signal
 - Common Mode Voltage for Analog Buffers (VCM)
- ASIC Analog Output
 - 16 differential outputs (referred to VCM)
 - Vref0
- Serial Digital Interface (dataIn, dataOut, clock, some Load/Read signals): LV-TTL
- Readout Digital Signals (trigger, dataReady, RO clock,...): LVDS
- Other Digital Signals: LV-TTL

- GEM analog spectroscopy signal

Moreover the detector shall be kept under thermal control, with a stability of $\pm 2^{\circ}\text{C}$.
For this reason a Peltier driver, under control of the CE, is foreseen inside the Back-End electronics.

The ASIC will be used in self-triggering mode in which the chip itself recognizes an event and prepares a rectangular area (Region Of Interest, ROI) to be read out by the Back-End electronics: the ASIC provides a differential analog output which shall be amplified and converted into an 8bit digital word by the BE Electronics.

As a baseline the BEE will use 5V CMOS/TTL digital levels, so a suitable buffer will adapt the TTL outputs of the Back-End to LV-TTL levels required by the ASIC.

Electrically, the BEE communicates with the GPD board with one or more flat cables for a total number of 60 lines, including power supplies and ground lines.

The GEM is connected to the BEE with an HV cable that carries the spectroscopic signal.
According to later development, a possible simplification of this interface can take place. In fact 14 analog signals can be kept on the ASIC if the only used readout mode of the ASIC is the self-triggered.
Moreover a further reduction of 15 lines is possible (trigger threshold) if they all the 16 threshold lines are put together on the ASIC.

The detector also requires three high voltage power supply lines (HV) in the range 0 ... 2-3KV and currents of a few nanoampères (see Table 6-3).

As a baseline these HVs shall be derived using resistive voltage divider, keeping the higher value programmable through an 8bit DAC.

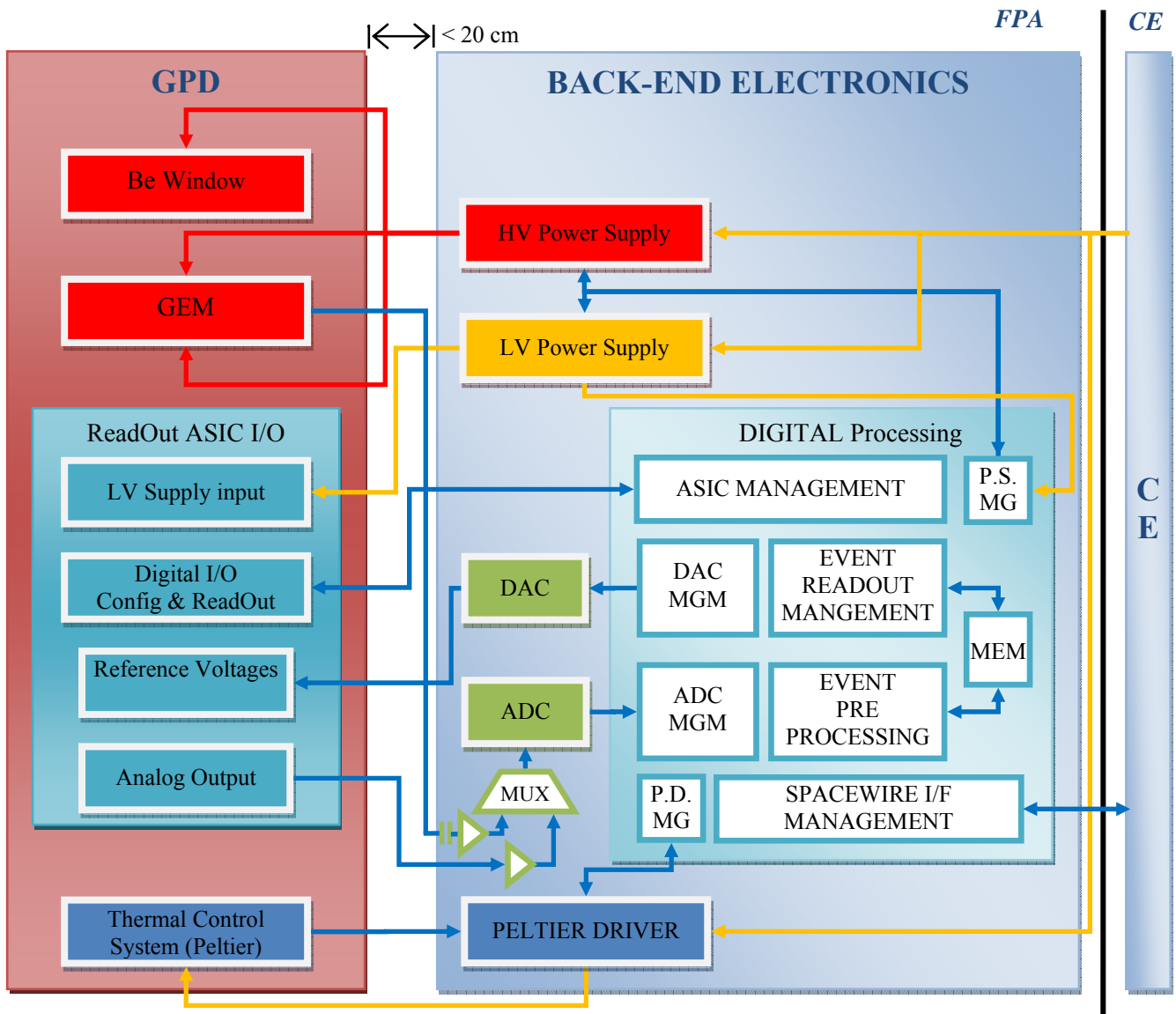


Figure 6-6: Block diagram of the GPD and the Back-End Electronics

6.1.8.3 BEE - Digital Processing Functional Description

This section illustrates the core functions of the back-end, whose architecture is depicted in the next figure.

The serial link with CE is used to configure the ASIC and the Back-End processing itself when the Instrument is in idle mode; during observation the same link is used by CE to read the science processed data. Also the digital HK are read by this link.

A dedicated logic implemented in FPGA will be in charge of the ASIC management for event readout: it is essentially a sequencer that moves, according to pre-defined steps, the ASIC signals dedicated to get ROI coordinates and get all the analog values of the detected charges.

In parallel with this action, the ADC manager will drive the 8-bit ADC to sequentially digitize the pixel charges and store them in a dedicated memory area.

At the end of the charge readout, another sequence take place to store two pedestal samples for each pixel of the ROI. It is mainly composed of a delay (4-500 μ s) followed by the same ROI readout sequence used to acquire the pixel charges.

After pedestal acquisition, the pixel-by-pixel average is calculated by the FPGA and then subtracted to the corresponding acquired pixel charge.

The last processing step is the so-called *zero-suppression*. Aim of this step is to reduce the data to be transferred to CE, discarding the pixels whose pedestal subtracted charge is below a threshold common to all the chip. For example a typical ROI is made of 1000 pixels but the average number of fired pixels is around 50, so this step is able reduce the event size by ten.

A DAC manager is in charge to set an analog threshold, common to all the chip, that fixes the chip triggering level.

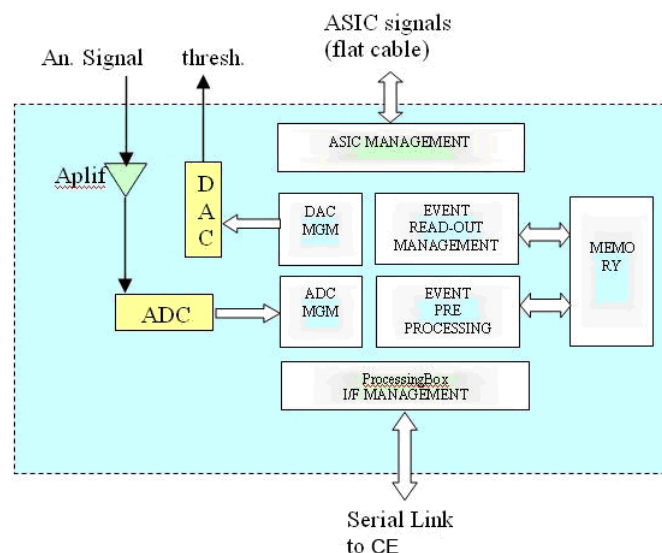


Figure 6-7: Back End Digital Processing Architecture

The Back-End memory will implement the following main areas related to events data:

- Acquired charge (1kWord)
- First Pedestal Acquisition (1kWord)
- Second Pedestal Acquisition (1kWord)
- Calculated Pedestal (TBC, 1kWord)
- Pedestal Subtracted Data (TBC, 1kWord)
- Event Header Data (time-tag, aux info)
- Output Buffer (managed in a FIFO manner) of at least 16 zero-suppressed events (> 16 x 256 word = 4kword)

Memory size will be minimum 32k x 16bit.

The analog section depicted in the above picture is a differential amplifier because the ASIC output section is made of two complementary lines (out+ and out-) with a common mode V_{cm} of 1.5V.

6.1.8.4 BEE – CE Interfaces Description

Three types of interfaces are present. First of all a primary power bus from which all power supplies needed by the Back-End itself and the Detector are carried out.

It has been chosen to directly supply the Back-End with the primary power for two main reasons:

- In this way the “back-end” and/or “back-end + detector assembly” is a *stand-alone* unit/subsystem, that can be tested and integrated in parallel without the CE, which otherwise will become a bottleneck in the AIV flow
- The path of the high voltage cables is thus minimized (the solution with the HV DC/DC inside the detector assembly has been discarded due to noise and thermal considerations).

A serial digital LVDS data interface is then provided for science, command and digital housekeeping exchange with the processing unit.

Considering a peak rate of 5000 events/sec and assuming the average data size for a single photon of 1016 bits and a margin factor of 2, we get a peak data rate on this link of about 5Mbit/sec (see Section 6.4.6.2).

Logically connected to this interface there is the clock line for the Back-End Electronics (12MHz TBC, supplied by the processing unit) and the interrupt line used by BE to prompt the processor that some data (e.g one or more event data) is ready to be read.

From the point of view of the data exchanges, as a preliminary exercise, we list here a possible layout of the science packets exchanged from ASIC to BEE (raw format) and from BEE to CE (pre-processed data)..

		16 bit word	word id
header	Packet Type ID (RAW)		0
	Event Time (MSW)		1
	Event Time		2
	Event Time (LSW)		3
	ROI X width: ΔX		4
	ROI Y width: ΔY		5
	ROI corner: X0		6
	ROI corner: Y0		7
pixels data	Pix 0: charge (Q0)		8
	Pix 1: charge (Q1)		
		
	Pix N-1: charge (QN-1)		7+N
	END MARKER		8+N

For a typical event of 50x20 ROI (in which $50 \cdot 20 = \Delta x \cdot \Delta y = N$): 800128 bit/ev

Figure 6-8: Science Data Packet (RAW format) – from ASIC to BEE

		16 bit word	word id
header		Packet Type ID (PROC)	0
		Event Time (MSW)	1
		Event Time	2
		Event Time (LSW)	3
		AUX info	4
		Nr of pixels (N)	5
		ROI corner: X0	6
		ROI corner: Y0	7
		Pix 0: Δx(8bit), Δy(8bit)	8
		Pix 0: charge (Q0)	9
pixels data		Pix 1: Δx(8bit), Δy(8bit)	
		Pix 1: charge (Q1)	
		
		Pix N-1: Δx(8bit), Δy(8bit)	
		Pix N-1: charge (QN-1)	7+N*2
		END MARKER	8+N*2

For a typical event of 50 zero suppressed pixels: 1728 bit/ev

Figure 6-9: Science Data Packet (Pre-Processed data) – from BEE to CE MEM

The last interface is an analog differential line used to transmit to the CE the analog HK values to be periodically acquired.

The baseline foresees that this line is multiplexed on the Back-End in order to limit the harness between the two units.

6.1.8.5 Control Electronics

The CE is in charge of managing the following interfaces:

- Three serial interface with the three instrument to:
 - configure the corresponding Back-End and Front-End unit;
 - manage the digital HK periodic acquisition
 - retrieve the science data
- manage one multiplexed differential analog line to periodically acquire the analog HK of each instrument (voltages, currents, temperatures,...). We assume to acquire up to 16 (TBC) analog values (already conditioned inside the BE box);
- manage three dedicated interrupts lines to trigger the science data retrieval of the already pre-processed data from the BEE;
- manage one filter wheel for each detector (the presence of this wheel is TBC).

- Drive one Peltier driver (inside the Back-End) for each instrument, to implement the detector thermal controls with an accuracy of $\pm 2^{\circ}\text{C}$;
- Manage the non regulated primary power bus in order to carry out all the secondary voltages needed by the unit;
- filter the non regulated primary power bus for the BEE;
- manage the data interface with the spacecraft. This link is used to get TC from the Spacecraft and to send both Science and HK telemetry packets.
- Manage the Pulse Per Second synchronization signal line in order to perform the event time-tagging with the required accuracy ($50\mu\text{s}$ TBC);

The box high level architecture is shown in the following picture.

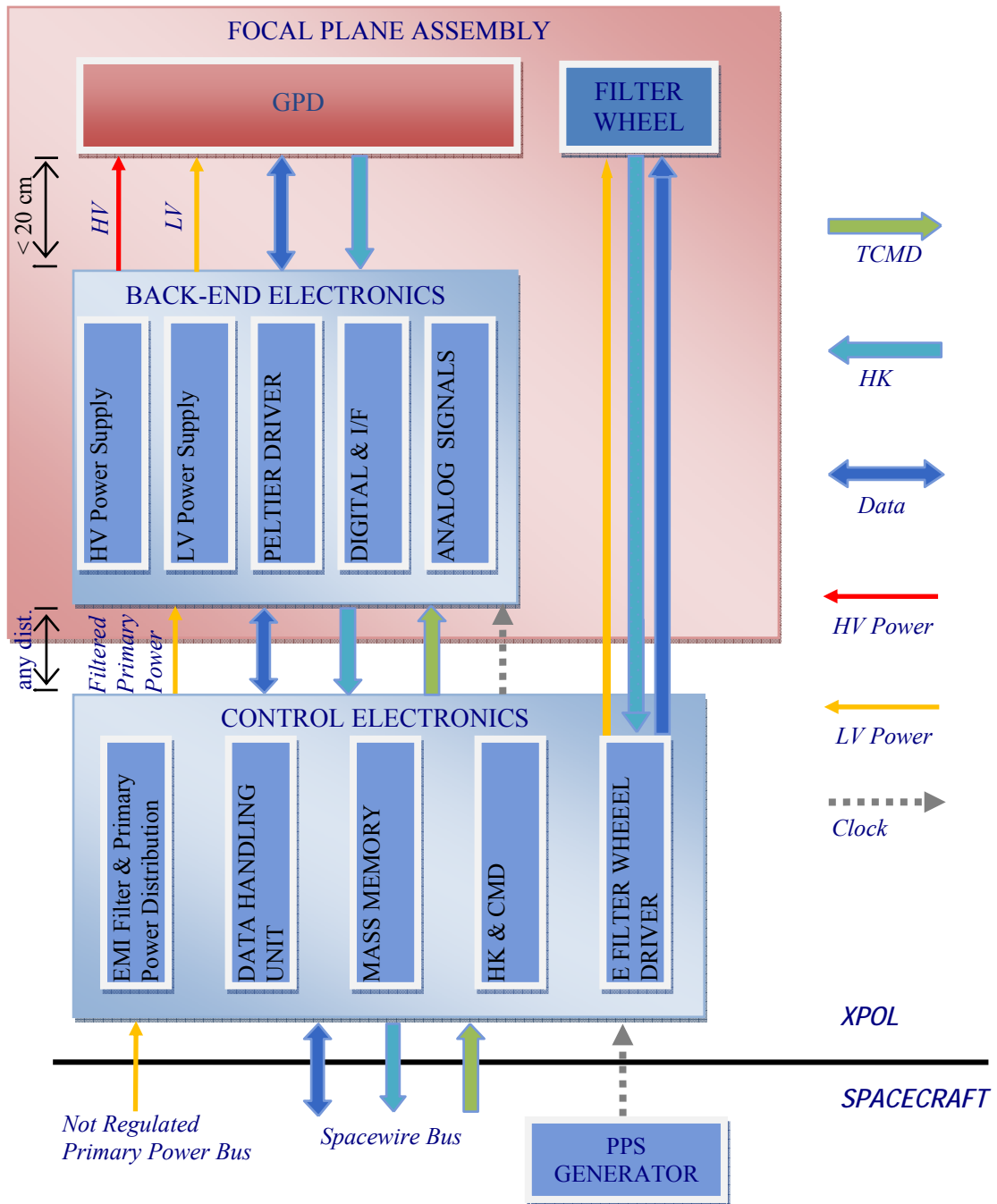


Figure 6-10: CE Interfaces and Functions

From the functional point of view, the CE shall also:

- Parse and execute the TCs coming from the S/C
- Generate scientific and HK telemetries;
- Generate messages, warnings and errors reports;
- Manage the Instrument Operative Modes;
- Implement the detector thermal control algorithms;
- Control the positioning of the Filter Wheel (TBC);
- A to D convert all the instrument analog HK lines both for thermal control, position control and HK purposes;
- Perform the Instrument Control Function, i.e. the active monitoring of some instrument safety critical parameters in order to implement a nearly real-time reaction to avoid damages;
- In case of high science data rates, store this data into an instrument Mass Memory (implemented inside the CE or shared with the IXO payloads);
- Perform science data processing

6.1.9 On-board software

The on board software will be capable of:

- Decoding and executing telecommands
- Formatting the data according to Table 6-8 and Table 6-9
- Performing pedestal subtraction from the data after the acquisition of each frame.
- Performing the evaluation of the impact point, the photon energy and of the emission angle for sources approximately brighter than 0.3 Crab. This will be accomplished evaluating the I, II and III momentum of the charge distribution and identifying the side of the track from where the photoelectron is ejected.

6.1.10 Ground support equipment

6.1.10.1 Electrical ground support equipment

At the present time the GPD control and data acquisition is done through a VI graphic interface developed in LABVIEW. The VI performs a bidirectional communication through a 100Mbps TCP connection between the DAQ and a portable PC running Windows XP. For the following phase an EGSE will be adopted.

6.1.10.2 Mechanical and optical ground support equipment

The present mechanical accommodation is very compact. No dedicated Mechanical GSE has been designed so far, but due to the light weight of the detector and associated electronics we foresee that the weight and the complexity of the Mechanical GSE will not be cumbersome. For example we designed and built a very compact facility for the calibration of the X-ray polarimeter. For the following phase a mechanical GSE will be developed.

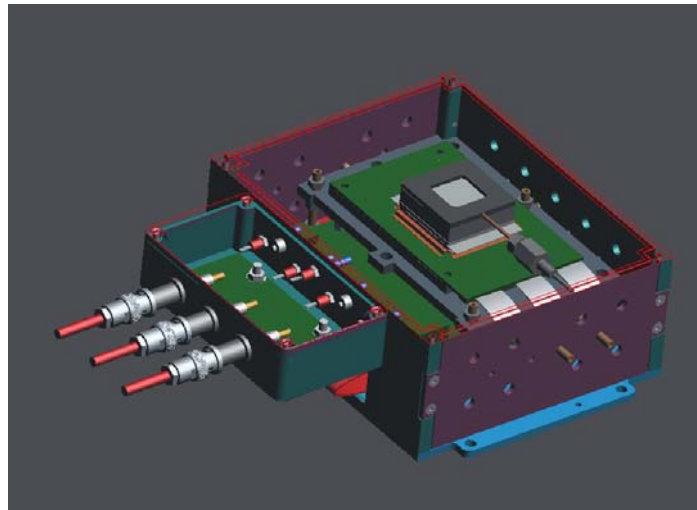


Figure 6-11: Schematics of the laboratory box containing the detector and the interface electronics.

6.1.11 Instrument mode description

6.1.11.1 Operating modes

The XPOL instrument will be operating by execution of a limited number of predefined observation sequences to be stored in the spacecraft DPU that the spacecraft receives at a previous communication window.

Calibration modes are:

- Electric calibration mode of pedestals (filter A = FW closed)
- Electric calibration mode by test pulse (filter A = FW closed)
- Calibration with radioactive source Fe55 (filter E)
- Calibration with radioactive source mixed (filter F)
- Calibration with polarized source (filter G)

The science modes are:

- Normal (Filter B = all open). No post-processing
- Diaphragm (Filter D = f.o.v partially covered). No post-processing
- High rate (Filter B = all open). Post-processing
- Extremely high rate (Filter C = all field attenuated) Post-processing

All these science operative modes are the same from the point of view of detector/FEE configuration, time tagging, A/D conversion and zero suppression. They differ for the strategy to avoid overwhelming the mass memory in case bright sources are observed. In the normal mode data after zero suppression (pre-processing), the track image, are stored to MM to be further forwarded to telemetry. In high rate, when the XPOL observation is over and the telescope is allocated to another instrument, data are recovered from MM, compressed by CE DHU with onboard analysis of polarization (post-processing) and stored again in MM. In case the target source is faint and another stronger source is present in the FOV, the latter can be removed by the use of a diaphragm: this is the diaphragm mode. In case of an extremely bright source, that could exceed

the capability of data handling or the dead-time quality limit ($< 5\%$), all the field will be attenuated with a filter C.

The XPOL MM is dimensioned (16GByte) to store data from a 5000 s observation of a 1 Crab source. The same function could be performed on the P/L Mass Memory provided that it is made available for the time needed for post-processing. The processing time will normally be < 20 times the acquisition time. The data flow for a very bright source (to obtain good spatial resolution), i.e. the Crab observed for more than 9 hours. The same function could be performed on the P/L Mass Memory. The stored data can be post-processed by the CE and after compression reduced to < 1 GByte, which could be downloaded over subsequent telemetry windows at suitably lower rate interleaved with normal science data, or special communications windows requested for this download.

The XPOL will be launched with the filter wheel in closed position (A). The filter wheel's position 'A' will be used to prevent excessive charged particle fluence (solar flare or local magnetospheric storms), or to protect for micrometeorites or spacecraft attitude loss. Autonomous Safe mode may be required in addition to pre-programmed command.

Calibrations

Internal calibrations will occur frequently to ensure the stability of instrument operation with respect to X-ray energy-ADC gain function etc. This can be done via special observations in appropriate filter wheel position, and most efficiently during spacecraft slew.

Electrical calibration:

- Pedestals (offset subtraction)
- Gain calibration (pixel equalization)

Pedestal calibration can be performed once every 2 hours while gain calibration once every 12 hour. The Pedestal calibration of the entire chip will take 2 min.

Physical calibration (internal calibration):

The two calibration positions on the filter wheel are to be used regularly to verify the performances (measure the level of absence of modulation across the detector area) and physically calibrate XPOL.

Calibration with a ^{55}Fe source as well as with fluorescence by target materials (e.g. Ti, Cu etc.) using a ^{109}Cd (e.g.) source can be performed every 2 hour of observation for 10 min. If the calibration source will be placed internally to the detector body, collimated on a far angle of the chip, a continuous calibration during observation can be performed.

Astrophysical calibration:

Calibration Standard

Polarization.

Previously measured X-ray polarized source :

Crab Nebula: 5 ks 2/year.

Calibration of the angle swing:

6.2 Mechanical Interfaces and Requirements

6.2.1 Location requirements

The GPD+FW unit of XPOL is hard-mounted on the focal plane interface plate of the spacecraft, with no special location requirements. The BEE unit must be located close to the GPD+FW unit, on top (side-by-side layout) or bottom side (top-bottom layout) of the focal plane interface plate provided that the HV connectors distance is less than 20cm. There are no special location requirements for the CE that can be located anywhere wrt the BEE unit.

6.2.2 Alignment requirements

The instrument optical axis should be aligned with the Z-axis of the S/C. Since the Field of view (FOV) of the present instrument is 2.6 arcmin and its size is 15 mm, it should become aligned in the S/C within an accuracy of <5 arcmin with the Z axis and +/- 0.75 mm in the X and Y axis, with a knowledge of +/- 0.15 mm. The focal plane of the instrument, defined to be half-way in the drift region of the polarimeter, should be at the focal plane of the telescope to an accuracy of +/- 3 mm (TBV).

6.2.3 Pointing requirements and performance goals

The generic pointing requirements for XPOL can be found in Part 3 along with the rest of the instruments. Any instrument specific requirements are discussed here.

Pointing requirements are driven by the need to accurately locate the point sources into the detector field of view. Timescales of reconstruction knowledge appropriate to the image time resolution (~1ms)

(1) AME

The drift region of 1 cm of XPOL anticipates a blurring effect of 7 arcsec due to the inclined penetration of X-ray photons coming from X-ray optics at 20 m of focal length. Therefore the requirement of 1 arcsec of AME is more than adequate for XPOL.

(2) RPE, APE, Long Term attitude stability

At each event is assigned a time tag with high accuracy.

Normal/weak sources

For normal/weak sources the data are downloaded into telemetry on event by event base (zero-suppressed pixel energy content and coordinates) and post-processed on-ground. The impact point is calculated with an accuracy of the same order of the optics (see below).

Strong sources

For strong sources a processing on board occurs. On-ground the post-facto reconstruction permits to recover the nominal performances (position location and photoemission angle) in a way which is not affected by the RPE, APE and long Term attitude stability which therefore do not drive the scientific capability of XPOL. Care will be taken in choosing the diameter when designing the diaphragm (in case of use of a filter wheel) to take into account the drift stability and pointing accuracy.

6.2.4 Interface control drawing

At the moment we do not have an instrument control drawing.

6.2.5 Instrument mass

Here below we show the mass budget.

Table 6-4: XPOL mass distribution

Item	Assumption	Unit mass [kg]		Margin [%]	Total mass [kg]	
Focal Plane Assembly						
GPD		0.4		20	0.5	
FW + prebaffle* + mech I/F		2.85		20	3.4	
BEE		1.55		20	1.9	
FPA Total		4.8		20	5.8	
Associated Electronics						
CE		3.5 [†]	4 [‡]	20	4.2 [†]	4.8 [‡]
XPOL Total		8.3[†]	8.8[‡]	20	10[†]	10.6[‡]

* possible electrostatic grid included

[†] XPOL with shared Mass Memory

[‡] XPOL with dedicated 16GByte Mass Memory

The mass budget value includes all the XPOL units (mechanical I/F plates and boxes included), in particular:

- FPA
 - GPD + FW + pre-baffle + mechanical I/F unit
 - BEE (I/FE, HVPS) unit
- CE unit with and without the MM board

and excludes:

- harness

6.3 Thermal Interfaces and Requirements

6.3.1 Temperature limit in space environment

The XPOL non operative temperature (e.g. launch, not observing/calibrating) is -15°C to $+45^{\circ}\text{C}$. The operative temperature of the GPD gas cell is $10^{\circ}\text{C} \pm 2$ and it will be maintained by a Peltier cooler managed by the XPOL associated electronics. The other items (FW, BEE and CE) will work in the operative temperature range $-10/+40^{\circ}\text{C}$

Table 6-5: XPOL temperature limits in space environment

Item	Operative [$^{\circ}\text{C}$]	Non-operative [$^{\circ}\text{C}$]
Focal Plane Assembly		
GPD	10 ± 2	$-15 / +45$
FW	$-10 / +40$	$-15 / +45$
BEE	$-10 / +40$	$-15 / +45$
Associated Electronics		
CE	$-10 / +40$	$-15 / +45$

6.3.2 Temperature limits in laboratory environment

The Gas Pixel Detector can work at environmental temperature, however best performances are obtained when working at $10 \pm 2^{\circ}\text{C}$.

6.3.3 Temperature sensors

We foresee to use temperature sensors within the detector and the associated electronics to monitor the temperature during flight.

6.3.4 Heaters

No instrument heater is foreseen. If needed, the Peltier can be operated to heat the GPD.

6.3.5 Thermal schematics

The units' mechanical interface plates act as thermal interfaces. In Figure 6-12 are shown the I/F plates of the sectioned FPA units and of the CE unit. The S/C Focal Plane structure should be thermo-regulated as indicated in the next paragraph.



Figure 6-12: (left) GPD+FW and BEE Thermal I/F plates; (right) CE Thermal I/F plate

6.3.6 Thermal control requirements

The S/C Focal Plane structure is supposed to be thermo-regulated to maintain the temperature of all the units within the operative and non-operative ranges. A Peltier cooler managed by the XPOL associated electronics will help to maintain the GPD gas cell at the operative temperature of 10°C within the required ±2°C range. Referring to the XPOL power budget and assuming that the units' thermal radiation exchange is negligible, we can estimate the following thermal control requirements for the S/C at the I/F plates:

Table 6-6: XPOL thermal control requirements at the I/F plate

Item	Operative		Non-operative	
	Thermal load [W]	S/C I/F Temp [°C]	Thermal load [W]	S/C I/F Temp [°C]
	min	max		
Focal Plane Assembly				
GPD+FW I/F plate	2	6*	0	-15 / +45
BEE I/F plate	12	12	0	-15 / +45
Associated Electronics				
CE I/F plate	23.2	41.1	0	-15 / +45

*corresponding to the FW consumption (with GPD and BEE OFF and CE ON at min Thermal load)

6.4 Electrical Interfaces and Requirements

6.4.1 Electrical resources requirement summary

The instruments has its own power converters and power conditioning unit, it requires about 55 W (dedicated memory) or 37 W (shared memory) and 28 V from the satellite in the standard operative mode.

6.4.2 Instrument power distribution block diagram

A functional power distribution diagram is shown in Figure 6-10.

6.4.3 Power budget

Here below we show the power budget

Table 6-7: Power budgets

Item	Assumption	Unit power [W] with 20% margin		
		Operative mode	Standby mode	Survival mode (OFF)
Focal Plane Assembly				
GPD		2	0	0
Filter Wheel	see note*	6*	0	0
BEE	70% DC/DC efficiency	12	11**	0
Associated Electronics				
CE	70% DC/DC efficiency	41.1 [†]	23.2 [‡]	0
XPOL Total		55.1[†]	37.2[‡]	0

* The filter wheel driver is rarely activated and when it is activated the GPD and BEE can be OFF, so it contributes to the power budget in a nearly negligible way and is not added to the total power budget.

** HVPS board is OFF.

[†] XPOL with dedicated 16GByte Mass Memory

[‡] XPOL with shared Mass Memory, 18W (20% margin included) of power saving

6.4.4 Instrument modes duration

6.4.4.1 Instrument continuous mode duration

The XPOL instrument will be operating by execution of a limited number of predefined observation sequences to be stored in the spacecraft DPU that the spacecraft receives at a previous communication window.

Calibration modes are:

- Electric calibration mode of pedestals (filter A = FW closed): 2 min duration
- Electric calibration mode by test pulse (filter A = FW closed): 5 min duration
- Calibration with radioactive source Fe55 (filter E): 10 min duration

- Calibration with radioactive source mixed (filter F): 10 min duration
- Duration is 10 min each 2 hours of observation.

The science modes are:

- Normal (Filter B = all open). No post-processing
- Diaphragm (Filter D = f.o.v partially covered). No post-processing
- High rate (Filter B = all open). Post-processing
- Extremely high rate (Filter C = all field attenuated) Post-processing

All these science operative modes are the same from the point of view of GPD/BEE configuration, time tagging, A/D conversion and zero suppression. They differ for the strategy to avoid overwhelming the mass memory in case bright sources are observed. In the normal mode data after zero suppression, the track image, are stored to MM to be further forwarded to telemetry. In high rate, when the XPOL observation is over and the telescope is allocated to another instrument, data are recovered from MM, compressed by the CE DHU with onboard analysis of polarization (position, time and angle) and stored again in MM. In case the target source is faint and another stronger source is present in the FOV, the latter can be removed by the use of a diaphragm: this is the diaphragm mode. In case of an extremely bright source, that could exceed the capability of data handling, all the field will be attenuated with a filter C.

The duration of the observation depends on the source strength and the sensitivity to be reached. Typical observation can be in the range of 1000-10000 s

6.4.4.2 Instrument peak mode duration

During observation of bright sources (at level of more than 0.3 Crab till about one Crab), the instrument will work in indirect mode (or post-processing). In the indirect mode XPOL will process on board the analog data and will provide the impact point and the emission angle for each collected photon. This will permit to reduce the telemetry load and the mass memory requirement of a factor of 16. This mode will last up to 15 ks for the brightest sources.

6.4.5 Telecommands

For each observation the XPOL requires TBC commands to define operating modes, window configurations, filter wheel position etc. Low bit rate interface only.

6.4.6 Telemetry

6.4.6.1 Telemetry requirements (TBD)

The telemetry should be able to download up to 1 Mbit/s for bright sources

6.4.6.2 Telemetry description

Housekeeping telemetry

XPOL will generate TBD housekeeping at TBD rate

Science telemetry

Data rates

The detector chip is triggered from an event and provides a sub-frame (or Region of Interest (ROI)) which includes the photoelectron track as output.

Processing electronics provides a compression, independent on the source flux, called zero-suppression (pre-processing) and possibly a further compression depending on the source flux (post-processing). For each event, the zero suppression forwards only the pixels with non zero-charge to the memory, which gives an average compression factor of 3.

Weak source

For data rates to memory (pre-processed data) lower than 1 Mbit/s, corresponding to source fluxes below 0.3 Crab (from medium flux extragalactic sources or low flux galactic source up to high flux galactic source), all the information contained in the memory without further processing are downloaded on-ground. For each event the information on the address of each pixel within the sub-frame (12 bit) and on its energy content (8 bit) are provided. Also, the absolute coordinates of the sub-frame (9 bit X and 9 bit Y) and the Energy and Time of the event provided by the GEM are provided. The evaluation of the emission angle is derived on ground.

The bit assignment for pre-processed data is summarized in the following table:

Table 6-8: Bit assignment for pre-processed data

GEM		ASIC CHIP							
For each event:						TOT	For each hit pixel:		TOT
Time bit	Energy bit	RVC bit		RL bit			RPC bit	RPH bit	
		Coord. X	Coord. Y	Coord. X	Coord. Y		Coord.	Energy	
18	8	9	9	6	6	56	12	8	20

Bright source

If the data rates to memory (pre-processed data) are larger than 1 Mbit/s, corresponding to source flux larger than 0.3 Crab (a bright galactic source), the data in the memory is processed on-board (post-processed data). The estimations of the absorption point, of the emission angle and of a quality parameter are calculated event by event.

Time and Energy are provided by the GEM, also, event by event.

The following table defines the bit assignment for post-processed data to be downloaded to ground (for source fluxes above 0.3Crab):

Table 6-9: Bit assignment for post-processed data

ASIC CHIP						
GEM For each event:						TOT
Time bit	Energy bit	Absorption point bit		Emission angle bit	Quality parameter bit	
		Coord. X	Coord. Y			
18	8	9	9	10	8	62

If the source flux is larger than 1.4 Crab (corresponding to 5000 count/s), the source can be acquired with the Filter Wheel on Position C (with transmission filter of Be 150µm thick to reduce the count rate of a possible 10 Crab source to 5000 counts/s) to maintain the dead time <5%.

Below are calculated the expected bit rates downloaded in the on-board memory and in telemetry for two sources with weak and bright flux and for the counts/s limit:

1) Weak source (<0.3Crab) : **MCG-6-30-15** (2.7 mCrab = 9.7 counts/s) :

Average Number of pixel in ROI/ event = 160 BEFORE ZERO-SUPPRESSION

Average Number of pixel /event = 48 AFTER THE ZERO-SUPPRESSION

COMPRESSION FACTOR = 3.3

Bit rate to XPOL memory to be downloaded to ground.

$$48 * (8+12) * 9.7 + (18 + 8 + 9 + 9 + 6 + 6) * 9.7 = 9.9 \text{ kbit/s}$$

2) Bright source (>0.3Crab): **Crab Nebula** (1 Crab = 3600 counts/s)

Average Number of pixel in ROI / event = 160 BEFORE ZERO-SUPPRESSION

Average Number of pixel /event = 48 AFTER THE ZERO-SUPPRESSION

COMPRESSION FACTOR = 3.3

Bit rate to XPOL memory.

$$48 * (8+12) * 3600 + (18 + 8 + 9 + 9 + 6 + 6) * 3600 = 3.66 \text{ Mbit/s}$$

Bit rate to be downloaded to ground after the on-board emission angle determination

$$(18 + 8 + 9 + 9 + 10 + 8) * 3600 = 0.22 \text{ Mbit/s}$$

II COMPRESSION FACTOR = 16.4

3) count/s limit: 5000 counts/s corresponding to a 1.4 Crab source or a filtered 10 Crab source

Average Number of pixel in ROI / event = 160 BEFORE ZERO-SUPPRESSION

Average Number of pixel /event = 48 AFTER THE ZERO-SUPPRESSION

COMPRESSION FACTOR = 3.3

Bit rate to XPOL memory.

$$48 * (8+12) * 5000 + (18 + 8 + 9 + 9 + 6 + 6) * 5000 = 5.08 \text{ Mbit/s}$$

Bit rate to be downloaded to ground after the on-board emission angle determination

$$(18 + 8 + 9 + 9 + 10 + 8) * 5000 = 0.31 \text{ Mbit/s}$$

II COMPRESSION FACTOR = 16.4

Table 6-10: Data rates summary

event rate	to MM (pre-processed data)	telemetry to ground
<1000 cts/s (unfiltered)	1016 bit/event	1016 bit/event
1000-5000 cts/s (unfiltered)	1016 bit/event	62 bit/event (post-processed)
>5000 cts/s (filtered)	1016 bit/event	62 bit/event (post-processed)

6.4.7 Electrical interfaces

All the electrical interfaces with the spacecraft are through the Control Electronics (see Figure 6-10): satellite power, commanding, housekeeping and science data transport to the spacecraft computer. A redundant channel is foreseen.

The connection to the spacecraft computer systems is done via the SpaceWire connection.

The requirement for the absolute timing accuracy to be provided by the spacecraft (and ground segment) is better than 50 μs (TBC).

6.5 Electromagnetic Compatibility and Electrostatic Discharge Interface

6.5.1 Susceptibility requirements

XPOL does not need any magnetic field to operate, the only bias is bias voltages. The instrument can withstand rather high magnetic field strengths and as such the requirement on ambient magnetic field levels are not foreseen to be very strict.

Situations in which the XPOL performance could be influenced by magnetic fields are described below:

- On the photoelectron itself, possibly modifying its direction: to obtain a polarization angle resolution of 1 deg and residual modulation values of less than 1%, the lower limit to be deflected is about 0.001 Tesla at 50mm from any face of the GPD cover.
- On the drift of the primary charges produced by the electron. This can be the case only if the gyration time is comparable or less than the collision time of electrons during the drift which randomize the velocity distribution. Typical collision times are of the order of 10^{-11} s therefore in order to see an effect on a drift parameter (drift velocity and diffusion) fields of the order of 1 Tesla or larger are necessary.
- Effects on XPOL readout chip. No effects are foreseen on ASIC CMOS readout chip up to levels of 0.1-1 Tesla
- The Interface Electronics will be designed to be insensitive to magnetic field at the level foreseen for the location of XPOL with an adequate margin.

Should it be necessary, shielding (μ -metal tapes, metal strips etc.) that can reduce magnetic fields must satisfy the requirements in Table 6-11.

6.6 Optical Requirements

6.6.1 Stray-light requirements

Beryllium window is opaque to optical stray light. A baffle is foreseen to prevent X-ray stray light to reach the detector.

6.6.2 Baffling requirements

To attenuate the diffuse X-ray background, the instrument requires a baffle that can be a common baffle for all on axis instruments. The requirement is a normal transmission of X-rays $< 1/100$ at 10 keV.

The XPOL active area diameter d is of $1.5\sqrt{2}$ cm and, for a focal length $F = 20$ m, it corresponds to a FOV of 2.6×2.6 square arc minutes.

Possible configuration with an instrument-provided pre-baffle should be considered. The pre-baffle will be placed on top of the filter wheel. It will be made of carbon fibre possibly with a gold evaporated surface to absorb diffuse X-rays.

6.6.3 Charged particles deflector

Space plasma can induce two effects:

- Variation in the drift field due to a high voltage drop of the Be window polarized at about -2000 V
- the impact of energetic ions, accelerated by the negative potential will produce the emission of secondary electrons when impacting the detector window. Such electrons are accelerated back toward the satellite structure and they produce X-rays when impacting on the surfaces of the materials surrounding the detector.

To prevent those effects a charged particles deflector must be placed satisfying the requirements listed in Table 6-11 and Table 6-12.

An electrostatic grid deflector can be mounted on top of XPOL FPA if auxiliary particles deflectors will not provided.

Table 6-11: EMC environment and requirements

<i>Requirements</i>		<i>Notes</i>
charged particles with $E < 1\text{Mev}$ <i>max current</i>	$< 1 \cdot 10^{-10}$ A @ the detector Be window	the detector Beryllium window stops heavy charged particles until energy of 1Mev
charged particle with $E > 1\text{Mev}$ <i>max count rate</i>	< 0.1 Hz @ the detector Be window	
<i>max magnetic field module</i>	$< 1 \cdot 10^{-3}$ T @ 50mm from any face of the detector cover	values above the limit produce performance degradation of the detector due to electron path shifting

Table 6-12: Charged particles deflector requirements

<i>Requirements</i>		<i>Notes</i>
IXO auxiliary magnetic deflector	compatible only if the deflector satisfies the max magnetic field module and the other EMC requirements in Table 6-11	potentially EMI problems
accommodation	at least 90mm above the XPOL focal plane to avoid mechanical interference	See Figure 6-4
XPOL electrostatic grid deflector	must satisfy the EMC requirements in Table 6-11	needed only if no auxiliary deflector will be provided
characteristics	it could consists of 50 μ m wires connected to the bus power line through XPOL	
accommodation	at least 90mm above the XPOL focal plane to avoid mechanical interference	see Figure 6-4

6.7 Transportation, Handling, Cleanliness and Purging Requirements

6.7.1 Transportation requirements

There are no specific transportation requirements.

6.7.2 Handling requirements

No particular care should be taken in handling except, probably, care of the Beryllium window. Therefore a protective Kapton membrane for transportation has been devised.

6.7.3 Cleanliness requirements

Some cleanliness should be guaranteed against dust both for the filter wheel and for the Beryllium window. We assume that the electronics will be protected by the provided units' boxes.

6.7.4 Purging requirements

The XPOL will most probably not be launched with the experiment body in vacuum conditions. Thus, a vacuum suitable instrument door is not required.

Contamination is prevented prior to launch by gaseous Nitrogen purging and environmental contamination control. In addition, the Focal Plane Assembly is protected during launch by the filter wheel in its closed position.

6.8 Ground and Flight Operation Requirements

6.8.1 Ground and pre-flight operation

On ground XPOL will be operated with radioactive sources to check the functionality. Nevertheless, careful calibration will be performed by using x-ray tubes monochromatic and polarized by means of Bragg crystals.

6.9.3 Flight Model

A full flight model will be delivered.

6.9.4 Flight Spare Model

A flight spare at subsystem level will be delivered.

7 CRITICAL-ANGLE TRANSMISSION GRATING SPECTROMETER (CAT-GS)

7.1 Instrument Description

7.1.1 Introduction

The Critical-Angle Transmission Grating Spectrometer (CAT-GS) is a wavelength-dispersive spectrometer for high-resolution spectroscopy in the energy band between 0.3 and 1.0 keV. It consists of one or two transmission grating arrays that are placed just aft of the telescope mirrors in the convergent telescope beam, and a readout camera on the fixed instrument platform. (This document focuses on the case of two grating arrays, placed on azimuthally opposite sides from each other, with azimuth being in the x-y plane.) The grating arrays hold a number of grating facets in a fixed position and orientation relative to the mirrors. The gratings disperse x rays according to wavelength and focus them along a straight line (dispersion axis) into a spectrum that is recorded by the camera. The center of each grating facet touches a Rowland torus that also contains the telescope focus and the fixed blaze position in the spectrum. The CAT gratings are blazed, and therefore the diffraction efficiency is maximized around the direction of specular reflection off the sidewall of a grating bar. The direction of specular reflection coincides with the direction of the blaze position.

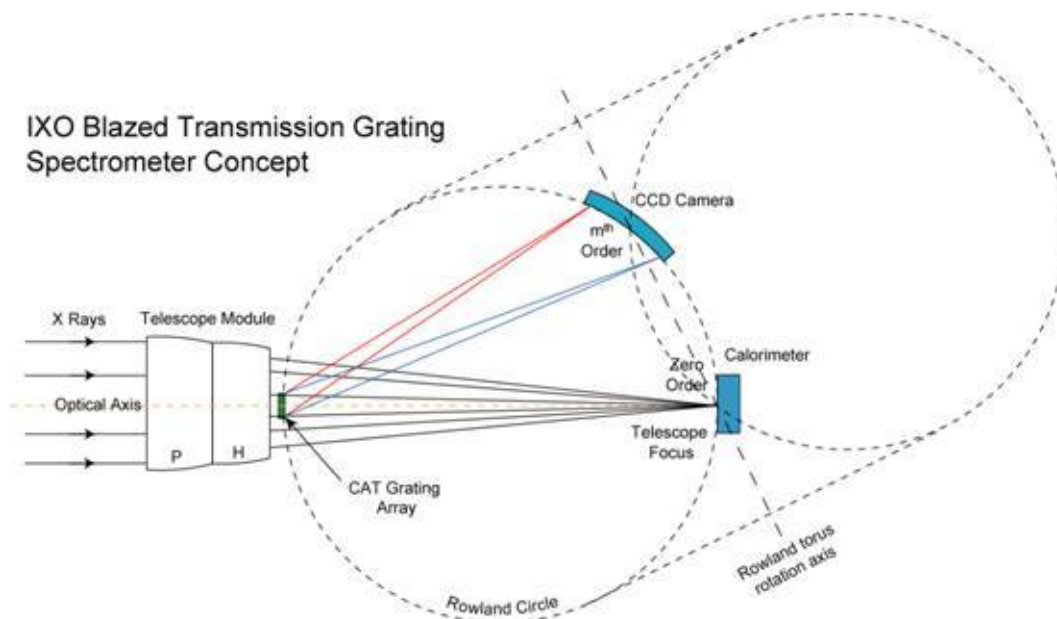


Figure 7-1 Side view of CAT-GS concept. The blue rays symbolize x rays of shorter wavelength than the red rays, but in the same diffraction order.

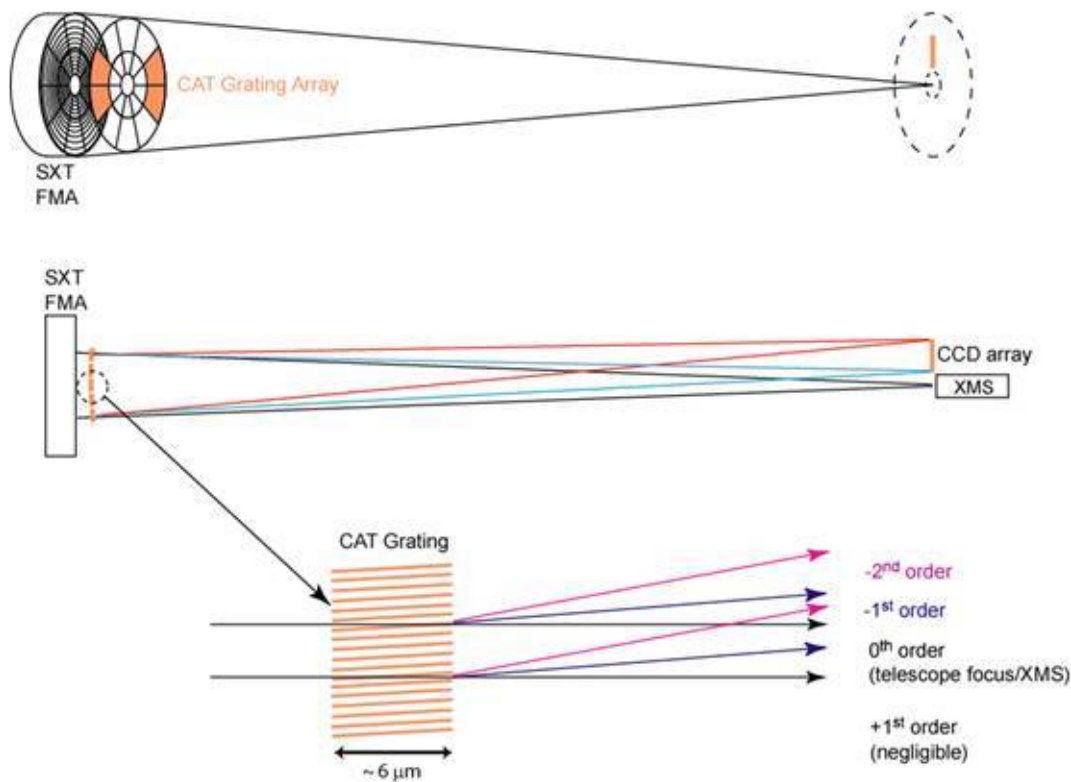


Figure 7-2 Schematics of CAT-GS. Top: Perspective view. Middle: Side view. Bottom view: Blow-up of CAT grating cross section.

The CAT-GS is based on the heritage of the optical design for the HETGS (High Energy Transmission Grating Spectrometer) and ACIS (AXAF CCD Imaging Spectrometer) instruments on Chandra. It has the following important features, many of which are significant improvements over Chandra:

Mass: Dispersion is achieved through transmission gratings close to normal incidence. These gratings only have to be a few micrometers thick, and are therefore light-weight. The mass of the grating array is dominated by the supporting structures that hold the membrane-like gratings in place.

Alignment tolerances: The transmission grating mount is extremely alignment insensitive, especially for diffraction orders that lie within a few degrees of the directly transmitted (0th order) beam. Alignment tolerances are therefore typically on the order of several to many arcminutes, despite the 5 arcsec telescope PSF.

Diffraction efficiency and effective area: The CAT gratings blaze very efficiently for wavelengths with a critical angle of total external reflection that is greater than the angle of incidence onto the grating bar sidewalls. The summed diffraction efficiency of all blazed orders for a given wavelength is on the order of 50% and therefore leads to high effective area.

Spectral resolution: Since the CAT gratings are blazed, shorter wavelengths contribute in higher diffraction orders and can therefore be detected with higher resolution. In addition, the CAT-GS takes advantage of the

anisotropic projected scattering from the grazing-incidence mirrors through sub-aperturing. This can easily improve resolution by a factor of 2-3 without placing a lot of demands on the telescope mirrors themselves.

Transparency and synergy with other instruments: Since the CAT gratings are so thin, they also become almost completely transparent at higher photon energies. This leads to the welcome effect that other focal plane instruments (such as the XMS) that have better energy resolution at higher energies lose very little effective area and can operate simultaneously with the CAT-GS, even if the gratings were to cover the whole mirror aperture.

Polarization and modelling: Silicon CAT gratings have negligible polarization sensitivity at soft x-ray wavelengths. Their diffraction behaviour is straight-forward to model, well understood, and agrees well with experimental results.

7.1.2 Instrument performance specifications

The performance requirements for the mission that are addressed by the CAT-GS are:

- Spectral resolution $E/\Delta E > 3000$ (FWHM).
- Effective area $> 1000 \text{ cm}^2$.

Both requirements apply to point sources in the energy band 0.3 – 1.0 keV. The CAT-GS will meet and exceed these requirements depending on fulfilment of the following other IXO key requirements:

- Mirror effective area $> 3 \text{ m}^2$ at 1.25 keV.
- Angular resolution < 5 arcsec (HPD) over the 0.3 – 10 keV range.

Furthermore, the effective area goal of $> 3000 \text{ cm}^2$ can easily be obtained by increasing the area of the grating arrays with minimal increase in mass (< 10 additional kg), without any changes to the camera, and without compromising the spectral resolution requirement.

7.1.3 Instrument configuration

The CAT-GS consists of two grating arrays just aft of the telescope mirrors, and a camera on the fixed instrument platform (FIP).

The grating arrays are passive devices that do not require any power. It is assumed that due to their proximity to the mirrors they will profit from the temperature control of the mirrors.

The camera consists of a linear array of CCDs and its housing (Camera Assembly), detector electronics and power supply (Detector Electronics Assembly - DEA), and the Digital Processing Assembly (DPA), containing the digital processor.

7.1.4 Instrument optical design – filters

We assume a 10 nm Al Optical Blocking Filter (OBF) directly deposited onto the CCDs. Technology development for such thin filters is still necessary. Since the level of straylight is unknown at this point, the filter thickness (and correspondingly the geometrical grating area) might need to be revisited.

7.1.5 Instrument units' mechanical design and dimensions

7.1.5.1 Grating arrays

The two grating arrays cover 30 deg. each in azimuth, and the radial range of 1.146 m to 1.591 m. This corresponds to covering a total of four mirror modules of the outer ring of modules in the NASA slumped-glass mirror (SGM) option. (For both the SGM option and the ESA silicon pore optics (SPO) option it seems advisable to match the grating coverage to the mirror module layout in order to minimize obscurations/shadowing and to maximize mechanical stiffness with minimal mass.)

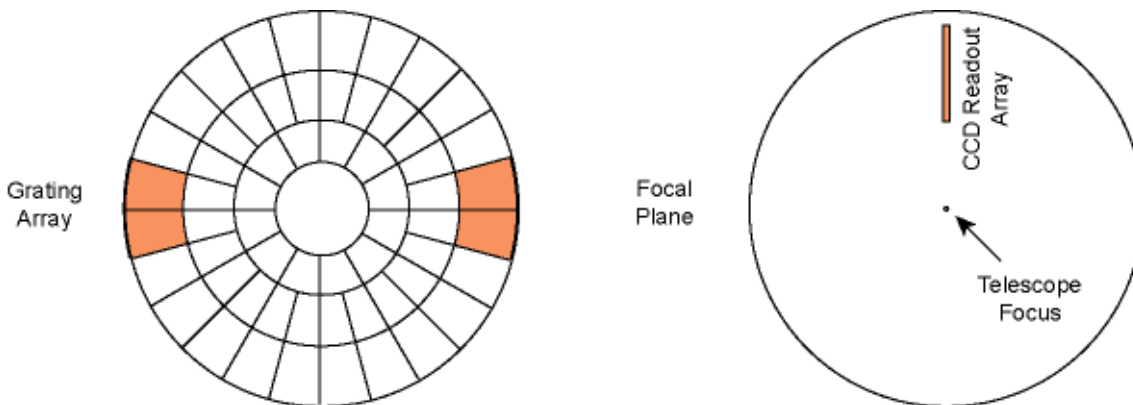


Figure 7-3 Schematic showing grating array coverage of the mirrors (left) and camera placement on the FIP.

With this coverage we expect effective areas of $\sim 1000 - 1,350 \text{ cm}^2$ in the $0.3 - 1.0 \text{ keV}$ band.

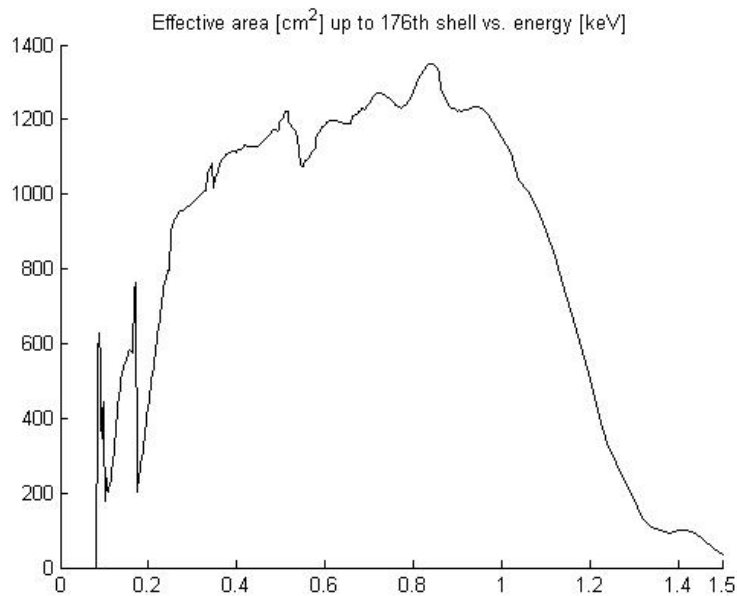


Figure 7-4 Theoretical effective area collected by the camera.

Our assumptions are based on a mirror model by Paul Reid (SAO) (file "1 sxt config_area data_ir_3.2mOD_20mFL_5amfov_2005 chandra const_73-175+187-302+320-460_mirror only_no

margin_gsfc_fma_m=732_020509.dat"), theoretical diffraction efficiencies of a 200 nm-period silicon CAT grating (duty cycle = 0.15, thickness = 6492 nm, 1 nm native oxide, 1.5 deg. incidence angle), and a 10 nm aluminum filter on a CCD camera with reasonable CCD efficiencies. We also assume a hierarchical set of support structures with three levels, each of which obscures 10% of the open area. (For calculations of the 0th order transmission the partial transparency of the finest support level should be taken into account). Preliminary analysis of x-ray data for existing CAT grating prototypes currently shows diffraction efficiencies in the range of 80-100% of theoretical values.

7.1.5.1.1 CAT gratings and Level I supports

The CAT gratings consist of high aspect-ratio silicon grating bars, suspended on their sides by integrated silicon support bars (Level I supports) that are monolithically etched out of the same silicon crystal. Our goal is for the Level I supports to cover no more than 10% of the geometric grating area A_g . The mass of Level I is given by

$$M_1 = A_g \times 6.11 \times 10^{-4} \text{ cm} \times (0.10 + 0.18) \times 2.33 \text{ g/cm}^3 = A_g \times 3.99 \times 10^{-4} \text{ g/cm}^2.$$

7.1.5.1.2 Level II supports

The Level II supports consist of a microfabricated honeycomb (or other TBD) structure of 0.5 mm thick silicon and covers no more than 10% of the geometric grating area. Its mass is

$$M_2 = A_g \times 0.05 \text{ cm} \times 0.10 \times 2.33 \text{ g/cm}^3 = A_g \times 0.0117 \text{ g/cm}^2.$$

7.1.5.1.3 Level III supports/grating facet frames

The Level III supports consist of a ~ 2 mm thick, ~ 2-5 cm pitch micromachined metal grid made of Invar or similar low-CTE (or Si-matched CTE) material. Its mass is given by

$$M_3 = A_g \times 0.2 \text{ cm} \times 0.1 \times 8.0 \text{ g/cm}^3 = A_g \times 0.160 \text{ g/cm}^2.$$

The Level III supports also serve as a frame for each individual grating facet that mounts to the grating array structure. We assume that each grating facet is ~ 5 cm x 5 cm in size and optimized in shape to minimize gaps in grating coverage.

7.1.5.1.4 Mass of grating facets

The mass of the grating facets is dominated by the Level III frames. The geometrical area that needs to be covered by grating facets is ~ 5400 cm². This can be achieved with ~ 215 facets of 25 cm² area each at a total mass of <1.1 kg, including mounting screws.

7.1.5.1.5 Grating array structure (GAS)

The grating array structure consists of two identical units. It holds the grating facets in place and connects to a rigid and stable spacecraft structure, such as structural components of the mirror assembly. The GAS is modelled after the HESS (HETG Element Support Structure) of the Chandra HETGS.

The main structure coincides with mirror module walls or supports. It consists of spokes (radial), main rings (azimuthal, $r = 1.143 \text{ m}, 1.594 \text{ m}$), and sub-rings (azimuthal, $r = 1.256, 1.368, 1.480$). The cross sections of spokes and rings are approximately rectangular (narrow in x,y, longer in z). Borrowing from the HESS we assume the following cross sections and total lengths:

Structure	cross section	length
Spokes (6):	2.4 cm ²	2.742 m
Main rings (2):	3.3 cm ²	2.866 m
Sub-rings (3):	1.14 cm ²	4.298 m

The volume of this structure is 2094 cm³. The mass of this structure depends on the material:

Aluminum:	5.66 kg (Chandra)
Beryllium:	3.87 kg
AlBeMet®162H:	4.40 kg

We consider these mass estimates to be conservative upper limits, since they are based on the HESS, which was never aggressively light-weighted. We believe that the above GAS *masses could easily be reduced by 20%* through smart engineering.

The grating facets are mounted to the GAS in a way that minimizes stress transfer between facets and GAS due to thermal expansion mismatch, etc. On Chandra this was successfully done via single-point mounts. Due to the relaxed alignment tolerances of transmission gratings this should also be sufficient for IXO.

7.1.5.2 Camera assembly

The Camera Assembly (CA) is mounted via an interface adapter to a focus mechanism, which in turn is connected to the Fixed Instrument Platform (FIP). The Camera Assembly holds the CCD array, which connects to the Detector Electronics Assembly (DEA) via harnesses between connector panels on the CA and DEA.

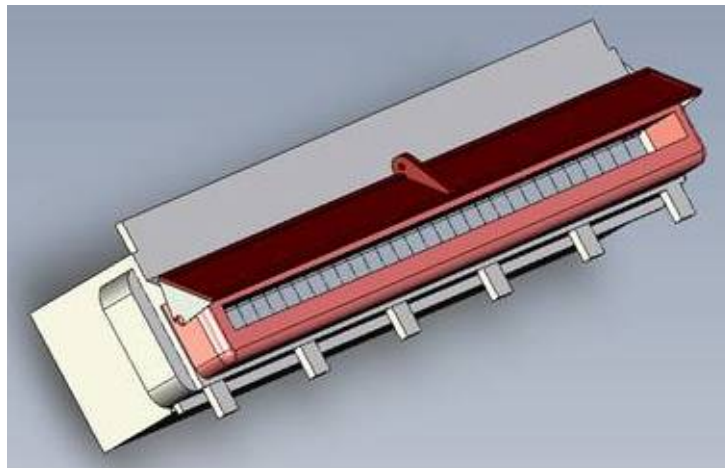


Figure 7-5 XGS Camera Assembly

7.1.5.3 Detector Electronics Assembly

See table in Section 7.2.5.

7.1.5.4 Digital Processing Assembly

See table in Section 7.2.5.

7.1.6 Mechanisms

7.1.6.1 Camera focusing mechanism

The diffracted beams transmitted by the gratings converge towards the spectral focus. The camera has to be positioned on the surface of the Rowland torus to within +/- 0.1 mm to achieve optimal spectral resolution. The width of a spectral line in the dispersion direction widens proportional to the cone angle of the marginal rays from the grating arrays in the dispersion (= x) direction. For example, if the camera is out of focus by 0.5 mm, an initial resolution of $R = 5000$ would degrade to 4500. Since the spacecraft probably can not maintain this tolerance through construction, launch, and years of operation in space, there needs to be a focusing mechanism that allows translation of the camera towards the center of the grating arrays. Its resolution should be no less than 0.1 mm. Its range is determined by the expected excursions of the focal plane from its nominal position relative to the telescope mirrors. We expect this focusing mechanism to form the interface between an interface adapter (which connects to the camera assembly) and the FIP.

7.1.6.2 Camera Assembly Protective Door

A two position (open/closed) protective cover will be an integral component of the CAT-GS Camera Assembly. Its primary purpose will be to protect the detector, during ground transportation and launch, due to any debris entering the camera opening and impacting the detectors. This door will be closed during launch and kept closed during the initial out gassing period once on orbit around L2. The inside of the door will (tbd) be equipped with an x-ray radioisotope source to allow for diagnostics both on the ground and prior to door opening on orbit. It is TBD if these door sources will be used as part of the in-orbit calibration. Once opened in orbit the door will be able to be closed again, but it is not anticipated that this will be a regular occurrence. The door will be able to be commanded open and closed by way of commands sent to the instrument via its standard command interface between the spacecraft and the Digital Processing Assembly (DPA). The door controller electronics will be housed in the CAT-GS Detector Electronics Assembly (DEA). This door will not be required to maintain a vacuum seal either during ground operations or during launch. The Camera Assembly will provide the necessary venting paths during both ground operations and launch ascent, but actively controlled vent valves are not anticipated.

7.1.7 Instrument units thermal design

7.1.7.1 Gratings and grating array structure

The individual grating facets are expected to be mounted to the GAS in a stress-free fashion that prevents deformation of the facets due to CTE mismatch between GAS and grating facets. The following requirements need to be met:

- Thermal motion of facets must stay within alignment requirements.
- Grating period must be maintained to within one part in 5×10^4 to prevent loss in resolution.

Assuming that thermal expansion of the grating facets is dominated by the CTE of silicon ($2.6 \times 10^{-6} /K$), the latter point requires temperature gradients $\Delta T < 7.7$ K across the grating arrays.

The first point is not expected to be a problem, but has not been investigated in detail.

It is expected that the GAS is thermally connected (conduction, radiation) to the telescope optics in a fashion that easily meets the above requirement on ΔT . Potential additional thermal loads on the thermal control of the optics due to the presence of the GAS are not considered here.

7.1.7.2 Camera thermal design

The CCD Focal Plane will be passively cooled to approximately -100 C via thermal straps connected to a radiator facing deep space that is mounted to the back of the Camera Assembly housing. It will then be warmed up to its nominal operating point of -90 C using trim heaters mounted to the focal plane paddle. It is intended to thermally isolate the focal plane from the camera housing and the Camera Assembly from the fixed platform to the extent practical. The power dissipated by the Camera Assembly is dominated by the trim heater on the focal plane, as the electronic power dissipated by the detectors is negligible. Focal plane temperature control, during science observations, will be actively controlled to -90 C +/- 0.3 C. Currently understood design assumptions are that the fixed platform the camera assembly housing is mounted to (via the spacecraft provided interface adapter and focus mechanism) will operate nominally at -100 C, and that there will be a sunshade that will eliminate direct views of the sun by the Camera Assembly radiator. The surface area of the back of the Camera Assembly is capable of dumping ~5 W (at -100 C) to space and will be designed as the camera radiator. The focal plane control electronics will reside in the Detector Electronics Assembly (DEA). Elevated temperature focal plane bake out modes for decontamination or radiation damage annealing are TBD.

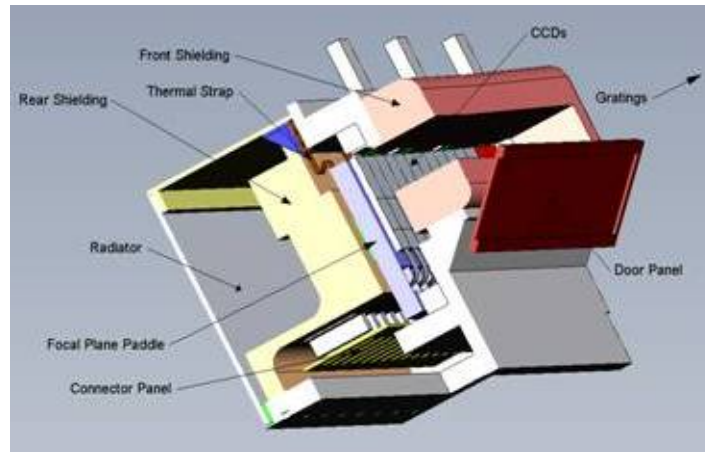


Figure 7-6 XGS Camera Assembly cross section.

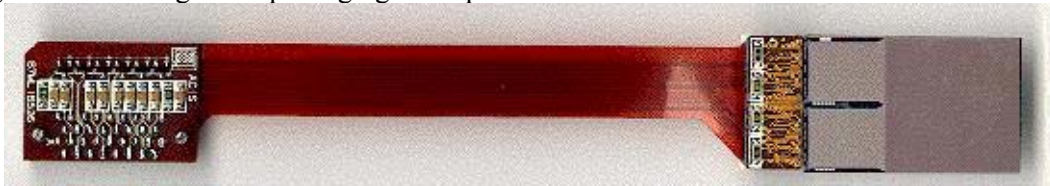
The door mechanism placement is TBD, The two likely places for it are either directly mounted to the Camera Assembly or mounted directly to the mirror facing side of the Fixed Instrument Platform. Trade studies for the door placement will take into account mechanical, thermal and calibration source considerations.

The two electronic boxes that go with the Camera Assembly will be mounted by the spacecraft in a fashion that keeps them within their survival limits while in a non-operating mode and within their operating limits while they are in one of their operating modes. There is no active thermal control of the instrument's electronic boxes by the instrument itself. Final surface treatments and MLI requirements are TBD and will be determined by the thermal design analysis done at spacecraft level. While the detailed design of the electronics is done, it is anticipated that standard mil-spec type parts will be used and that an operating temperature range of -35 C to +35 C (as an example) electronic box to spacecraft interface will be specified.

7.1.8 Electrical design

The CAT-GS detector system is broken down logically and physically into three separate assemblies that will be interconnected by electrical harnesses.

The first assembly is called the *Camera Assembly* and it houses a cooled focal plane made up of 32 CCID41 back illuminated framestore style CCDs. The CCDs are mounted in a 1x32 configuration that approximates the Rowland circle defined by the CAT grating assemblies. This assembly will have minimum electronics associated with it, as it will contain just the detectors, a JFET on each of the four outputs of each CCD, some discrete ESD protection components and a flexprint to the camera assembly bulkhead. The following illustrates the general packaging concept for the individual detectors.



This particular device is mounted in its front illuminated configuration as it is easier to show the imaging area and the smaller framestore area of the device. The silicon CCD detector and one end of the flexprint are mounted to a ceramic substrate and interconnected with bond wires. The other end of the flexprint has the connector, which will mount to the bulkhead of the camera assembly. Given the results of spacecraft level stray light analysis, any necessary optical blocking filter will be applied directly to the back illuminated surface of the CCD.

The CCID41 consists of an imaging area and two separate framestore areas. The two framestore areas each have a split bidirectional serial shift register allowing for the simultaneous operation of four output nodes. The CCID41 is equipped with a charge injection register that is used to help mitigate the detrimental effects of the dominant type of radiation damage expected to occur over the course of the mission.

The configuration of this detector, along with the design of its control electronics, allows for the 24x24um pixels in the imaging area to be summed on chip in the shift register and output node to create “super-pixels” that are multiples of 24 um. An example frame readout rate, for a 1x8 pixel summing mode, using all four output nodes operating at 500Khz, would be each detector generating a 1024Cx128R pixel image frame every 68 ms (14.7Hz for frame readout).

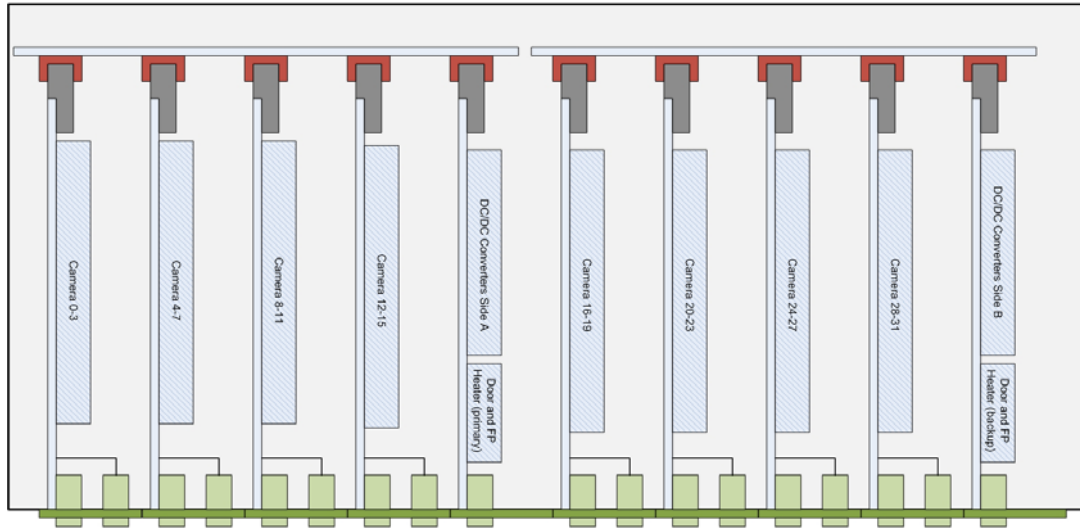
On the focal plane paddle, the CCDs will be mounted using the same design and procedures developed for the Chandra ACIS program. In addition to the CCDs, there will be several RTDs and heater elements used for thermal control of the focal plane.

Mounted to the camera assembly (tbd) will be a door mechanism and several position sensors. The door open/close function will be actuated by a (tbd) mechanism.

The CCDs will be designed and fabricated at the MIT Lincoln Laboratory (MIT-LL), while MIT Kavli Institute for Astrophysics and Space Research (MKI) will be responsible for the camera housing design, fabrication as well as the individual detector level calibration.

The second assembly will be the *Detector Electronics Assembly* (DEA), whose primary purpose will be to provide all the control signals to the CCDs in the Camera Assembly and to digitize the video output from those CCDs. There will be command channels from the Digital Processing Assembly (DPA) to the DEA in order to set the DEA’s clock sequencer memory, command registers and bias levels. There will also be data channels from the DEA to the DPA to send digitized video data and miscellaneous housekeeping data. Additionally, the DEA will provide all the necessary secondary regulated voltages and the control circuitry for the focal plane thermal control and the door mechanism. The packaging design will be based on a ruggedized cPCI format. The DEA will be designed and fabricated at the MKI.

IXO-XGS Strawman DEA Layout (Top View)
 Rev02 2/11/09



Assumes basic cPCI packaging

Figure 7-7: Detector Electronics Assembly

The final electronics assembly is the *Digital Processing Assembly* (DPA). This unit will do all of the data processing on image frames, generated from the DEA, to accomplish the x-ray event extraction algorithms. This includes such things as bias correction, event neighbourhood extraction, bad pixel filtering, etc. This unit will be the command and data interface to the spacecraft via a Spacewire based electrical interface. It is anticipated that the DPA processing modules will be selected from a vendor that offers space qualified single board computer based systems, as the use of standardized interfaces is envisioned. Examples of such potential vendors are MDA, SEAKR, Space Micro, GSFC Space Cube, etc. Flight software development and verification for the DPA will be the responsibility of MKI.

The following block diagram provides a general overview of the CAT-GS detector system.

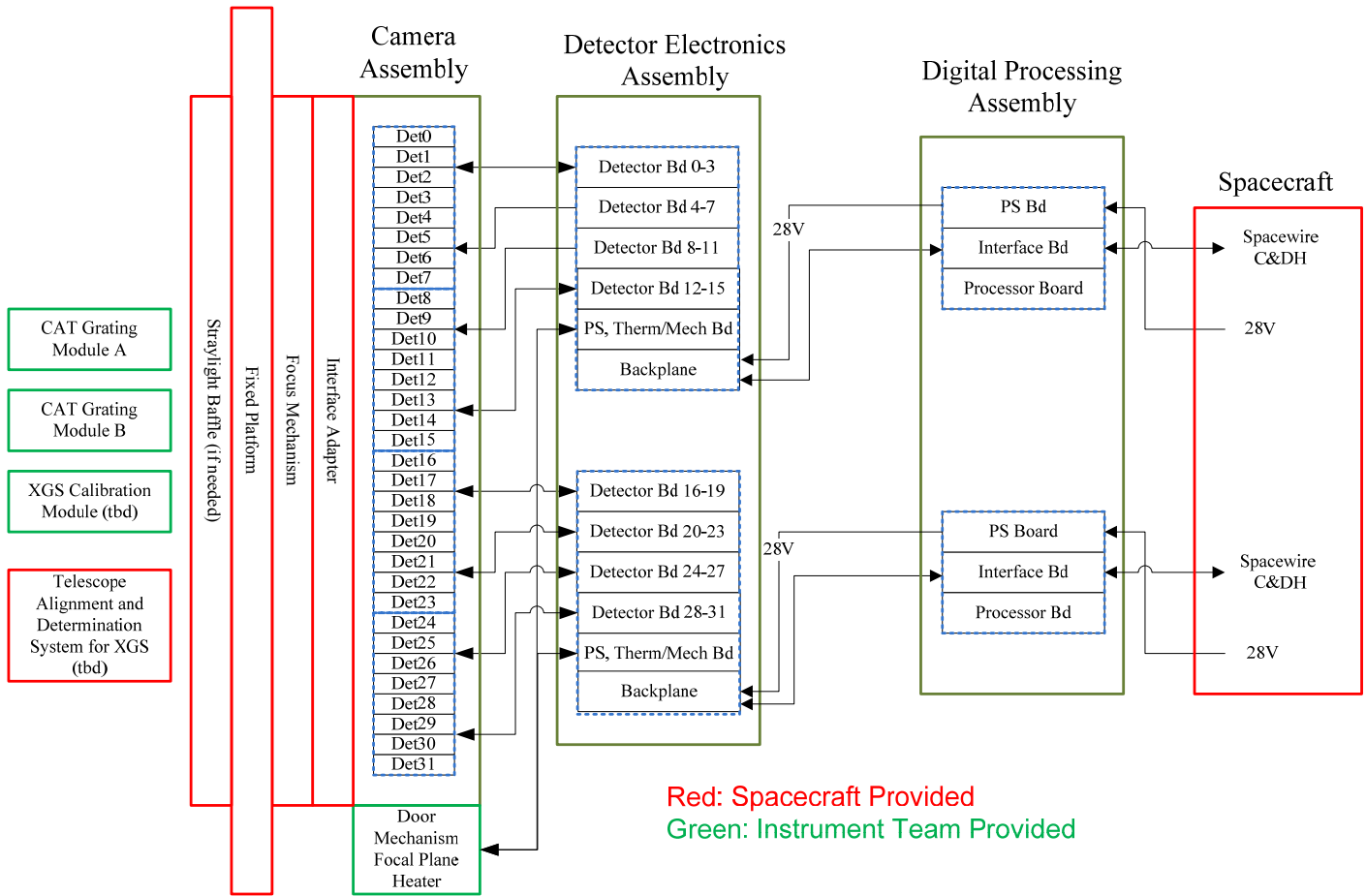


Figure 7-8 XGS Block Diagram

7.1.9 On-board software

The CAT-GS onboard software performs the following functions:

- S/C Interface Functions
 - Receipt of commands and configuration data from the s/c
 - Formatting & transmission of science & HK data to s/c
- CCD configuration & readout control:
 - CCD bias and clock level configuration
 - CCD readout sequence configuration & control. Readout modes include:
 - **Timed exposure** readout mode, in which each CCD is exposed for commanded period and then read out. The readout operation consists of a rapid transfer of the image from the CCD image area to its framestore area, followed by readout of the framestore. This is the nominal mode for most science observations. This mode supports on-chip binning and commandable exposure time. It is expected that for most observations, each 1024 row by 1026 column CCD will be binned into 8-row by 4 column sums before readout. The minimum exposure time in this mode will be 19 ms (TBR).
 - **Windowed** readout mode digitizes out only a subset of CCD rows in each frame. This allows proportionately shorter frame times than can be achieved in timed exposure mode.
 - **Continuous** readout mode provides the shortest effective exposure time. In this mode the CCD imaging-area and framestore-area parallel drivers are clocked simultaneously once per row readout. In this mode the effective exposure time is determined by the time required for a CCD charge packet to traverse the dispersed spectrum in the cross-dispersion direction. In this mode the nominal exposure time is approximately 64 times shorter than in timed exposure mode.
- Onboard data system configuration & data processing
 - Data processing mode control
 - Data processing/extraction. Major data processing modes include:
 - **Bias determination** In this mode a ‘bias’ or zero-signal level is computed and stored for every pixel present in a given readout mode. The bias determination algorithm processes multiple readouts to find and remove signal produced by charged particles and photons incident on the detector, and to reduce the effects of readout noise on the bias computation. Following Chandra/ACIS practice, bias may be determined before the start of each observation. Bias frames may optionally be telemetered to the ground.
 - **Event extraction** This is the processing mode used for ordinary science observations. Bias-corrected CCD data are compared with a threshold to identify candidate X-ray events. Neighborhoods around candidate events are extracted and tested against various programmable selection criteria (local maximum, amplitude, and ‘grade’ or ‘pattern’. Acceptable candidates are formatted for telemetry. Rejected candidates are counted.
 - **Raw mode.** In this mode CCD output is packaged for telemetry to the ground without processing. This is intended as a diagnostic mode.
 - Data compression algorithms may optionally be applied to the output of the various data processing modes. The compression is lossless and is intended for transmission of bias maps and raw-mode data.
- Mechanism control (door, cal. Source.) (TBD: Are these software functions?)

- Housekeeping (HK) configuration. Functions include:
 - CCD temperature control
 - Bakeout
- HK data configuration and collection

7.1.10 Ground support equipment

7.1.10.1 Electrical ground support equipment

TBD

7.1.10.2 Mechanical and optical ground support equipment

TBD

7.1.11 Instrument mode description

7.1.11.1 Operating modes

Two operating modes are anticipated for the instrument:

- Timed Exposure Mode (TE)
- Continuous Clocking Mode (CC)

-Operation modes apply for all 32 (1024x1026 exposed pixels) devices simultaneously. Events are recognized by a set of 255 flight grades.

-The TE mode collects data for a pre-selected frame time (68 ms -- 10 s [TBC]). After this integration time, charge is transferred to the frame store region within ~[TBD] ms. A nominal full frame time is set to 3.2 s [TBC]. This mode allows a 3x3 pixel event recognition (faint mode, F), a 5x5 pixel event recognition (very faint mode, VF).

-In TE mode all 32 devices can be operated simultaneously with sub-arrays (see *windowed mode* in 7.1.9), where only a selected continuous number of rows are registered. The minimum sub-array for all devices is 128 rows, the maximum some number between 128 and 1024 with flexible choice of start row.

-The CC mode continuously clocks data through each CCD (2.87 ms/row [TBC]) and its frame-store. The instrument accumulates data into a buffer until a virtual detector of size 512 rows and 1024 columns is filled. A baseline 3x3 event algorithm (F) is applied to this mode.

The onboard software also allows TE and CC mode to be operated in graded (G) mode where (F) events can be pre-graded into a smaller set of standard grades [TBD] (see also 7.1.9).

While not subjected to an external radiation source - which can either be a calibration source or an X-ray target - all 32 devices will frequently generate bias maps. Bias maps contain the amplitude of the charge in each pixel in the absence of external X-rays and determine the internal instrument background.

7.1.11.2 Non-operating modes

In order to achieve optimal performance from the readout system, there are two conditions that are required. The first is that the focal plane array is being controlled to its nominal temperature operating point. The second is that the CCDs have been clocking in whatever operating mode they will be using for the upcoming observation for a given number of minutes. Aside from staying within its survival temperature limits, there are no aspects of the instrument that need continuous operation to meet its mission requirements.

- **Standby Mode** will be defined as the mode where the focal plane temperature is maintained at its' operating point, the instrument commands can be processed and housekeeping data can be acquired (essentially it will be everything operating except the acquisition and transfer of science data from the Camera Assembly).
- **Off Mode** will be defined as a full power off for the instrument. The instrument will be kept inside its survival limits by the spacecraft (typically by controlling survival heaters mounted to or near the instrument assemblies). The spacecraft will also monitor the temperature of the instrument assemblies during this period.

There is a mode that is TBD at the moment, as it is not clear it would be necessary (or used). For now we shall refer to it as **Decontamination Mode**. It involves elevating the temperature of the focal plane high enough to drive off contamination that has accumulated on the imaging area surface of the CCD.

7.2 Mechanical Interfaces and Requirements

7.2.1 Location requirements

7.2.1.1 Grating arrays

There are two identical grating arrays. Each array is bounded by an inner arc (radius ~ 1.146 m) and an outer arc (radius ~ 1.591 m), and two radial spokes 30 degrees apart (see Figure 7-3). The arrays are arranged just aft of the telescope optics in mirror-symmetric fashion, with the mirror plane defined by the dispersion axis (camera center line) and the telescope optical axis (z-axis). For simplicity we assume that the dispersion direction coincides with the telescope x-axis. However, the whole GAS/camera design can be rotated around the z-axis if this is deemed advantageous for other reasons (placement relative to sun shade, etc.). The GAS conforms to a Rowland torus as shown in Figure 7-1. (Details of the Rowland torus are TBD. Figure 7-1 shows one possible implementation.) The GAS should be as close to the optics as reasonably possible for maximum dispersion and minimal mass. We envision the GAS to be rigidly attached to mirror supporting structures.

7.2.1.2 Camera location

The camera is mounted to a focusing mechanism that connects to the FIP. It holds a linear array of 32 CCDs. The individual CCDs follow the surface of a Rowland torus that also intersects the telescope focus and the grating facets. The CCD array is oriented in a radial direction from focus, with the center of det0 ~ 725 mm from focus and the center of det31 $\sim 1,475$ mm from focus.

7.2.2 Alignment requirements

Due to the limited azimuthal coverage of the telescope mirrors with CAT gratings, sub-aperturing effects are expected to boost the resolution from $R \sim 2100$ (no sub-aperturing) to $R > 4500$. The alignment requirements for the whole grating array given below are derived under the assumption that $R = 5000$ (resolution element ~ 210 micron FWHM), and that each tolerance can independently broaden the resolution element by 10%, leading to a resolution of 4500, which still exceeds the goal of 3000 by far.

If we consider the alignment tolerances of an individual facet within the GAS and assume that misalignments between facets contribute independently, we see that the same tolerances apply to individual facets.

Alignment tolerances for gratings relative to ideal position/orientation:

Translation along optical axis:	$\Delta z < 0.394$ mm (relative to mirror node)
Translation along x:	insensitive*
Translation along y:	insensitive*
Grating roll (rot. around z axis):	< 14.3 arcmin (limited by $\frac{1}{4}$ of CCD width (det31))
Grating pitch (rot. around y axis):	< 6 arcmin at far end of camera < 20 arcmin on blaze
Grating yaw (rot. around x axis):	insensitive*

* "Insensitive" neglects the fact that translations and rotations also remove gratings from the Rowland torus. Translation along x and y also introduce deviations from the ideal z-position and roll, pitch, and yaw angles. However, these are higher order effects. Rotations will also contribute to Δz in proportion to the length of the lever arm. For 5 cm grating facets this would lead to a yaw requirement of less than 54 arcmin rotation around the facet center.

7.2.3 Pointing requirements and performance goals

Acquisition $\pm 1/8$ CCD = ± 30 arcsec radial

Knowledge < 0.2 arcsec (relative to zeroth order)

Pointing stability < 0.2 arcsec/68ms (absolute)

Pointing control $\pm 1/8$ CCD = ± 30 arcsec radial/day

We do not know how well the mirrors can be aimed at or aligned with respect to the instrument platform via an extendable boom. If it is not guaranteed that the spectrum falls within $\pm 1/8$ CCD within the center of the camera CCDs in the cross-dispersion direction, then a y-translation stage might be necessary to center the camera on the spectrum.

Wavelength calibration:

Knowledge of the the zeroth order position is important for determination of the absolute wavelength scale. For our baseline configuration using a Lorentzian form for the grating LSF, we estimate that a line sampled with 4 bins per FWHM and 10 counts peak can be centroided to $0.1 \times$ FWHM (and less in proportion to $1/\sqrt{\text{max counts}}$), a desirable target for the dispersed line centroid. The calorimeter sampling is less (~ 3 pixels per resolution element), but is adequate for counting statistics to dominate the centroid error. Thus, any grating observation will easily have sufficient counts to centroid the zeroth order to the same level as the line, yielding a wavelength accuracy on the order of 0.2 times the grating FWHM. However, to maintain an

absolute wavelength scale in order to conduct accurate velocity measurements, there needs to be length reference between the calorimeter/other detectors at focus and the readout camera with a precision of better than about 0.1 times the grating FWHM. For the required resolution of 3000 this is 0.035 mm. Thus we require knowledge of the distance between 0th order center (at telescope focus) and spectral line center (on camera readout array) to about 35 microns.

(Relevant plate scale:

1/10th of resolution element: for R=3000 this is 0.1 x 350 micron = 35 micron
 for R=5000 this is 0.1 x 210 micron = 21 micron ~ 0.2 arcsec.)

7.2.4 Interface control drawing

(can be part of 7.1.5 at this stage)

7.2.5 Instrument mass

Unit	Dimension (cm) H x W x D	Mass (kg)	Mass inc. 20% margin (kg)	Location
CAT Grating Module A	6 × 50 × 82	2.31	2.77	FMA
CAT Grating Module B	6 × 50 × 82	2.31	2.77	FMA
Camera Assembly (CA)	23 × 89.2 × 17.8	28.0	33.6	Fixed Platform
Detector Electronics Assembly (DEA)	15 × 41 × 20	6.0	7.2	<1m from Camera Assembly
Digital Processing Assembly (DPA)	11 × 15 × 11	2.5	3.0	<4m from Detector Electronics Assembly
		41.12	49.3	
<i>Other CATGS related not included here</i>				
Camera Interface Adapter		TBD	TBD	
Focus Mechanism		TBD	TBD	
Stray Light Baffle		TBD	TBD	
CATGS Calibration Module		TBD	TBD	
Telescope Alignment and Determination System for CATGS		TBD	TBD	
Assembly Interconnect Harnesses		TBD	TBD	

Table 7-1 Mass Properties for the individual units

7.3 Thermal Interfaces and Requirements

7.3.1 Temperature limit in space environment

7.3.1.1 Gratings and grating array structure

We do not anticipate that temperature limits for gratings and grating arrays would be drivers for other parts of the observatory. However, detailed studies of potential failure modes or irreversible misalignments due to extreme temperature excursions have not been performed to date.

7.3.1.2 Camera focal plane

Focal plane temperature will be controlled to -90 ± 0.3 C.

7.3.2 Temperature limits in laboratory environment

7.3.2.1 Gratings and grating array structure

Gratings and GAS should be kept at standard laboratory/room temperature. Large and/or fast temperature fluctuations should be avoided. Condensation development on the gratings must be avoided.

7.3.2.2 Readout system

The allowable temperature limits for the CAT-GS readout system in the laboratory are the same as in space. When the unit is operating at a temperature below the dew point, it must be in either a dry nitrogen or vacuum environment to prevent condensation from developing on the instrument.

7.3.3 Temperature sensors

TBD

7.3.4 Heaters

TBD

7.3.5 Thermal schematics

TBD

7.3.6 Thermal control requirements

See Section 7.1.7.

The Detector Electronics Assembly (DEA) and the Digital Processing Assembly (DPA) will utilize Mil Spec components and packaging that could reasonably be expected to support derated non-operating survival limits of -30 C to $+55$ C.

The Camera Assembly, which is expected to operate colder than standard spacecraft electronics assemblies such as the DEA and DPA, is expected to have derated non-operating survival limits of -120 C to $+70$ C.

7.4 Electrical Interfaces and Requirements

7.4.1 Electrical resources requirement summary

RF

7.4.2 Instrument power distribution block diagram

7.4.3 Power budget

The CAT-GS Detector System will be provided nominal 28VDC +/-TBD bus power from the spacecraft. Power converters in the DEA and DPA will generate the necessary secondary voltages needed for the operation of the system. These regulated/filtered voltages are TBD, but are typically 3.3V, 5V, 12V, -12V and 24V. The instrument design will contain current limiting provisions at the board level to prevent a failure on a single board from propagating to the rest of the instrument.

Table 7-2: Power requirements

Element	Average (W)	Peak (W)	Bakeout (W)	Standby (W)	Safe Hold (W)
CAT Grating Module A	0	0	0	0	0
CAT Grating Module B	0	0	0	0	0
Camera Assembly (CA)	5 (note 1)	tbd	tbd	tbd	0 (note 2)
Detector Electronics Assembly	50	tbd	tbd	tbd	0 (note 2)
Digital Processing Assembly	41	tbd	tbd	tbd	0 (note 2)
Total w/o margin	96	tbd	tbd	tbd	0
Total inc 20% margin	115.2	tbd	tbd	tbd	0
<i>Other CATGS related not included here</i>					
Camera Interface Adapter	0	0	0	0	0
Focus Mechanism		tbd			
Stray Light Baffle					
XGS Calibration Module					
Telescope Alignment and Determination System for CATGS					
Assembly Interconnect Harness					

Note 1: Dissipated by the trim heaters in the Camera Assembly from power provided by the DEA

Note 2: Assumes survival heaters powered by spacecraft to keep units in survival range, if necessary,

7.4.4 Instrument modes' duration

Unlike the other instruments the CAT-GS is always at its focus. Therefore we expect continuous science operations.

7.4.5 Telecommands

TBD

7.4.6 Telemetry

We expect a peak data rate of 1.5MB/s of science data. This accommodates a 10 Crab source. Typical observations will require ~ 10 kB/s.

7.4.6.1 Telemetry requirements

Transmission of all relevant detection data for the highest rate X-ray sources results in the following data rate estimate. Assuming a maximum source intensity of 10 Crab, the count rate expected will be $\sim 70,000$ count/s. (A quick estimate can be obtained by noting that you get 10 ph/cm²/s/keV at 1 keV from the Crab. The spectrum goes as E^{-2} in ph/keV units, which is flat in ph/Å units but there's a factor of 1/12.4 conversion. At 10 Crab, you get 8 ph/cm²/s/Å into a band-pass of about 20 Å [10-30 Å, for an NH of 10²¹], multiply by 50% for the transmission of the ISM, gives about 8×10^4 events/s.) For the full, un-processed data, we estimated 320 bits per event (5×5 PHAs at 12 bits each + 20 bits for other) or 40 Bytes per event. So, the max data rate is actually about 2.8 MB/s. This assumes no binning either on the sensor, or in the backend electronics.

If we now assume binning into 2 'super-pixels' (each 1×8 pixels) in cross-dispersion direction and 3 in the dispersion direction, we only need 6 PHAs instead of 25, a reduction by a factor ~ 3.5 to 800kB/s.

The exposure is likely to be only long enough to obtain 1×10^5 cnt/pixel (to allow for 0.3% statistics), which would take about 100 ks. The maximum storage estimate is about 80 GB. Other targets would be 100× fainter, for "typical" data rates of 8 kB/s. Note that when operated while pointing at a typical XMS target, however, the data rate is likely to be even lower

In practice, the use of the instrument will ensure that the maximum sustained data rate will be kept below 750 kbits/s. This will be achieved for otherwise high-rate sources by using on-board data selection, processing and compression options to retain the key science data of the observation while staying within the data rate limit.

7.4.6.2 Telemetry description

7.4.6.2.1 Housekeeping telemetry

TBD

7.4.6.2.2 Science telemetry

TBD

7.4.7 Electrical interfaces

The data electrical interface to the spacecraft will be pair of bi-directional Spacewire connections to the spacecraft command and data handling (C&DH) subsystem. The instrument will do real time x-ray event extraction and deliver the event data to the C&DH system as soon as it is processed. The Spacecraft will provide the necessary onboard storage to buffer the event data for downlink. In addition to primary science data, there will be secondary science data and engineering housekeeping delivered to the spacecraft for downlink. Commands to the instrument, either as uplinked from the ground or issued by the spacecraft onboard computer will be delivered to the instrument via this interface.

The other electrical interface, from the spacecraft to the CAT-GS detector system, will be unregulated bus power (nominally 28V). The CAT-GS detector system will generate its own internally used regulated voltages from this bus power and provide the necessary EMI filtering to limit conducted emissions back on the bus.

It is likely that the spacecraft may want to mount their own thermal sensors and survival heaters on several, if not all three of the CAT-GS detector system assemblies. Accommodations for such elements are anticipated and not considered to impact the current design concepts.

7.5 Electromagnetic Compatibility and Electrostatic Discharge Interface

7.5.1 Susceptibility requirements

The CAT-GS detector system electronics (DEA and DPA) do not anticipate having any specific issues associated with complying with standard Mil-Std 461 emissions and susceptibility requirements. Standard spaceflight design and fabrication practices will be used to assure compliance. Any significant mission specific changes to standard levels will of course need to be reviewed.

The Camera Assembly does however contain a large opening exposing the focal plane during operation to the optical bench cavity. Unlike previous missions, such as Chandra and Suzaku, the optical blocking filter will be directly deposited on the CCD (as opposed to be mounted on a frame connected to the camera housing). EMI implications of the direct opening into the cavity containing the CCDs will need to be reviewed.

The CCDs used in the Camera Assembly are extremely static sensitive and appropriate precautions will need to be taken during assembly and handling. Once assembled and connected to their electronics, precautions against such things as rapid venting when inside a vacuum chamber needs to be observed. Once on orbit around L2, issues associated with spacecraft charging are not envisioned to be an issue.

7.6 Optical Requirements

7.6.1 Stray-light requirements

The CAT gratings will diffract out-of-band (FUV through NIR) radiation from celestial sources away from the detector. Scattered out-of-band light from the Sun or from bright celestial sources may produce unwanted background in the CAT-GS detectors. Noise (or temporal variation) in this background could compromise the spectral resolution and therefore the order-sorting capability of the CAT-GS detectors.

Stray-light induced background should be limited to less than 5 photo-electrons per ‘super-pixel’ (a 1×8 pixel summed on chip, assuming 24μm pixels) per read (68ms integration time), which implies that the maximum tolerable flux of out-of-band photons is $\Phi_{\text{stray}} < 1.6 \times 10^6 \text{ ph-s}^{-1}\text{-cm}^{-2} / T_{\text{obf}}$, where T_{obf} is the transmission of the optical blocking filter on the CAT-GS CCDs. With $T_{\text{obf}} = 1$, the requirement is:

$$\Phi_{\text{stray}} < 1.6 \times 10^6 \text{ ph- s}^{-1}\text{-cm}^{-2}.$$

7.6.2 Charged particle requirements

TBD

7.7 Transportation, Handling, Cleanliness and Purgings Requirements

7.7.1 Transportation requirements

The CAT grating sectors, bagged in contamination free bags (nylon/poly) and secured in their shipping containers will be ground transported in an air ride van, or equivalent.

Each reusable container will have a gross weight of order 90 kg and size of order 1.25 m × 1.00 m × 0.5 m. Ambient temperature will be within -18 to +40 C, monitored by direct measurement. Vibration, shocks, etc. will be limited to 9.5 g, monitored by direct measurement. There is no constraint on the air pressure, although monitoring by direct measurement is suggested.

7.7.2 Handling requirements

While in their shipping containers there are no special handling requirements beyond those given in 7.7.1 Transportation requirements.

There should be no contact with the thin grating membranes of the CAT grating sectors. Detailed procedures and GSE will be provided for the removal of the flight CAT grating sectors from their shipping containers and their installation into the observatory in close proximity to the telescope optics.

7.7.3 Cleanliness requirements

Contamination of the CAT grating sectors will not exceed "level 350A"(*) as monitored by accompanying witness samples. Relative humidity will not exceed 50% as monitored with a dessicant indicator. Cleanliness of the focal plane surface is TBD, and will set to meet the low energy quantum efficiency requirements of the Camera Assembly.

(*) MIL-STD-1246: the "350" sets specific particulate count/size limits and the level "A" requires NVR below 108 Å total.

7.7.4 Purgings requirements

Purgings may be required for the CAT grating sectors to maintain the requirements listed in Section 7.7.3.

The Camera Assembly will be fitted with a port to allow for purging with lab grade dry nitrogen during ground operation. This purge will facilitate minimizing contamination of the detectors and corrosion of the bond wires. The Detector Electronics Assembly and Digital Processing Assembly will contain conformal coated circuit boards and will not require purging.

7.8 Ground and Flight Operation Requirements

7.8.1 Ground and pre-flight operation

Operating modes on ground and pre-flight are generally identical to in-flight operations [TBC] (see 7.8.2). Operations and data processing include all items described in 7.1.9 and 7.1.11.

7.8.2 Flight operations

All 32 devices are either operated in TE (VF, F, G) or CC (F, G) mode (see Sect. 7.1.11.1).

The instrument remains operative all the time using the two operating modes described in Sect. 7.1.11. Data processing as described in Sect. 7.1.9 is always available. All devices will frequently generate bias maps during slew operations or other off-target positions.

External calibration source (ECS) exposure [TBD]: in case a movable external calibration source is provided, all 32 devices may always be able to operate in TE or CC mode once exposed to the ECS.

7.8.3 Contamination Requirements

In order to meet EOL quantum efficiency requirements, a maximum NVR deposition rate of TBD angstroms/year, at the surface of the focal plane, will be required. This NVR accumulation is expected to result from spacecraft and payload outgassing during the course of the mission. Decontamination bakeouts, as part of the on orbit contamination mitigation strategy, are TBR.

7.9 Deliverable Models and Ground Support Equipment

7.9.1 Structural Thermal Model

7.9.2 Engineering Qualification Model

7.9.3 Flight model

7.9.4 Flight spare model

7.10 Other requirements

There needs to be a significant discussion on contamination control at the observatory level. Contamination has the potential to reduce the effective area below requirements.

8 OFF-PLANE X-RAY GRATING SPECTROMETER (OP-XGS)

8.1 Instrument Description

8.1.1 Introduction

The purpose of the OP-XGS is to provide high spectral resolution, $\lambda/\Delta\lambda > 3000$, at low energies, 0.3-1.0 keV as a complement to the X-ray Microcalorimeter System. The spectrometer consists of an array of reflection gratings in the off-plane mount that diffracts light onto an array of dedicated CCDs. Light intersects the surface of the grating at grazing incidence, 2.7° , and nearly parallel to the groove direction. This maximizes the illumination efficiency on the gratings. Furthermore, the groove profile can be blazed to preferentially diffract light to only one side of zero order thus increasing the efficiency further. The blaze angle is chosen to maximize efficiency around 35 \AA in first order (1 keV efficiency peaks in 3rd order) and is set to 12° . The off-plane geometry leads to diffraction along an arc at the focal plane. A summary of the generic off-plane geometry is shown in Figure 8-1.

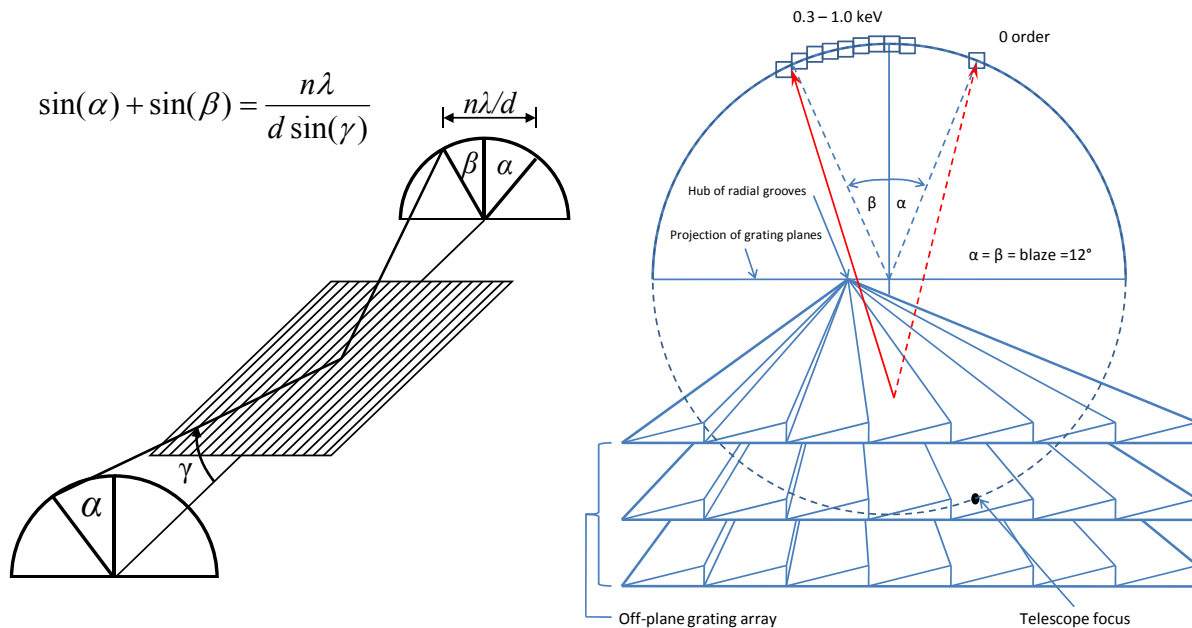


Figure 8-1: On the left an incoming ray of light intersects a grating in the off-plane mount with an azimuthal angle of α and graze angle of γ . Light is diffracted to an angle of β , dependent on wavelength and according to the grating equation. The diagram to the right shows the arc of diffraction at the focal plane and depicts several off-plane gratings placed in an array in order to collect light from some fraction of a telescope beam.

The viewing orientation for the diagram on the right is normal to the focal plane. Therefore, we are looking approximately down the optical axis. In this orientation the gratings are extending from the focal plane toward the observer. In reality, the gratings will not extend from their position in the spacecraft all the way to the focal plane, but this situation is shown here for illustrative purposes. The red lines show two possible

paths for a ray of light intersected by a grating. If the light was allowed to continue unimpeded by gratings, then it would propagate to the telescope focus which happens to lie in the grating focal plane along the circle defined by the arc of diffraction. The dashed red line shows specular reflection into zero order, which lies vertically displaced from the telescope focus, while the solid red line depicts a diffracted beam on one side of zero order.

This diagram illustrates several of the key concepts that will be utilized for IXO. First, given the shallow graze angle necessary for efficient reflection of X-rays, several gratings will need to be placed into an array to capture the appropriate section of the telescope beam and ultimately achieve the required effective area. A small, representative section is shown in the figure. Second, this figure demonstrates the concept of blazing the grating grooves to maximize efficiency in only plus or minus orders. Third, the grating grooves will also exhibit a radial profile as opposed to typical parallel grooves. In order to maintain a constant graze angle over the array, the gratings are fanned such that the radial grooves of all gratings converge to a point on the focal plane denoted as the hub. This radial profile will match the convergence of the telescope beam which will maintain a consistent α over the array, thus nullifying any aberrations caused by the gratings. Therefore, the spectral resolution obtained by the gratings will be limited by the quality of the telescope. Spectral lines will be approximately Gaussian with a FWHM equal to the HPD of the telescope PSF. However, the effective telescope PSF can be minimized by only sampling a fraction of the beam. Limiting the azimuthal coverage of the grating array, or in other words subaperturing, will decrease the FWHM of the spectral lines thus increasing spectral resolution.

The high illumination efficiency combined with the use of a blazed grating ensure high throughput in diffracted orders. Furthermore, the use of radial profiles and the technique of subaperturing will maximize spectral resolution. In this way an off-plane reflection grating spectrometer will be able to meet the requirements for IXO.

8.1.2 Instrument performance specifications

Spectral Resolution	$\lambda/\Delta\lambda > 3000$ over bandpass
Effective Area	$> 1000 \text{ cm}^2$ over bandpass
Bandpass	0.3 – 1.0 keV

Table 8-1: Instrument performance specifications

8.1.3 Instrument configuration

An off-plane grating array can achieve the instrument performance requirements at any position along the optical axis from just aft of the optics to just 3 m away from the focal plane. However, due to CCD accommodation at the focal plane along with mass considerations, it was determined that a convenient position to place the grating array would be at the spacecraft avionics bus which is located ~6.5 m downstream from the optics (in the NASA MDL configuration). This places the grating array 13.5 m away from its focal plane. Figure 8-3 shows the placement of the grating array relative to the rest of the spacecraft. The telescope beam enters the grating array with a graze angle of 2.7° and is then reflected away from the telescope focus onto an array of CCD chips. The array is mounted to the forward side of the avionics bus facing the optics. The placement is independent on azimuth, but was chosen to conveniently place the CCD camera on the Fixed Instrument Platform (FIP). A close-up of this position is shown in Figure 8-2. As seen in Figure 8-1, the CCDs lie along the arc of diffraction. Therefore, the CCD camera box is oriented orthogonal to the radial direction. Some CCD electronics are located in the camera head but an external CCD electronics box will also be required.

Figure 8-4 takes a closer look at the grating array mounted to the spacecraft bus. The array is mounted to the forward side of the bus, the side facing the optics. In this way it is free from any interference with avionics

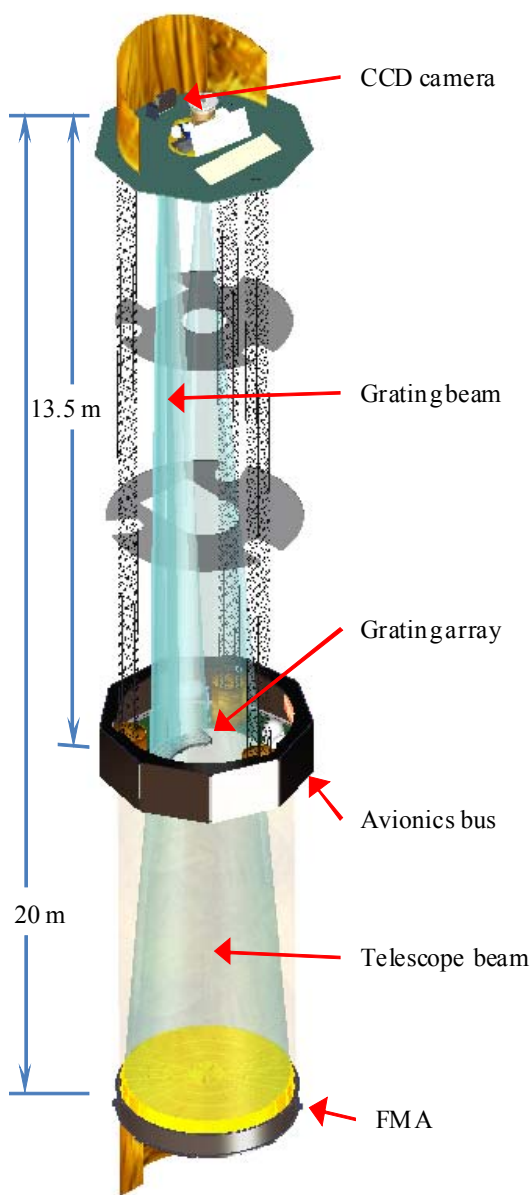


Figure 8-3: Grating array position relative to the spacecraft. Placing the gratings at the avionics bus results in a separation of 13.5 m from the focus (NASA MDL configuration).

equipment, electronics or the deployable masts. There is ample room for the structure in addition to heaters (not shown) which stabilize the temperature of the gratings around room temperature. The heater controller box is mounted in proximity to the grating array to minimize mass and cabling required.

Figure 8-5 details the individual components of the grating array. The most basic component of the array is an individual grating. Each grating will have a blazed (at 12°), radial groove profile that matches the convergence of the telescope beam. A groove density of 5500 grooves/mm is adequate to achieve the spectral resolution requirements and is currently well within the state of the art in grating manufacturing. We will also study the effects of going to higher densities and therefore higher dispersion both from technical and scientific perspectives to optimize the science return for minimal technical risk. The reflective face of the grating, which contains the grooves, measures $100\text{ mm} \times 100\text{ mm}$. The body or “substrate” of the grating changes in thickness, starting at 2 mm on one edge, increasing to 4 mm at the center and then thinning back down to 2 mm at the opposite edge to form a trapezoidal profile as evident in model on the left side Figure 8-4. This viewing orientation looks at the back of the grating. The reflective surface is on the opposite side and contains the grooves which run approximately vertical. Trapezoidal substrates allow for tighter packing in a module and increased throughput. This trapezoidal substrate is then light-weighted to provide mass savings without overly decreasing the structural integrity of the substrates. The current packing of the modules leads to a mechanical throughput of 70%. However, this number may be increased through additional light-weighting. This will be studied in the future, but is not critical in achieving the requirements.

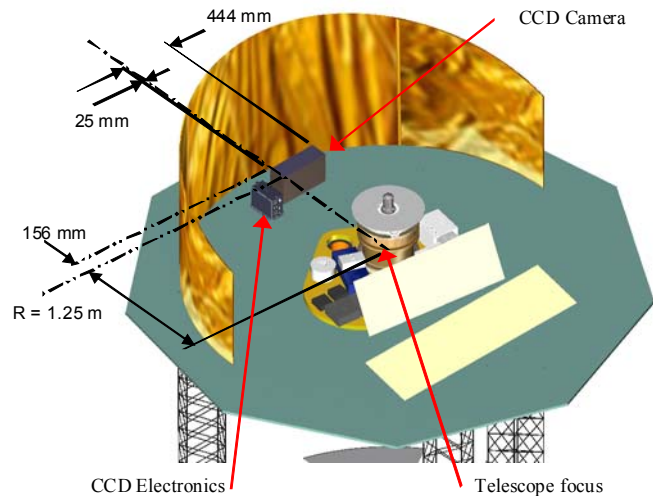


Figure 8-2: CCD position on the FIP. Approximate size of the camera and position relative to the telescope focus are given (NASA MDL configuration).

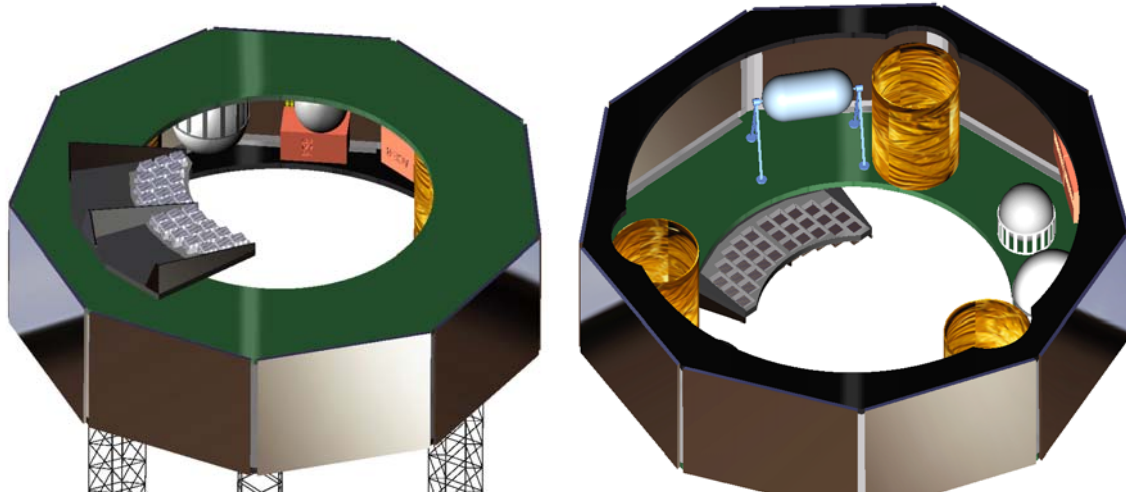


Figure 8-4: Placement of the grating array on the avionics bus. On the left the array is mounted on the forward side of the bus, facing the optics. The deployable masts are visibly protruding from the other side. The figure on the left shows the underside of the bus which houses the avionics and deployable mast mounts (NASA MDL configuration).

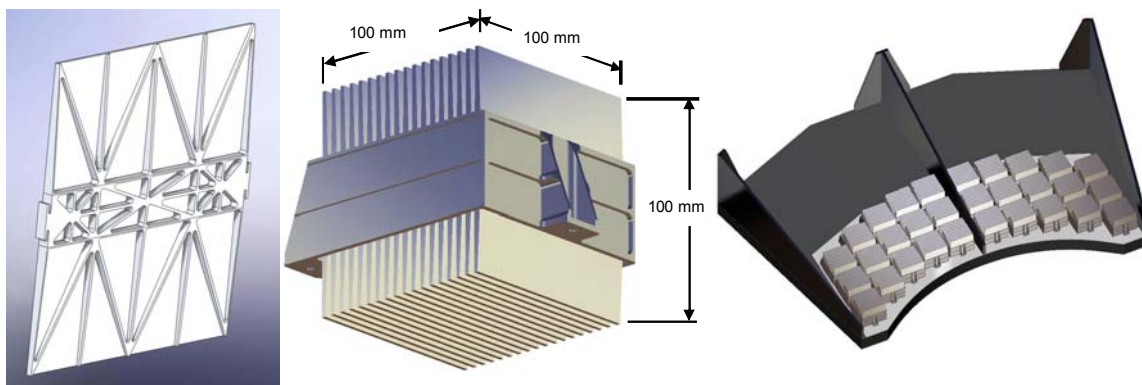


Figure 8-5: The backside of an individual grating is shown on the left. The structure has been light-weighted to reduce mass. The tabs on the side, near the middle, are used to mount each grating into a module as shown in the center. Each module houses 18 gratings. 30 modules are then co-aligned into an array as shown on the right. The modules utilize three mount points for adjustment in tip, tilt and piston.

The next component in Figure 8-5 is a grating module. Each module holds 18 gratings. The tabs on the side of the grating, which are evident on the left of the figure, epoxy into a groove on the interior surface of the module structure. Mounting the gratings in this way minimizes mechanical effects of the module mount on the grating surface such as the transmission of mechanical and thermal stresses. The gratings are not parallel to one another. Given that an individual module intersects a range of angles from the converging telescope beam, the gratings are fanned over a small range of angles to maintain the 2.7° graze over the extent of the module and ultimately the array. 30 of these modules are co-aligned into an array as shown on the right of the figure. Each module has three mount points to adjustment tip, tilt and piston for alignment. The main body of the grating array structure which mounts to the avionics bus is constructed from Glass Fiber Reinforced Polymer (GFRP) facesheet with an aluminium honeycomb. A titanium frame is bonded to this main body using a fiberglass CTE buffer layer and mechanically captured. The modules then mount to this

titanium frame. It is important to note that the module and array structures shown here are capable of achieving the performance requirements with modest weight and little obscuration. However, we will study methods for further optimization of the structure to decrease mass and obscuration.

8.1.4 Instrument optical design – filters

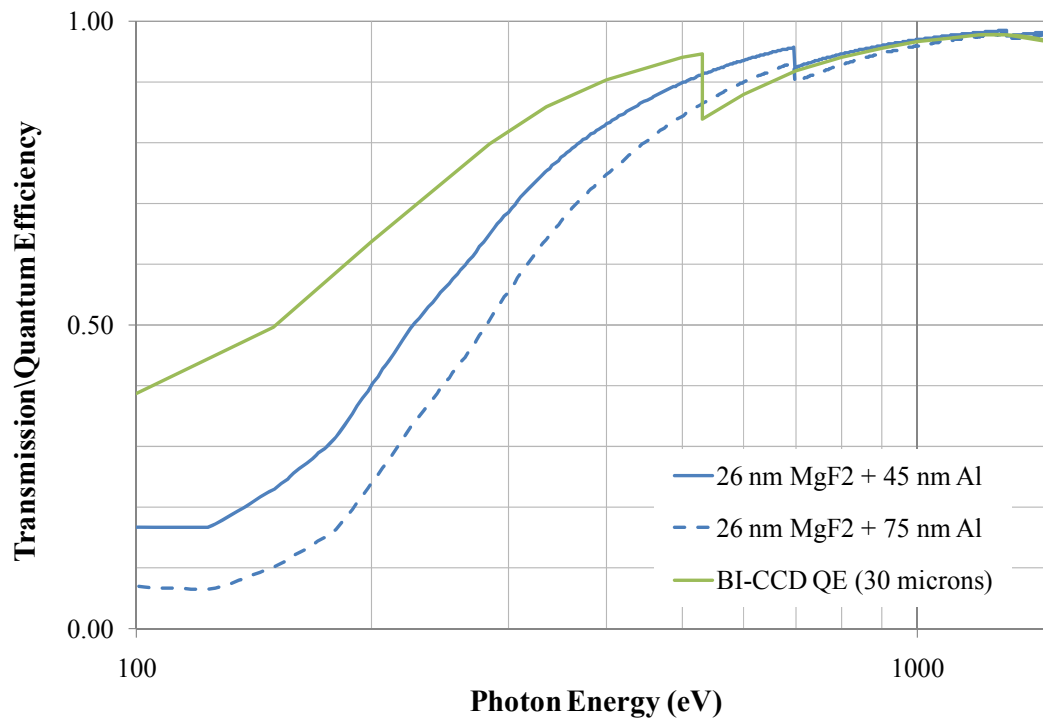


Figure 8-6: Soft X-ray transmission through the optical blocking filter comprised of 26 nm MgF₂ plus 45 nm Al and the modelled quantum efficiency of a 30 μ m, back-illuminated CCD in the energy range 0.1-1.1 keV

The optical blocking filter has high TRL from XMM which can be used as a baseline, and comprises a 26 nm layer of MgF₂ and a 45-75 nm layer of Al deposited directly on the CCD giving a reduction in stray light between 10^2 - 10^5 . We anticipate making refinements to the XMM-type filter, so here assume the thinnest XMM filter as the baseline for performance estimation purposes, which is consistent with the >100x frame rate over the XMM RGS. The expected attenuation of soft X-rays due to the optical blocking filter is shown in Figure 8-6. We choose this layer since it maximizes the 200-400 eV transmission which will enhance the soft X-ray science.

8.1.5 Instrument units' mechanical design and dimensions

A dimensioned drawing of the placement of the grating array on the spacecraft bus is given in Figure 8-7. This figure gives the dimensions of the grating array itself as well as its orientation relative to the telescope beam that passes through the central hole of the bus. The outermost extent of the telescope beam is the outer dash-dot green circle in this figure. The grating array intersects the telescope beam over a limited range of azimuth and over a limited range of outer radii. Using only outer annuli has the benefit of conserving the high energy throughput of the inner annuli. Also given in the figure is a finite element analysis of a completely populated array. The results show that the natural frequency of the first mode is above 50 Hz and increases to around 100 Hz by the third mode.

In addition to the grating array, a thermal control unit measuring approximately 23 x 30 x 8 cm with 3 electronics boards must be accommodated in the spacecraft nearby. Proximity is desired due to the potentially large number of heaters and temperature sensors that will need to be controlled which generate a significant amount of harness. See additional details in section 8.1.7 below.

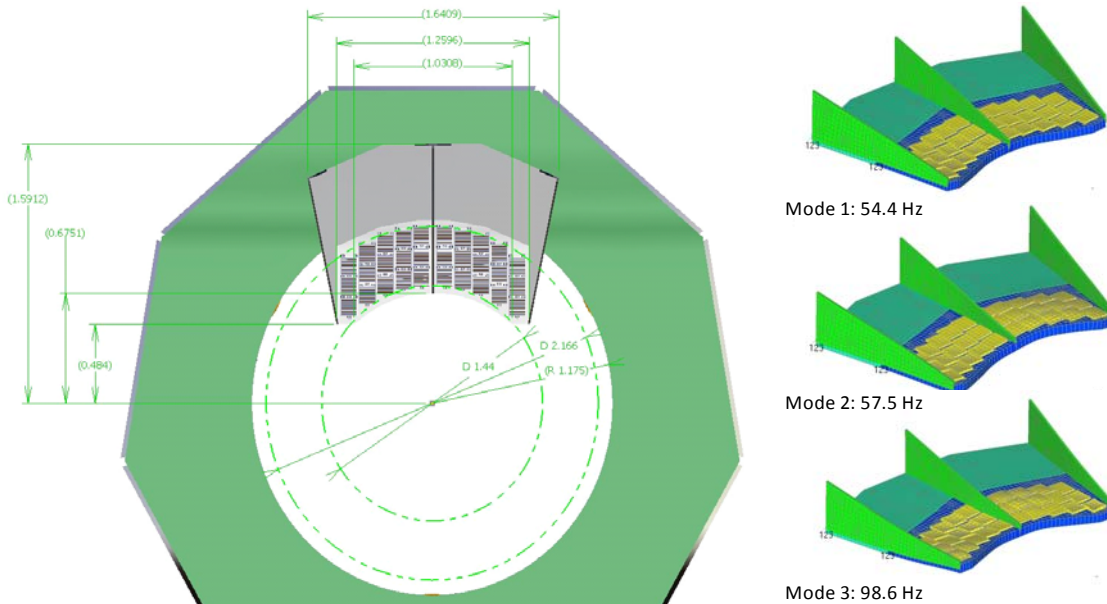


Figure 8-7: Left: Dimensioned drawing of the grating array size and position on the spacecraft bus (NASA MDL configuration).. Dimensions are in meters. Right: Finite element analysis results of the first three modes of the array structure.

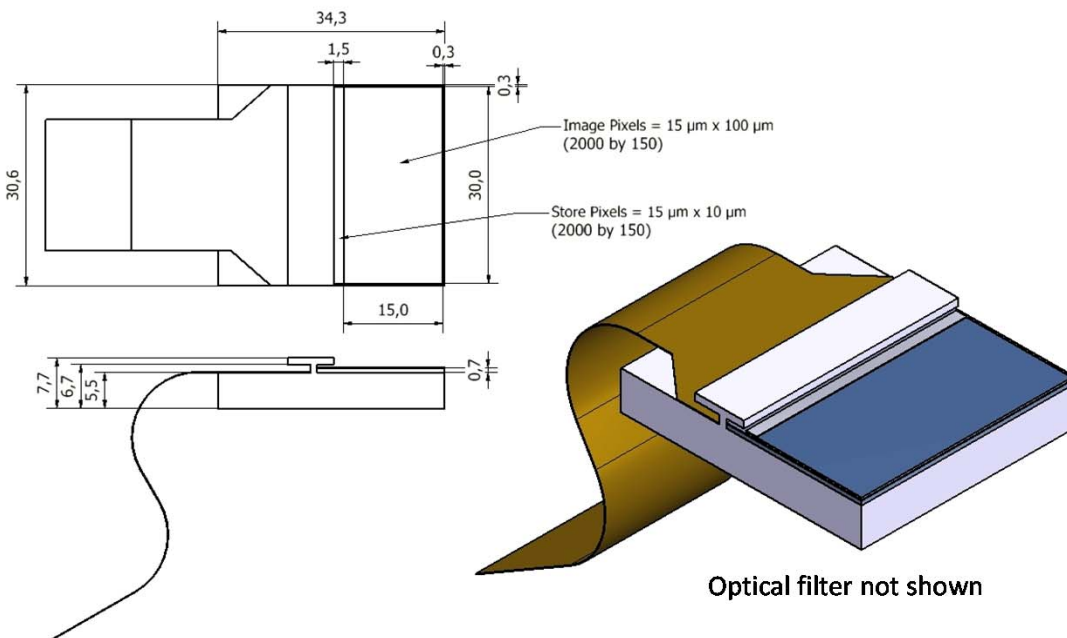


Figure 8-8 : Dimensions of a single CCD.

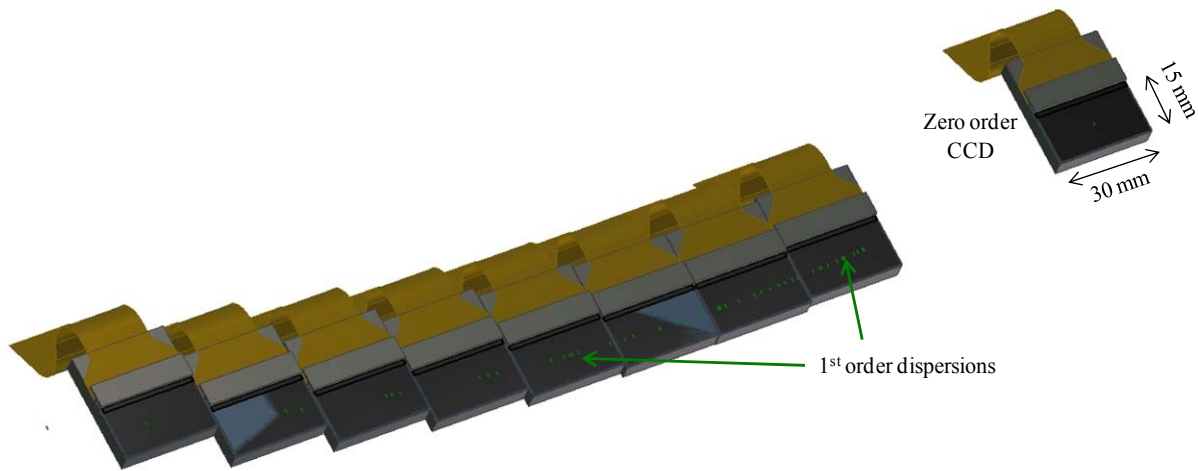


Figure 8-9: Model of the 9 CCD array.

Figure 8-8 gives the dimensions and characteristics of a single CCD. Each CCD measures 30 mm x 15 mm and is three side abutable. The pixels measure 15 μm in the dispersion direction and 100 μm in the cross dispersion direction. The larger pixel size will allow for a faster frame rate. Figure 8-9 shows how the 9 CCDs will be placed in the array. The zero order CCD is displaced from the rest of the array which collects light in the required bandpass. Figure 8-10 gives dimensions to this array and displays the position of the arc of diffraction as well as the position of various wavelengths on the detectors (vertical lines). These vertical lines, in no way, mimic the true point spread function of the spectral lines, but are just shown for reference.

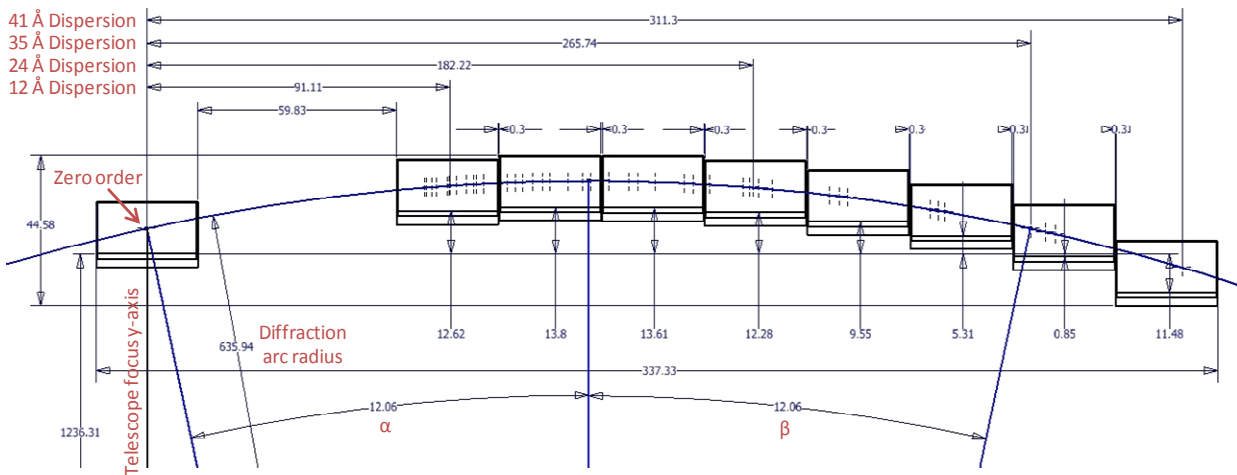


Figure 8-10: Dimensioned drawing of the CCD array with dimensions in mm. The arc of diffraction with corresponding wavelength positions are shown for reference. The vertical lines do not duplicate the actual spectral line PSF.

In addition to the grating array, a thermal control unit measuring approximately 23 x 30 x 8 cm with 3 electronics boards must be accommodated in the spacecraft nearby. Proximity is desired due to the potentially large number of heaters and temperature sensors that will need to be controlled which generate a significant amount of harness. A CAD model showing the placement of the thermal control unit within the spacecraft bus is shown in Figure 8-11. The unit is highlighted with a red circle. See additional details in section 8.1.7 below.

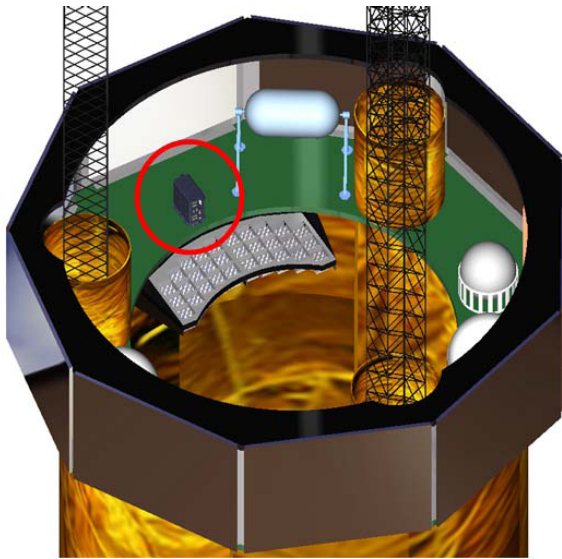


Figure 8-11 : Thermal control unit placement within the spacecraft bus (NASA MDL configuration).

8.1.6 Mechanisms

No mechanisms are required for the baseline 1,000 cm² OP-XGS configuration.

8.1.7 Instrument units' thermal design

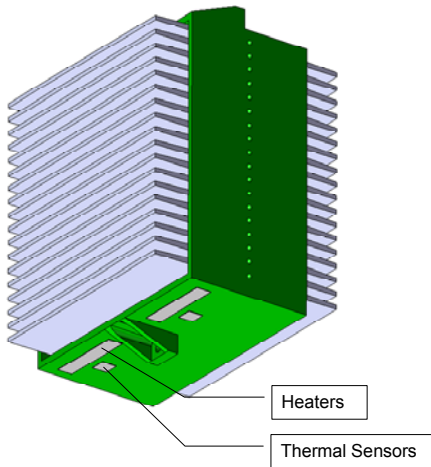


Figure 8-12: An individual grating module using a slightly modified mounting design from Figure 8-5, is shown with the nominal location of heaters and temperature sensors installed.

The XGS grating array will be heated to 23 ° C (see Chapter 8.3.1). Thermal design trade studies will be performed to determine the optimum method of heating based on optical-thermal requirements. The optical-thermal requirements will be based on the allowable radial and axial gradients and absolute temperature differences from 23 ° C required to maintain optical alignment and performance. Beryllium was selected for the gratings for its high specific stiffness, but also has high thermal conductivity, which will aid in minimizing thermal gradients.

Figure 8-12 shows the individual grating module with heaters and temperature sensors installed. Each module hosts 4 heaters and 4 temperature sensors to provide redundancy and to detect and correct any gradients in the module. An alternative design is under study which would replace the titanium mounting

bracket for the grating array with a beryllium insert and then mount the heaters to the insert rather than the grating modules. This is attractive as fewer (but larger) heaters could be used, but the thermal and structural designs for this alternative have not been studied to verify similar performance.

The CCDs in the array must be cooled sufficiently to suppress the leakage (dark) current and mitigate in-flight radiation damage. The CCDs will have a maximum operating temperature of -90°C and minimum of -120°C , stabilized to $\pm 0.2^{\circ}\text{C}$ during operation. This level of control is routinely accomplished for space based detectors.

The CCDs will be affixed to a bench that has a thermal link to a passive radiator. Heaters and platinum resistance thermometers (PRTs) in a feedback loop will be used to control the operating temperature of the array.

8.1.8 Electrical design

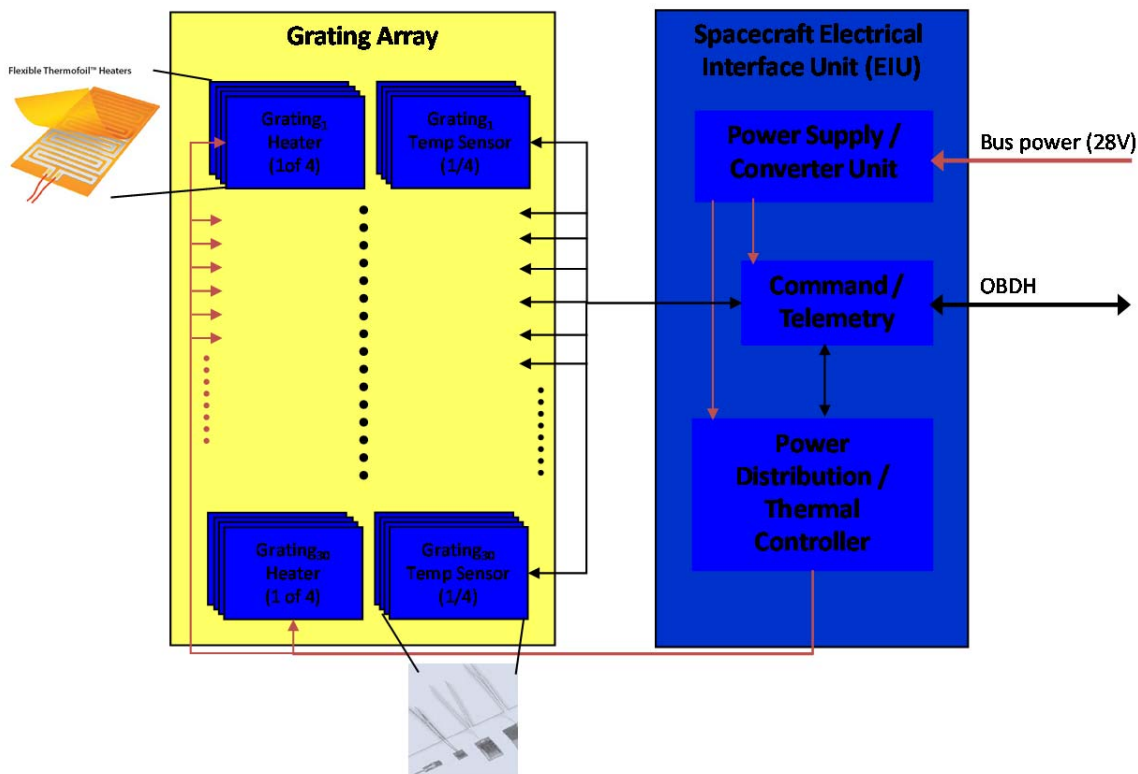


Figure 8-13 : Heater electronics box diagram

The heater electronics box is relatively simple, comprised of a command and control slice, a power converter slice, and a power distribution slice. These boards are all based on heritage Northrop Grumman designs and require no new technology, only new packaging. Figure 8-13 shows the notional heater electronics block diagram. Trades to reduce the number of heaters and temperature sensors will only change the complexity of the individual boards but not impact the overall electronics design. .

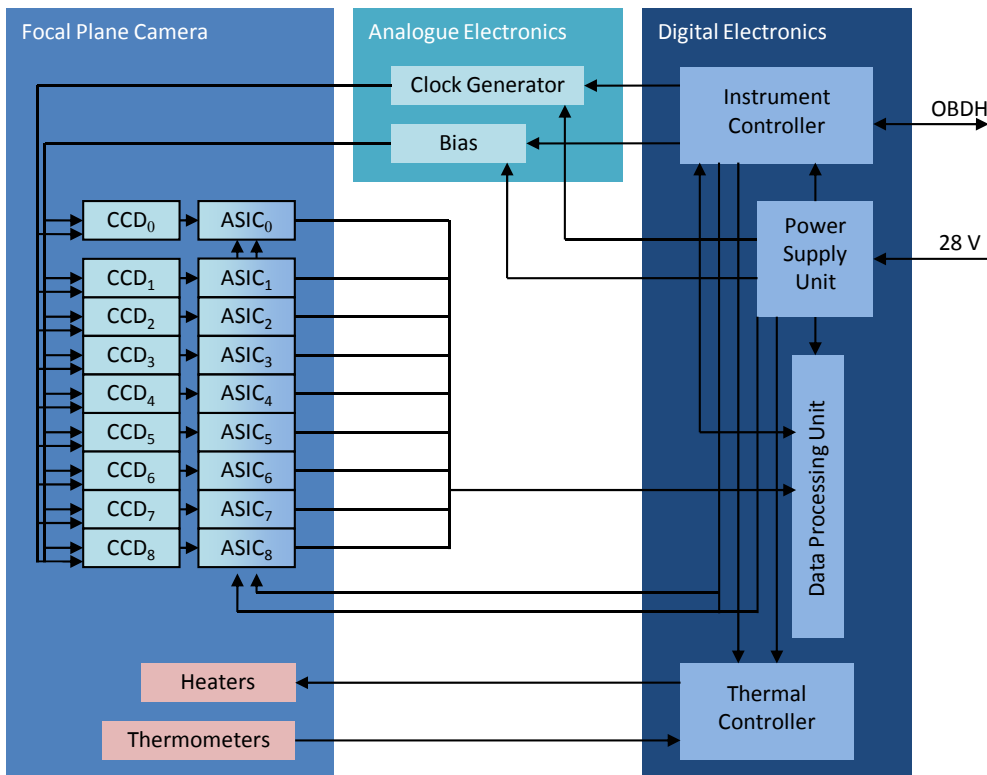


Figure 8-14: XGS camera electrical block diagram.

The electrical block diagram of the XGS camera system is shown in Figure 8-14. It consists of the focal plane camera and two separate units to handle the analogue and digital circuitry. The interface to the spacecraft's On Board Data Handling bus (OBDH) is via the Instrument Controller that configures the clock sequence programs and bias potentials for driving the CCDs. The Instrument Controller also configures the timings for the correlated double sampler (CDS) and 16-bit ADC conversions of the close-coupled, 8-channel readout ASICs and passes the digitally processed output (Data Processing Unit) of the camera to the OBDH. The temperature of the CCD bench is programmable via the Instrument Controller and regulated by the Thermal Controller.

8.1.9 On-board software

The on board computer (OBC) that is used for mirrors and spacecraft temperature control will also be used to control the XGS grating array temperature. This allows for set-point adjustments to accommodate aging effects.

8.1.10 Ground support equipment

8.1.10.1 Electrical GSEs

The OP-XGS EGSE will have provision for monitoring the grating temperature and switching power to the grating assembly heaters.

A test rack and PC are required to drive the CCD array. The array will need to be housed in a sealed enclosure capable of being evacuated to $\sim 1\text{E-4}$ mbar, by use of a turbo-molecular pump, to enable the CCDs to be cooled by a commercially available refrigeration pump system to between -120°C and -50°C . A heater, thermometer and temperature controller will be required to stabilise the operating temperature.

For gain calibration and charge transfer efficiency monitoring a similar configuration is baselined to that employed by the RGS camera on XMM-Newton. A Cm^{244} source fluoresces Al and Teflon targets to provide characteristic photon emissions of Al-K α (1485 eV) and F-K α (676.8 eV).

8.1.10.2 Mechanical and optical GSEs

The OP-XGS MGSE will include contamination covers for the grating assembly and CCD detector assembly with provisions for dry nitrogen purge during I&T and preparation for launch. Handling fixtures and shipping containers for the XGS components will also be provided.

The Optical GSE for the XGS will include corner cubes attached to the grating assembly to facilitate alignment in the spacecraft coordinate system, plus laser light sources that can be mounted on the grating assembly to check the alignment of individual gratings.

8.1.11 Instrument mode description

8.1.11.1 Operating modes

For the majority of observations the CCDs will operate in frame transfer mode, whereby the entire image areas are integrated for a finite time before being rapidly transferred into the store sections for readout via the parallel output nodes (frame rates based on 4 outputs per CCD). The frame integration time will be programmable to ensure enough photon counts in zero order can be obtained, whilst optimized to minimize the integration of stray-light. A maximum frame rate of 32 Hz is possible in this mode with a noise equivalent signal of $\leq 8\text{ e}^-$ rms.

A fast science mode (up to ~ 4100 Hz) will enable the observation of bright sources with minimal pile-up of photons. In this mode the frame is continuously clocked towards the readout registers, integrating light for time the each row-well takes to be clocked through the imaging area. Vertical spatial resolution is lost as the image data is in 1-dimension only (horizontal), preventing over-sampling of the PSF's astigmatism.

A calibration mode will enable the performance of the camera system to be monitored in conjunction with the calibration source.

The grating array temperature will be held at $23 \pm 0.5^{\circ}\text{C}$ during operational mode.

8.1.11.2 Non-operating modes

In the non-operating mode the camera electronics, including the CCDs, can be powered down and the overall power consumption is reduced. Upon power on, the CCDs must be given sufficient time to stabilize to the operating temperature.

The XGS grating array shall be held between -20 and $+40^{\circ}\text{C}$ during survival mode. This is consistent with the *Chandra* (and presumed IXO) mirror thermal control mode requirement.

8.2 Mechanical Interfaces and Requirements

8.2.1 Location requirements

Initial installation requirements for the gratings have been calculated given that the optics and CCDs are in their nominal positions. These requirements are $\delta_x = \pm 3$ mm, $\delta_y = \pm 1.5$ mm, $\delta_z = \pm 130$ mm, $\theta_x = \pm 0.8'$, $\theta_y = \pm 1.5'$, $\theta_z = \pm 3.5'$, where z is in the direction of the optical axis, x is the dispersion direction and y is the cross-dispersion direction (quasi-normal to the grating face). Rotation about x is grating pitch, rotation about y is grating yaw and rotation about z is grating roll.

8.2.2 Alignment requirements

The XGS will be aligned relative to the spacecraft coordinate system using corner cubes attached to the grating assembly. Laser light sources will be mounted to the grating assembly to check alignment.

The Optical GSE for the XGS will include corner cubes attached to the grating assembly to facilitate alignment in the spacecraft coordinate system, plus laser light sources that can be mounted on the grating assembly to check the alignment of individual gratings.

Grating-to-grating alignment requirements can be expressed as $\delta_x \sim$ millimeters, $\delta_y = \pm 39\mu\text{m}$, $\delta_z \sim$ millimeters, $\theta_x = \pm 0.9''$, $\theta_y = \pm 0.5'$, $\theta_z = \pm 0.4'$, where x is the dispersion direction, y is normal to the grating surface, z is parallel to the groove direction, δ 's are translations parallel to the specified axis, and θ 's are rotations about that axis.

8.2.3 Pointing requirements and performance goals

Given the requirements above, the pointing requirements are driven by maintaining position of the spectral line to within a FWHM of a spectral line, i.e. no degradation in spectral resolution. These pointing requirements are then $\delta_x = \pm 0.49$ mm, $\delta_y = \pm 3$ mm, $\delta_z \sim \pm$ tens mm, $\theta_x = \pm 1.9'$, $\theta_y = \pm 0.4''$, $\theta_z = \pm 3.7''$, where z is in the direction of the optical axis, x is the dispersion direction and y is the cross-dispersion direction (quasi-normal to the grating face). Rotation about x is grating pitch, rotation about y is grating yaw and rotation about z is grating roll.

8.2.4 Interface control drawing

A detailed ICD is not available at this time. An ICD will be developed as the host vehicle design matures. In general, the grating module will be mounted to the upper deck of the spacecraft as shown in Figure 8-4 using a hard mount arrangement with shims if required for alignment purposes. Just inside the spacecraft on the opposite side of the deck, the thermal control unit will be mounted which will be cabled to the temperature sensors and the heater units. This unit will need to interface with the spacecraft electrical system via a Remote Interface Unit (RIU) to get bus power and provide command and telemetry interfaces. Standard bus harness practices will be used to connect the thermal control unit to bus power and communication. Standard IEEE-1553 or similar command and telemetry protocol as defined by the spacecraft will be used.

8.2.5 Instrument mass

Spacecraft Bus Component	Quantity	Mass per unit [kg]	Total Mass [kg]
Grating array			44.7
array structure	1	7	7.0
Platform insert	1	12	12.0
Module structure	30	0.33	9.9
Grating	540	0.028	15.1
Mounting Screws NAS1352	90	0.002	0.2
Mounting Nuts MS1043	90	0.0004	0.0
Washers	90	0.006	0.5
Grating Thermal Control			10.2
Power Converter	1	1.2	1.2
Command and Telemetry	1	1.2	1.2
Minco thermofoil heaters HK5568	120	0.002	0.2
Minco thermal sensor S665	120	0.002	0.2
Power distribution assembly	1	1.2	1.2
Cable harness	480	0.01	4.8
Total			54.9

Table 8-2: OP-XGS masses for spacecraft bus components

Instrument Module Component	Quantity	Mass per unit [kg]	Total Mass [kg]
CCD Camera			19.7
enclosure	1	2.0	2.0
Proximity electronics card	1	1.9	1.9
90 filters per card			
36 preamps per card			
27 ASICs per card			
Radiation shielding	1	8.0	8.0
Cold finger	9	0.1	0.9
Thermal control card	2	0.5	1.0
radiator	1	5.0	5.0
CCDs	9	0.1	0.9
Drive Electronics			4.2
enclosure	1	1.0	1.0
Signal processing card	4	0.5	2.0
40 ADC's per card			

Housekeeping card	2	0.3	0.6
Drive thermal control card	2	0.3	0.6
Digital Processing electronics			2.2
Enclosure	1	1.0	1.0
Bus interface	1	0.3	0.3
Camera control Card	1	0.3	0.3
Discriminator	1	0.3	0.3
Command card	1	0.3	0.3
Total			26.1

Table 8-3: OP-XGS masses for instrument module components

The total instrument mass without margin is 81.0 kg (97.2 kg including 20% margin).

8.3 Thermal Interfaces and Requirements

8.3.1 Temperature limit in space environment

To minimize alignment errors during operations, the XGS grating array should be held at the same temperature in flight as it was during assembly and alignment, room temp 23 ° C. This is necessary because the thin gratings will be made of a structural material, Beryllium which has a moderate coefficient of thermal expansion. The grating modules are assumed to be cold in the absence of heaters due to the thermal balance of the spacecraft. Thus the OP-XGS gratings will be heated to the required temperature of 23±0.5 ° C. The sizing of these heaters will be dependent on the overall system thermal design. Under survival and safe mode conditions, grating temperature only has to be maintained within -20 to +40° C.

The CCDs will operate between -120°C and -80°C.

8.3.2 Temperature limits in laboratory environment

The XGS temperature must be held to 23±0.5 ° C during alignment. Ambient temperature conditions will be controlled by room temperature control adjusted for thermal inputs due to lighting, and worker proximity. The CCDs will operate between -120°C and +25°C.

8.3.3 Temperature sensors

The baseline design uses 4 Minco model S665 thermal tab sensors per grating module, for a total of 120 sensors in the grating array. These are fixed to the sides of the grating modules, 2 per mounting side as shown in Figure 8-12.

The CCD array will have 8 platinum resistance thermometers (PRTs), located on the focal plane camera above and below CCD₀, CCD₁, CCD₅ and CCD₈. The data from these sensors will be used by the Thermal Controller to ensure a homogenous heat distribution throughout the array.

8.3.4 Heaters

We have baselined using Minco polyimide flexible heaters configured to provide sufficient heating without being too large for mounting. For example, the Minco model HK5568R13.1 can provide up to 2W of heating at 5V in a package that is 0.25 x 1 inch (6.3 x 25 mm) for each. The exact configuration will be determined during the design phase. However, we have assumed that each module will have 4 heaters mounted to it near each of the sensors as shown in Figure 8-12. This results in a total of 120 heaters which are controlled by the thermal control unit. As mentioned in Chapter 8.1.7, this is a large number of heaters and a trade is proposed to see if control could be done at the inserts or at the platform assembly level.

Four heater elements are required on the focal plane camera to regulate the operating temperature of the CCDs. These will be located on the rear surface of the cold bench, below CCD₀, CCD₁, CCD₅ and CCD₈.

8.3.5 Thermal schematics

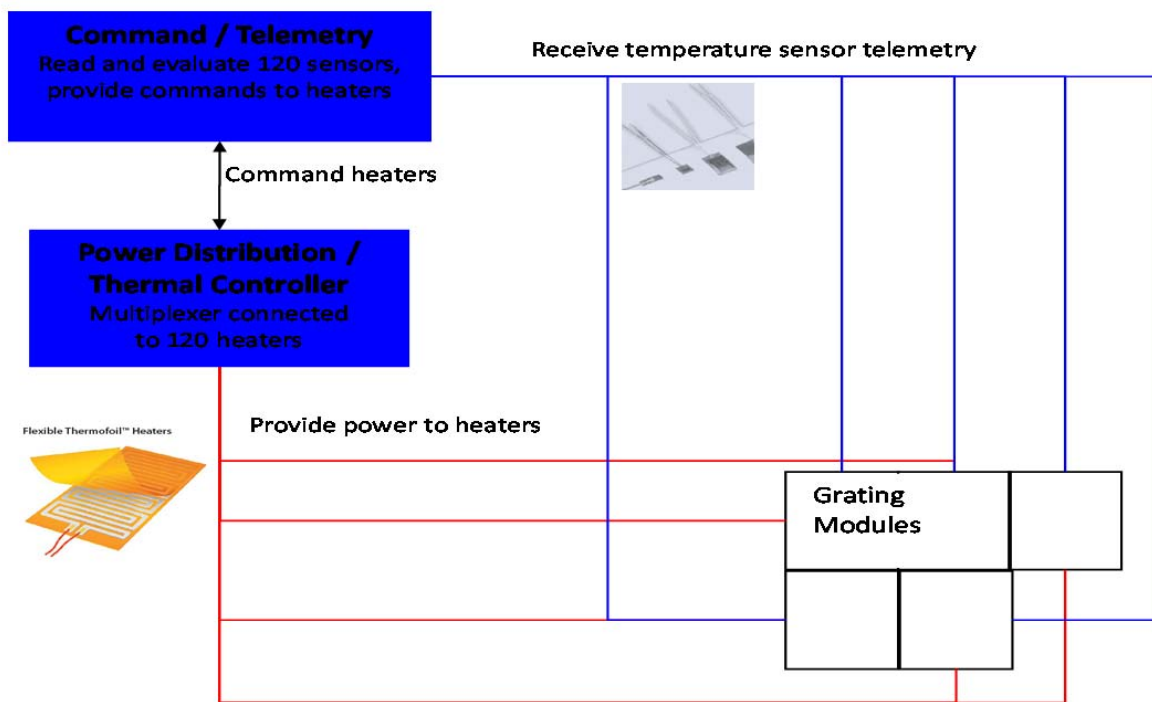


Figure 8-15: Thermal control schematic for the grating array at the module level.

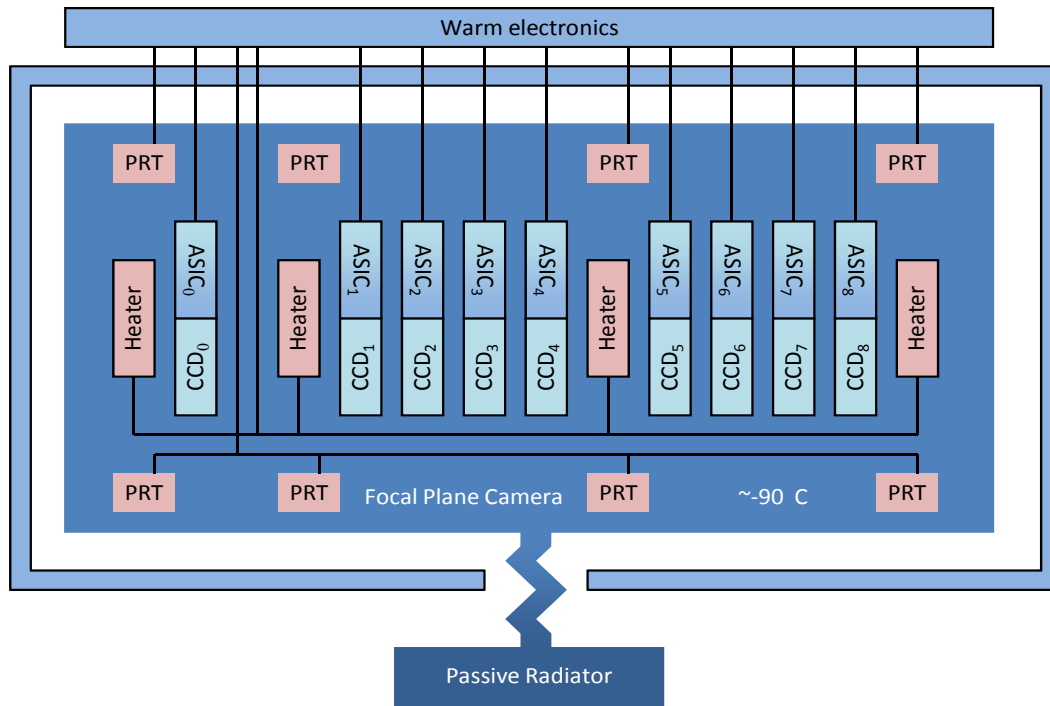


Figure 8-16: Thermal control schematic for the CCD camera.

8.3.6 Thermal control requirements

The ± 0.5 K requirement on the gratings is driven by maintaining flatness over the gratings in the pitch direction. A thermal design trade study will determine the optimum heater type and layout.

The CCDs will operate between -120°C and $+25^{\circ}\text{C}$ in the laboratory and between -120°C and -80°C in space environment. The CCDs must be controlled to ± 0.2 K during operation to maintain the performance stability and allow dark frame subtraction. The exact operating temperature will be determined by the overall thermal environment and the radiator performance. Adjustment of the operating temperature over time is expected but on a scale of months to years, with stability expected on the order of days to weeks.

8.4 Electrical Interfaces and Requirements

8.4.1 Electrical resources requirement summary

The grating thermal control unit receives unregulated bus power, nominally 20 – 38V. The included power conditioning and conversion slice provides the required interface for the temperature sensors and heaters. CCDs require a 28 V power supply.

8.4.2 Instrument power distribution block diagram

See Figure 8-15 for grating thermal control system.

8.4.3 Power budget

Table 8-4: Grating array thermal control power budget (without margins).

Thermal Control Unit	Nominal Power [W]	Maximum Power [W]
Command and Telemetry	1	2
Power Converter	1	5
Power Distribution Assembly	1	2
Minco Heater (120)	10	120
Minco Sensors (120)	1	5
Total	14	134

Table 8-5: XGS CCD Electronics power budget (without margins)

CCD Electronics	Unit Power [W]
Pre-amps	2.5
ASICs	2.5
Thermal Control	15
CCDs	3
ADCs	2.5
Housekeeping	2
Bus Interface	4
Camera Control	4
Discriminator	10
Signal Processors	2.5
Total	48

8.4.4 Instrument modes' duration

8.4.4.1 Instrument continuous mode duration

The camera array will default to frame transfer readout, with a frame rate of 32 Hz.

8.4.4.2 Instrument peak mode duration

When the event detection unit can no longer distinguish incident photon energies due to mixed pile-up, caused by excessive flux, the camera will temporarily switch into the fast science mode.

8.4.5 Telecommands

Commands will be required to initiate and terminate thermal control of the grating array. Analysis will be required to determine if heaters can be disabled for launch and safemode operations or if thermal limits will be exceeded for hardware safety.

8.4.6 Telemetry

8.4.6.1 Telemetry requirements

Thermal control of the grating array will be done autonomously by the thermal control unit when commanded by the spacecraft. The commanding will be part of the spacecraft command set as it is anticipated that the heaters will need to be operated when the instrument is in safe mode (as survival heaters). During commissioning, the data from the temperature sensors and commanded power for heaters will be requested once per minute (each sensor read at a rate of 0.5 seconds with 60 seconds between reads). During nominal operations, the data will be collected for each sensor and heater sequentially at a rate of one reading per second, with each individual sensor being read every 2 minutes. This data will be supplied in the housekeeping data stream from the spacecraft.

8.4.6.2 Telemetry description

TBD

8.4.7 Electrical interfaces

The power for the grating thermal control unit can come directly from the spacecraft with minimal harness required.

8.5 Electromagnetic Compatibility and Electrostatic Discharge Interface

8.5.1 Susceptibility requirements

CCDs will have no requirements on magnetic fields.

For operation at L2 halo orbit, the dominant source of radiation will be from solar protons. Some degree of shielding will be required to protect the CCDs. The exact thickness will require a detailed study combining radiation modelling of the environment with the spacecraft, with readout rate/frame time, operating

temperature and EOL resolution requirement. In the meantime we assume a local shielding thickness equivalent to 2 cm Al to be wrapped closely around the array.

8.6 Optical Requirements

8.6.1 Stray-light requirements

Stray light is defined as radiation at wavelengths greater than 12.4 nm (0.1 keV) which reaches the OP-XGS detectors. Stray light shall contribute less than 10 percent of the detector noise.

8.6.2 Baffling requirements

Stray light baffling will be required to maximize the signal-to-noise ratio for the XGS detectors. The shroud around the fixed metering structure between the optics and spacecraft bus, plus the shroud around the deployable optical bench and baffles between the spacecraft and the instrument module should prevent stray light from reaching the detector array. Additional stray light protection may be provided by filters over the detector array and radiation shielding around the detectors.

8.7 Transportation, Handling, Cleanliness and Purging Requirements

8.7.1 Transportation requirements

A shipping container will be provided to ship the grating array and the detector array as needed. The units will be designed to survive the environmental shock and thermal environment specified in the IXO environmental specification. To maintain cleanliness, a clean dry nitrogen purge is required at all times when the instrument is not in a Class 1000 or better cleanroom. A purge interface will be provided with the shipping container.

8.7.2 Handling requirements

Both grating array and detector plane will be handled via best practices for space flight instruments. Full documentation will be developed under contract.

8.7.3 Cleanliness requirements

The OP-XGS gratings and detectors are sensitive to molecular and particulate contamination. The XGS contamination requirements are similar to those of the IXO mirror assembly. The contamination budget for the XGX shall be 500A (TBR) and less than 0.1% area coverage due to particulates.

8.7.4 Purging requirements

The grating array and CCD camera will be under vacuum or dry, UHP nitrogen purge during all ground operations.

8.8 Ground and Flight Operation Requirements

8.8.1 Ground and pre-flight operation

The system will be tested in the laboratory under flight like conditions. Soft X-ray testing and calibration will occur in vacuum. Outside of testing the instrument will be under purge. Prior to launch, contamination mitigation covers will be removed from the grating array.

8.8.2 Flight operations

The XGS will be launched at atmosphere.

8.9 Deliverable Models and GSE

8.9.1 Structural thermal model

A detailed structural-thermal model will be built based on optical model. The structural-thermal model will then be used to verify mounting stress and temperature control requirements.

A detailed structural-thermal model of the CCD array will be built to verify the temperature control requirements for the power dissipated by the array for the two operating modes.

8.9.2 Engineering qualification model

Several engineering qualification models for the gratings will be constructed starting with the grating substrate, going into the separate grating modules (how to mount 18 gratings in a module and metrology necessary), into module-to-module alignment, into array population. We will also need to develop hardware for final alignment of grating array to optics once installed. We propose to build a complete engineering qualification model of the grating platform and inserts, using thermal mass models that for the most part are simple lump masses but for a few consist of a full up set of grating substrates (uncoated) and grating modules to put through environmental testing. The location of the high fidelity mass models will be selected based on the structural thermal model to verify survivability at the highest stress locations.

8.9.3 Flight model

The flight unit will consist of a fully populated and verified grating module and CCD detector array plus all associated flight electronics.

8.9.4 Flight spare model

A complete flight spare is not considered practical given typical instrument development budgets. However, three populated grating modules and flight electronic boards will be developed as spares in addition to any of the qualification model hardware that can be refurbished and used as a flight spare. In addition, sufficient CCDs will be procured to ensure a full set of flight spares will be available at the detector level, though not integrated into a detector module. These spares can be used either to replace damaged CCDs in the flight module if this occurs or be mounted into a full module if the risk assessment by the program determines this should be done.

Part 3 Payload Accommodation and Interfaces

1 INTRODUCTION

The accommodation of the IXO reference payload and relevant interfaces to the Spacecraft are described in the following sections. This chapter is included to facilitate further definition of the interfaces between instruments and platform and to provide background information on the accommodation of the instrument in the spacecraft that could be used as input to future studies and any foreseeable Announcement of Opportunity for the actual instrument provision.

The content of this part of the PDD is based on the preliminary design of IXO mission performed by SRE-PA in ESA CDF activities in 2008-2009 [RD-5] and on the results of the earlier payload accommodation study performed by industry over 2006/07 (parallel competitive activity with Astrium and AAS). It should be noted that the actual instrument accommodations will be revisited during the system level studies to be performed as part of the IXO assessment phase within the Cosmic Vision mission selection process.

The identification of a resource-efficient configuration will be crucial in the context of the system level IXO design in view of meeting two main goals: a) ensure compatibility with programmatic constraints especially for defining clean interfaces for cryogenic sub-systems b) optimise the resource usage so that the mission can be made as affordable as possible, and especially maximise the resources (mass) devoted to the mirror sub-system.

It is also important to stress that the results obtained from the payload accommodation studies have been used to define a list of specific technology development activities, with particular regard to the cryogenic chain definition and its readiness level. Additional development activities will address instrument specific issues, such as focal plane detectors and read-out electronics.

Finally, this part of the PDD considers a payload suite consisting of all instruments described in part 2, with exception of the OP-XGS.

2 ACCOMMODATION

2.1 Instrument accommodation issues

As explained in the Payload Overview section (Part 1 Section 6), the IXO straw man payload includes 6 instruments, two of which, WFI and HXI, are co-aligned and foreseen to be delivered as a single instrument. Five instruments are operated in the telescope's primary focus, one at any time (except WFI/HXI), and are therefore mounted on a movable instrument platform (MIP) with four positions and a global focus adjustment capability (TBC). Only CAT-XGS is not operated in the primary focus, but intercepts dispersed light along a strip extending radially from the primary focus at distances between 0.7-1.5 m. CAT-XGS is located on the Fixed Instrument Platform (FIP) and will always be operated simultaneously with one of the four on-axis instruments. In order to alleviate the complexity of the XMS accommodation, testing and allow for a minimum of 5 years operations, it has been decided that the cryogenic chain for XMS is cryogen-free and operates with a room temperature cryostat and active pre-cooling. In the section below, we will discuss possible accommodations of all units.

The distribution of the different instrument units over the MIP and FIP is driven by individual instrument constraints and the general aim to minimise the amount of harness which has to be routed from the MIP to the FIP. In the case of the ESA CDF design this harness was routed through the MIP rotation/focus mechanism. The instruments' accommodation constraints and the ESA CDF configuration are listed in Table 2-1.

Table 2-1: Accommodation constraints for the IXO instruments and configuration as in the ESA CDF

Instrument	Accommodation (in ESA CDF)				constraints
	Movable platform		Fixed platform		
	units	Mass [#] (kg)	units	Mass [#] (kg)	
WFI	FPA HPP (2x)	56.3	Brain/framebuilder PCU	26.5	- radiator close to detector - HPPs on FPA - distance HPP-BFB <4m - distance HPP-PCU <4m
HXI	HXI-S HXI-E	27.3	HXI-D	5.2	- Co-mounted with WFI - radiator close to detector - distance S-E <2 m - distance E-D <10 m
XMS[#]	Dewar assy FE LCD DE (4x)	270.0	JTD (2x) PCD (2x) ICU (2x) EP PSU (2x)	81.1	- strict magn field req at detec - distance dewar-FE <0.5m - distance FE-DE <1 m - distance dewar-LCD <1 m - distance dewar-other <3 m
HTRS	Detector+FW Electronics	31.9	-	-	- detector 12 cm out of focus - distance det-electr <1 m
XPOL	FPA BE CEE	10.6	-	-	- distance FPA-BE <20 cm

CAT-XGS	-	-	CA DEA DPA	58.2	- gratings on mirror assy - distance CA-DEA <1 m - distance DEA-DPA <4 m
total		396.1		171.0	

including margins

with European cryogenics option

2.2 Instrument alignment requirements

The alignment requirements of the individual instruments are collected in Table 2-2.

Table 2-2: Instrument alignment requirements

	WFI detector	HXI detector	XMS detector	HTRS detector	XPOL detector	CAT-XGS detector	CAT-XGS gratings
Lateral (X,Y)							
Accuracy	+/-1 mm	+/-0.5mm	1 mm	+/-1 mm	+/-0.75mm		
knowledge			0.05 mm			<0.035mm [#]	
stability			0.1				
Focus (Z) offset	0	<+25mm	0	- 12 cm	0	0	
Accuracy	+/- 1mm		0.5 mm	+/-1 mm	+/-3mm		+/-0.4mm
knowledge			1 mm				
stability			0.5 mm				
⊥ Z (arcmin)	<0.35'	<5'		<0.35'	<5'		

required knowledge of distance between 0th order image on WFI/XMS and spectral lines on CAT-XGS

3 INTERFACES

3.1 Data handling system

The spacecraft shall provide the main data handling system with which the instruments shall communicate. As all instruments require different type of processing the spacecraft provided data handling system (DHS) will not do any instrument specific data processing, instead such processing will be performed by the instrument processors. However, in case some high level process (e.g. data compression) is common for all instruments this processing might be performed in the spacecraft DHS.

The present baseline assumes that the interface between the instruments and the spacecraft DHS will be based on SpaceWire. The mass memory required to store the processed data between successive downloads will be provided by the spacecraft DHS. The mass memory of the spacecraft will be sized to accommodate 2 days of science data, so as to be able to cope with a failed telemetry downlink sequence. Table 3-1 shows the corresponding required mass memory size, calculated for 1 day of continuous observation for each instrument operating at maximum expected data rate.

Table 3-1: Data rate and mass memory table. The data rate is after instrument processing and mass memory requirement is only mass memory required for storing of processed science data.

Instrument	Maximum Data rate - nominal	Maximum Data rate – high background	Max. total data acq time (ks)	Mass memory (Gbit)	Mass memory (Gbit) incl. 100 % margin
WFI	0.45 Mbps	0.5 Mbps	86.4	43.2	86.4
HXI	1 Mbps	1 Mbps	86.4	86.4	172.8
XMS	0.84 Mbps	0.84 Mbps	86.4	72.6	145.2
HTRS	<20Mbps	<20Mbps	TBD	TBD	TBD
XPOL	5.1 Mbps	5.1 Mbps	86.4	128 ^b	256
CAT-XGS	0.75 Mbps	0.75 Mbps	86.4	64.8	129.6
MAX: CAT-XGS + WFI/HXI	2.20 Mbps	2.25 Mbps	86.4	194.4	388.8

^b limited by XPOL internal MM (128 Gbit)

Worst case, for the combination of CAT-XGS and WFI/HXI, the required mass memory is ~390 Gbit. It is assumed that here that HTRS will not be driving the total mass memory requirement, but rather the observation time for HTRS will be limited by the available mass memory.

Alternatively, during the IXO CDF activities at ESA [RD-5] a reference observation scenario [RD-6], consisting of a sequence of observations of different sources with different instruments and with realistic durations has been used to more accurately model the MM and telemetry requirements. It should be noted that the sequence of observations was not optimised for data volumes, and CAT-XGS and HTRS were allowed to contribute up to 1.5 and 1.0 Mbit/s, respectively. This exercise predicted a maximum required MM of 368 Gbit (TBC), assuming nominal daily X-band downloads during ~1.5 hrs (8 Mbps), and allowing exceptional 4.5 hrs daily downloads. The total data volume was dominated by CAT-XGS and HTRS simultaneous observations, and therefore probably an overestimate since most likely, the HTRS data volume will be truncated, rather than its bit rate. To allow for missing one daily pass, the MM was increased to 512 Gbit.

3.2 Power

The spacecraft is in charge of delivering protected primary power at 28V. It is assumed that a distributed approach to DC/DC conversion shall be adopted. Some instruments need a wide range of low voltage and high voltage supplies for detector operation that would be provided by each instrument's own PCDU.

The power system is sized to provide sufficient power to one operating instrument and one instrument ready to be operated, in addition to CAT-XGS, which is always operating. For the cryogenic systems it is assumed that the pre-cooling chain will always be on. In Table 3-2 the power system sizing is shown. The maximum power demand at any time is 1544 W, during operation of CAT-XGS and XMS simultaneously, with WFI/HXI in STANDBY mode, and the other instruments in SLEEP mode

Table 3-2: Power demands for instruments. Power demand is including 20% margin and dc-dc conversion efficiency of 70% has been accounted for

Instrument	operational (W)	standby (W)	SLEEP (W)
WFI ¹	283.1	283.1	73.9
HXI ¹	61.0	61.0	0
XMS (incl coolers)	1067.6	618.5	560.4
HTRS	164.6	17.1	17.1
XPOL	55.1	34.2	0
CAT-XGS ²	114.2	115.2	TBD
MAX continuous power³	1067.6+115.2+283.1+61.0+17.1 = 1544.0 W		

¹ WFI and HXI are assumed to be operated as a single instrument

² CAT-XGS is always ON

³ this is the maximum possible power requirement with CAT-XGS + one on-axis instrument operating (XMS), one ready for operation (WFI/HXI), and the others at minimum power

3.3 Thermal

The instrument complement on the IXO instrument platforms has a wide range of thermal requirements, from the cryogenic instrument XMS, to the cold WFI, HXI and CAT-XGS and (almost) room temperature instruments such as XPOL and HTRS.

It is currently assumed that all instruments except for XMS can be cooled passively. Cryogenic coolers are required to cool the XMS. Any radiator required by the cryogenic chain of XMS is not discussed further in this section.

As IXO is located at L2 in a stable thermal environment, the radiator design can be simple, consisting of only flat panels. The most challenging instrument to cool passively is the WFI which needs to radiate at least 30 W of power at 210 K. This implies a very large thermal strap and dictates that the detector shall be located close to the dedicated radiator. Since WFI and HXI are integrated, further heat will need to be transferred from the HXI detectors putting even stricter demands on the thermal control. A further complication arise from the different operating temperature of HXI at T=233 K

The elements that can be at room temperatures, such as instrument control electronics, power supplies etc. are assumed to be commonly controlled with the rest of the spacecraft components with room temperature radiators.

Using this interface philosophy the following radiator sizes are calculated based on a full un-obstructed view to deep space and shown in Table 3-3.

Table 3-3: Temperature requirements and dissipations for the instruments. The distribution of instrument units over the platforms is reflecting the ESA CDF configuration.

Item	Operating temperature (K)	Dissipation ¹ (W) incl 20% margin	
		Movable platform	Fixed platform
WFI focal plane	210K	30.1	-
WFI remaining elements	290 K	117.6	113.8
XMS detector	50 mK	0	-
XMS remaining elements	290 K	687.4	363.2
HXI focal plane	233 K	26.0	-
HXI remaining elements	290 K	26.0	9.0
HTRS focal plane	253 K	17.1	-
HTRS remaining elements	290 K	130.3	-
XPOL GPD ²	283 K	2.0	-
XPOL remaining elements	290 K	53.1	-
CAT-XGS detector	173K	-	6.0
CAT-XGS remaining elements	290 K	-	109.2

¹ excluding filter wheel operation

² Controlled by Peltier

3.4 Cryogenics

The definition of the optimum interface between the PI and the prime contractor is particularly difficult for missions using cryogenic equipment. In fact, specific effort has been made in the context of the XEUS DSC instruments accommodation study (conducted in the time frame Q1/06 – Q1/07) to identify optimised interfaces, with specific emphasis on the cryogenic chain required for the Cryogenic Instrument (see chapter 3 in part 2). Given their critical role on overall system performance, impact on the AIV/T schedule and close interfaces to the spacecraft subsystems, it is recognized that, although the cryogenic chain could be split at some appropriate interface (e.g. around 2.5K) between a prime-contractor and PI, an overall cryogenic architect and responsible needs to be appointed at some appropriate point in time.

In the current IXO study and in the absence of a well-defined interface and procurement strategy, the entire cryogenic chain is now tentatively described as part of the instrument. The cryogenic chain is currently assumed to be an actively cooled system with a room temperature interface to the S/C. Various options are described in section 2 and these will be subject of further study, at instrument level as well as at S/C level. It could be anticipated however, that, in later phase of the project, different interfaces may become relevant. In order to facilitate an objective comparison and trade-off between these and future designs of the entire cooling chain, all interface requirements are collected in a separate document [RD-7] and the complete cooling chain will be studied in the frame of the industrial and instrument assessment studies.

3.5 Baffling and particle deflection

The relevant instrument parameters for stray light and charged particle suppression are listed in Table 3-4.

Table 3-4: instrument specifications relevant for X-ray baffling and particle deflection. Drivers for baffles and particle deflectors are indicated in orange

	Instruments					
	On axis					Off axis
	WFI	HXI	XMS	HTRS	XPOL	CAT-XGS
FoV: sky (arc min) focal plane (cm)	18.0 ∅ 10.5 ∅	12.0x12.0 7.0x7.0	5.4x5.4 3.14x3.14	- 3.0 ∅	2.6x2.6 1.5x1.5	-
Filter stack: Fixed	70nm Al + 35nm Si ₃ N ₄ + 35nm SiO ₂	N.A.	210nm Al + 280nm Poly- imide	100nm Al	50 μm Be	10nm Al TBC
movable	100 nm Al + 300nm Poly- propylene	See WFI	120nm Al +200nm Poly-imide	N.A.	N.A.	none
Energy range for particle deflection	<20 keV	N.A.	<20 keV	TBD	N.A.	<2keV (TBC)
E _{max} defl. (keV): protons electrons	75 keV 21 keV	N.A.	78 (113) ^a keV 21 keV	100 keV 21 keV	N.A.	TBD
B _{max} (T)	~1e-3 T	~1e-3 T	<1e-4 T ^b <1e-3 T ^c	~1e-3 T	~1e-3 T	TBD
Diffuse X-ray bkgnd from outside FoV	<0.001 cts/s/cm ² (0-15keV)	Eq 200μm LoS Au (1/e att @ E=70keV)	<0.02 cts/s/cm ² /keV (0-10keV)	<0.001 cts/s/cm ² (0-15keV)		TBD
UV/Vis straylight	<10 ¹² ph/s/cm ²	N.A.	<2.5 10 ⁹ ph/s/cm ²	<3 10 ¹⁰ ph/s/cm ²	N.A.	<2 10 ⁶ ph/s/cm ² (TBC)

a: 113 keV is a goal requirement which includes the energy loss in the movable filter, 78 keV does not

b: during cool down of the superconducting shield through its transition to prevent flux trapping

c: at any other time during (non)-operation to prevent flux trapping in the superconducting shield when cold

3.5.1 X-ray stray light baffles

A consequence of the deployment concept with a shroud is that there is only a partial solid and opaque tube connecting the Mirror Assembly with to the Instrument Platform. In particular the shroud is more or less transparent at X-ray photon energies above a few keV. In addition, it may be damaged by micrometeorites during the mission life time such that the visible stray light level may become unacceptable. Therefore, the instruments need additional shielding against X-ray photons that may reach their detectors from directions

other than the mirror, as well as any optical stray light. The amount of shielding depends on the X-ray energy range covered by the instruments and their internal stray light provisions (filters, baffles).

To simplify the interface to the instruments a small PI provided baffle could be envisaged. This baffle would bridge the gap between the instruments radiation aperture and the main baffle on the FIP, and thus it would add some extra mass. Whether such a baffle is beneficial needs to be evaluated for the different instruments, but it is expected that having such a baffle would for instance simplify the thermal control and potentially help to reduce further any contamination effects.

3.5.2 Optical stray light baffling

The instrument's requirements with respect to optical stray light intensities are also listed in Table 3-4. Optical stray light sources could be (in order of severity):

- optical contributions of celestial sources through the mirror, either in the FoV or by single or multiple reflections from outside the FoV. Most instruments have fixed or movable filters to reduce this light
- solar light entering the telescope tube through holes punctured in the relative thin deployable shroud during the mission by micro-meteorites. Current estimates during the ESA-CDF suggest that these could be problematic for CAT-XGS
- stray light induced by the metrology system (only if this is operated during observations). Careful design could mitigate this

3.5.3 Particle deflectors

The issue of charged particle background is related to the collimating effect of the X-ray mirrors of XMM-Newton and Chandra for low energy (up to a few hundreds of keV) charged particles (electrons and protons). A similar effect is expected for IXO. Magnetic diverters are foreseen to reduce the particle flux on the detectors. The relevant drivers for the design and accommodation of the diverters are the required deflection efficiency, preventing the obstruction of the X-ray light paths, mass optimisation, and residual magnetic fields at the detectors. Such deflectors could in principle be placed anywhere between the Mirror Assembly and the Focal Plane. However, placing them closer to the Mirror Assembly implies much larger mass (TBC) than placing them on the instrument platform. The current baseline is therefore to place these deflectors on the instrument platform.

The instruments' requirements with respect to charge particle deflection are also listed in Table 3-4 above. They refer to:

- the maximum energy of the protons and electrons that need to be deflected, based on the band pass that needs to be cleared from charge particle signals, and the relevant filter thicknesses to calculate energy loss of these particles
- the area in the Focal Plane from which the particles have to be deflected

3.6 Pointing requirements

TBD

4 SPACE CRAFT PROVIDED ITEMS

The definition of optimal interfaces between S/C (prime) provided items and instruments (PI) provided units is considered of large importance to reduce the technical and programmatic risks associated with the mission development. To elucidate the interfaces between the payload and the spacecraft, to maintain overall coherency in the procurement of the key mission elements and to reduce the overall development risk, the concept of Payload Support Elements is introduced. The PSE are items procured separately from any scientific instrument but required for their accommodation on-board (*e.g.*, baffles and mass memory storage). Other areas calling for direct involvement of industry in the design and procurement is represented by the stray light baffle and charged particle diverters required by most instruments. These facilities will most likely be common for all on-axis instruments, but physically detached from each from them. Although in future project phase changes to the mission configuration and corresponding S/C design are possible, the design solutions described below will be considered as the baseline.

As mentioned before in par. 3.4, the cryogenic system is currently described as part of the XMS instrument. However, in view of the complexity of the system and of its interfaces with the S/C, the procurement of the cryogenic system may well be detached from the instrument. For this reason, the cryogenic system is provisionally listed here as a PSE item.

Presently the PSE items are considered as S/C provided and the following are currently envisaged as listed in Table 4-1.

Table 4-1: List of PSE items

Item	Description
Movable instrument platform	provides 4 fixed (TBC) instrument positions and global focussing capability +/- tbd mm
On-axis translation mechanism(s)	Currently not foreseen, depends on accuracy and stability of S/C deployment
On-axis instrument baffle with door	Limits FoV off all on-axis instruments to fixed telescope structure in order to suppress X-ray stray light, door is required within the contamination control philosophy for IXO
CAT-XGS stray light baffle/camera mount	Currently not part of CAT-XGS, placeholder
CAT-XGS focussing mechanism	Needed if the S/C deployment accuracy and stability are insufficient
CAT-XGS translation mechanism	Currently not foreseen, depends on accuracy and stability of S/C deployment
Charged particle deflection system for on-axis instruments	Deflects charged particles up to instrument defined maximum energies away from the instruments FoV in the primary focus
Charged particle deflection system for CAT-XGS	TBC: currently not clear if needed
Optical stray light baffling	TBC: at TBD positions in the telescope tube; currently not clear if needed
Telescope Alignment Monitoring system (TAM)	Measures the alignment of each individual instrument with respect to the mirror
Instrument calibration source facility	Currently not foreseen, may be needed for CAT-XGS
Mass Memory (part of Data Handling subsystem)	Provides data storage for all instruments; sized to hold up to 48 hrs of data, 512 Gbit (TBC)
Cryogenic system for XMS	A cryogen free system with active cooling from 300K (TBC) providing a base temperature of 50 mK

The list of PSE is subject to further updates following the planned system level assessment study. It is foreseen that a consolidated list will be provided with the release of any future Announcement of Opportunity for the instruments provision.

A further description of the above PSE items is given in the next paragraphs

4.1 Alignment equipment

A telescope alignment monitoring system (TAM) will be provided in order to ensure sufficient accurate knowledge of the instruments' alignment and positioning with respect to the telescope and to each other. Most likely this will include dedicated equipment for each of the instruments on the MIP and FIP. Depending on whether or not the system will be used continuously during observation, stray light mitigation may be necessary. The ESA-CDF report [RD] includes a section on this item.

The alignment accuracy of the detectors with respect to the telescope focus may depend on the instruments internal alignment and stability, the alignment of the instruments' with respect to the MIP and FIP, the stability and reproducibility of the MIP and FIP position, and, probably mainly, on the accuracy and stability of the S/C deployment mechanism. The necessity of instrument translation and focussing mechanisms depends on the whether the sum of all uncertainties exceeds the alignment requirements listed in Table 2-2. It is currently foreseen (based on ESA CDF results) that no translation stages are required, but there will be a single focussing mechanism for the entire MIP, and one for the CAT-XGS on the FIP.

4.2 Stray light and background related equipment

4.2.1 X-ray Baffling

In the section below an estimate of the required baffle sizes is given, based on:

- A 1.9m radius of the mirror, which is placed at 20m in front of the detector planes
- The baffle should limit the view of the detectors to within the solid support ring at the edge of the fixed telescope tube, defined by a 3.0 m diameter (TBC) circle at 10.7m distance from the Focal Plane
- The effect of the pointing accuracy and position accuracy of the MA with respect to the IP has been taken into account
- The effect of a possible misalignment and of the stability of the alignment between detector and baffle has not been taken into account
- The baffle should be opaque to the diffuse x-ray background to a level specified by the individual instruments
- No optimisation (shape of edges, vanes) has been done to mitigate optical stray light, except for black paint at the inside (include in mass budget)

A sketch of the deployed S/C configuration with the relevant dimensions is shown in Figure 4-1, left. It is assumed here that the main telescope tube attached to the mirror assembly is completely opaque to energies up to 40 keV, and therefore any X-ray stray light can only come through the shroud. Figure 4-1, right shows the calculated transmission of the shroud (modelled as consisting of 76.2 μm of Kapton and Mylar each) for normal incidence. Clearly, the shroud provides sufficient shielding for CAT-XGS, but not for any of the other instruments. Therefore, for the on-axis instruments a common baffle on the fixed instrument platform is foreseen, which restricts the unobstructed view of any of the instruments to the inside of the telescope tube

and provides sufficient x-ray attenuation in the relevant energy range for all instruments. The driver for the size of the baffle is obviously the FoV of WFI.

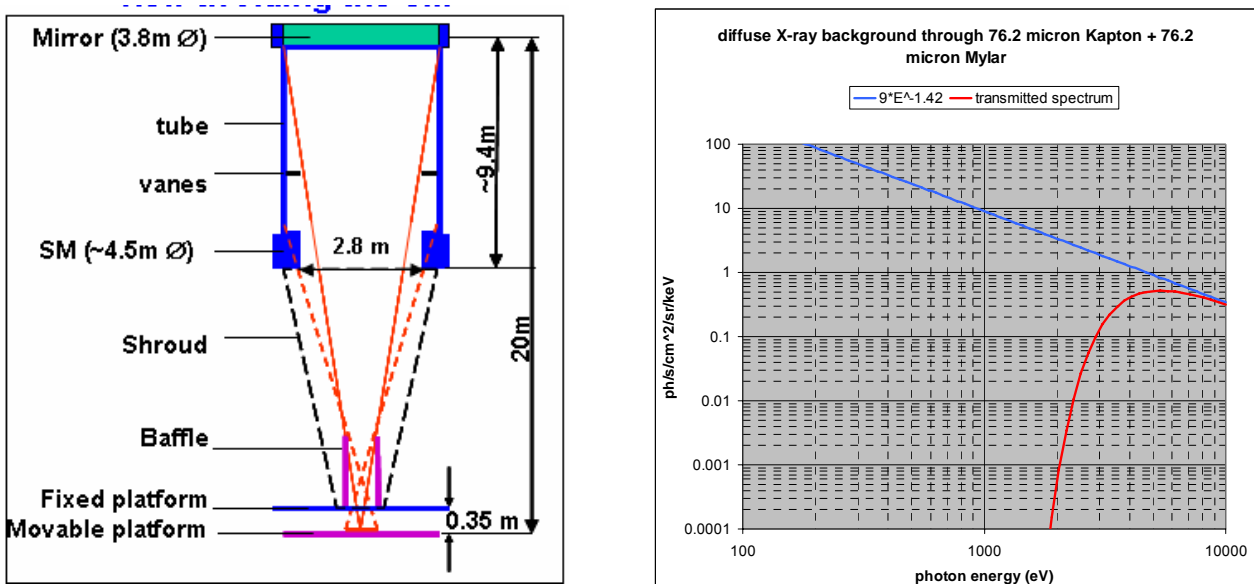


Figure 4-1: left) schematic representation of the deployed satellite. Right: calculated attenuation of the diffuse X-ray back ground spectrum by the shroud (normal incidence)

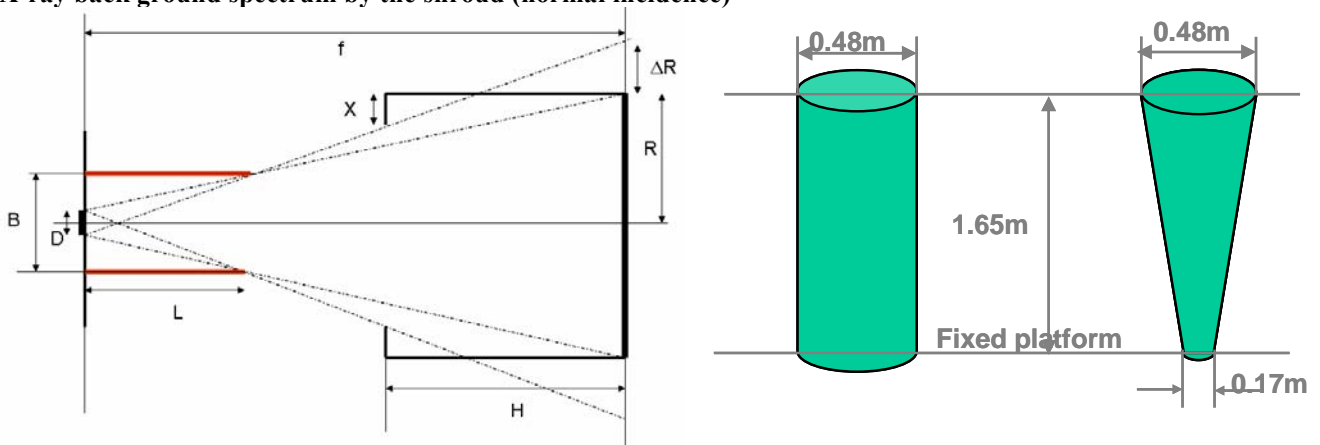


Figure 4-2: left) Geometry used to calculate the baffle dimensions. right) resulting baffles sizes for two possible configurations. A 0.35m distance between fixed platform and the focal plane is assumed.

The length L and diameter B of the baffle are given by (see Figure 4-2):

$$L = \frac{fD}{D + \Delta R} \quad \text{and} \quad B = \frac{2RD + D\Delta R}{D + \Delta R}, \quad \text{with} \quad \Delta R = \frac{(R + D/2 - X)f}{f - H} - (R + D/2)$$

Here $f=20\text{m}$ is the telescope focal length, $R=1.9\text{m}$ is the mirror radius, $D=10.5\text{cm}$ is the WFI detector diameter, $H=9.3\text{m}$ is the length of the fixed telescope tube, and $X=0.4\text{m}$ is the dimension that limits the radius of the telescope tube at the detector side. The quantity ΔR is equivalent to an effective width of a skirt around the mirror. To account for a pointing error of 1 arcmin and a detector displacement error of 1 mm, the quantities R and X have been adapted to $R=1.907\text{ m}$ and $X=0.404\text{ m}$ in the calculation. Displacement Error (RDE), representing the lateral displacement of the MA wrt the centre of the detector. The 1'AAE corresponds to a 6 mm shift of the MA wrt to the optical axis (and a slight tilt which is neglected here) which

can be accounted for by increasing R by 6 mm and decreasing ΔR by 4mm in the equations above. The ± 1 mm RDE is accounted for by increasing R and ΔR by 1mm. The resulting baffle sizes are shown in the last 2 columns of Table 4-2. The resulting baffle dimensions are $B=0.48$ m and $L=2.00$. Correcting for a 0.35m distance between movable and fixed platform, the physical length of the baffle mounted on the fixed platform would be 1.65m.

Table 4-2: On-axis baffle dimensions and mass

	cylindrical	conical
Length (measured from the fixed instrument platform)	1.65m	1.65
diameter	0.48m	0.48m (top), 0.17m (bottom)
Mass (incl. mounting and door)	19.0 kg	13.4 kg

In order to provide sufficient attenuation up to 40 keV (as required for HXI) the baffle could be coated with a gold layer with a graded thickness equivalent to 200 μ m along the line of sight. Figure 4-3 shows the attenuated diffuse X-ray background spectrum, assuming a 5 steradian view to the sky through the Au-coated baffle. Note that the X-ray background will by far dominate the particle background above ~ 40 keV. Further optimisation (e.g graded shielding to reduce secondary emission) may be necessary.

The shape of the baffle could be simply cylindrical, but a conical shape will of course be more mass efficient (see Figure 4-2, right). Dimensions and mass estimates (based on 2mm CFRP, 200 μ m LoS Au, and 20% additional mounting structure, and a door at the top) are shown in Table 4-2.

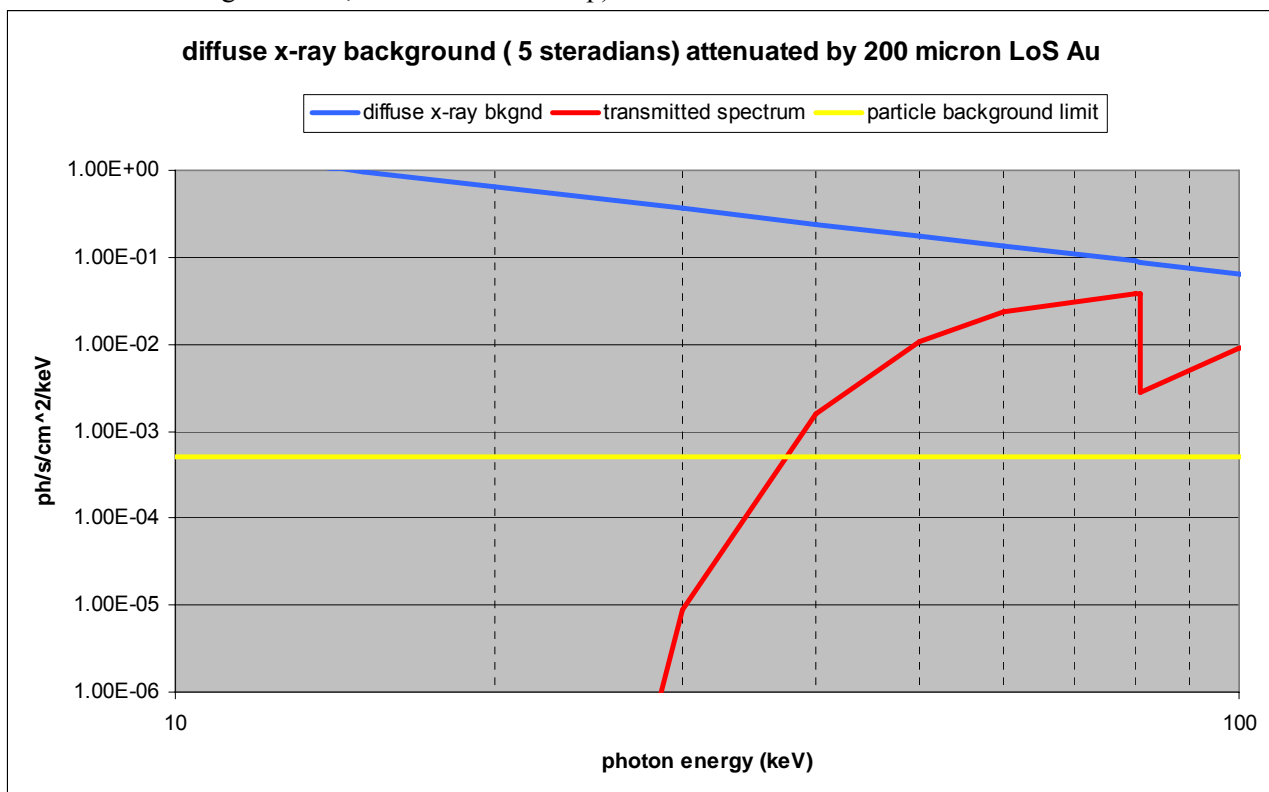


Figure 4-3: attenuated diffuse X-ray background spectrum, assuming a 5 steradian solid angle view to the sky through the Au-coated baffle.

It should be noted that, in the absence of a shroud, CAT-XGS would require an extremely large baffle with an estimated length of order 4-5m, which would probably interfere with the S/C deployment concept. Currently a relatively small stray light baffle which is integrated in the instrument is foreseen for CAT-XGS.

4.2.2 Optical stray light baffling

A preliminary stray light analysis was performed during the ESA CDF [RD-5] concentrating on the effect of micrometeorites induced holes in the shroud. It was estimated that the total hole area after 10 years in orbit is $\sim 4 \text{ cm}^2$. It was found that:

- the on-axis baffle length needs to be $\sim 2\text{m}$ to meet the stray light requirements for WFI and XMS. This would be well matched to the X-ray baffling requirements.
- XGS needs a baffle of 3-5m to meet its stray light requirement (defined for the case without Al filter on the CCDs). Clearly this issue needs further attention.

Stray light from the metrology is not foreseen to be a problem, provided that the proper measures (collimation, high quality optical components etc) are in place.

Additional stray light baffling or vanes at TBD positions in the telescope may be required to suppress optical stray light propagating through the mirror assembly.

4.2.3 Charged particle deflectors

The following assumptions have been made for evaluating which charged particles need to be deflected away from the detector sensitive areas:

- Radiation damage issues are not taken into account here: these will need to be addressed separately
- It is sufficient to deflect away from the detector sensitive area only those particles that would give rise to signals in the energy band of the respective instruments. The upper energy limits for the instruments have been increased to give some margin for pile-up analysis (see E_{max} row in Table 3-4)
- Particles will lose energy when passing through any filters included in the instrument. This energy loss has been accounted for by using both the proposed fixed filter thickness for each instrument as well as possible additional filters in the filter wheel (see Table 3-4).

The resulting maximum proton and electron energies to be deflected are listed in Table 3-4. It should be noted that the *total* flux of charged particles incident on the detectors may not be reduced significantly, since the low energy particles are only a small fraction of this total flux. Further input from the instrument teams is needed to evaluate if this is acceptable.

X-POL is different since it has a $50 \mu\text{m}$ thick Be entrance window, which will stop all low energy protons up to $\sim 6 \text{ MeV}$. However, an electrostatic grid is necessary here to prevent contact between plasma and the HV part of the instrument. This grid is included in the instrument.

HXI is mounted behind WFI. The latter has a Si thickness of $450 \mu\text{m}$ which will stop all protons up to $\sim 6 \text{ MeV}$ and all electrons up to $\sim 200 \text{ keV}$. Any protons at 6 MeV will probably not be focussed by the mirrors (TBC), while electrons at $E > 200\text{-}300 \text{ keV}$ will be deflected sufficiently efficient if the deflection magnets are designed for proton deflection up to $> 100 \text{ keV}$.

Using the approximation that the deflection angle scales as B/\sqrt{E} , it appears that for the on-axis instruments WFI probably is the driving instrument: are roughly equivalent: WFI requires a lower maximum energy of particles to be deflected than XMS, but over a 3 times larger deflection angle. The magnet systems could be accommodated close to the detectors on the instrument platform or further away at the level of the Service Module or the Mirror Assembly. As the former is likely to be more mass efficient, this option is evaluated in a little more detail here. During the Payload Accommodation studies for XEUS (refs) a magnet system was designed to be mounted in the instrument baffle of WFI for a detector area of $7 \times 7 \text{ cm}^2$, a maximum energy to be deflected of 50 keV , and a telescope F# about 2x larger than for IXO. This system consisted of (see

Figure 4-4) two permanent magnets (NdFe 42H, NEO 45) of 10x15x2 cm at 0.6m from the detector with a total mass of 4.4kg. Using the above crude scaling, the estimated field strength for IXO would be $\sim 1.7\times$ higher, suggesting total mass of ~ 7.5 kg. In addition the magnets may have to be slight larger: tentatively we assign ~ 10 kg of mass (without margin). These magnets are mounted in the common baffle for the on-axis instruments. Note that the residual field at the detectors position would be ~ 10 Gauss, which is currently compliant with all instrument requirements, except the XMS requirements during cool down. It could be considered, however, to choose the most optimum position of the MIP during cool down of the XMS, and provide extra shielding at that position, if necessary. A full optimisation with respect to accommodation, mass and residual magnetic field is needed.

For CAT-XGS, being an off-axis instrument, the geometry is more complicated, and possibly more favourable, since the innermost CCDs are more than 2 degrees from the optical axis. In addition, the energy band of CAT-XGS is < 2 keV, and CAT-XGS has an intrinsic rejection capability through the well-defined relation between photon energy and position along the detector. Therefore, currently no dedicated particle deflection system is foreseen for CAT-XGS. If such a system would be required it is not obvious how it could be implemented effectively, due to the large length of the detector.

It should be noted that a careful analysis of the charged particle distribution in the focal plane is presently lacking

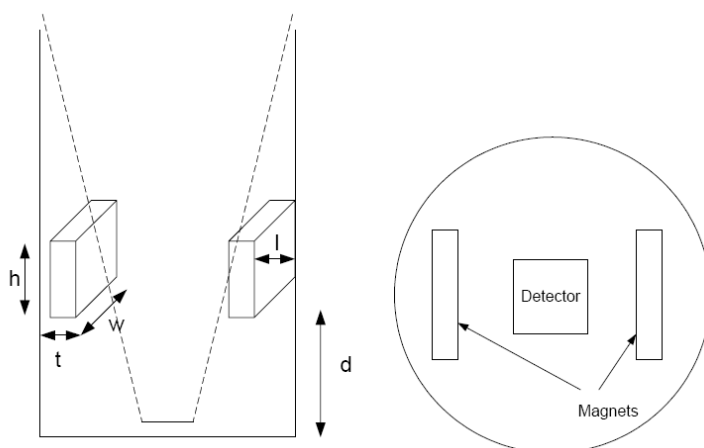


Figure 4-4: configuration of the particle deflecting magnets in the common on-axis instrument baffle

4.3 Cryogenic chain for XMS

Several options for this system are described in part 2 chapter 3 (XMS) and many more probably exist. In order to facilitate an objective comparison and trade-off between these and future designs of the entire cooling chain, all interface requirements are collected in a separate document [RD-7].

4.4 Additional Items

4.4.1 CAT-XGS baffle, mount and wavelength calibration sources

The CAT-XGS-CAT description in section 2 does explicitly mention some additional required but not included items:

- a stray light baffle + camera mount

- a wavelength calibration source

These are listed as a place holder; they are not necessarily S/C provided items.